Title
Improving Preclinical Testing of Deformity Correction Surgery

Author
Borkowski, Sean Leo

Publication Date
2015

Peer reviewed|Thesis/dissertation

UNIVERSITY OF CALIFORNIA

Los Angeles

Improving Preclinical Testing of Deformity Correction Surgery

A dissertation submitted in partial satisfaction of the

requirements for the degree Doctor of Philosophy

in Biomedical Engineering

by

Sean Borkowski

2015

ABSTRACT OF THE DISSERTATION

Improving the Standard for Preclinical Testing of Deformity Correction Surgery

by

Sean Borkowski

Doctor of Philosophy in Biomedical Engineering

University of California, Los Angeles, 2015

Professor Edward Ebramzadeh, Co-Chair

Professor Harry McKellop, Co-Chair

With advancements in deformity correction surgical strategies, such as the use of thoracic pedicle screws, invasive surgical resections, and correction maneuvers involving high forces, surgeons are pushing the limits of deformity correction in children and adolescents. Unfortunately, due to the lack of an adequate in-vitro model, many clinical questions surrounding these treatments remain unanswered, leading to clinical uncertainty and surgical risk. For the past three decades, in-vitro models have almost universally included the application of pure bending moments in cadaveric spines to produce kinematic responses. Pure moments are intended to produce a constant bending moment along the length of the spine, and offer the advantage of reproducible testing regardless of spine length or stiffness. With this model, the resulting kinematic spine responses have been compared for the evaluation of simulated destabilized and implanted conditions, either with dynamic stabilization or rigid fusion devices.

However, the pure moment model was not selected to simulate intraoperative conditions. Moreover, alternative loading models have not been adequately explored.

The purpose of the proposed study was to evaluate three preclinical spine testing models: 1) the traditional pure moment preclinical testing method in spine biomechanics; 2) a novel simultaneous multi-planar loading protocol to represent the three-dimensionality of scoliosis deformities; and 3) a novel torsional loading protocol using a custom-built simulator intended to mimic a representative surgical correction maneuver employing high-magnitude in-vitro torque application. Each of the three models was applied to cadaveric thoracic spines to evaluate the safety and efficacy of representative intraoperative surgical techniques during deformity correction surgery. Specifically, safety and efficacy was measured by quantifying differences in thoracic spine range of motion and strength as a function of surgical resection and loading type. In addition to expanding the loading schematics for preclinical scoliosis testing, the proposed study evaluated and improved upon the validity of using elderly cadaveric specimens for preclinical testing of pediatric spine disorders and treatment, a major criticism of pediatric spine biomechanics. Unlike previous studies where intervertebral disc health has been ignored, the proposed study classified changes in the structural response of the spine as a function of disc health, thereby producing more specific conclusions towards the applicability of the results in the pediatric and adolescent communities.

Under single plane Pure Moments, wide posterior releases provided significant increases in motion beyond that provided by routinely performed releases, with thoracic spine range of motion increases of as much as 12-17° following the clinical releases. This result substantiates the use of wide posterior releases as a supplemental tool in increasing the flexibility of the

thoracic spine. Moreover, in specimens with healthy intervertebral discs, multi-level releases provided more pronounced releases, nearly doubling the increase in motion. Furthermore, under the multi-planar loading protocol, the releases were effective in providing simultaneous three-dimensional increases in motion, suggesting their potential use in cases of three-dimensional deformity, such as adolescent idiopathic scoliosis.

The results were further developed under the simulated intraoperative correction technique, direct vertebral rotation. Thoracic spine strength was established, with an average failure moment of 33.3Nm, significantly less that the torques purportedly applied intraoperatively. Additionally, following the posterior release, single level ROM increases of as much as 19° were observed at failure, the most clinically relevant magnitude of motion increase measured to date using an in-vitro model. Using strength predictions based on the relationship between BMD and thoracic spine strength, safe limits of loading can be applied to produce significant increases in flexibility. Even applying as little as 25% of the failure load, the achievable increase in range of motion more than doubled compared to that predicted using 4Nm pure moments, the typical pure moment magnitude. In addition to providing safety and efficacy data towards predictions of deformity correction, the novel model highlighted the limitations of traditional in-vitro models, and may promote the use of novel experimental design in evaluating many spine problems.

In its entirety, the study introduced novel spine biomechanics testing methods which challenged the traditionally used pure moment model, and improved upon its limitations. In turn, the clinical applicability of preclinical scoliosis biomechanics testing results improved as well. Using these novel testing methods, the study helped to provide clinical guidelines for the

efficacy and safety of posterior surgical releases and correction techniques. The improved clinical applicability of the results may also serve to stimulate development in other areas of spine testing, such as evaluations of disc degeneration, where the pure moment model has become increasingly unsuitable, as treatment has trended away from solid fusion and towards motion-preserving implantations. With improved models and experimental design, preclinical spine testing will begin to make a greater impact on the clinical outcome for children and adolescents. Moreover, the clinical decision making and outcome for all spine patients, young or old, will improve.

The dissertation of Sean Borkowski is approved.

Warren S. Grundfest

Daniel T. Kamei

James V. Luck, Jr.

Sophia N. Sangiorgio

Harry McKellop, Committee Co-Chair

Edward Ebramzadeh, Committee Co-Chair

University of California, Los Angeles

2015

This work is dedicated to

James, Eileen, Patrick, Nicole, Dylan and Alexis Borkowski

My Father, Mother, Brother, Sister, Nephew and Niece

TABLE OF CONTENTS

ACKNOWLEDGEMENTS

While this document is represented by a single name, the work and impact represents the efforts of teams of individuals who provided me with the support, knowledge, and opportunity to lead these investigations.

I would like to thank and acknowledge my coauthors that helped with the published articles which contributed to this work, including the publications in Spine Deformity and the European Spine Journal - Dr. Ebramzadeh, Dr. Sangiorgio, Dr. Scaduto, Dr. Bowen, Dr. Kwak-Lee, and Dr. Frost. I would like to additionally thank the coauthors on my other published manuscripts.

To my committee members, Drs. Ebramzadeh, Sangiorgio, McKellop, Kamei, Grundfest, and Luck, I truly appreciate all of your support and guidance throughout my graduate career.

Dr. Kamei, you provided more than the necessary support and guidance – you lit a flame, you instilled confidence, and you led by example…for all of us.

Thank you to Dr. Luck, and all of the faculty and staff at Orthopaedic Institute for Children for providing me and my coworkers an opportunity to work in the field of Orthopaedics, and to have the opportunity to conduct meaningful research each and every day.

Thank you to all of my fellow students who helped me along the way. I would never have made it without your help and your support.

Dr. Park and Dr. Campbell, thank you for your support, guidance, and most of all, your friendship.

Dr. Ebramzadeh and Dr. Sangiorgio, from day one, you provided nothing but loyalty, support, mentorship, and love. I will always be thankful for the journey, and for the way in which you embraced me from day one. We will always be a team.

Ashleen Knutsen, thank you for your support. You provided me with confidence every day, as I knew you always had my back. You never wavered. I appreciate forever the bond that we built, and the support that you provided me.

To all of my friends, thank you.

To my family, thank you. The Santry family, thank you. The Borkowski family, thank you.

Mom, Dad, Pat, Cole, D, Lexi…words will never describe. Thank you. This is us.

CURRICULUM VITAE

I. EDUCATION

M.S. in Biomedical Engineering, March 2010
University of California Los Angeles, Los Angeles, CA

B.S. in Biomedical Engineering, May 2008
Rutgers University, New Brunswick, NJ

II. ACADEMIC APPOINTMENTS

Research Assistant/Ph.D. Student,
Implant Biomechanics Laboratory
The J. Vernon Luck, Sr. Orthopaedic Research Center
Orthopaedic Institute for Children (Formerly Los Angeles Orthopaedic Hospital) and University of California, Los Angeles
Fall 2008 to Present

III. HONORS AND AWARDS

- ***Best Poster, Pediatrics***, American Academy of Orthopaedic Surgeons (AAOS) 2014 Annual Meeting, New Orleans, LA, March 2014
- ***"Editor's Choice"*** Top Nine publications selected by the ASME Journal of Biomechanical Engineering to represent their best publications of 2012: "Site-Specific Quantification of Bone Quality Using Highly Nonlinear Solitary Waves," *ASME J. Biomech. Eng.
- ***Finalist: John H. Moe Award for Best Basic Science Poster Presentation***, Scoliosis Research Society (SRS) 47th Annual Meeting & Course, Chicago, IL, October 2012***Presentation of the Best Paper,*** 21st Annual Research Day, Orthopaedic Hospital, Los Angeles, CA, 2012
- ***Presentation of the Best Paper,*** 20th Annual Research Day, Orthopaedic Hospital, Los Angeles, CA, 2011

IV. BIBLIOGRAPHY

PUBLISHED ARTICLES

1. Sangiorgio, S.N., Sheikh, H., **Borkowski, S.L.,** Khoo, L., Warren, C.R., Ebramzadeh, E. "Comparison of Three Posterior Dynamic Stabilization Devices." Spine. 2011. 36(19):E1251-8.

2. Yang, J., Silvestro, C., Sangiorgio, S.N., **Borkowski, S.L.**, Ebramzadeh, E., De Nardo, L., Daraio, C. "Nondestructive Evaluation of Orthopaedic Implant Stability in THA Using Highly Nonlinear Solitary Waves." Smart Materials and Structures. 21 (2012) 012002 (10 pp).
3. Sangiorgio, S.N., Ebramzadeh, E, **Borkowski, S.L.**, Oakes, D.A., Reid, J.J. Bengs, B.C. "Effect of Proximal Bone Support on the Fixation of a Press-Fit Noncemented Total Hip Replacement Femoral Component." Journal of Applied Biomaterials & Functional Materials. 2013; 11(1):e26-34.
4. Silva, M., Knutsen, A., Kalma, J.J., **Borkowski, S.L.,** Bernthal, N.M., Spencer, H.T., Sangiorgio, S.N., Ebramzadeh, E. "Biomechanical Testing of Pin Configurations in Supracondylar Humeral Fractures: The Effect of Medial Column Comminution." J Orthop Trauma. 2013; 27(5):275-80.
5. Yang, J., Sangiorgio, S.N., **Borkowski, S.L.**, Silvestro, C., De Nardo, L., Daraio, C., Ebramzadeh, E. "Site-specific Quantification of Bone Quality using Highly Nonlinear Solitary Waves." Journal of Biomechanical Engineering. 2012; 134(10):101001.
6. Sangiorgio, S.N., Ebramzadeh, E., Knutsen, A.R., **Borkowski, S.L.,** Kalma, J.J., Bengs, B.C. "Fixation of Non-Cemented Total Hip Arthroplasty Femoral Components in a Simulated Proximal Bone Defect Model." Journal of Arthroplasty. 2013; 28(9): 1618-24.
7. Sangiorgio, S.N., **Borkowski, S.L.**, Bowen, R., Scaduto, A.A., Frost, N.L., Ebramzadeh, E. "Quantification of increase in 3-Dimensional spine flexibility following sequential Ponte osteotomies in a cadaveric model." Spine Deformity. 2013; 1:171-178.
8. Zionts, L., Ebramzadeh, E., Knutsen, A., **Borkowski, S.L.**, Avoian, T., Sangiorgio, S.N. "Accuracy of Radiographs in Assessment of Displacement in Lateral Humeral Condyle Fractures." J Child Orthop. 2014; 8(1): 83-9.
9. **Borkowski, S.L.,** Ebramzadeh, E., Sangiorgio, S.N., Masri, S.F. "Application of the Restoring Force Method for Identification of Lumbar Spine Flexion-Extension Motion Under Flexion-Extension Moment." J Biomech Eng. 2014; 136(4).
10. Knutsen, A.R., Avoian, T., Sangiorgio, S.N., **Borkowski, S.L.,** Ebramzadeh, E., Zionts, L.E.. "How Do Anterior Tibial Tendon Transfer Techniques Influence Forefoot and Hindfoot Motion?" Clin Orthop Relat Res. 2014 Nov 25. [Epub ahead of print].
11. Tan, T.L., **Borkowski, S.L.,** Sangiorgio, S.N., Campbell, P.A., Ebramzadeh, E. "Imaging Criteria for the Quantification of Disc Degeneration: A Systematic Review." JBJS Reviews. *In-Press*.

NOTABLE ABSTRACT PRESENTATION

1. **Borkowski, S.L.**, Sangiorgio, S.N., Bowen, R.E., Scaduto, A.A., Kwak Lee, J., Ebramzadeh, E.: Challenging the Standard for Pre-Clinical Testing of Deformity Correction Surgeries. AAOS Annual Meeting, New Orleans, LA, 2014.

1 Background

1.1 Brief Historical Perspective on Spine Biomechanics

For centuries, professionals of many trades have recognized the importance of spine biomechanics, including doctors, scientists, mathematicians, philosophers, and artists. Whether it was the iron corset designed by Ambroise Pare for spine deformity correction in the 1500s,[1,2] the first spine biomechanics textbook written by Giovanni Alfonso Borelli in the 1600s,[3] or the theories of deformity correction by Jean-Andre Venel in the 1700s,[4] the contributions to the field were widespread. Despite primitive medical practices and technologies, by appreciating the mechanical, geometrical, and mathematical aspects of spine conditions, these early pioneers developed theories still employed today. For example, Jean-Andre Venel recognized the coronal and transverse plane components of scoliosis deformity, and theorized two primary correction maneuvers to reduce the deformities: (1) axial traction and (2) transverse forces in the form of derotation.[4] The first principle, axial traction, was the primary correction force employed in the revolutionary Harrington instrumentation system.[5] Meanwhile, today, the primary correction maneuvers still follow the second principle, that is, application of transverse forces through, for example, derotation and direct vertebral rotation (DVR).[6,7] The culmination of such contributions by these pioneers built the foundation for spine biomechanics, a field which has been essential in the understanding, diagnosis, and treatment of spine pathologies and conditions.

In the early to mid-1900s, theories describing the cause of various spine pathologies led to the development of early models for in-vitro spine biomechanics. While the causes of back pain were largely unknown, structural changes to the intervertebral disc could be seen on x-rays, including intervertebral disc space narrowing. It was postulated that when structural changes

occur, the ability of the intervertebral disc to resist strain would be compromised.[8] To test this and many other theories, early in-vitro studies began investigating the load-displacement behavior of human cadaveric spines under compression loading.[8] The biomechanical testing of spines quickly transitioned beyond axial loads to include bending moments, which produced flexion, extension, and lateral bending rotations, and torsional moments, which produced axial rotation.[9-12]

Prior to the establishment of any loading or testing standards, loads and moments varied in magnitude and method of application among different research groups. Bending and torsion were produced in thoracic and lumbar functional spine units (FSUs), for example, using dead weights,[12] dead weight pulley systems,[11] and pneumatic actuators.[13] Meanwhile, other groups produced bending by applying off-axis compression,[9,10] or compression to slightly bent spines.[14] Furthermore, the magnitudes of applied moments varied. Specifically, magnitudes ranged from 2 Nm in thoracic spines[10] to more than 10 Nm in lumbar spines.[12]

However, despite these differences in experimental setup and moment application, the primary objective of the majority of these early models was simple: determine the fundamental displacement and rotational properties of the spine in response to applied loads and moments. For example, White *et al*.[9,10] applied 2 Nm of bending through pneumatic actuators and dead weight pulley systems to thoracic FSUs, producing approximately 4-20° in flexion-extension, 5-13° in lateral bending, and 3-14° in axial rotation. However, due to different loading setups and conditions, the results across studies varied widely. Markolf *et al*.[11] applied higher loads (6.8 Nm) to thoracic FSUs using a dead-weight pulley system, but reported smaller motions than those reported by White *et al*.[9,10] About a decade later, Panjabi *et al*.[13] used a linear force vector

to produce forward flexion moments between 2-6 Nm, which spanned the moment magnitudes applied by White *et al*.[9,10] and Markolf *et al*.,[11] and reported even smaller motions than those previously reported, with average motions of 1.4° and 1.0° in flexion and extension, respectively.

Despite the wide range of results, these early studies provided some key foundational concepts in spine biomechanics. First, there are large variations in the rotational properties of nominally equivalent cadaveric spines, that is, cadaveric spines with the same intact structural support, such as intervertebral discs and connective soft tissue and ligaments. While differences in the loading protocols inevitably contributed to the wide variability in range of motion of the FSUs across studies, these differences were not a result of testing artifacts.[12] Instead, the reported ranges within each study suggested the inherent variability in cadaveric spines. This concept still applies today, even with the application of standard testing methods, but this will be further explored later in this work.

In addition to the variability in motion among cadaveric spines, the early studies demonstrated the complex, nonlinear hysteretic response of the spine under applied bending loads,[11] as demonstrated by the nonlinear load-displacement and torque-rotation curves. Finally, early studies highlighted the benefits of studying primary motions (i.e. sagittal plane rotation in response to a flexion bending moment), coupled motions (i.e. coronal plane rotation in response to a flexion bending moment), and stiffness.[15,16]

While the initial studies provided some of the foundational concepts in spine biomechanics, it became clear in the 1980s that a major change was needed. As discussed by Dr. Manohar Panjabi,[17] biomechanical testing of new instrumentation systems began to parallel the development and manufacturing of these same systems, leading to an increased number of spine

biomechanics studies. The designs included, for example, pedicle screws,[18] spinal rods,[5,18,19] sublaminar wires,[19] anterior vertebral body screws,[20,21] laminar and pedicle hooks,[5,18] and plates.[22] Meanwhile, the devices were tested using various loads, specimen lengths (i.e. one level functional spine units vs. 6-level T12-sacrum specimens), specimen types (i.e. human or porcine), loading rates, and outcome variables. Consequently, comparisons of the results across studies were not easily performed.[17]

With the increase in popularity, acceptance, and use of biomechanical studies, together with the increase in popularity of fusion instrumentation to treat spine conditions, it was clear that a standard method of testing was necessary to evaluate and compare the different devices and systems. At the time, the idea of a standard method was very reasonable. These early instrumentation systems, while having different designs, had one common functional goal: provide rigid fusion to the spine. Because the designs shared this common functional goal, the ability of different systems to achieve this function could be compared. For example, to prove a particular implant could provide solid fusion, the in-vitro results should demonstrate that the fixation system minimized motion at the implanted level. Then, to compare one implant's ability to minimize motion compared with another implant's, the stiffness measurements could be compared. This standard became *Pure Moments*, a concept that would transform biomechanics, and become the standard in the spine community from the 1980s through the present day.

1.2 Pure Moment Testing

The following section provides a description of the design of, the assumptions in, and the applications of the pure moment testing model for preclinical spine biomechanics testing. As such, this chapter has been broken down into three major subsections: Design, Assumptions, and Applications.

1.2.1 Design

Pure Moment Theory

In the early 1980s, with the growth in popularity of spine implants and devices, the need for preclinical spine biomechanics testing increased.[17] A method was needed to test the new devices in a reproducible and repeatable manner that could predict potential in-vivo performance of the devices, prior to clinical use in patients. This method and standard was *Pure Moments*.[17]

A pure moment, or a force couple, is a system of forces which produces a net moment without producing a net force. Similarly, the system produces rotation without producing translation. The theory of pure moments is described by two applied bending moments of equal magnitude and opposite direction at the left and right ends of a straight rectangular beam. During such bending, shear force is zero across the beam. Consequently, the only forces acting on the beam are the moment couple. As such, loading is equivalent along the entire length of the beam. Moreover, under the same applied moment couple, the load at every cross section would be the same regardless of the dimensions of the beam. This concept was adopted by the spine biomechanics field,[17,23,24] and for more than three decades, has remained the gold standard in spine biomechanics and spine flexibility testing.

As discussed, by applying pure moments to the spine, the moment at each cross section of a test specimen remains constant throughout testing, regardless of the amount of rotation that occurs.[17] The advantages of pure moments for spine biomechanics have been discussed thoroughly, demonstrating the model's importance.[17] This discussion can be applied to loading setups used in the literature to illustrate the points. Specifically, two studies, one by White *et al*.[10] and one early study by Panjabi *et al*.,[13] can illustrate the disadvantages of alternative loading setups. As discussed in the literature,[17,23] three primary methods can be employed to produce bending in the spine: (1) off-axis compression;[9,10] (2) cantilever bending;[13] and (3) pure moments.

In the first mode, that is, (1) off-axis compression, a compressive load is applied to the spine at a distance from the centroid of the vertebral body to produce bending. For example, to produce flexion in thoracic FSUs, White *et al*.[9,10] applied a compressive load at a point between the central-most point and the anterior-most point of the superior vertebral body. In that setup, when the spine is in the vertical position and a small compressive load is applied, the resultant moment would be relatively constant along the length of the FSU, as minimal rotation would be produced. However, as soon as larger compressive loads are applied and larger flexion rotations are in turn produced, the moment profile along the length of the spine will vary. Moreover, the moment profile would continuously change as a function of the amount of rotation in the spine. These differences would be substantially magnified when applying loads to multi-level specimens, which the majority of studies in the literature have used, as the total rotation would increase. The corresponding testing results would be significantly affected by this variability along the length of the specimen. Consequently, this method of loading, that is off-axis compression, is susceptible to large errors.

In the second mode, that is, (2) cantilever bending, a horizontal load vector is applied to the superior vertebral body of the spine to produce bending in either the sagittal or coronal planes. For example, to produce flexion in thoracic FSUs, Panjabi *et al*.[13] used pneumatic cylinders to apply an anterior-directed horizontal force vector to the superior vertebra, while the inferior vertebra was rigidly fixed to the test table. In that setup, the moment profile increases linearly along the spine from superior-to-inferior, with the minimum moment occurring at the point of load application, and the maximum moment occurring at the base of the inferior vertebra. In other words, as the distance between the point where the horizontal force is applied and a point at the cross-section of interest increases, the moment increases as well. Similar to off-axis compression, the differences between the moments at the superior and inferior segments become more pronounced with multi-segment specimens, in turn affecting the results. In a more recent article, Horton *et al*.[25] used a cantilever bending setup to apply a 25N horizontal force vector to T1, in turn producing flexion and extension in a full-length human thoracic spine. Using published geometrical properties of the thoracic spine,[23] the distance between the force vector (top of T1 vertebral body) and the T1-T2 disc space would be approximately 21 mm. The moment at the T1-T2 disc, therefore, would be approximately 0.5 Nm. In contrast, at the T11-T12 disc space which lies approximately 292 mm from the force vector, the moment would be approximately 7.3 Nm. Clearly, the difference between the moments applied at the superior discs and inferior discs would be substantial, and in turn, would affect the results. Furthermore, if, for example, the authors sought to produce a typical in-vitro thoracic spine moment of 5Nm at T1-T2, a horizontal force of 238N would need to be applied. However, while this force would produce the desired 5Nm moment at T1-T2, it would produce a destructive moment of 69.5Nm at T11-T12. Consequently, a full-length thoracic spine could not be utilized in that example

study. Therefore, like off-axis compression, cantilever bending loading setups are subject to errors and disadvantages.

With these two modes of testing, comparisons across the literature are difficult as the results are dependent upon the type of loading, the point of load application, the geometrical properties of the spine, and the amounts of rotation produced.

Unlike modes (1) off-axis compression and (2) cantilever bending type loading, in mode (3), i.e. pure moments, the applied moment remains constant throughout testing along the length of the entire specimen, regardless of the amount of rotation produced or the geometrical properties of the specimen.[17] Because of this, the moments are controllable and highly reproducible, providing an unbiased, repeatable platform for the testing of spinal fixation devices. In turn, comparisons of the results across the literature could be performed.

Within pure moment testing, two methods of moment application have been performed: the stiffness method and the flexibility method.[17] In the stiffness method, a rotation is applied to the spine, and the resulting moments and forces are recorded. The stiffness method is mainly limited, however, in that it (1) constrains the motion to a specified direction, and (2) predetermines the axis of rotation of the spine, both of which are not physiological. Contrarily, in the flexibility method, a load or moment is applied to the spine, and the resulting motions are recorded. The main advantage to the flexibility method is that it allows the spine to move physiologically, with unconstrained motion in all planes. This method, that is pure moment testing with the use of the flexibility method, became the standard of testing.[17]

Pure moments gained widespread use to compare various instrumentation systems and provided the spine testing framework for the next three decades.

Applying Pure Moment Loads to Cadaveric Spines

Pure moment testing has been used extensively throughout the literature for the past three decades. Depending on both the question of a given study and the experimental apparatus capabilities of a given research group, moments are typically applied in flexion, extension, left and right lateral bending, and left and right axial rotation. These in-vitro moments are typically applied to fresh-frozen, human cadaveric spine specimens. Specimens may include the entire thoracic spine (T1-T12),[26,27] partial thoracic spines (e.g. T1-T6),[28] or functional spine units (e.g. T4-T5).[11,29] As discussed, one advantage of pure moment testing is that, because the moment is equivalent at every cross section of the spine, the loading profile at each disc would be equivalent, regardless of whether a study tests full length thoracic spines (T1-T12), partial segments, or functional spine units. This allows for comparison of results obtained from these various specimen lengths across studies performed at different institutions.

Several testing machines and apparatuses have been developed to apply pure moments to the spine for kinematic testing. Historically, moments have been applied using systems including weights and pulleys,[30] pneumatic cylinders,[13] and linear bearings and cables.[31] However, in most of these systems the moments could only be increased incrementally, and thus a continuous moment-rotation response could not be measured. Meanwhile, other more recent systems have included the use of these previous technologies in conjunction with uniaxial load frames;[32] however, these systems required manual adjustments throughout testing and were susceptible to off-axis moments as a result of changes in the axes of the cables.

Wilke *et al*.[33] developed the first spine tester that was truly capable of applying and controlling continuous pure moments, while maintaining six-degrees of freedom. The 6-*dof*

system used a combination of stepper motors and pneumatic cylinders to apply forces and moments; however, only the superiorly potted vertebra could be controlled. More recently, fully-equipped machines have been designed and employed in spine testing which allow for simultaneous control multiple degrees of freedom. For example, robotic machines have been designed which attach to and control the superior aspect of the spine; however, only 6-*dof* can be controlled.[26]

Unlike these models, the present study employs a hydraulic-based spine simulator which allows for full control over 8-*dof*.[28,34] The hydraulic load frame is capable of applying pure, unconstrained moments. Unlike previous systems, the load frame used in the present study is equipped with gimbals on both the inferior and superior of the machine, allowing control of both the inferior and superior vertebrae of the spine. This allows for more dynamic loading scenarios, and more freedom of control. A similar system has been used at other centers.[35]

Dependent Variable Measurements from Pure Moment Testing

As discussed, for in-vitro biomechanical flexibility testing, moments and loads are typically applied to cadaveric specimens to produce flexion-extension, lateral bending, and axial rotation.[17,24] The specimens are typically first tested intact, that is, prior to disruption of their structural support (intervertebral discs, bony structures, ligaments, facet joints, costovertebral joints, and connective tissue).[24] This intact condition serves as the baseline flexibility for a given specimen. Then, the spine is tested following destabilization, a simulated injury, and/or device implantation. Following testing, the conditions of the spine are compared to evaluate, for example, the increase in motion following destabilization or the increase in stiffness following implantation.[28,34,36,37] From these pure moment experiments, nonlinear, hysteretic moment-

rotation curves are generated and used for analysis. Typically, the range of motion (ROM) is the primary parameter extracted from these curves to assess differences between conditions, representing the two rotational endpoints of moment-rotation curves.[24,38-40] Using mainly ROM values, conclusions are made, and clinical predictions of the effects of destabilization, injury, or implantation are postulated.

In addition to ROM, other parameters extracted may include the neutral zone, defined as the amount of rotation that occurs from the neutral position in each plane prior to significant increase in stiffness,[24,37] the elastic zone,[24] or stiffness.[24]

1.2.2 Assumptions

The following section outlines the primary assumptions associated with Pure Moment testing. As the present work will focus on scoliosis and preclinical testing of deformity correction, the assumptions will be discussed as they pertain to the thoracic spine.

In pure moment testing of cadaveric thoracic spines, several major assumptions are made in the experimental design:

1. *Loading magnitudes are non-destructive.*
2. *Loading levels produce physiological motions.*
3. *Primary stabilizers include ligaments, discs, and connective tissues.*
4. *Quasi-static loading and loading design minimizes viscoelastic effects.*

Loading Magnitudes are Non-Destructive

For the thoracic spine, pure moments are applied within the range of 2-7.6Nm.[27,31,35,41-43] In 1971, White and Hirsch applied 2 Nm moments to thoracic functional spine units to produce

flexion-extension, lateral bending and axial rotation.[10] Soon after, in 1972, Markolf *et al*.[11] applied approximately 6.8 Nm moments to produce the three modes of bending; however, the moment magnitudes were not justified. It was not until 1976 that Panjabi and White applied 9 Nm moments to thoracic spine FSUs with justification.[15,16] In their work, the authors stated that "[the] loads were limited to these values in order to prevent damage to the motion segments and permit subsequent testing." In other words, non-destructive loading was applied. Throughout the literature, authors use this same argument as justification for repeated testing on cadaveric specimens. The nondestructive loading is defined as loading that does not damage the specimens[15-17] and does not cause any permanent (plastic) deformation to the stabilizing ligaments of the spine.[44] This allows for, as discussed, repeated testing on the same cadaveric specimens so that various conditions can be compared, e.g. the intact condition compared with an implanted condition.

Loading Levels produced Physiological Motions

In addition to being nondestructive, the loading magnitudes were chosen on the basis that they also produced physiological motions. In 1989, Yamamoto *et al*.[45] applied 10 Nm moments to lumbar spines with the justification that the magnitudes were capable of producing physiological motion, as well as being nondestructive. These two assumptions were often linked, and even transitioned beyond the original intention to include alternate definitions. For example, the applied loads have been equated with physiological loads to produce the conclusion that because the applied loads were physiologic, damage to the specimens would not occur.[17]

It is often noted that the loads applied in-vitro may not accurately represent the magnitude of loads and moments experienced in-vivo; however, due to simplifications of in-vitro

modeling, the safe in-vitro loads have been accepted. Despite the limitations and simplifications, the safe, non-destructive, physiological motion-producing loads and moments provide sufficient motion and moment-rotation responses to compare implants and fixation devices across the literature.

Primary Stabilizers include Ligaments, Discs, and Connective Tissues

Thoracic spine specimens are dissected to remove all fat and muscle tissue, while keeping intact the bony structures (vertebral bodies, posterior elements), ligaments (anterior longitudinal ligament, posterior longitudinal ligament, interspinous and supraspinous ligaments, ligamentum flavum, capsular ligaments), intervertebral discs, and costovertebral joints.[24] It is assumed that the ligaments, intervertebral discs, and connective tissues provide the majority of the structural stability in cadaveric thoracic spines.

Quasi-static Loading and Loading Design Minimizes Viscoelastic Effects

The pure moment loading rates and methods of application are designed to be quasi-static. In other words, the moments are applied at rates in which the effects of inertia and mass can be ignored.

In addition, the connective tissues of the spine, that is, the intervertebral discs and ligaments, are viscoelastic materials. As such, the response of these structures to loading depends on the rate of load application and the time duration that a particular load is applied. To minimize these viscoelastic effects, as discussed earlier, the magnitudes of loads applied have been chosen to prevent and minimize plastic deformation to the stabilizing tissues. In addition, typically five cycles of loading are applied to the spine in every given direction. The third or sometimes fourth

cycle of loading is used for analysis. This serves to precondition the specimen, allowing the hysteresis of the spine to stabilize and become repeatable. Finally, studies have investigated the rates of load application which effectively minimize the time-dependent responses of the connective tissues. Specifically, rates of between 0.5 deg/s and 5 deg/s have been applied to minimize such time-dependence.[24] By the same token, under moment control, loads are typically applied at a rate of 0.1 Nm/s.[46]

1.2.3 Applications

In the early days of spine biomechanics testing, these assumptions were made and accepted on the basis of determining the general motion behavior of the thoracic spine in cadaveric experiments, and to compare the stability of the thoracic spine following rigid fusion provided by fusion instrumentation. At the time, the assumptions were largely valid. A primary reason for these assumptions was to isolate the effects of different instrumentation systems. As many of the fusion systems, by design, intended to eliminate motion at a given motion segment in the spine, the motions at a given level following instrumentation were small. Moreover, the differences in motions at a given level between two different instrumentation systems were small as well. As such, by standardizing the testing methods and creating a set of standard assumptions, the small changes between fusion systems could be detected.

Applications of the pure moment model in the thoracic spine are widespread, including testing of, for example, pedicle screw systems,[47,48] anterior instrumentation systems,[49] sublaminar cables and wires,[46] nitinol stapling,[50] transverse connectors,[35] and hybrid systems.[51] As originally intended, the Pure Moment model was beneficial in characterizing the general

range of motion of thoracic spines, as well as evaluating and comparing these fusion devices and instrumentation systems.

For example, Deviren *et al*.[47] evaluated the stability of pedicle screw/rod systems for fixation of the thoracic spine in a human cadaver model (T4-T12). Pure moments of ±4Nm were applied to produce rotation in each anatomical plane in three conditions: intact, following bilateral facetectomies, and again after various combinations of screw placement and numbers of screws. Each screw configuration significantly stabilized the spine compared with the destabilized condition; however, only the least-stabilized configuration, i.e. bilateral screws at the inferior-most and superior-most vertebrae, was significantly less stable than the other configurations. The results suggested similarities in stiffness, at least immediately post-operatively, in the other combinations, including all-pedicle screw configurations and alternating-level configurations. These results could then be immediately used for surgical decision making. For example, a scoliosis surgeon may choose a configuration with less anchor points to limit operative time, blood loss, and cost; however, other factors must obviously be weighed as well, as less anchor points may result in weaker correction maneuvers, and in turn, less obtainable deformity correction. Additionally, the results can only predict performance for the immediate post-operative condition.

As pure moments allow for standardized comparisons across the literature, the results reported by Deviren *et al*.[47] can be used to put the results of other studies into context. For example, Jones *et al*.[51] applied pure flexion-extension and lateral bending moments to 3-level human cadaver thoracic spines, before and after instrumentation with either pedicle screw-based or hybrid-based constructs (i.e. combinations of screws and hooks). No significant differences were reported in either flexion-extension or lateral bending stiffness between the two groups.

The stiffness of the screw constructs in flexion-extension and lateral bending (4.1±7.5 Nm/deg and 4.4±7.4 Nm/deg, respectively) compared to the results reported by Deviren *et al*.,[47] in which all-pedicle screw constructs had stiffness magnitudes of 2.6±6.7 Nm/deg and 1.7±4.4 Nm/deg in flexion-extension and lateral bending, respectively. While the averages are somewhat different, the standard deviations overlap. Jones *et al.*,[51] however, applied moments of between 1.5-2Nm, whereas Deviren *et al*.[47] applied moments of 4 Nm. With a repeatable and consistent loading model, the results of these two studies could be easily compared. Specifically, in addition to all-pedicle screw constructs which both groups analyzed, the various pedicle-screw construct configurations, tested by Deviren *et al*,[47] could be compared to the hybrid configuration tested by Jones *et al*.[51] As the results of these studies suggested the adequacy of pedicle screw and hybrid constructs to stabilize the thoracic spine, other measures must be used for decision making between the two constructs, such as pull-out strength, lateral push-out strength, implant cost, clinical outcome, etc.

In addition to comparisons of similarly tested constructs, due to the reproducibility of *Pure Moment* testing and the comparative nature of the results, the results of small changes in simpler experiments, such as the use of cross-connectors, could be applied to the more complex arrangements tested by Deviren *et al*.[47] For example, in simpler models, the addition of cross-connectors significantly increased the stiffness of thoracic spine constructs in axial rotation.[35,52] Specifically, the addition of 1- and 2- connectors provided increases in axial rotation stiffness of 20% and 35%, respectively.[35] This information can then be reapplied to existing results. In the study by Deviren *et al*.,[47] following fixing thoracic spines with all-pedicle screw-rod constructs, less than 3° of flexion-extension and lateral bending motion remained; however, axial rotation ROM was still nearly 9°. It could be expected that, with the addition of 2 cross-links, for

example, the axial stiffness could be reduced by approximately 35%, and the axial rotation ROM decreased. A risk-benefit analysis could then be conducted to determine whether or not the morbidity and cost of adding cross-links to the all-pedicle screw construct would be worth the additional stiffness.

In these thoracic spine studies,[35,47,51,52] and similar to many studies investigating the effects of rigid fusion in the cervical and lumbar spines,[53-57] the pure moment model served its purpose. The model enabled the comparison of various fusion instrumentation systems across different instrumentation designs, different specimen types and conditions, and different research centers with various experimental setups and loading capabilities. Due to the initial successes of these models, as well as the ease of utilizing validated standards of testing, the pure moment model became the global standard in all of spine biomechanics. The use of the model became widespread, and studies assessed a variety of clinical applications, including fusion surgery,[35,47,51-57] intraoperative surgical resection,[27,29,58] and motion-sparing devices devices.[37,59,60]

Unfortunately, in many of these cases, the *Pure Moment* model design and assumptions may not be applicable. Consequently, for many spine fields, spine biomechanics has largely failed to have a clinical impact, placing a reliance on often flawed and limited patient studies. Improvements and expansion of the typical testing methods may provide more clinically relevant and impactful results, and in turn, may ultimately benefit patient care.

To demonstrate the necessity and benefits of improving upon the currently used testing methods, the present study focuses on the field of scoliosis biomechanics.

1.3 Applying Pure Moments for Scoliosis Biomechanics

1.3.1 Definition of Scoliosis

Scoliosis is often defined very simply: a sideways curvature of the spine.[61] This definition arises from the physical appearance of a scoliosis patient, and from the 2D projection of a deformed spine on an anterior-posterior (AP) radiograph. From these perspectives, scoliosis deformities appear as lateral curvatures in the frontal plane, with C- or S-shaped curvatures.[61,62]

However, in actuality, scoliotic spines have complex, three-dimensional curvatures, with abnormal motion segment rotations in the coronal, sagittal, and axial planes.[6,63] Specifically, idiopathic scoliosis is often coupled with some hypokyphosis (lordosis) at the apex of the scoliosis curvature, as well as rotational deformity (i.e. transverse plane deformity) away from the concave apex of the scoliosis.[64] Moreover, the vertebral bodies themselves are often physically deformed, e.g. wedged vertebrae,[64] resulting in random geometrical properties.

Objectively, the presence of scoliosis is determined by two factors: (1) asymmetry of the spine during forward bending, and (2) a Cobb angle (measure of scoliosis deformity in the coronal plane) of $\geq 10°$.[65] With increasing severity of the abnormal curvature, scoliosis may have negative effects on pulmonary function (vital capacity), self-image due to the cosmetic aspects of the deformity (i.e. rib hump), ability to perform various activities, and cardio-respiratory function, to name a few. Consequently, for many scoliosis patients, surgery is recommended over conservative treatment, such as bracing. Specifically, surgery is typically recommended for AIS patients with Cobb angles in excess of 45°,[66] and in adult patients with Cobb angles greater than 50°-60°.[67]

1.3.2 Clinical and Societal Impact of Scoliosis

According to the HCUP Nationwide Inpatient Sample, over the 10 year period from 2001 to 2011, more than 168,000 patients were discharged in the US with a primary diagnosis of spine deformity or related conditions.[68] In 2011 alone, over 20,000 US patients were diagnosed with these same conditions, resulting in a national bill of over $3.6 billion.[68] These conditions included a variety of abnormalities, including scoliosis, kyphosis, and lordosis deformities.

Adolescent idiopathic scoliosis (AIS) is both the predominant spine deformity and the predominant form of scoliosis, affecting approximately 80% to 85% of all scoliosis patients. The reported prevalence of AIS is typically reported to range from 1%-3%,[69] with reported incidence in excess of 5% of children.[70] In 2010 and 2011 alone, US hospitals discharged more than 12,000 adolescent patients with idiopathic scoliosis, costing the nation more than $1.8 billion.[68] Moreover, according to a study by Kamerlink *et al*.,[71] a single AIS surgery costs, on average, $31,414.

As AIS affects some of the youngest orthopaedic patients who require permanency in their treatments, the instrumented-fusion should provide stabilization for many decades of life. In addition, institutional requirements to reduce costs associated with and maximize the efficiency of spine surgery continue to expand.[72] Therefore, given the enormous societal and economic costs of spine deformity, it is essential that the treatments of these conditions are optimized.

1.3.3 Overview of Posterior-Only Approaches and Implants

Since the 1960s, when scoliosis surgery became popularized, surgery consisted of placing anchors into the vertebral bodies of the spine, and connecting the anchors by way of a solid rod.[5]

Over the years, the anchors have transitioned from laminar hooks to pedicle screws, and the rods have transitioned from one-rod systems to two-rod systems; however the goals of instrumentation have remained constant. These goals include correction of the deformity, solid and successful fixation and fusion, and maintenance of the correction. To understand the concepts and motivations of current implants and surgical techniques, an appreciation of the historical innovations is necessary.

In the early 1960s, Dr. Paul Randal Harrington revolutionized scoliosis and spine deformity correction with his internal fixation system, known as Harrington instrumentation.[5] Harrington's original design included a single rod connected to two hook anchors at the proximal and distal ends, and utilized internal axial traction for straightening the deformity. Axial traction had been used for centuries before Harrington, dating back as far as Hippocrates (1460-1375 BC) and Galen (130-200 AD).[73] Moreover, and as discussed earlier, axial traction had been suggested as one of the primary correction maneuvers necessary to reduce scoliosis deformities in the 1700s.[4] Harrington's system provided internal traction, applying tension through a ratcheted mechanism along the concavity of the curvature. This system was capable of applying larger forces than external traction, and had the advantage of applying internal forces directly to the spine.

However, the Harrington instrumentation suffered a major drawback: it failed to correct the spine in three-dimensions. As discussed earlier, scoliosis is often simply defined as an abnormal lateral curvature, or a coronal plane deformity; however, in actuality, the deformity occurs in three-dimensions. Therefore, while compression-distraction using the ratcheting Harrington system provided apparent coronal plane correction, with coronal correction of 32%-

69%,[74-79] the other components of the deformity, that is, the abnormal sagittal and axial components, were ignored. Consequently, many patients suffered from postoperative flat back syndrome,[74,76,77] with reported rates as high as 52%,[78] as the natural curvatures in the sagittal and axial planes were not restored. Patients also suffered from progression of their scoliosis deformities due to the fact that the anterior column, i.e. the anterior vertebral bodies and anterior disc spaces, continued to grow through natural growth processes, while the posterior column, i.e. the posterior element complex, was rigidly fixed through the Harrington system. This process and common complication has become known as crankshaft phenomenon.[80,81] Other complications associated with the Harrington system included loss of correction,[74,76,82] low back pain,[74,75,78] pseudarthrosis,[76,77] and implant failure.[74,76,77]

Due to the inabilities of the Harrington instrumentation to correct deformities in three-dimensions, in 1976, Dr. Eduardo R. Luque created a segmental system of instrumentation.[19] This system utilized a rod anchored by proximal and distal connections, similar to Harrington's system;[19] however, the rod was connected to the spine through sublaminar wiring. Specifically, in addition to the proximal and distal anchors, the Luque system provided segmental sublaminar wire-rod connections at each vertebral segment within the fusion. Then, during surgery, at each segment, the sublaminar wires were tightened to the rod at each segment, in turn applying a translational corrective force to the spine. With these two developments over Harrington instrumentation, that is, segmental fixation and translational corrective forces, Luque instrumentation provided stronger resistance to implant failure,[83] better maintenance of natural thoracic kyphosis and lumbar lordosis,[84] less loss of correction,[76] and more control over the rotational aspects of the curvature. However, the sagittal and axial post-operative curvatures

were still not ideal. Additionally, as the sublaminar wires pass through the spinal canal, there was a high risk of neurological complications and/or damage to the spinal cord.[85,86]

Despite advancing from Harrington's system to Luque instrumentation, the unnatural postoperative curvatures and high incidence of debilitating surgical and postoperative complications necessitated further implant development. In 1984, Drs. Yves Cotrel and Jean Dubousset developed Cotrel-Dubousset (CD) instrumentation which provided a monumental advancement in scoliosis surgery, and provided the backbone for the instrumentation systems used for deformity correction today.[18] Their system used multiple rods, segmental fixation by way of multiple transverse process, pedicle, and laminar hooks, and later, through pedicle screws. In this system, the first rod was attached on the concave side of the curvature. This rod was then derotated, increasing the thoracic kyphosis and translating the curved spine into the midline of the body. Then, the second rod, placed on the convex side, applied sequential compression and distraction at desired levels. Transverse connectors were used to link the rods. This system was the first to utilize derotation correction maneuvers, the second principle of deformity correction proposed by Venel in the 1970s.[4] Derotation remains one of the primary correction maneuvers utilized in surgery today.

The CD instrumentation system offered improved curve correction over previous designs,[74,87,88] as well as better control and maintenance of the sagittal curvatures.[88,89] This system was the first to recognize the advantageous capabilities of pedicle screws to provide three-column fixation of the spine. However, this instrumentation brought on a new wave of surgical complications – a major one being proximal junctional kyphosis.[90-92] Additionally, the true ability to provide transverse plane rotational correction has been questioned.[6] Variations of

this system were used over the years,[93] including the hybrid system of thoracic hooks and lumbar pedicle screws, a system still currently used in practice today.

While posterior-only fusion for scoliosis correction was being developed, various surgeons were exploring the possibilities of anterior approaches to scoliosis surgery. The motivating force behind anterior surgery was the hypothesis of greater correction over shorter fused segments of the spine, obviating the need for long posterior fusions.[94] The first system, proposed by Dwyer in 1964,[21] utilized a combined anterior-posterior approach, with posterior surgical release and anterior fixation. Screw fixation was achieved through the lateral side of the vertebrae on the convex side of the curvature, and a cable was threaded through the screw heads. However, this system was associated with curve progression and pseudarthrosis, amongst other complications.[95,96] Modifications to the Dwyer system included Zielke and Halm-Zielke instrumentation, which included threaded rods, fluted rods, and derotators; however, high rates of complication were reported, including implant breakage, loss of correction, and pseudarthrosis.[97-99] More recently, Kaneda *et al*.[100] developed a segmental system which consists of a vertebral plate and two vertebral screws per vertebra, with dual rods connecting the vertebra; however, despite the developments of these systems and many others, posterior-instrumentation remains the standard.

1.3.4 Current Surgical Techniques

Recently, the use of all-pedicle screw based posterior instrumentation has become more popular in favor of hook and hybrid constructs due to the three-column fixation of pedicle screws. The three-column fixation, that is the fixation from the posterior elements to the anterior vertebral body, allows sophisticated three-dimensional correction maneuvers,[11,101,102] greater

axial pullout strength and tangential force resistance than previously used pedicle and laminar hooks,[103,104] and significantly improved curve correction over hook and hybrid constructs.[93,102,105,106] With these improvements, surgeons can apply correction maneuvers intraoperatively to reduce and correct spine deformities.

Intraoperatively, in addition to the all-pedicle screw instrumentation, surgeons typically use a combination of posterior releases and posterior correction maneuvers to achieve deformity correction.[6,93,102,107-112] As scoliosis and spine deformities are often extremely rigid, surgeons must increase in the flexibility in the spines for correction. Specifically, prior to applying the correction maneuvers in surgery, such as traction,[73] derotation,[113,114] cantilever bending,[115] or more recently direct vertebral rotation (DVR),[6,7] posterior releases are performed,[108,110] removing specific structures and ligaments from the spine to increase the flexibility of the rigid spine curvature. For example, facetectomies may be performed by removing the facet joints bilaterally at multiple levels of the spine,[110] or Ponte osteotomies may be performed by resecting not only the facet joints, but the interspinous and supraspinous ligaments, the ligamentum flavum, and portions of the spinous processes as well.[108,112] With these releases, the flexibility of the rigid curvatures may increase.

Following release, correction maneuvers are applied. More specifically, loads and moments are manually applied to the spine by the surgeon, as the curvature is manipulated to reduce the deformity and connect the pedicle screws with the bilateral rods. Recently, one such correction maneuver employed by surgeons is direct vertebral rotation (DVR).[6,7] With DVR, a device with large lever arms is attached to the pedicle screws at multiple levels of the spine through which surgeons can apply torsional loads to the spine. These loads result in axial rotation of the spine, which both corrects the axial component of the scoliosis curvature and rotates the

apparent coronal plane deformity into a more normal, physiological sagittal curvature. Compared to traditional methods of applying compression-traction,[73] lateral forces,[19] or rod derotation,[113,114] DVR allows surgeons to apply segmental axial rotation to the spine in surgery, thereby maximizing the correction.[6]

While the current standard includes the use of posterior pedicle screw/rod instrumentation systems with concurrent posterior-releases and correction maneuvers, many controversies still exist in the clinical literature with each aspect of surgery. For example, there is substantial controversy in the literature debating whether all-pedicle screw constructs truly provide greater deformity correction than hybrid systems using screws, hooks, and wires.[93,105,106,116-126] Similarly, despite good clinical outcomes using various wide posterior releases, the results fail to comprehensively support using such releases to supplement routinely used total facetectomies.[111,112,127] Another example controversy surrounds posterior correction maneuvers. Specifically, despite the ability to apply large correctional forces to the spine using newer correction maneuvers, such as DVR,[7] the safety of such procedures has not been established, and has therefore been questioned due to intraoperative and postoperative pedicle fractures.[128]

With the combination of posterior-instrument strength, invasive surgical resections, and high magnitude correctional loads, surgeons are continually pushing the limits of deformity correction surgery to achieve the goals of maximum correction and prolonged maintenance of normalcy. To help resolve the controversies surrounding these techniques, as well as many other questions in the literature surrounding the treatment of not just spine deformity, but degeneration, trauma, and other conditions requiring spine fusion, preclinical models must be developed, improved, and applied.

1.3.5 Assumptions and Testing Considerations for the Thoracic Spine

With the introduction of pedicle screws and three-column fixation in the 1980s coinciding with the boom in fusion instrumentation systems, naturally, the *Pure Moment* testing model was being applied to evaluate and compare scoliosis fusion instrumentation. In addition to the general *Pure Moment* testing model and experimental design assumptions discussed earlier, including assumptions regarding moment magnitudes, nondestructive loading, and minimizing viscoelastic effects, several additional assumptions are needed for the thoracic spine and scoliosis.

Structural Assumptions for the Thoracic Spine

When using a cadaveric model for evaluating thoracic spine conditions and treatments, several structural issues must be considered. Specifically, in-vivo spine stability and stiffness is primarily provided by three factors: (1) soft tissue, that is, the discs, ligaments, connective tissues, and muscles; (2) the ribcage, sternum and thoracic cavity; and (3) intra-thoracic and intra-abdominal pressure. However, several assumptions and simplifications are typically necessary for cadaveric thoracic spine models with regards to these three stabilizing factors listed above.

(1) Stabilizing tissues, including the intervertebral discs, ligaments, costovertebral joints, connective tissues, and muscle forces (i.e. paraspinal and trunk muscles);

As discussed earlier, thoracic spine specimens are typically dissected to include the bony structures (vertebral bodies, posterior elements), ligaments (anterior longitudinal ligament, posterior longitudinal ligament, interspinous and supraspinous ligaments, ligamentum flavum,

capsular ligaments), intervertebral discs, and costovertebral joints.[24] The muscles, however, are resected away prior to experimentation. In cadaveric specimens, the muscles are inactive, and consequently, provide minimal structural support. As a result, the muscles are not included in the model. Moreover, during surgery, the muscles are largely inactive as the patient is anesthetized and lies prone on the surgical table.[25] Consequently, in many scoliosis biomechanics studies, muscle forces need not be simulated.

(2) The ribcage, sternum, and thoracic cavity;

In addition, the ribcage and sternum are often removed, while keeping intact the costovertebral joints and posterior 5-cm of the ribs.[13,29] In these studies, it is assumed that the stability provided by the ligaments, intervertebral discs, and connective tissues is sufficient to evaluate the kinematics and flexibility of the cadaver thoracic spines. Despite these typical assumptions, some previous studies have demonstrated that the ribcage significantly contributes to the motion of the thoracic spine.[27,129-132]

Watkins *et al*.[27] demonstrated that the sternum and ribcage provided 31.4% of the thoracic spine stiffness in axial rotation, 39.8% in flexion-extension, and 35.4% in lateral bending. Feiertag *et al*.[129] showed no significant increase in either flexion-extension or lateral bending with a single rib head release in thoracic torsos, with change in motion of $< 2°$; however, had the entire ribcage been removed, and assuming a somewhat equal contribution of each rib head release, significant increases in motion may have been produced. Oda *et al*.[29] loaded thoracic FSUs under pure moments, demonstrating significant increases in flexion-extension following right costotransverse joint resection, and in lateral bending and axial rotation following both right and left costotransverse joint resection; however, these resections were performed

after laminectomy and bilateral total facetectomies. Brasiliense *et al*.[131] demonstrated the largest stabilizing effects of the ribcage. Specifically, the ribcage provided 78% of the thoracic spine stability; however, the pure moment was applied equally through the spine, ribcage and sternum, whereas the rest of the literature applied pure moments directly to the spinal column, as specified in the standard. The results of these studies are consistent with an early computer model, which emphasized the importance of the ribcage in providing stability during bending.[132]

Despite the evident stiffness produced by the ribcage and sternum, the majority of thoracic spine in-vitro testing is performed with these structures removed prior to testing.[13,35,43,46,47,133-136] As a result, the motions reported in these preclinical models may only represent estimates of in-vivo motion.

(3) Intra-thoracic and intra-abdominal pressure;

In-vivo, the associated pressures of the thoracic and abdominal cavities provide stability to the thoracic spine;[137] however, these pressures have not been simulated in in-vitro experiments using cadaveric models. Therefore, once again, the resulting motions may only represent estimates of true in-vivo motions.

Deformity Assumptions for Scoliosis Biomechanics Studies

In thoracic scoliosis biomechanics studies, another major assumption is that the increase in motion of a thoracic spine during loading following a surgical release, that is an 'obtainable deformity', is equivalent or symmetric to the potential deformity correction in a scoliosis patient. This model was introduced by Ashman *et al.*[138] more than twenty years ago, and as the investigators admit, "differences between imposing a deformity with an implant and correcting a

deformity with an implant may also be significant."[138] To date, no quantitative data exists to support or disprove this assumption; however, this theory is assumed throughout the spine biomechanics literature.[58,129]

Cadaveric Assumptions for Scoliosis Biomechanics Studies

While spines with normal straight curvatures may not be ideal, scoliotic spines are simply unavailable for research at this time, much less scoliotic spines from the pediatric population. Some studies have stated the need for a model representing scoliosis deformity to test instrumentation; however because of the complex three dimensional properties of the deformity, it is hard to determine the physical loads placed on the instrumentation systems.[49,139] Moreover, even if scoliotic spines were obtainable for preclinical testing, the specimens would not have identical curvatures. Instead, there would be a wide range of curve magnitudes, curve types, curve direction (i.e. contribution of the deformity in the coronal, sagittal, and axial planes), vertebral geometries (e.g. wedging), and disc spaces. While straight spines may be limited in that they are from donors without gross deformity, a major advantage of using straights spines is that many of these uncontrollable variables can be minimized.

Currently, very little data exists comparing the mechanical properties of normal and scoliotic spines. Andriacchi *et al*.[132] created a mathematical computer model to compare the responses of normal and scoliotic spines, with and without rib cages, to a lateral bending moment. Moments were applied to T1 to produce lateral bending of a full spine model. Both normal and scoliotic spines had a similar response to lateral bending moments, which were similar to the cantilever bending moments created during deformity correction surgery in the 1970s.[19] The results, while somewhat primitive, suggest a similarity between the responses of

normal and scoliotic spines. To date, studies have justified using 'straight spines' as opposed to 'deformed spines' by citing these results.[129]

Despite the evident limitations, e.g. availability of deformed cadaveric specimens or deformed composite spines,[49,139] in-vitro studies of spine deformity using cadaveric models are still routinely performed and accepted in the literature.[139] Studies accept these limitations as inherent, and perform the experiments on straight, un-deformed, often elderly cadaveric specimens.[129,140]

Another major limitation cited throughout the biomechanical literature is the lack of availability of spines from pediatric donors.[24] Cadaveric spines available for laboratory research are typically limited to elderly specimens, with some degree of bone and disc degeneration.[49,141,142] However, despite potential differences due to these natural aging processes and anatomical differences between pediatrics and adults, the complex nonlinear tissues are largely simulated. Both pediatric and adult spines alike are comprised of viscoelastic soft tissues which produce nonlinear responses under loading. Replication of these viscoelastic properties is essential, particularly in the preclinical testing of scoliosis and deformity surgery.

Additionally, due to the varying degrees of disc degeneration, bone quality, and general health of cadaveric specimens, there is also a wide range of flexibility amongst these same cadaveric specimens. However, these large deviations in flexibility are not a property unique to adult cadaveric spines. Instead, it is an inherent characteristic of all human spines, young or old, healthy or deformed. For example, in one cohort of 76 AIS patients, standing Cobb angles ranged from 41.3-95° and bending Cobb angles ranged from 9.1-60.8°.[139] Similarly, in a separate

cohort of 66 AIS patients, standing Cobb angles ranged from 48-78° and bending Cobb angles ranged from 22-47°.[105]

Therefore, human cadaveric spines are the most representative and appropriate model for the preclinical testing of scoliosis, regardless of the age of the donor. Having said this, there are ways in which the limitations could be minimized. As discussed, one major limiting factor in cadaveric specimens from adult donors is the varying degrees of disc degeneration, resulting in a wide range of biomechanical properties. This limitation could potentially be minimized by evaluating the health of each specimen, and subsequently stratifying the biomechanical results according to disc health. For example, histology of the intervertebral discs could be obtained following testing, as it is a reliable and sensitive method of investigating disc pathology,[143-145] with improved detection over imaging techniques.[144,145] Using established degeneration scoring systems,[146-148] the disc health could be related to the resulting biomechanical responses. Such an analysis may help to justify using elderly spines to make conclusions for the pediatric population; however, previous biomechanical studies of spine deformity correction have largely ignored this variable. This will be discussed in more detail later in this work (Section 1.4).

In summary, in-vitro biomechanical tests using cadaveric specimens assume that the specimens represent a valid model for in-vivo comparison and application. In-vitro measured motions and spine response are accepted as reasonable for making in-vivo predictions, while it is understood that the motions and responses may only be estimates of true in-vivo measurements. In-vivo spine motion and stiffness may be affected by muscle forces, anatomical structures (i.e. sternum and ribcage), thoracic cavity pressures, or by anatomical (i.e. growth plates) and health

(i.e. deformity) factors associated with aging. However, despite the limitations, fresh-frozen human cadaveric specimens remain the best model for testing.

1.3.6 Benefits and Applicability of Pure Moments for Scoliosis

As discussed extensively, the *Pure Moment* model and experimental design became the routine and standard biomechanical testing method for nearly all fields of spine biomechanics, including scoliosis. As scoliosis, and particularly adolescent idiopathic scoliosis, primarily affects the thoracic spine, the biomechanics of the thoracic spine pre- and post- instrumentation must be established. The *Pure Moment* model offered a useful tool to characterize the normal motion of the thoracic spine, which is necessary as a baseline for comparing the effects of posterior-releases or posterior instrumentation. In addition, and as it was originally intended, the *Pure Moment* model offered a platform to compare various types of posterior fusion devices in the thoracic spine.

1.3.6.1 Typical Range of Motion of Thoracic Spines

Over the past three decades, major advances have been made in various aspects of spine surgery.[6,18,102,149,150] In light of these advances, thorough knowledge of the kinematics of the human spine, and in particular, its range of motion (ROM), plays an important role in many phases of diagnosis, treatment, and follow-up of most spine disorders.

The ROM of each spine segment, or functional spine unit (FSU), is arguably the most basic and fundamentally important parameter in establishing its function. Unlike many joints such as the knee or elbow, motion of spine segments, particularly thoracic spine segments, are difficult to measure ¬in-vivo without invasive procedures. Moreover, noninvasive in-vivo

measurements,[151-157] such as skin marker-based measurements, are affected by many uncontrollable variables. Consequently, most studies that have evaluated thoracic spine ROM have used in-vitro cadaveric models,[9,10,47,135,158] the majority of which have used *Pure Moments*.

Functional Spine Units (w/out Ribcage/Sternum)

Nearly four decades ago, Drs. White and Panjabi published typical ROM for each level of the human spine.[23] For the thoracic spine, the values were largely based on both the experience of the authors and the thesis work of Dr. White,[9] who applied off-axis compression and torsional loading to produce bending and axial rotation in cadaveric spines, respectively. Specifically, reported motions ranged from 2-20° in flexion-extension, 6-26° in lateral bending, and 4-28° in axial rotation, depending on the level.[23] However, this publication preceded the widespread usage of biomechanical testing standards, and more specifically, *Pure Moments*. Notwithstanding, both clinical[154,155] and in-vitro[29,41,42,50,130,159,160] studies frequently reference the ROM ranges reported in White and Panjabi's spine biomechanics textbook,[23] cited more than 3700 times according to Google Scholar, for comparison or evaluation of their own respective results. On the other hand, since this work was published, numerous more recent studies have reported the ROM of cadaveric thoracic spines, the majority of which have generally applied established testing standards.[17,24] No study to date has summarized the thoracic ROM reported in this literature. Without such a summary, the large variability amongst the literature makes the reported motions difficult to interpret.

Hemi-segments (w/out ribcage and sternum)

Similar to the individual FSU results, large variability exists amongst the literature studying the motions in hemi-thoracic segments.

Specifically, several studies have applied pure moments to multi-level thoracic spines, e.g. testing T3-T11[35] or T4-T12.[47] Under ±4 Nm pure moments, Deviren *et al*.[47] measured T5-T11 motions of approximately 17±2° in flexion-extension, 30±2° in lateral bending, and 39.5±2° in axial rotation. Kuklo *et al*.[35] found similar results by applying pure moments of ±6 Nm to T4-T10 segments, producing intact motions of 14.01±4.90° in flexion-extension, 20.01±7.04° in lateral bending, and 34.75±9.38° in axial rotation.

Kothe *et al*.[134] characterized motions of shorter segments, i.e. 4-level mid-thoracic segments and 4-level lower-thoracic segments, and reported smaller motions. Specifically, mid-thoracic segments, on average, rotated 6.2±1.4° in flexion-extension, 10.6±3.2° in lateral bending, and 12.1±2.4° in axial rotation. Lower-thoracic segments had smaller ranges of motion, with average ROM of 5.7±2.1° in flexion-extension, 6.7±1.2° in lateral bending, and 4.8±1.4° in axial rotation. Balabaud *et al*.[43] reported similar motions in flexion-extension and axial rotation; however, only 2-level thoracic spines were tested.

Full thoracic spines (w/out ribcage)

Under pure moments of ±2 Nm in flexion-extension and lateral bending, and ±5 Nm in axial rotation, Watkins *et al*.[27] reported full thoracic range of motion of 13.17° (3.11-29.29°) in flexion-extension, 16.04° (3.71-27.96°) in lateral bending, and 33.60° (11.95-67.55°) in axial rotation. If the motions are estimated for each of the tested levels T1-T12, assuming an equal contribution of motion at each level, segmental motion would be approximately 1.2° in flexion-extension, 1.5° in lateral bending, and 3.1° in axial rotation. Each of these values are substantially lower than any of the reported motions by White and Panjabi.[23]

Full thoracic spines (w/ ribcage and sternum)

Few studies have characterized the motion of the entire thoracic spine, with the ribcage and sternum intact, under pure moments. Watkins *et al*.[27] reported T1-T12 motion of 7.93° (2.64-15.64°) in flexion-extension, 10.36° (3.71-27.96°) in lateral bending, and 23.03° (6.17-51.44°) in axial rotation. Recently, Healy *et al*.[26] reported larger motions in the thoracic spine, with full T1-T12 motions of 26.9±10° in flexion-extension, 42.06±19.04° in lateral bending, and 43.69±16.87° in axial rotation. Feiertag *et al*.[129] and Horton *et al*.[25] both characterized motion of the entire thoracic torso; however, cantilever loading was applied. Brasiliense *et al*.[131] also tested full length thoracic torsos; however, the pure moment was applied to the entire torso, rather than the spinal column, and raw motion data was not reported.

As shown, the *Pure Moment* testing model and experimental design have been widely applied throughout the literature to characterize the intact motion of cadaveric thoracic spines. The model has produced results to provide a general idea of the typical motions in cadaveric specimens. However, despite the standardized model, large variations exist amongst the studies. Additionally, it is difficult to interpret the true effectiveness of the model in describing typical motions, as no study to date has summarized the reported motions from *Pure Moment* studies throughout the literature.

1.3.6.2 Comparison of Scoliosis Fusion Implants

As discussed, due to the reproducibility and cross-sectional equivalence of *Pure Moments*, the model provides an adequate platform to compare instrumentation systems for spine fixation (Section 1.2). Under *Pure Moments*, the ability of various fusion-constructs to provide stability to the thoracic spine has been demonstrated, including sublaminar cables and wires,[46]

anterior instrumentation,[49] hybrid systems,[51] and all-pedicle screw systems,[47,48] to name a few. Moreover, other variables have been evaluated, including screw placement,[47] screw density,[47] and presence of transverse cross-connectors.[35,52]

As originally intended, the *Pure Moment* model was beneficial in evaluating and comparing fusion devices and instrumentation systems used in cases of scoliosis and spine deformity. Consequently, over time, the *Pure Moment* model has been applied to areas beyond the comparison of fusion instrumentation, including surgical resection and intraoperative correction. However, in such cases, the *Pure Moment* model may not applicable, as the general assumptions are largely inapplicable. As such, scoliosis biomechanics has lacked major clinical impact, and preclinical cadaveric studies are rarely performed.

1.4 Limitations of Pure Moments and Alternative Methods

As discussed, despite the initial design and assumptions of the *Pure Moment* model being intended for characterizing the general characteristics of spine kinematics and for comparing fusion instrumentation, the model has been nearly universally applied for all preclinical spine biomechanics. For example, the *Pure Moment* testing model and experimental design has been routinely applied to questions regarding the intraoperative treatment of scoliosis and spine deformity. However, due to the limitations of the model in this regard, the results have been inconclusive and inconsequential.

1.4.1 Limitations of Pure Moment Testing Results in Scoliosis

Posterior-Release Potential

Despite posterior-based surgical procedures being performed for deformity correction for more than 50 years,[5] the surgical techniques are continually debated; however, the general procedure includes three primary phases: (1) resection of anatomical structures to increase the flexibility in the curve, (2) force application to correct the deformity, and (3) fixation using instrumentation. The first step, that is, resection of anatomical structures, is necessary as the physiological bending limits of scoliotic spines prevent natural alignment. For example, Hasler *et al*.[139] reported standing Cobb angles in AIS patients ranging from 41.3-95°, which under physiological loads bent to Cobb angles ranging from 9.1-60.8°. Similarly, Dobbs *et al*.[105] operated on AIS patients with Cobb angles of 48-78°, which bent to Cobb angles of 22-47°. In these types of patients, particularly those with curves which after bending still retained large

deformity, surgical releases are necessary to add flexibility to the deformity. However, the effectiveness of specific releases has not been adequately quantified.

One common posterior-only procedure used in scoliosis deformity surgery is a total facetectomy, which involves the bilateral removal of the inferior facets of each of the vertebrae along the length of the deformity.[110,161] More recently, surgeons have suggested the use of Ponte osteotomies and wide posterior releases to supplement facetectomies in cases of rigid AIS.[107,112] These wide posterior releases are more invasive than the routinely performed total facetectomies as they involve not only resection of the inferior facets, but the additional resection of the inferior half of the spinous process of the vertebra superior to the osteotomy site, the interspinous ligament, and the ligamentum flavum.[108] As a supplemental procedure to provide additional flexibility for correction, a number of these releases may be performed. However, it remains unclear exactly how much additional correction is attainable. Moreover, it is unclear whether the additional correction warrants the more invasive procedure which requires longer operative times and results in increased blood loss intraoperatively.[111,127] Consequently, the techniques are continually debated throughout the literature,[111,112,127,162,163] representing one example of the type of scoliosis controversies which often remain largely unresolved.

The importance of understanding the effects of and quantifying the effects of each surgical release cannot be understated. This data is necessary for the preoperative planning of each individual patient so that they receive optimal treatment. This information would not only assist surgeons and clinicians in understanding current surgical release procedures, but it would also shed light on new surgical options. As stated by White and Hirsch,[10] "[the] surgeon who treats scoliosis would be interested in whether or not the release of these structures would allow

for a greater degree of correction of the scoliotic spine." The ideal way to obtain such information is through preclinical models and preclinical testing.

The pioneers in this realm of scoliosis literature were White and Hirsch[10] who tested thoracic functional spine units (FSUs) in flexion-extension, lateral bending, and axial rotation, both before and after the release of anatomical structures. Using compressed-air to apply loading to thoracic FSUs, spines were tested intact, and following the removal of the posterior elements, which in this study, included the facet joints, the intertransverse ligaments, the ligamentum flavum, the inferior one-half of the laminae, and the spinous process. As determined by extensometers and displacement gauges, motions in the sagittal and transverse planes were significantly larger in magnitude following the resection of the posterior elements. Specifically, on average, flexion-extension motion increased by as much as 5°, while axial rotation motion increased by as much as 9°; in lateral bending, increases were smaller. Based on the results, it was thought that perhaps more derotation could be achieved during scoliosis surgery following the removal of the posterior elements. Stemming from the results of this study, several groups have performed various destabilization studies, removing different elements in various orders, to continue to build on the results of this foundational study.

Panjabi *et al.*[13] loaded thoracic FSUs following the resection of various structures in a posterior-to-anterior sequence. Cantilever bending was produced by applying a horizontal load vector to the superior vertebra to produce flexion and extension, while the inferior vertebrae held rigid. Following the resection of posterior structures all the way to the anterior column, increases of 1.8° and 0.5° were produced in flexion and extension, respectively. However, the contributions of individual structures were not reported.

While the two pioneering studies by White *et al*.[10] and Panjabi *et al*.[13] provided basic information regarding thoracic spine motion and the contributing structures, the *en bloc* and sequential resections were not based on typically performed surgical resections; consequently, further studies were necessary. To begin to develop data which may improve intraoperative correction prediction, the information truly valuable to the surgical community, the increase in motion, or decrease in stiffness, of the spine following surgical-specific resections was needed.

However, despite the early attempts at quantifying the effects of various ligaments and structures to thoracic spine stability, and the recent trend towards using posterior-only techniques for correcting spine deformity, few biomechanical studies since have investigated the kinematic and biomechanical effects of specific posterior-only surgical procedures.[25,29,58,129,164] Amongst the studies that have been performed, definite conclusions are difficult to make due to differences in the results, as well as differences in the biomechanical methods.

Feiertag *et al*.[129] analyzed motion in flexion-extension and lateral bending following sequential releases, posterior to anterior. In the study, six full-length thoracic spines, including the ribcage and sternum, were tested using the general principles of the *Pure Moment* protocol; however, it is unclear whether pure moments were truly produced. Following unilateral, one-level total facetectomy, no increase in motion was observed in either flexion-extension or lateral bending, with changes in ROM of less than 1°. It was not until rib head resection and discectomy procedures were performed that significant increases in motion were observed, suggesting the necessity of anterior release; however, the posterior release performed, that is, single-level unilateral facetectomy, is substantially less invasive than what would typically performed intraoperatively.

Horton *et al*.[25] used a similar setup to Feiertag *et al*.[129] to characterize thoracic spine flexion-extension flexibility following posterior release. In contrast to Feiertag *et al.*,[129] Horton *et al.*[25] performed a surgically-relevant release. Specifically, bilateral total facetectomies were performed at four levels, spanning T4-T8, on full-length thoracic spines including the sternum and ribcage. When performing this posterior release first, which would commonly be the case clinically for complex scoliosis deformity correction cases, an average increase in flexion-extension of only 2.5°, or 12.7% flexibility, was observed across the entire thoracic spine, T1-T12. Similar to Feiertag *et al*.[129], anterior releases had a more substantial effect on ROM.[25] Interestingly, when performing the posterior facetectomies following anterior release, flexion-extension ROM increased by an average of 6.7°, which suggests a nonlinear effect of various releases, depending on the sequence in which they were performed.

In addition to the full thoracic spine studies performed by Feiertag *et al*.[129] and Horton *et al*.[25], some studies have evaluated the effects of removing posterior structures in thoracic FSUs; however, the motions were rarely quantified. Specifically, Oda *et al*.[29] applied *pure moments* to thoracic FSUs following laminectomy with bilateral total facetectomy, a combination comparable to the Ponte osteotomy and other similar wide posterior releases. Compared to the intact condition, range of motion increased by 38%, 37%, and 45% in flexion-extension, lateral bending, and axial rotation, respectively. However, the significance of these normalized increases is unclear, as the raw motion of each FSU was not reported. In another study, Anderson *et al*.[164] applied *pure moments* to thoracic FSUs to determine the effect of removing all posterior structures, also comparable to the wide posterior releases. Following the single-level release, 68% of the total stiffness was lost in flexion; however, the effects on extension, lateral bending,

and axial rotation were not tested. Additionally, and similar to the study performed by Oda *et al.*[29], no raw motion data was reported.

More recently, Wollowick *et al*.[58] applied pure torsional moments to hemi-thoracic spine segments before and after single-level posterior-releases. Similar to previous models, the single-level release included the removal of the interspinous ligament, inferior and superior facets, spinous process, lamina, and ligamentum flavum, i.e., a wide posterior release. Single level increases in axial rotation ROM following this release were less than 2° (0.8-1.9°).

Other studies have evaluated the removal of anterior structures, the ribcage and sternum, and the rib heads;[27,131] however, posterior releases were not performed. In addition to these previous studies, releases have been evaluated under *pure moments* in canine models;[130,159] however, the relevance and applicability of the canine model to the human spine remains unknown.

Comparison to Clinical Results

In order to evaluate the results produced in these previous cadaveric spine biomechanics studies, comparisons to the clinically reported corrections following similar releases are necessary.

The Smith-Petersen Osteotomy is a posterior column shortening procedure. The SPO, originally described in 1945 by Dr. Smith-Petersen,[165] was intended for patients with ankylosing spondylitis and rigid kyphosis. More recently, the SPO has become analogous with the Ponte osteotomy,[108] as the two surgeries are reported as nominally interchangeable. Meanwhile, others have described wide posterior releases, which involve seemingly equivalent surgical resections.

These procedures are comparable to those performed in the aforementioned biomechanical destabilization studies.

With the exception of the axial rotation ROM increases reported by White and Hirsch,[10] ROM increases throughout the literature following posterior-release have been less than 5°,[25,58,129] even with the use of multi-level releases. Meanwhile, in clinical reports, the increases have been much larger.

In a study by Cho *et al*.,[166] the Smith-Petersen Osteotomy (SPO) was compared with the Pedicle Subtraction Osteotomy (PSO), an extremely invasive procedure involving resection of large portions of the vertebral bodies. The two procedures were compared for use in cases of fixed sagittal imbalance, primarily in the lumbar spine. For the SPO group (n = 30), the majority of patients suffered from idiopathic scoliosis as adolescents, and consequently, had existing instrumentation in the lumbar spine, most commonly the Harrington system. This caused disc degeneration, with imbalance primarily occurring distally. The average age of the adult patients in the SPO group was 40.1 ± 11 years. The average correction of the kyphotic angle at the site for which the Smith-Petersen Osteotomy was performed was 10.7° ± 3.2°, per osteotomy. From this result, the authors suggested that, with a single SPO, approximately 10° of sagittal correction could be achieved.

Geck *et al*.[108] reported similar results in adolescents and young adults with thoracic spine deformities. Specifically, Ponte osteotomies were performed in 17 patients with Scheuermann's Kyphosis. The adolescent patients' average age was 16.4 years, with a range of 14-25 years. Despite the differences between this study and the aforementioned study by Cho *et al.*[166] in terms of patients (adolescents versus adults), deformities (Scheuermann's kyphosis versus fixed

sagittal imbalance), and primary deformity locations (thoracic versus lumbar), similar results were reported.[108] Specifically, average sagittal correction was 9.3° per osteotomy, with a range of 5.9° to 15°.

Based on these results, it has been routinely suggested that Ponte osteotomies may provide between 5-15° of correction in the sagittal plane.[107,167] However, as discussed, flexion-extension motion increases reported in the biomechanical studies were substantially smaller following posterior-releases. Even in the study by White and Hirsch,[10] where the largest corrections were reported, the average increases were less than 5°.

Comparison to Clinical Results: Lateral Bending (Coronal Plane)

Despite the suggested use of similar wide posterior-releases for fixing coronal deformities and the reportedly routine use of these procedures in cases of AIS, few studies have evaluated deformity correction following these releases.[111,112,127,162,163] In these studies, the primary outcome variable evaluating the effectiveness of the releases is deformity correction (Cobb angle correction), reported as a percentage. However, the amount of correction provided by the releases can only be estimated as the number of releases, the level at which those releases were performed, and the location of the Cobb measurement are rarely reported.

Pizones *et al*.[111] reported that the wide posterior releases were performed at all levels along the major curvature; however, they did not report the location of the major curve. The major curve Cobb angle improved from an average of 59.3º preoperatively to 18.1º postoperatively, or an average correction of approximately 41.2º. Conservatively, if the major curve included all thoracic levels from T2-T12, as described in the Lenke classification system,[168] this would correspond to approximately 4.1º per wide posterior release; however, this

is likely an underestimation, as the major curve likely included less than 10 vertebral levels. However, if the preoperative flexibility was accounted for, that is, a bending flexibility of 35°, only 2.4º of correction was achieved per wide posterior release. In comparison, the standard posterior release (similar to a facetectomy), which was performed in a separate group of patients, resulted in 3.4º of correction per release. Once again, this estimation would be lower if preoperative flexibility was accounted for, with less than 1º of correction per release.

In another study, Halanski *et al*.[127] did not report whether or not osteotomies were performed at each level of the curvature; however, an average of 9 levels and 8 levels were fused in the osteotomy and facetectomy groups, respectively. Assuming that a posterior release was performed at each level, this would correspond to approximately 5.6º of correction per osteotomy, or approximately 5.4º per facetectomy. Similar to the results reported by Pizones *et al*.,[111] if preoperative flexibility is accounted for, the per-level corrections decrease to approximately 3.4º and 2.7º per osteotomy and facetectomy, respectively.

Shah *et al*.[112] also applied Ponte osteotomies for cases of AIS, with an average of approximately 4 Ponte osteotomies per patient; however, like the studies by Pizones *et al*.[111] and Halanski *et al*.,[127] the levels at which the osteotomies were performed and the Cobb angle was measured were not reported. Therefore, an approximation of the per-level corrections could not be obtained. However, Shah *et al*.[112] did suggest the importance of the Ponte osteotomies in not only improving the coronal curvature, but restoring a more normal thoracic curvature as well, with approximately 2.5º of sagittal correction per osteotomy. Their results highlight the potential ability of Ponte osteotomies to increase flexibility of the curvature in multiple dimensions, as well as the coupling effects of scoliosis correction maneuvers.

In the lumbar spine, Shufflebarger *et al*.[163] performed wide posterior releases at all instrumented levels, with fusions ranging from T9 to L4. Coronal Cobb angle correction was, on average, 42º, or 17º when taking into account preoperative flexibility. Conservatively, assuming the longest fusion possible from T9-L4, or seven levels, the correction per wide posterior release would be 6º or 2.4º, depending on whether or not flexibility was considered. In their earlier patient cohort,[162] the results were not detailed enough to make an approximation.

Overall, the clinical results suggest conservative coronal plane ROM increases ranging from 2.4-6 º per wide posterior release. As these are conservative estimations, in many cases, these increases were likely larger. In comparison, biomechanical studies have reported smaller increases in lateral bending. Specifically, with the exception of T1-T2 FSUs,[10] which in most cases would not be included in a scoliosis fusion, increases in lateral bending ROM have been less than 2º.[10,129]

Comparison to Clinical Results: Axial Rotation (Transverse Plane)

As discussed, scoliosis is a complex, three-dimensional deformity with abnormalities in the sagittal, coronal, and axial planes.[6,63,64] One major factor in evaluating the effectiveness of various releases, maneuvers, and instrumentation systems is the ability of that particular treatment to correct the deformity in the axial plane. While previous clinical literature using posterior releases is limited in the reporting of axial plane correction, approximate corrections can be determined.

Cotrel and Dubousset[18] introduced the concave rod rotation maneuver in an attempt to provide increased correction of the axial deformity associated with AIS curves compared to previous techniques used with, for example, Harrington rods or Luque wires.[169] However, even

with pedicle screws and such rod derotation maneuvers, vertebral rotation correction magnitudes have been small.[6,170,171] For example, Fu *et al*.[171] reported minimal improvements in apical vertebral rotation of 25 AIS patients instrumented with pedicle screw constructs. Specifically, RA_{ml} improved from 25.5±4.6 º to 22.6±5.3 º at 2 years, and RA_{sag} improved from 13.9±3.0° to 13.0±4.0° (~6.5%) at 2 years. Similarly, in 21 AIS patients, Lee *et al*.[6] reported apical vertebral rotation (RA_{sac}) was 16.1±6.1º preoperatively and 15.7±6.2º postoperatively, or 2.4% correction. Di Silvestre *et al*.[170] reported larger corrections, with approximately 4.2º of apical rotation correction, or 14.8%, in 30 AIS patients. In their study, Smith-Petersen osteotomies were performed prior to correction, which may have accounted for the increased correction.

In comparison, with more powerful rotational correction maneuvers, such as direct vertebral rotation (DVR), the apical vertebral rotation has drastically improved.[6,169,170,172] Lee *et al*.[6] compared the results from a simple rod derotation maneuver with 17 AIS patients who underwent a DVR maneuver. In contrast to the minimal correction using rod derotation, in the DVR group, apical vertebral rotation significantly improved from 16.7±5.7º preoperatively to 9.6±5.6º postoperatively. Asghar *et al*.[172] reported similar results in 32 AIS patients, with apical vertebral rotation improving from 21.3º to 8.5º using DVR. Kadoury *et al*.[169] reported correction from 19±7º to 5±4º. Di Silvestre *et al*.[170] reported apical vertebral rotation correction of approximately 17º, or 63.4%. Interestingly, Di Silvestre specifically reports having performed Smith-Petersen Osteotomy (SPO) at the apical levels, and achieved higher magnitudes of correction as compared with the patient cohorts reported by Lee *et al*.[6] or Asghar *et al*.[172] It has further been suggested that the rotational corrections can be improved when using monoaxial screws as compared to multi-axial screws.[173]

In contrast to these large axial vertebral rotation corrections reported using pedicle screw constructs and DVR maneuvers (5.1-17º), increases in axial rotation reported in biomechanical studies have been substantially smaller. Of the thoracic spine biomechanics studies, only three evaluated the effects of posterior surgical release on axial rotation range of motion.[10,29,58] White *et al*.[10] reported increases in axial rotation ROM ranging from approximately 9º at T1-T2, to less than 2º at T10-T11 and T11-T12. Similar to these reported increases in the lower thoracic spine, Wollowick *et al*.[58] reported increases of less than 2º. Meanwhile, the work by Oda *et al*.,[29] the only other study evaluating axial rotation following posterior release, did not report the magnitudes of increase in ROM.

Overall, there are clear differences between the suggested correction potential of various releases in the clinical literature in comparison to the biomechanics literature. This may be in large part due to the inherent assumptions and design of the *Pure Moment* model, which were intended to evaluate general spine characteristics and to compare fusion instrumentation. The model was not selected to simulate physiological loading conditions nor intraoperative loading conditions. However, to date, alternative testing models and loading conditions have not been adequately explored. With improvements to the preclinical testing model, perhaps more clinically relevant data may be produced.

In-Vitro Thoracic Spine ROM

As discussed previously, the pioneering work of White and Panjabi established ranges of motion in cadaveric thoracic FSUs.[23] Specifically, per-level motions ranged from 2-20º, 6-26º, and 4-28º in flexion-extension, lateral bending, and axial rotation, respectively.[23] Additionally, 'representative' angles for each level were reported, with angles ranging from 4-12º, 10-18º, and

4-18º in flexion-extension, lateral bending, and axial rotation.[23] Similarly, several other studies reported intact thoracic spine ROM using the pure moment model, and close variants therein.[9,10,13,25-27,35,43,46,47,129,133,134,174] However, the reported motions do not always coincide.

For example, at the T11-T12 motion segment, White and Panjabi reported ranges of motion of 6-20º in flexion-extension, 10-20º in lateral bending, and 4-6º in axial rotation.[23] Meanwhile, despite applying a relatively large in-vitro thoracic moment of 7.5 Nm, Oxland *et al*.[133] reported mean motions of approximately 5.1º in flexion-extension, 7º in lateral bending, and 3.6º in axial rotation, all smaller in magnitude than the lowest ROM reported by White and Panjabi.[23] Similarly, according to the ROM reported by White and Panjabi, T5-T11 motion could range from 18-50º in flexion-extension, 50-88º in lateral bending, and 48-96º in axial rotation.[23] However, Deviren *et al*.[47] reported mean ROM of 29.9º in lateral bending and 39.3º in axial rotation, substantially less than even the previously reported lower ranges of motion; flexion-extension motion was closer to the lower range, with a mean of 17.3º.

Therefore, despite the application of a standard protocol, i.e. the *Pure Moment* testing model, wide ranges of motion have been produced in the thoracic spine. While the large variability may partially be attributed to the inherent variability in human spine flexibility, it may also be a result of the many changeable factors within the *Pure Moment* model. Once again, and similar to the limitations of previous models evaluating the effects of posterior destabilization, the limitations and contradictions in the results suggest the need for improvements and expansion of the traditional preclinical testing model.

1.4.2 Limitations of the *Pure Moment* Testing Model and the Experimental Design Assumptions for Scoliosis Application

Pure Moment Design/Assumption: Single Plane Pure Moment Loading

Limitations: During intraoperative correction of thoracic spine deformity, surgeons use a combination of complex, three-dimensional loads, including compression-distraction, bending moments, torsion, shear, and lateral forces.

As discussed, the *pure moment* model is designed on the basis of applying single-plane pure moment couples to produce single-plane rotations.[17,24] For example, *pure moments* are applied about the anterior-posterior axis of the spine to produce lateral bending rotations about this same anterior-posterior axis. Similarly, *pure moments* are applied about the vertical axis of the spine to produce axial rotations about this same axis, and *pure moments* are applied about the lateral axis of the spine to produce flexion and extension rotations. The primary motions are analyzed, and conclusions are largely based on these motions. However, in many applications, such as scoliosis, single plane motions may not be sufficient in comprehensively evaluating various aspects of surgery. For example, coupled motions, or multi-planar motions, may be affected differently than the single plane motions.

Coupling and coupled motions have long been acknowledged as crucial variables in scoliosis biomechanics.[175] Spine biomechanics studies have reported marked coupling of axial rotation and lateral bending in the thoracic spine,[175] consistent with AIS, which is a complex three-dimensional deformity largely involving transverse and coronal deformities.[6] Correspondingly, three-dimensional multi-planar intraoperative forces are necessary to achieve optimal deformity correction. As discussed, early instrumentation systems, which centered on fixing the coronal component of the deformity through uniplanar and unidirectional

intraoperative forces,[5,19,83] failed to achieve three-dimensional correction. Instead, large axial plane and sagittal plane abnormalities remained postoperatively despite satisfactory outcomes in the coronal plane.[74,76,77] Subsequent instrumentation designs, beginning with CD instrumentation,[18] aimed to provide not only coronal correction, but sagittal and transverse plane correction as well. With these new instrumentation systems came new correction maneuvers which apply complex, three-dimensional intraoperative correction loads, such as rod derotation[18,113,114] and segmental direct vertebral rotation.[6,7] Moreover, with a host of correction maneuvers available, combinations are used to include rod derotation,[18,113,114] rod translation,[176] cantilever bending,[115] compression-distraction,[73] and direct vertebral body rotation,[6,7] resulting in complex correctional loads. For example, Chang *et al*.[177] suggested combining DVR and cantilever bending for maximum control of correctional forces in all three dimensions.

Despite the importance of coupled loads in the correction of AIS, biomechanical studies to date have predominantly used single plane *pure moments*, and similar single plane testing modes, e.g. cantilever bending. Moreover, the majority of these *pure moment* studies have ignored coupled motions altogether.[13,25,27,29,58,129,130,164] While single plane *pure moments* provide many answers with regards to intraoperative scoliosis questions, alternative models must be explored to adequately and more comprehensively evaluate intraoperative situations.

Pure Moment Design/Assumption: Physiological Motion

Limitations: During intraoperative correction of thoracic spine deformity, physiological motions are not produced, as the surgeons apply corrective torques and forces, not physiological torques and forces, to fix the deformity.

The magnitudes of bending moments applied in *Pure Moment* testing of cadaveric spines have partly been chosen on the basis that such moments can produce physiological ranges of motion.[17,45] As discussed in previous chapters, normal thoracic spine motion has been extensively studied under pure moments;[29,35,47,134] however, the majority of the studies evaluated the motion of the thoracic spine without the ribcage or sternum. With the ribcage and sternum intact, arguably the closest representation of the *in-situ* human thoracic spine, average motions have been reported between 7.93-26.9°, 10.36°-42.06°, and 23.03-43.69° in flexion-extension, lateral bending, and axial rotation, respectively.[26,27] Meanwhile, in healthy patients, Willems *et al*.[155] reported mean motions across T1-T4, T4-T8, and T8-T12 of approximately 16.8-20.3° in flexion-extension, 11.8-25.6° in lateral bending, and 20.1-47.4° in axial rotation. Similarly, Fujimori *et al*.[151] reported full thoracic axial rotation ROM of 24.9±4.9°, with segmental motion ranging from, on average, 0.5-2.6°. Therefore, the clinically measured physiological motions correspond well with the results from the biomechanical testing.

On the other hand, during the intraoperative correction of scoliosis, the physiological loads and motions are exceeded to achieve optimal deformity correction. This is particularly true in severe cases rigid AIS. For example, Dobbs *et al*.[178] reported follow-up of 34 AIS patients who underwent posterior-only spine fusion. For these patients, the preoperative thoracic Cobb angle was 94.3° (90-111°). Preoperatively, these curves bent to a Cobb angle of 76.4° (70-95°). In other words, under physiological conditions, and under patient-initiated lateral bending motion (side bending), the apex of the thoracic spine bent approximately 17.9°. Therefore, for this cohort of patients, the mean physiological range of motion in 'lateral bending' was nearly 18°. Then, intraoperatively, the patients' spines bent, on average, an additional 23.3°, as the immediate post-operative Cobb angle was 53.1° (44-72°). Similar trends have also been reported

in cases of less severe AIS curvatures. For example, Kim *et al*.[106] reported on a cohort of 26 patients who received pedicle screw based spine fusion. In these patients, Cobb angles bent preoperatively from 63° to 30°, and were corrected even further during surgery, resulting in an average postoperative Cobb angle of 15.8°. Therefore, the typical physiological motions of these patients were exceeded during scoliosis surgery.

In order to correct the spines beyond their inherent physiological range (i.e. bending Cobb angles), the intraoperative forces must exceed the typical physiological forces applied by the patient. With the increased strength of pedicle screws over previous instrumentation,[103,104] techniques have been developed for the application of large correctional forces to the spine, such as direct vertebral rotation (DVR).[6,7] With these large correctional forces, larger corrections can be achieved. Unlike many questions which require the application of *pure moments*, such as the quantification of general thoracic spine motion or the comparison of fusion instrumentation systems, questions regarding intraoperative correction and surgical techniques require improved and supplemental models for more comprehensive analyses and preclinical predictions.

Pure Moment Design/Assumption: Non-Destructive Loading

Limitations: Non-destructive loading is essential in comparing conditions of a given spine, for example, comparing the intact spine after injury, and after solid fusion. However, during deformity correction, the magnitudes of loading exceed the conservative 'non-destructive' in-vitro force and torque magnitudes. Moreover, as the ligaments, and even the intervertebral discs, are often resected prior to corrective maneuvers, the 'non-destructive' notion becomes less important.

Pure moment magnitudes were selected based on two criteria: (1) magnitudes which produce physiological ranges of motion,[17,45] and (2) magnitudes which are non-destructive and do not cause plastic deformation of the intervening tissues or spine structure, thus allowing repeated testing, e.g. before and after sequential destabilization.[16,17,44] For the preclinical testing of scoliosis and spine deformity correction, these two criteria are less important. As discussed above, the first criterion no longer applies because the physiological ranges of motion are exceeded during surgery. Similarly, the second criterion no longer applies as the intraoperative loads exceed the elastic properties of the human spine.

Whereas *pure moments* are designed to err on the conservative side of the yield strength of the intervening bony and soft tissues, that is, designed to apply loads that produce elastic deformation, intraoperative correction techniques are designed to err on the conservative side of ultimate strength. Wagner *et al*.[128] go as far as to state that "[as] we strive to achieve near anatomic reduction of the spinal deformity, the biologic limitations of vertebrae are approached." This statement is supported by the literature, with many reports of intraoperative complications in AIS surgery, including pedicle fracture.[128,179-182] Moreover, surgeons have reportedly applied DVR torque magnitudes in excess of 100 Nm.[7] While torsional failure of the spine may not occur, the pedicle fractures suggest that the elastic limits of the spine structures are surpassed during surgery.

Intraoperative pedicle fracture can be a debilitating complication, as screw plow could result in aortic abutment.[128] Moreover, pedicle fracture in the spine results in weaker constructs, as the screw-bone interfaces may be compromised, potentially having long-term effects on the fusion and outcome of scoliosis correction surgery. However, while pedicle and vertebral fracture may be of great consequence, the integrity of the disc and ligaments are more or less

ignored. Moreover, while it is often necessary to have ample open-disc space for optimal correction,[107,108] the deformation of the structure, i.e. elastic or plastic deformation of the disc, is also ignored.

The overall goals of scoliosis correction are to correct the deformity, achieve solid fusion, and maintain correction over the long-term. As the fusion relies primarily on solid bone-screw interfaces, it makes sense that there is large concern over the integrity of the bony structures, e.g. the pedicles. In addition, it follows that there is little concern over the soft tissue connections, e.g. discs and ligaments, particularly considering that many of these structures are often removed during surgery to provide additional flexibility in the curvature. Therefore, while safe loading limits must be established and applied to prevent future pedicle fracture and bony failure, the loads are clearly destructive. As such, the non-destructive loads typically applied during *pure moments* may not be the most representative for the simulation of intraoperative techniques and scoliosis correction.

Moreover, throughout the literature, a range of applied non-destructive loads have been applied in the thoracic spine. Specifically, applied moments have ranged from 2 Nm – 7.6 Nm.[27,31,35,41-43] Not only are these applied moments likely substantially smaller in magnitude than those applied intraoperatively, but the low range of applied moment magnitudes also results in moment-rotation curve variability amongst studies.[29,133,136,183-186] For example, in two previous studies,[29,136] there were large differences in the degree of non-linearity at the same moment endpoint. Specifically, the representative curve reported by Oda *et al*.[29] was largely linear at the 2Nm endpoint. In this linear range, the nonlinear response of the tissues has not been reached, and thus, a minimum stiffness occurs. On the other hand, Busscher *et al*.[136] reported a representative curve with a largely nonlinear relationship at 2 Nm, with near maximum stiffness

occurring. In these two examples, removing the same structures in each of these studies following intact testing may yield significantly differing results. Moreover, in a case where the moment magnitudes are vastly different, such as comparing the results of a study which employed a maximum moment of 2 Nm with a study which used a maximum moment of 8 Nm, clearly, there may be differences between the moment-rotation relationships at the moment-endpoints. For example, Ellingson *et al*.[183] reported a representative moment-rotation curve for a lumbar FSU. At 2 Nm, 4 Nm, 6 Nm, and 8 Nm, the total ROM was approximately 4°, 7°, 9°, and 10°.

These differences in loading inevitably produce differences in the reported results, and in turn, may affect their clinical applicability. This also could, in part, account for the wide ranges of motions reported throughout the literature in the testing of cadaveric spine specimens.

Pure Moment Design/Assumption: Minimizing Viscoelastic Effects

Limitations: When comparing different conditions of the spine, i.e. intact versus fused, it is important to minimize viscoelastic effects during repeated *Pure Moment* testing to facilitate the comparisons; however, during corrective surgery, maximizing the value of the creep/relaxation effects of the spine may be beneficial.

One of the key benefits of the *pure moment* model is the ability to produce consistent and reproducible results. To achieve this, the loading application was designed to, as much as possible, minimize the viscoelastic effects of the tissues.[24,31] Specifically, a series of loading-unloading cycles are applied to precondition the spine specimens, typically including two or three preconditioning cycles before measurements are recorded.[24,31,187] After such preconditioning, the hysteresis loop stabilizes, resulting in reproducible moment-rotation curves

over subsequent cycles. The nonlinear, biphasic hysteresis loops, that is, a region defined by large increases in rotation under small incremental increases in torque and a region defined by high stiffness and small rotations under increases in torque, can then be accurately reproduced and analyzed.[31] Prior to such preconditioning, experiments produced largely linear, single-phase moment-rotation relationships.[15,16]

To further minimize the viscoelastic effects, specific loading rates have been established. For example, when using hydraulic actuators to apply *pure moments* to human cadaveric spines, rates are typically applied between 0.5º/s and 5.0º/s.[24] Rates of lower than 0.5º/s could result in viscoelastic effects, and specifically, could result in creep, that is, continual deformation (or rotation) under a constant applied load.[188] Unlike hydraulic actuators which are capable of applying continuous loading rates (e.g. 0.5º/s, 0.5 Nm/s), more commonly used experimental setups, such as weights and pulleys, involve quasi-static loading in which the moments are applied and increased incrementally. For example, Yamamoto *et al*.[45] applied a maximum of 10 Nm in flexion-extension, lateral bending, and axial rotation, reaching the maximum moment in five equal steps (i.e. 2 Nm, 4 Nm, 6 Nm, 8 Nm, 10 Nm). Following each load application, 30 seconds of creep were allowed to minimize the viscoelastic effects, similar to many previous experiments.[45,133,187,189,190] This process helps to produce typical nonlinear biphasic hysteresis responses.

As discussed, all of these loading considerations were designed to minimize viscoelastic effects, or to 'reduce variations caused by viscoelasticity',[189] or to prevent 'creep effects'.[24] However, viscoelasticity and the effects of creep can be crucial tools in deformity correction. For example, using halo-pelvic distraction and intraoperative traction techniques, three phases of correction are described: (1) an initial elastic deformation phase, (2) a primary creep period

where the majority of the correction takes place under small increases in load, and (3) the secondary creep period where gradual correction occurs.[191,192] With such techniques, the maximum curve correction may occur after 10-12 days.[193,194] Similarly, with new techniques, such as shape-memory metal implants, constant small-magnitude loads which maximize the effects of viscoelasticity are applied for gradual deformity correction.[195]

The same principles of correction are employed with all-pedicle screw systems and derotation-type correction maneuvers, the current standard in deformity correction surgery. For example, Asghar *et al*.[172] applied segmental and en bloc derotation maneuvers to AIS patients, reportedly applying en bloc maneuvers over a period of approximately 20 minutes to overcome the viscoelastic properties of the tissues and provide maximal deformity correction. Therefore, rather than trying to minimize viscoelastic effects altogether or trying to prevent creep, the loading mechanisms should be designed to simulate the typical surgical maneuver and intraoperative loading application. With such simulations, more relevant results may be produced in preclinical biomechanical testing of scoliosis correction.

Pure Moment Design/Assumption: Normalized spine motions (% of intact)

Limitations: By normalizing the spine motions following resection of various structures or following various treatments to the intact spine, the assumption is made that all intact spines represent the same condition. While intact spines are nominally the same, and all include nominally equivalent structures, i.e. intervertebral discs, stabilizing ligaments, and connective soft tissues, the properties of these structures among different spines vary greatly. As such, prior to normalizing motions to the intact condition, other factors should be considered.

Finally, and also as discussed in previous chapters, cadavers from pediatric donors or from donors with untreated scoliosis are currently unavailable. Consequently, the majority of scoliosis biomechanics studies use cadaver specimens from elderly donors without gross structural deformities. The potential differences between straight adult cadaveric spines and deformed pediatric spines are acknowledged as limitations, and reported as such.[24,58] Moreover, there is often large variability amongst a sample of adult cadaveric spines, and while this may be representative of the true AIS patient population,[105,139,178] it is an experimental limitation. In an attempt to account for these differences, the results from each individual spine specimen following injury (i.e. simulated annular tear or simulated surgical release) or treatment (i.e. fusion) are typically normalized to the results of that same specimen in the intact condition.[40] However, rather than reduce the differences, this process only enables a comparison between specimens. Perhaps a more fundamental approach to normalization would provide a better minimization of the limitations associated with the use of adult cadaveric specimens.

Instead of solely normalizing on the basis of motions produced, a more fundamental approach would include normalizing on the basis of what contributed towards those produced motions. Under an applied torque, which is inherently controlled and accounted for in the experimental design, the spine motions produced are primarily a result of ***(1)*** the properties of the individual soft tissues of each spine, i.e. the intervertebral discs and connecting ligaments, and ***(2)*** geometrical constraints of a given spine, i.e. disc height.[196] For example, in theory, the maximum rotation achievable for a given spine segment would be the rotation which caused vertebral bone-on-bone contact; however, it is much more likely that the soft tissues would rupture or become severely damaged prior to such contact. Moreover, based on simple mechanics, it would be expected that there would be a simple inverse relationship between

intervertebral disc height and disc stiffness, which was verified in a simple FEA model.[197] Correspondingly, the same would be expected of ligaments. Both the properties of the individual soft tissues and the geometrical constraints of the spines are largely governed by the health of the intervertebral discs, as natural aging processes and degeneration may affect these properties, i.e. ligament hypertrophy[198,199] or disc space narrowing.[196] Therefore, by normalizing the specimens according to disc health, the results from healthy, non-degenerated spines can be targeted, and may provide more relevant information for pediatric spine patients.

While the quality of motion may be affected by other variables, many of which are immeasurable such as patient lifestyle, degeneration likely plays a dominant role. Kirkaldy-Willis and Farfan[200] hypothesized a three-phase process of degeneration, with an initial increase in segment motion and laxity followed by a subsequent period of decreased motion and increased stiffness. During the process of aging, soft tissue fibrosis may reduce the effectiveness of the tissues to resist forces, thereby increasing segmental motion.[196,198] At the same time, disc space narrowing and osteophytes formation may decrease segmental motion.[196] Therefore, with degeneration, a complex interaction between the individual soft tissues and spine geometries may exist, resulting in changes in spine mechanics.[196]

Several studies have analyzed lumbar spine motion as a function of intervertebral disc health, with varying results.[183,196,201-205] However, the effects of degeneration on thoracic spine ROM have not been well documented, as thoracic spine degeneration is less common than that of the cervical and lumbar spines. Panjabi *et al*.[13] analyzed thoracic FSUs in flexion and extension intact, and following sequential ligament resections. Following failure of the specimens, the intervertebral discs of each specimen were graded on a 0-3 scale; however, no analysis was performed on the basis of these grades.

Despite the lack of studies in the thoracic spine, disc degeneration clearly plays a role in the mechanics of the spine at a given level. However, scoliosis biomechanics studies have largely ignored these effects. While the literature is limited, one study examined ligament surgical samples from idiopathic scoliosis and adult herniated disc patients.[206] The ligament structure in the scoliosis patients were found to be normal, compared to the degeneration patients who demonstrated ligament fibrosis.[206] Moreover, as scoliosis, and in particular adolescent idiopathic scoliosis, affects the pediatric population, degeneration is likely not present. Therefore, normalization of the adult cadaveric spines according to health may reduce the limitations associated with adult cadaveric spine specimens, and may potentially produce more applicable results for the pediatric and adolescent populations.

1.4.3 Alternative Testing Methods

Despite the need for improved models beyond the traditional *Pure Moment* testing model and experimental design for preclinical spine testing, no alternative testing models have been adequately developed to evaluate intraoperative spine deformity conditions. While several ASTM standards have been established for preclinical evaluation of spine technology, they are limited to evaluating post-operative conditions (i.e. long-term cyclic testing of solid rigid fusion) and mechanical strengths of implants (i.e. ultimate strength or pull-out strength of a pedicle screw).

Cadaveric Testing – Alternative Models

Outside of the general *Pure Moment* model, or close variations therein, very few biomechanical experiments have been reported. Wiemann *et al.*[207] studied the effect of posterior surgical release on the required torque to achieve 25° of segmental correction in human thoracic

cadaveric spines; however, they did not examine linked screw constructs, did not report the torques required to produce the correction, and did not perform the rotations in a controlled, repeatable manner. Lam *et al.*[208] used a novel derotation simulator to determine which screw design, i.e. fixed-axis, uniplanar, or polyaxial, resulted in the most efficient rotation of the spine under a given applied moment; however, the spine was tested in only one condition (following facetectomies), the applied moment was small (i.e. 3 Nm), potential correction was not assessed, and human cadaveric specimens were not used.

ASTM Standards

For the spine, several ASTM standards have been established for a wide range of preclinical testing, such as the mechanical evaluation of individual implant components, intervertebral disc cages, and posterior pedicle screw-rod systems (Table 1).[209-221]

Table 1. ASTM Standards for Preclinical Testing of Spine-Related Devices

ASTM Standard	Name
F2077[220]	Test Methods For Intervertebral Body Fusion Devices
F1717[221]	Standard Test Methods for Spinal Implant Constructs in a Vertebrectomy Model
F1582[217]	Standard Terminology Relating to Spinal Implants
F2193[209]	Standard Specifications and Test Methods for Components Used in the Surgical Fixation of the Spinal Skeletal System
F2267[216]	Standard Test Method for Measuring Load Induced Subsidence of an Intervertebral Body Fusion Device Under Static Axial Compression
F2346[215]	Standard Test Methods for Static and Dynamic Characterization of Spinal Artificial Discs
F1798[210]	Standard Guide for Evaluating the Static and Fatigue Properties of Interconnection Mechanisms and Subassemblies Used in Spinal Arthrodesis Implants
F2624[214]	Standard Test Method for Static, Dynamic, and Wear Assessment of Extra-Discal Single Level Spinal Constructs
F2423[213]	Standard Guide for Functional, Kinematic, and Wear Assessment of Total Disc Prostheses
F2694[211]	Standard Practice for Functional and Wear Evaluation of Motion-Preserving Lumbar Total Facet Prostheses
F2790[212]	Standard Practice for Static and Dynamic Characterization of Motion Preserving Lumbar Total Facet Prostheses
F2706[218]	Standard Test Methods for Occipital-Cervical and Occipital-Cervical-Thoracic Spinal Implant Constructs in a Vertebrectomy Model
F2759[219]	Standard Guide for Assessment of the Ultra High Molecular Weight Polyethylene (UHMWPE) Used in Orthopedic and Spinal Devices

The majority of these standards, however, are not related to scoliosis testing. For example, standard ASTM 1717 can be applied to evaluate the stability and durability of a typical spine fusion assembly with posterior pedicle screws (or hooks, wires, etc.) and rods.[221] Additionally, ASTM F1798 can be applied to evaluate the strength of the interconnecting components, i.e. the screw-rod junction, of scoliosis instrumentation systems.[210] However, none of the standards are designed to evaluate intraoperative techniques, such as the effectiveness of surgical releases or the efficacy and safety of correction maneuvers. Moreover, the above mentioned standards to not evaluate spine range of motion in cadaveric specimens.

1.5 The Need for Improved Methods for Scoliosis Testing

As demonstrated, due to the literature being limited by the near-universal application of the *Pure Moment* testing model and experimental design for scoliosis biomechanics, evaluations of new techniques are often reliant on clinical studies. Unfortunately, many controversies exist in the literature which, with improved biomechanical models, could potentially be settled quicker. Moreover, clinical studies are often limited due to technique differences, the inability to isolate variables, and differences in the ways in which results are reported.

1.5.1 Unresolved Controversies

As discussed in previous chapters, the Ponte osteotomy and similar wide posterior releases have recently been suggested for use in cases of AIS, with suggested deformity correction potential of 5-15° per osteotomy.[107] Statements recur in the literature, stating that each millimeter of resection results in approximately 1 degree of correction.[107] The procedure has also been described to include an osteotomy width of between 7-10 mm, resulting in a correction of approximately 10° at a given level.[167] Despite the fact that, as discussed in previous chapters, previous biomechanics studies of surgical releases have suggested substantially smaller motions following each posterior release, wide posterior releases are routinely performed in cases of AIS. However, even with the evident prevalence of their use in AIS cases, there is conflicting evidence in the literature amongst clinical studies.

Shufflebarger and Clark[162] were the first to use wide posterior releases for coronal plane deformity, reporting on the follow-up of 10 patients suffering from lumbar and thoracolumbar AIS. The wide posterior release included the removal of the interspinous ligament, spinous

process, ligamentum flavum, and bilateral facet joints, analogous to a Ponte osteotomy. Interestingly, in their first report, several x-rays were taken at various stages of the surgical and follow-up process: standing preoperatively, bending preoperatively, after positioning the patient on the Jackson table, intraoperatively following initial correction maneuvers with instrumentation prior to surgical release, following posterior-release and final correction maneuvers, and postoperatively. Prior to surgical release, lumbar coronal curvatures were reduced 64%, increasing to 76% correction following wide posterior release ($p<0.005$). Moreover, the wide posterior releases significantly restored lumbar lordosis. Based on the results, the authors recommended the use of wide posterior release in correcting scoliosis deformities.

In a second study, Shufflebarger *et al*.[163] prospectively evaluated 62 patients with lumbar and thoracolumbar AIS treated with the same wide posterior release and pedicle screw-based instrumentation. Results were even more promising, with average lumbar coronal correction of 80%, improving from an average of 52 degrees (40-72) to 10 degrees (0-25) postoperatively. The operative time ranged from, on average, 2.36 – 2.8 hours, with average blood loss ranging from 500 – 675 mL, consistent with previous reports of AIS surgery. Additionally, like their original study, lumbar lordosis and sagittal kyphosis were normalized and restored. The additional correction in this study compared to the original, that is, 80% versus 76%, may be attributable to the use of pedicle screws compared to hooks. Beyond the increased three-dimensional flexibility of the spine, in both studies, the authors stress the benefit of the wide posterior release to increase the surface area for arthrodesis.[162,163] This increased surface area was hypothesized as the reason for the maintenance of correction over time.

Despite these early successes using wide posterior releases for the correction of AIS deformities, with reported coronal corrections of 76%[162] and 80%[163], few studies have been performed to evaluate the validity of these results, particularly in the thoracic spine. As discussed by Shufflebarger *et al.*,[162] the most common release is a facetectomy, typically performed bilaterally. In a more recent study, Pizones *et al.*[111] compared wide posterior releases, in 21 patients, with standard posterior releases, i.e., total facetectomies, in 25 patients. The wide posterior release was significantly more effective in reducing the coronal aspect of the deformity, with thoracic Cobb angle correction of 68.6% compared to only 57% correction with the standard posterior release. In this study, hybrid instrumentation was used, that is, hooks proximally, wires apically, and screws distally. With newer all-pedicle screw instrumentation, the correction percentage would likely increase. In their study,[111] the operative times were between 4 and 5 hours, longer than those reported by Shufflebarger *et al.*;[163] however, the fusion-lengths were likely shorter in the previous studies.

Most recently, Shah *et al*.[112] retrospectively analyzed the use of multiple-level Ponte osteotomies in 87 AIS patients. Similarly to Shufflebarger *et al*.[162,163] and Pizones *et al*.,[111] the coronal and sagittal plane deformities were improved postoperatively.[112] Specifically, coronal plane deformities were reduced by an average of 71.5%. Additionally, rib hump deformity was reduced from an average of 15 degrees preoperatively to 7.4 degrees postoperatively. They reported both longer operative time and more blood loss than those reported previously. However, despite the large rates of correction, the study was retrospective, and no control group was reported for the basis of comparison, both of which make the results difficult to interpret.

Despite the positive preliminary results for both lumbar[162,163] and thoracic scoliosis deformities,[111,112] other groups have abandoned the use of Ponte osteotomies for cases of AIS

altogether.[127,222] Halanski *et al*.[127] compared the use of total facetectomies with Ponte osteotomies in separate patient groups. Unlike previous studies, there was no significant difference in the percentage Cobb improvement, postoperative Cobb angle, or sagittal improvement. In their study, both surgical groups resulted in Cobb corrections of more than 80%, higher than those reported in previous reports. Moreover, significant increase in operative time and blood loss for the surgeries including Ponte osteotomies led the authors to abandon the procedure altogether.

Despite the conflicting evidence in the few existing reports, the use of these procedures appears to be widespread in the AIS community.[107,112] Therefore, definitive conclusions, either for or against, would be desirable. However, it is difficult to normalize the results between the studies due to variations in the curve magnitudes, preoperative curve flexibilities, and instrumentation. Moreover, the correction maneuvers employed are rarely described, despite having the ability to significantly impact the postoperative corrections. Additionally, the amount of correction obtained as a result of each surgical release is difficult to estimate, as the specific levels where the procedures were performed are rarely described. A well-controlled preclinical biomechanical study could address these limitations associated with the clinical studies, and help to predict the true performance of these procedures.

1.5.2 Uncontrolled Variables and Incomplete Reports

In specific situations, clinical studies fail to answer clinical questions due to conflicting evidence amongst the literature. This conflicting evidence, however, is often hard to compare due to lack of consistency between techniques, differences in confounding variables, and differences in the reporting of the results. In these cases, biomechanical testing could offer a

more reliable, consistent basis for comparison due to the ability to, all else equal, isolate variables.

In the previous discussion, two polarized conclusions were made based on clinical outcome. Compared to less-invasive techniques, Pizones *et al*.[111] reported significantly increased correction using wide posterior releases, and therefore advocated the technique. In contrast, Halanski *et al*.[127] reported no difference, and subsequently abandoned the procedures. However, due to differences in the variables, such as preoperative curve magnitudes, curve flexibility, and instrumentation, conclusions are difficult to make. Moreover, the specific correction maneuvers used were not stated, further complicating the comparison.

Perhaps the use of posterior-only releases is only useful when using specific implants constructs. In a study by Kim *et al*.,[106] pedicle screw constructs were compared with hook constructs for patients with AIS. In both groups, the surgical procedures were identical. The authors reported significantly better curve correction using pedicle screws versus hooks (75.6% postoperatively versus 49.9%). Despite the added expense of pedicle screws, the authors concluded that the use of pedicle screws offered significant advantages over hook constructs. This suggests that when isolated, there is a definite difference between different implant types. Therefore, the conclusions made from surgical release studies, such as Pizones *et al*.[111] and Halanski *et al*.,[127] may be specific to the specific instrumentation type used. However, due to the limited number of reports, it remains unclear clinically how much additional correction is provided solely by the specific procedure (i.e. Ponte osteotomy) compared to the type of instrumentation used.

Another possibility could be that the use of posterior-only releases provides added flexibility along the axis of correction when using direct vertebral rotation as the main maneuver (pedicle screws) compared to using apical translation or derotation as the main correction maneuver (hybrid systems). However, and once again, the variables in the clinical studies are often confounded, and worse, often unreported. Alternatively, perhaps other confounding variables are creating the differences in the results of these studies beyond the type of instrumentation, surgical release, or surgical correction maneuver.

Using another example, and as discussed in a previous chapter, the results from the clinical posterior-release literature conflict with the results from the biomechanical literature. For example, in comparison to apical corrections of 5.1-17° reported clinically,[6,169,170,172] biomechanical studies have suggested less than 2° of axial rotation increase following posterior release.[58] In the clinical studies, the change in apical vertebral rotation is reported as the difference between the preoperative rotation angle and the postoperative rotation angle; however, the initial flexibility in the axial plane of these curves is unknown.[6,169,170,172] Moreover, the specific soft tissue releases performed are rarely reported. Consequently, it is difficult to discern whether the achievable apical correction is attributable to the natural motion of the apical disc space under load, to the increase in flexibility following soft tissue resection, or to the powerful rotational correction maneuvers applied during surgery.

These represent just a few examples of the many controversies existing throughout the scoliosis literature. However, due to the limitations associated with current biomechanical studies, in-vitro data has not impacted many of these controversies. Consequently, the community has been reliant on clinical studies. However, and as discussed above, these studies

are clearly limited. Improved preclinical testing may serve to accelerate the process of answering and resolving the many clinical questions and controversies throughout the literature.

1.5.3 Untested Advancements

In addition to the conflicting evidence in the literature regarding specific procedures, e.g. posterior-releases, many new techniques and procedures remain untested. As discussed earlier, the increase in popularity of pedicle screw based systems has led to improvements in the correction maneuvers used during deformity correction surgery. With the improvements of pedicle screw systems over prior instrumentation systems, including three-column fixation,[76,101,102] stronger bone-implant fixation,[103,104] and improved curve correction,[93,102,105,106] new correction techniques are being applied. One such technique, direct vertebral rotation (DVR),[6,7] is applied to the spine for correction of the deformity in three dimensions. Compared to traditional methods of applying compression-traction,[73] lateral forces,[19] or rod derotation,[113,114] DVR allows surgeons to apply segmental transverse rotation directly to the spine in surgery.[6,7] With the advancement of such techniques, surgeons are applying higher torques than previously achievable directly to the spine, with torques reportedly in excess of 100 Nm.[7] As a result, this technique has become a typical correction maneuver in scoliosis deformity surgeries, with numerous short-term follow up studies recently published.[6,128,169,172,223-227]

However, despite the increase in use, the safety of the procedure has been recently questioned.[128] Wagner *et al*.[128] reported 7 cases (2.6%) of lateral pedicle screw "plow" following the DVR technique. Meanwhile, using other maneuvers, again at presumably lower moments and

forces than DVR, studies have reported intraoperative pedicle fracture and screw loosening.[110,179,228] For example, in a study by Di Silvestre *et al*.,[179] 13% of patients suffered pedicle screw fracture – 12 during pedicle screw insertion, and 3 during a rod rotation maneuver. These are potentially debilitating complications, particularly in patients with right thoracic scoliosis whose aorta is positioned more laterally and posteriorly,[229] where lateral pedicle screw plow could cause aortic abutment or severe aortic injury. Aside from intraoperative complications, other studies have reported pedicle screw-related aortic injury during follow-up.[230] Moreover, the true incidence of aortic and vascular injury is unknown, and likely, underreported.[230,231] The underreported risk may be partly due to the lack of postoperative CT scans in DVR follow-up reports,[119,126,169,173,177,223-227,232-236] since postoperative CT has been shown to be crucial in identifying high risk pedicle screws.

Furthermore, the risk of screw loosening and loss of screw purchase may be higher than reported due to the high incidence of pedicle screw malplacement. For example, in a study by Sarlak *et al*.,[237] 30% of pedicle screws were misplaced, of which 24 screws were deemed to have significant risk to the aorta and other vascular and airway structures. Moreover, Hicks *et al*.[238] reported an overall 15% pedicle screw malpositioning rate amongst studies with postoperative CT scans. In turn, in a typical AIS patient with 16 pedicle screws,[239] for example, and given a screw malpositioning rate of 15%,[238] the occurrence of that patient suffering from a misplaced pedicle screw may be unavoidable. As the "biological limitations of the vertebrae are approached" using DVR,[128] the overall construct strength following surgery may be compromised, particularly in these cases of misplaced pedicle screws.

In addition to the intraoperative risks of such high magnitude loading, the long-term risks of such surgeries are unknown. Paik *et al*.[240] demonstrated significantly lower pedicle screw pullout strength following a rod reduction maneuver compared to pedicle screw pullout strength prior to surgical loading. In DVR, where the applied moments and forces are presumably larger than those applied during rod reduction,[7] similar results should be expected.

The biomechanical literature suggests significant risks to the spine at such high torque magnitudes as well. Specifically, in the lumbar spine, flexion-to-failure tests have reported ultimate failure ranging from 59 Nm – 156 Nm.[241,242] Miller *et al*. evaluated the strength of lumbar FSUs and reported no specimen failures before 59 Nm in bending or torsion;[243] however, failure moments were not reported. In a recent study, Bisschop *et al*.[244] evaluated the ultimate torsional failure strength of lumbar FSUs before and after laminectomy. Specimens with high bone mineral density failed at an average of 58.9 Nm (43.8-79.2 Nm), while specimens with poor bone quality failed as low as 23.7 Nm. These reported values are all substantially smaller than the 100 Nm reportedly applied clinically during deformity correction surgery.[7] Further, it would be expected that the strength of the thoracic spine compared to that of the lumbar spine would be substantially weaker.

In addition to the overall strength of the spine, screw-bone failures have been reported at substantially lower torque magnitudes. Parent *et al.*[142] applied a transverse force to pedicle screws inserted in cadaveric thoracic spine vertebra and measured yield torques of 12.0 ± 4.9 Nm in the medial direction and 11.5 ± 5.1 Nm in the lateral direction, averaged over T4-L5 vertebra. Similarly, Cheng *et al.*[245] applied rotational torques through a clinically used vertebral column manipulator to thoracic spine segments for DVR, simulating the correction torques applied in

surgery. The authors compared the failure torques of the pedicle screw-bone interfaces when applying the rotational moment through a single screw, single level bilaterally linked screws, multilevel unilaterally linked screws, and quadrangular linkages. The failure torques for single screw linkages were similar to those reported by Parent *et al*.[245], with failure torques of 4.0 ± 1.4 Nm and 6.1 ± 2.5 Nm for medially and laterally rotated screws in T4 vertebra, respectively. However, new pedicle screw instrumentation allows for screw linkages to distribute the load amongst several screw-bone interfaces. Simulating a typical quadrangular linkage, that is bilateral pedicle screws linked amongst 4-vertebrae, Cheng *et al.* showed an average failure torque of 42.5 ± 16.5 Nm.[245]

However despite these findings, to date, the magnitude of torque that can be safely applied during deformity correction surgery has not been sufficiently quantified in the literature. Previous studies have shown that (1) pedicle screws are stronger than previous constructs, such as hooks and wires, with axial pullout strengths between 344 N – 1646 N;[103,104,246,247] (2) pedicle screws have stronger tangential strengths than previous constructs;[103] (3) pedicle screws exhibit lateral and medial strengths, when applied through a typical surgical lever arm, of between 4 and 12 Nm;[142,245] and (4) with more bone-screw interfaces, medial-lateral strength increases, with an average yield torque of over 40 Nm.[245] However, the effect of these surgical loads and torques affect the rotation of the motion segment and the health of the intervertebral disc at the level of correction are unknown. Moreover, the loads at which the risk of screw plow and intraoperative spine failure would outweigh the incremental increase in deformity correction have not been established. Unfortunately, these questions cannot be answered with the typical pure moment testing model and approaches.

As far back as the 1960s, the potential benefit of understanding clinical spine problems through in-vitro and bench top experiments was clear. The need was made clearer in the 1980s, as the development of new devices and implants for spine surgery expanded rapidly.[17,248] Even in those days, studies emphasized the importance of testing implants and devices using in-vitro biomechanical tests, prior to implanting the implants in patients.[249] As posterior-only procedures, techniques, and devices continue to evolve, and continue to increase in popularity, the need for biomechanical spine testing is as significant as ever. Moreover, the accuracy, sophistication, predictability, and clinical relevance of the in-vitro testing methods must parallel the growth of these surgical techniques and implant technologies.

1.6 Purpose and Aims of Proposed Study

While much has been learned from *Pure Moment* testing, including the basic properties of the thoracic spine and the strength and stability of various thoracic spine devices,[35,46,47,51] previous studies have failed to comprehensively answer several clinical questions. This has been particularly true in the field of scoliosis, where intraoperative procedures have been questioned and untested, ultimately resulting in conflicting evidence and, in turn, clinical risk.[110-112,127,128,163,179,228,230,231] As the *Pure Moment* model was not selected to produce intraoperative loading or surgical motions,[17] expansion of and improvement to the preclinical testing of spine deformity is necessary to better simulate such conditions and predict the clinical outcome of deformity correction surgery.

The current work demonstrates a case where the current testing model fails to comprehensively describe and predict clinical performance. In the current work, preclinical in-vitro testing of spine deformity surgery was performed to (1) evaluate the validity of pure moment testing for scoliosis biomechanics, (2) expand on the knowledge of thoracic spine properties and motion response to loading, (3) quantify the potential of specific posterior releases and posterior correction maneuvers for correcting spine deformity, and (4) define the safety limits of the thoracic spine under a typical correction maneuver.

The proposed work aims to:

1. Evaluate hemi-thoracic (5-level) spine flexibility in under standard *Pure Moments* in flexion-extension, lateral bending, and axial rotation as a function of four conditions: intact, and following three sequential wide posterior-only surgical releases.

2. Evaluate full thoracic spine flexibility under standard *Pure Moments* in flexion-extension, lateral bending, and axial rotation as a function of six conditions: intact, following standard *en-bloc* releases, and following four sequential wide posterior-only surgical releases.

3. Evaluate full thoracic spine flexibility under a novel combined multi-planar loading protocol producing flexion-extension with combined axial rotation, and lateral bending with combined axial rotation, as a function of six conditions: intact, following standard *en bloc* releases, and following four sequential wide posterior-only releases.

4. Design a custom direct vertebral rotation (DVR) simulator to accurately and reproducibly simulate surgical correction forces for in-vitro preclinical testing of deformity correction surgery.

5. Evaluate T10-T11 thoracic spine flexibility under simulated DVR.

6. Compare the three loading modes for the preclinical prediction of potential deformity correction: pure moments, combined multi-planar loading, and DVR simulation.

7. Establish the torsional limits of the thoracic spine under simulated DVR.

8. Evaluate the results from single-plane, multi-planar, and simulated DVR loading as a function of intervertebral disc health to improve the applicability of preclinical models for AIS.

9. Establish normal distributions of thoracic spine motion reported in the literature using in-vitro testing methods for a basis of comparison for the results produced in the above aims.

In its entirety, the study provides a detailed quantification of the effects of pure moments, combined moments, and simulated surgical moments on thoracic spine flexibility and behavior. Additionally, the study helps to provide clinical guidelines for safe torque limits in deformity surgery, and quantify deformity correction potential using specific releases. This study provides an example of the potential of non-standard testing to evaluate specific clinical questions. With such work, biomechanical results will be more applicable to clinical questions, and may potentially begin to have a greater impact on clinical decision making and clinical outcome in the fields of spine deformity.

2 Materials and Methods

2.1 Overview

The experimental protocol was designed to achieve the ***Aims*** (9) of the study, listed in the previous section (Section 1.6). The aims were achieved by applying in-vitro loading to human cadaveric thoracic spines, before and after posterior-release (Table 2).

Table 2. Experimental Summary

			Intact	Facetectomies	Ponte Osteotomy	Sequential Osteotomies
Experiment	Loading	Total Number of Specimens (N)	Number of Specimens Tested (n)			
1	Pure Moments	27	27	10	27	17
2	Multi-Planar	10	10	10	10	10
3	Simulated DVR	11	X	x	11	x
4	DVR-to-Failure	11	X	x	11	x

Four types of loading were applied: (1) *Single Plane Pure Moments*; (2) *Multi-Planar Loading*; (3) *Intraoperative Simulation*; and (4) *DVR-to-Failure*.

(1) *Single Plane Pure Moments*

Single Plane Pure Moment testing is the standard loading protocol universally applied throughout the literature for spine biomechanics, in-vitro spine testing, and characterization of spine kinematics before and after surgical release, injury, or implantation of a fixation device. The *Single Plane Pure Moment* tests were used to establish the benefits, drawbacks, and limitations of their use for preclinical scoliosis biomechanics. The testing was designed to achieve ***Aim 1*** and ***Aim 2***.

(2) *Multi-Planar Loading*

Following *Single Plane Pure Moments*, a custom-designed novel *Multi-Planar Loading* protocol was applied. The *Multi-Planar Loading* protocol was designed to evaluate the effects of combined moments on thoracic spine ROM before and after posterior-release. The combined moments provide a better representation of the types of loads applied intraoperatively, which are often three-dimensional. These multi-planar loads and moments are typically necessary in cases of scoliosis, where the deformity presents in three-dimensions, with abnormal rotations, i.e. deformity, in the axial, sagittal, and coronal planes. The *Multi-Planar Loading* tests were designed to achieve ***Aim 3***.

(3) *Intraoperative Simulation of Direct Vertebral Rotation (DVR)*

A custom-designed simulator was designed to simulate and replicate a typical surgical maneuver employed intraoperatively in cases of adolescent idiopathic scoliosis. Specifically, the custom-designed simulator applied simulated Direct Vertebral Rotation, producing a representative surgical correction maneuver, as well as replicating high-magnitude intraoperative moments. The *Intraoperative Simulation* was designed to achieve ***Aim 4*** and ***Aim 5***.

Additionally, following these tests, the results from the three previous loading protocols, that is, *Single Plane Pure Moments*, *Multi-Planar Loading*, and *Intraoperative Simulation*, were compared to evaluate the effectiveness and clinical relevance of each schematic. This analysis was designed to achieve ***Aim 6***.

(4) *DVR-to-Failure*

Finally, and following loading according to the *Intraoperative Simulation*, simulated *DVR-to-Failure* was applied to evaluate the torsional strength of the thoracic spine under axial rotation moment and to define safety limits under a typical surgical maneuver. These tests were designed to achieve ***Aim 7***.

Following the completion of loading according to *Single Plane Pure Moments*, *Multi-Planar Loading*, *Intraoperative Simulation*, and *DVR-to-Failure*, subsequent radiographic and histological analyses were performed to evaluate the intervertebral disc health of the tested specimens. The results of the above loading protocols were then re-analyzed as a function of specimen health to evaluate the usefulness and improve the applicability of using human cadaveric spines in preclinical studies of spine deformity. This analysis was designed to achieve ***Aim 8***.

Finally, numerous studies have reported the ROM of cadaveric thoracic spines. However, while there are generally established testing methods, e.g. pure moments, the specific parameters vary widely among different studies, such as loading rate, loading magnitude, and specimen condition. In part due to the wide variability amongst studies, the distribution of ROM in each segment of the thoracic region in the normal population has not been established. Therefore, a systematic MEDLINE search was performed to identify all of the studies in the literature which have reported cadaver thoracic spine motion. The reported results from the identified articles were reanalyzed to estimate the typical ROM at each segment of the thoracic spine in each of the three anatomical planes. This analysis was designed to achieve ***Aim 9***. Additionally, the analysis served as a baseline to compare the results of the biomechanical tests herein.

The results from the tests and analyses described above evaluated the typically used testing standard (*pure moments*), novel multi-planar moment protocols, and surgical simulations. In their entirety, the results provide a quantitative description of spine flexibility and strength before and after surgical release to quantify the correction potential and to define the safety limits of typically used intraoperative surgical techniques for deformity correction surgery.

2.2 Specimens

2.2.1 Cadaveric Specimens

24 fresh-frozen full-length human cadaveric thoracic spines were obtained from the International Institute for the Advancement of Medicine (IIAM, Jessup, PA) and Science Care (Science Care, Phoenix, AZ). Specimens were wrapped in saline-soaked gauze, and frozen in a -20º freezer prior to testing.[24]

The 24 thoracic spine specimens were separated into the following groups:

Group A: n=7 hemi-thoracic spines (T1-T6 or T7-T12)

Group B: n=10 full-length thoracic spines (T1-T12)

Group C: n=10 full-length thoracic spines (T1-T12)

2.2.2 Radiographic Analyses

Prior to testing, anterior-posterior and lateral radiographs of each spine were taken in the laboratory using an HP Faxitron Series™ x-ray system (438O5N, Hewlett Packard Company, Palo Alto, California) at standard 15% magnification. Radiographic analysis was performed on each specimen to determine disc and bone health. Each x-ray was evaluated for signs of gross deformity (i.e. scoliosis or kyphosis), tumors, or other diseases and abnormalities. Specimens with severe abnormalities were replaced.

In addition to standard AP and lateral radiographs, the bone mineral density (BMD) of each thoracic spine was determined by dual-energy x-ray absorptiometry (DEXA) using a Hologic 2000 bone densitometer (Hologic, Inc., Waltham, MA). The DEXA scans were

analyzed to exclude any specimens with abnormally poor bone quality. While t- and z- scores cannot be assessed for the thoracic spine, the raw BMD score can provide a general sense of the overall bone quality of each vertebral body.

Finally, specimens in ***Group C*** also imaged using MRI prior to testing. Both T1 and T2 weighted sagittal images were taken to determine the disc health of each specimen.

2.2.3 Dissection and Specimen Preparations

Prior to testing, specimens were removed from the -20º freezer and thawed at room temperature. Each thoracic spine was dissected of all skin, muscle and fat tissues, while maintaining the integrity of all vertebrae, posterior elements, bony structures, intervertebral discs, stabilizing ligaments, the posterior 5 cm of the ribs, and the costovertebral joints. Specifically, the following ligaments were kept intact: anterior longitudinal ligament (ALL), posterior longitudinal ligament (PLL), facet capsular ligament, ligamentum flavum, interspinous ligament, and supraspinous ligament. Previous studies in the spine biomechanics literature have routinely performed similar dissections prior to biomechanical testing.[13,29] In addition, the freezing and thawing procedures have been established in the literature to preserve the biomechanical properties of the cadaveric spine specimens.[24,174] Following thawing and dissection, the duration of mechanical testing on a given specimen was concluded within one day.

2.2.4 Potting and Alignment

Following pre-experimental radiographic analysis, each thoracic spine was potted and aligned for mounting in the spine simulator. The superior and inferior vertebra(s) of each

dissected spine segment were placed in a cylindrical fixture, 10 cm in diameter, and were potted in a low-temperature setting epoxy resin. In order to enhance the fixation of the spine within the epoxy resin pot, four to six 1.5-inch long, size 10 screws were screwed partway into the vertebral bodies.

For the specimens in ***Group A***, T1 (cranial) and T6 (caudal) were potted in the upper hemi-thoracic segments, and T7 (cranial) and T12 (caudal) were potted in the lower hemi-thoracic segments. For the specimens in ***Group B***, T1 (cranial) and T12 (caudal) were potted. For the specimens in ***Group C***, T1 was potted cranially, in addition to both T11 and T12 caudally. Note that in ***Group C***, both T11 and T12 were potted together to increase the fixation strength of the pot to withstand the high-magnitude applied moments.

Each potted vertebra was placed inside a 15-cm diameter aluminum mounting ring designed for aligning the anatomical planes of the spine with the axes of the load frame. For this alignment, two tri-planar laser levels were used (Stanley Crossline Level Max-CL2, Stanley Tools Product Group, CT). Using 16 pointed-tip stainless steel screws mounted on the ring and piercing the sidewall of the epoxy, the position of the pot was adjusted within the aluminum mounting ring to align the coronal plane (through the center of the vertebral body) and median planes of the vertebra with the axes of the load frame. The laser levels were set up to ensure proper alignment, verifying the planes against the anatomical landmarks on each vertebral body (i.e. spinous process, anterior longitudinal ligament, and intervertebral disc space), as well as against engraved lines on each of the aluminum mounting rings.

2.3 Experiments

2.3.1 Single Plane Pure Moments

2.3.1.1 Overview

Aim 1 and ***Aim 2*** were achieved by applying the standard in-vitro protocol to human cadaveric thoracic spines before and after sequential release. Specifically, *Single Plane Pure Moments* were applied to both hemi-thoracic segments and full-length thoracic spines.

2.3.1.2 Specimens

All specimens in ***Groups A***, ***B***, and ***C*** underwent *Single Plane Pure Moments* testing, according to the following protocol.

2.3.1.3 Load Frame

Following specimen preparation, pre-experimental radiographic analysis, and potting, each spine specimen was mounted in an MTS 858 8-degree of freedom mini-bionix servo-hydraulic load frame equipped complete with the Flextest System (MTS Systems, Minneapolis, MN), previously described (Figure 1).[28,34]

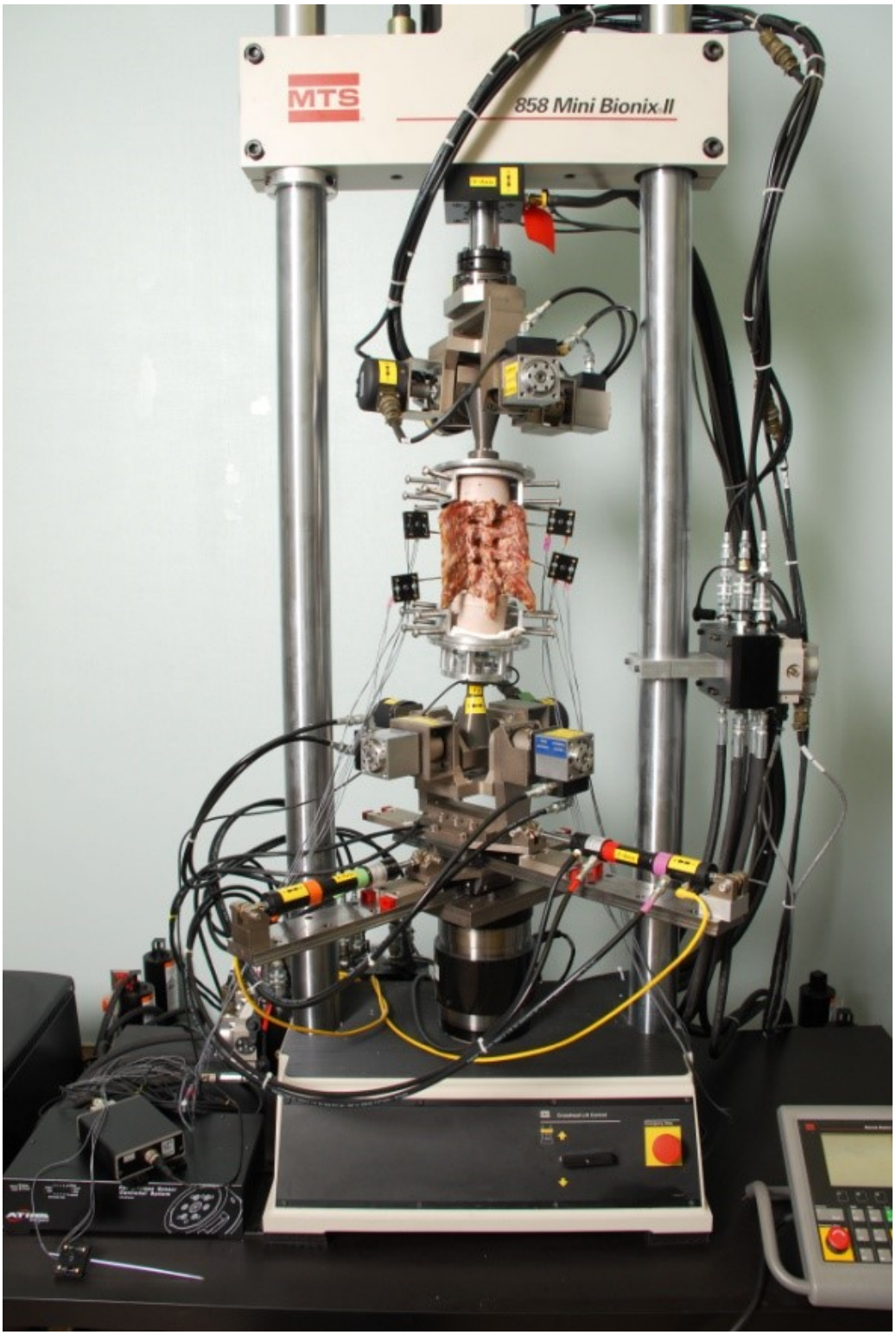

Figure 1. *Single Plane* pure moments experimental setup, with hemi-thoracic spine segment from *Group A*.[28]

For the single plane pure moment loading, each specimen was mounted in an inverted position such that the cranial vertebra was attached to the lower gimbals of the load frame and the caudal vertebra was attached to the upper gimbals of the load frame. In total, the spine machine was capable of independently controlling 8-*degrees of freedom* (Figure 2).

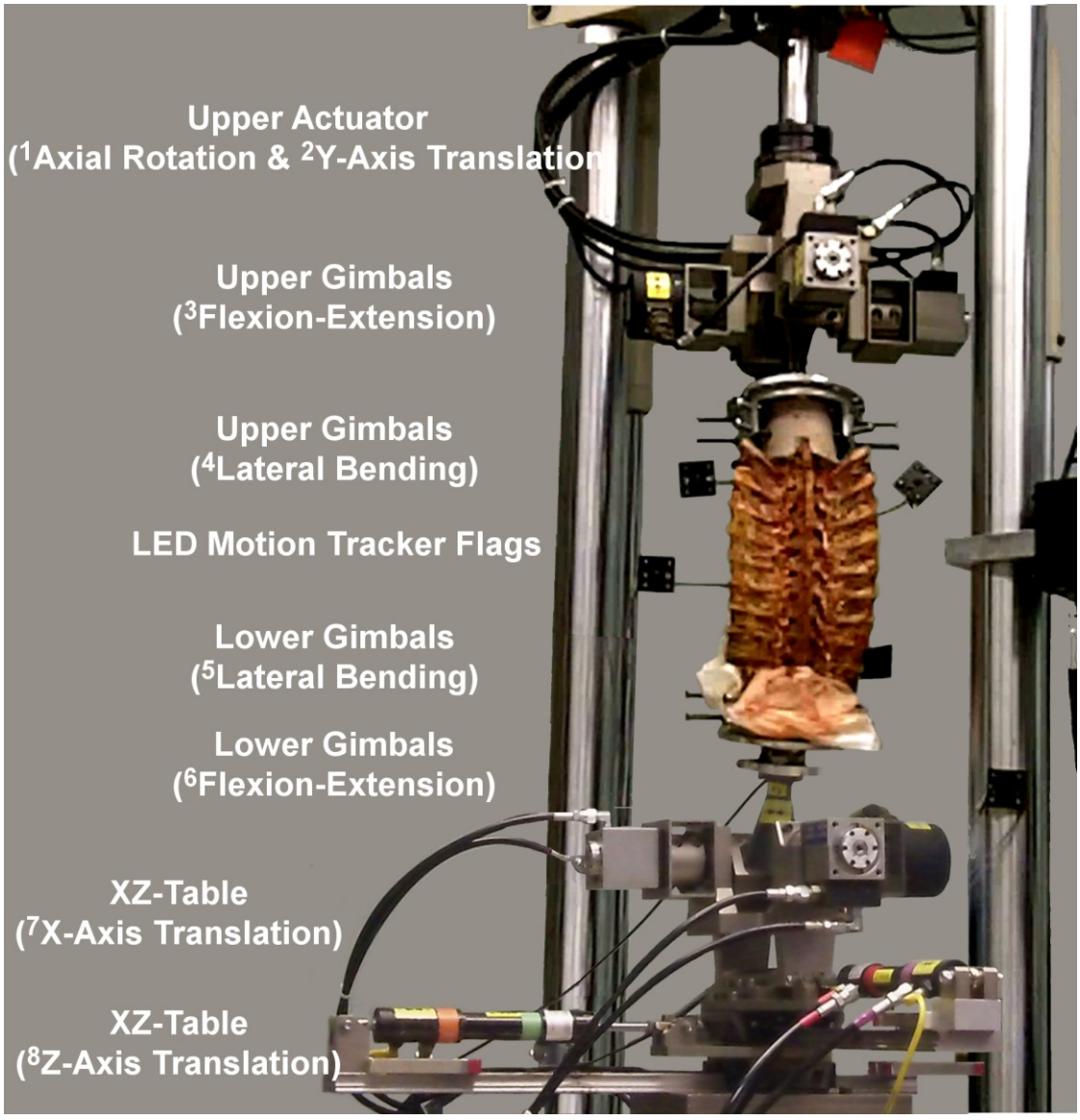

Figure 2. Representative photo of the experimental setup of specimens in *Group B and Group C*, and the 8-*dof* spine simulator. The degrees of freedom are denoted by the superscripts 1-8.[250]

The upper gimbals were attached to an axial-torsional actuator, together providing 4-degrees of freedom at the top of the machine: tension-compression (y-axis translation), axial torsion (rotation about the y-axis), superior flexion-extension (rotation about the x-axis), and superior lateral bending (rotation about the z-axis). The bottom gimbals were attached to a custom x-z table with two perpendicular linear bearings allowing transverse plane translation, together providing the remaining 4-degrees of freedom: x-axis translation, z-axis translation, inferior flexion-extension, and inferior lateral bending.

The x-axis translation and z-axis translation (transverse plane translation) were unconstrained to allow free translation in the transverse plane, effectively minimizing shear. Pure moments were applied such that the primary rotation was controlled, while the off-axis rotations were free to rotate.

Specifically, in flexion-extension,

- The inferior gimbals were controlled to produce flexion-extension rotation, with the upper gimbals flexion-extension rotation slaved, i.e. to match the bottom.
- The axial load was maintained at 0 N, allowing freedom in y-translation, i.e. cranial-caudal displacement.
- The lateral bending moment was maintained at 0 Nm, allowing freedom in lateral bending rotation.
- The torsional moment was maintained at 0 Nm, allowing freedom in axial rotation.

In lateral bending,

- The inferior gimbals was controlled to produce lateral bending rotation, with the upper gimbals lateral bending rotation slaved, i.e. to match the bottom.
- The axial load was maintained at 0 N, allowing freedom in y-translation, i.e. cranial-caudal displacement.
- The flexion-extension moment was maintained at 0 Nm, allowing freedom in flexion-extension rotation.
- The torsional moment was maintained at 0 Nm, allowing freedom in axial rotation.

In axial rotation,

- The upper actuator was controlled to produce axial rotation.
- The axial load was maintained at 0 N, allowing freedom in y-translation, i.e. cranial-caudal displacement.
- The lateral bending moment was maintained at 0 Nm, allowing freedom in lateral bending rotation.
- The flexion-extension moment was maintained at 0 Nm, allowing freedom in flexion-extension rotation.

2.3.1.4 Loading Protocol

Pure moments were applied using a hybrid loading scheme, with both position controlled rotation and moment controlled endpoints. Specifically, pure moments were applied in position (rotation) control at a rate of 0.5°/s until the maximum moment (M_{max}) is achieved. This protocol

was applied to produce the following pure moments: flexion-extension ($\pm M_{max}$), bilateral lateral bending ($\pm M_{max}$), and bidirectional axial rotation ($\pm M_{max}$). The moments were applied through the upper and lower gimbals for both flexion-extension and lateral bending testing, and through the axial-torsional actuator for axial rotation. Each pure moment was applied for five cycles, with the first two/three cycles used to precondition the specimen and the third/fourth cycle used for analysis. These methods were described according to the biomechanical testing standards in the literature to effectively minimize viscoelastic effects.[24]

For each of the three testing groups (***Group A***, ***Group B***, and ***Group C***), the following maximum moments were applied:

Group A: $M_{max} = \pm 6$ Nm

The maximum moment was chosen based on the typical range of moments applied in previous thoracic spine biomechanics studies. As deformity correction surgery involves the application of large correctional forces, an aggressive in-vitro magnitude was employed, i.e. ±6 Nm.

Wilke *et al*.[24] suggested pure moment magnitudes of ±7.5 Nm for the lumbar spine, ±5 Nm for the thoracic spine, and ±2.5 Nm for the cervical spine. Therefore, the value chosen in the present study for ***Group A***, that is ±6Nm, is similar to the value proposed by that particular article for thoracic spines. Other studies in the literature have also tested thoracic spines with the maximum moment of ±6 Nm.[35,185,251] Throughout the entire literature, moment magnitudes have been applied from as little as ±2Nm[27] to as much as ±7.6 Nm.[43] At ±6Nm, the magnitudes are well within the range of magnitudes applied in previous studies, and are small enough in magnitude to maintain stability in the machine throughout single-plane loading.

Group B: M_{max} = ±4 Nm

In this case, i.e. ***Group B***, a more conservative maximum moment (±4 Nm) was selected due to the higher risk of instability in the load frame with full-length thoracic spines. The ±4 Nm also falls well within the range applied in previous studies (2-7.6 Nm),[27,43] and has been applied in previous thoracic spine studies.[41,47,252]

Group C: M_{max} = ±4 Nm

Similar to ***Group B***, the conservative maximum moment (±4 Nm) was chosen in ***Group C*** to prevent instability in the machine with full-length thoracic spines.

2.3.1.5 Specimen Conditions

Group A: n=7 hemi-thoracic spine specimens

Specimens in ***Group A*** were tested in four conditions: (1) intact, and after three sequential Ponte osteotomies at (2) T2-T3 for superior hemi-thoracic segments (or T7-T8 for inferior hemi-thoracic segments), (3) T3-T4 (or T8-T9), and (4) T4-T5 (or T9-T10).

The sequence of releases for ***Group A*** specimens was chosen to evaluate the effects of sequential Ponte osteotomies on thoracic spine motion in all three planes, as compared to the intact condition.

Group B: n=10 full-length thoracic spine specimens

Specimens in ***Group B*** were tested in 6 conditions: (1) intact, (2) after 9 bilateral *en bloc* total facetectomies, and after four sequential Ponte osteotomies at (3) T7-T8, (4) T8-T9, (5) T6-T7, and (6) T9-T10.

The sequence of releases for ***Group B*** specimens was chosen to replicate the typical sequence of surgical releases that would be performed intraoperatively. In surgery, total facetectomies are typically performed at all instrumented levels. Therefore, testing following release (2) evaluated the effectiveness of *en bloc* total facetectomies in increasing the range of motion of the thoracic spine, as compared to the intact condition. Then, as would be performed clinically, sequential supplemental Ponte osteotomies were performed. This represents an important clinical decision making step in evaluating the usefulness of supplemental osteotomies as compared to the typically performed *en bloc* total facetectomies.

Group C: n=11 full-length thoracic spine specimens

Specimens in ***Group C*** were tested in three conditions: (1) intact, (2) after bilateral facetectomy at T10-T11, and (3) after Ponte osteotomy at T10-T11.

The sequence of releases for ***Group C*** specimens was chosen for the same reasons as those in ***Group B***, as described above.

The conditions outlined above are defined as follows:

Intact: The intact condition was the first condition tested in all groups, and consists of the thoracic spine segment dissected of all skin, muscle and fat tissue. The vertebrae, bony structures, intervertebral discs, stabilizing ligaments, posterior 5 cm of the ribs, and the

costovertebral joints were intact. The specific ligaments remaining intact included the anterior longitudinal ligament, posterior longitudinal ligament, facet capsular ligament, ligamentum flavum, interspinous ligament, and supraspinous ligament.

Note: For specimens in Group C, bilateral pedicle screws were inserted from T7-T10, prior to 'intact' testing. The primary level of interest, that is T10-T11, was intact as defined above. The levels from T7-T10 included bilateral total facetectomies for insertion of the pedicle screws. Previous studies have defined the 'intact' condition similarly in such cases.

Bilateral Total Facetectomy (Figure 3 and Figure 4): Each total facetectomy included the complete removal of the facet joints on both sides of the spine. The entire facet joint capsules were removed, while keeping intact the posterior ligaments, including the posterior longitudinal ligament, ligamentum flavum, interspinous and supraspinous ligaments.[110,161]

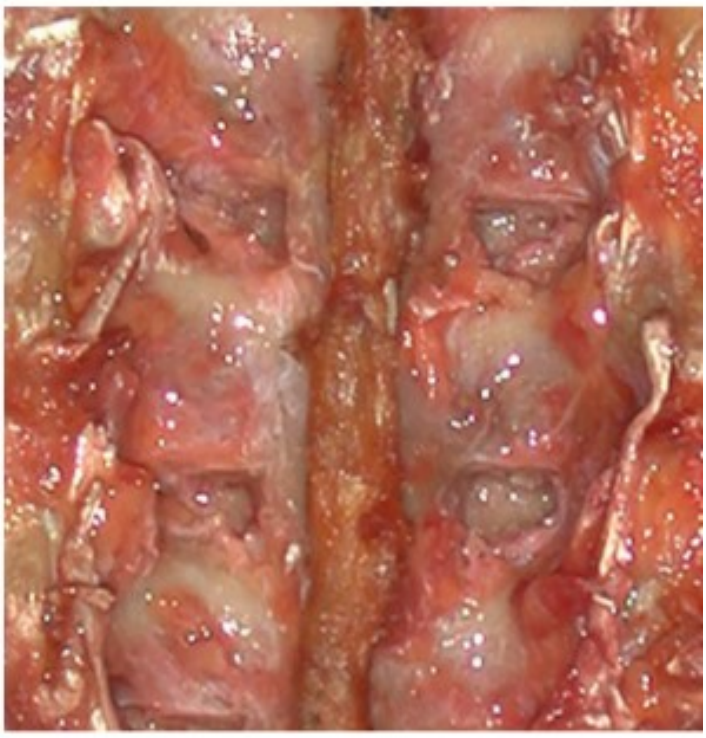

Figure 3. Representative bilateral total facetectomies at two adjacent levels of the thoracic spine.[250]

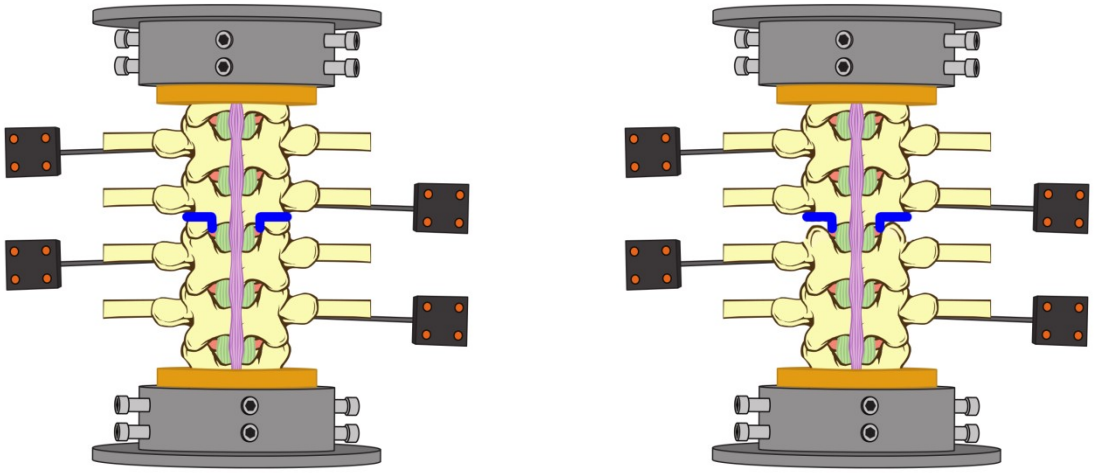

Figure 4. Representation of a bilateral total facetectomy in the coronal plane (posterior view) before (left) and after (right) bilateral facetectomy.

Ponte Osteotomy (Figure 5 and Figure 6): For each osteotomy, in addition to a bilateral total facetectomy, the following structures were resected: the inferior half of the spinous process of the vertebrae superior to the osteotomy site, the interspinous ligament, and the ligamentum flavum.[108]

a.)  b.) 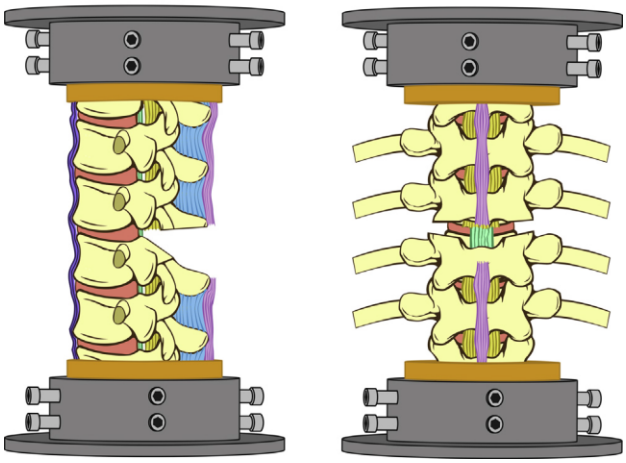

Figure 5. a.) Representative Ponte (chevron) osteotomies at two adjacent levels of the thoracic spine;[250] b.) Representation of Ponte osteotomy in the sagittal (left) and coronal (right) planes.[25]

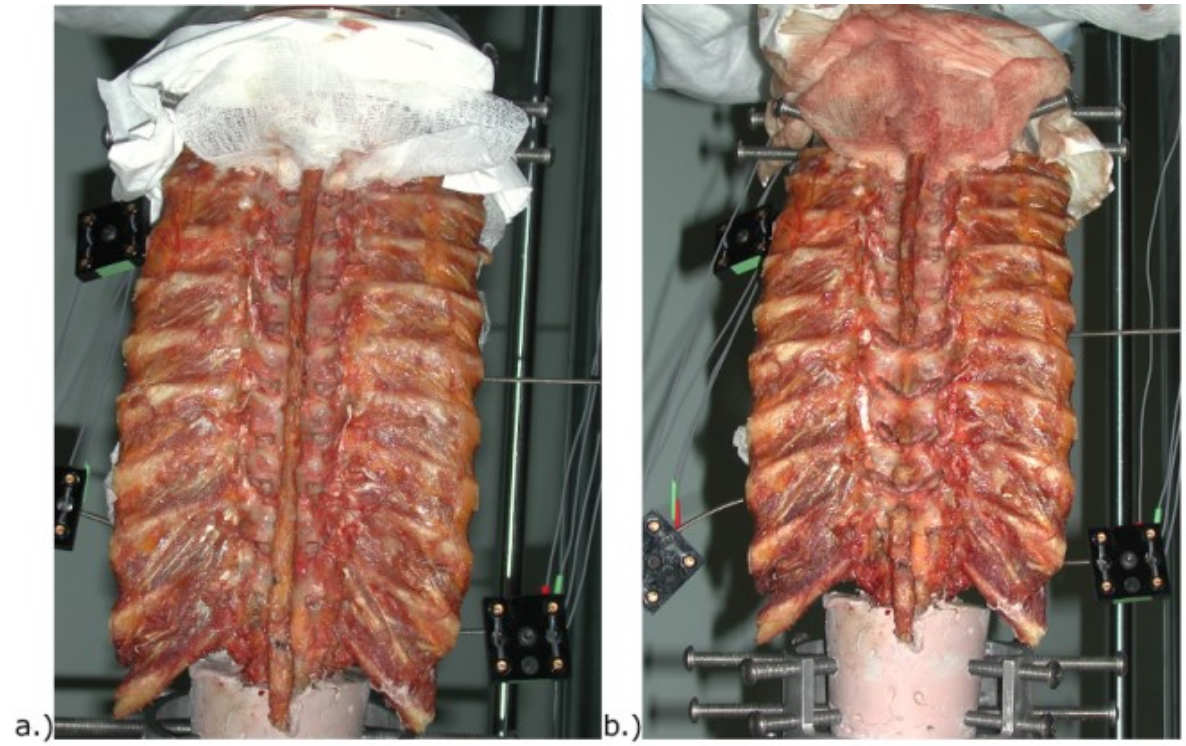

Figure 6. Representative photo of full-length cadaveric thoracic spine following a.) 9-*en bloc* bilateral total facetectomies (T2-T11), and following b.) 4 additional supplemental Ponte osteotomies (T6-T10).[250]

2.3.1.6 Range of Motion Measurements

To measure all of the 3D translations and rotations of all vertebrae of interest, an Optotrak 3020 Motion Capture System (Northern Digital Inc, Waterloo, Ontario, Canada) was used. The system has an accuracy of 0.1 mm and 0.1°, and a resolution of 0.01 mm. The accuracy and precision of this machine has been independently verified.[253] The system uses infrared light-emitting diode (LED) markers connected to the system. The positions of these LED markers are captured by three charge-coupled devices paired with three lenses at a total

sampling frequency speed of 3.5 kHz. The software calculates the 3D position for each marker and displays the coordinates for each marker position in real time.

First, a global reference frame was established by mounting a motion tracker flag to the MTS testing frame. A flag consists of four LED markers mounted in an approximately 2 sq. inch, non-collinear arrangement on a custom plastic mounting square. The global (MTS) reference frame was continuously measured with respect to the motion capture system's inherent location. This established a fixed coordinate reference frame, and minimized the effects of any vibrations of the MTS machine during loading.

Then, flags were attached to each of the vertebral bodies of interest in a given experiment. Each flag was mounted to vertebrae using a custom-designed probe apparatus. Specifically, depending on the size of a given vertebra, 0.5" to 1" bone screws were screwed into each vertebral body, alternating between the lateral left and right sides. For example, in upper hemi-thoracic segments, bone screws were inserted on the lateral left side of T2 and T4, and on the lateral right side of T3 and T5. Each bone screw was adapted to allow the insertion of a threaded probe into the screw head. After screw insertion, a threaded probe was inserted to each screw. Then, the motion flag was mounted on the opposite end of the probe, positioned such that the motion tracking system could view the location of the four LEDs throughout the progressions of spine bending and rotation.

For each group of specimens, flags were mounted in locations to allow specific analyses on each group of spines (Table 3). Specifically, in ***Group A***, flags were mounted on each of the unconstrained vertebral bodies, i.e. T2-T5 or T8-T11 (Figure 7). In ***Group B***, flags were

mounted on T2, T6, T10, and T11 (Figure 8). In ***Group C***, flags were mounted on T2, T7, T10, and T11.

Table 3. Motion Tracker Flag Arrangements and Range of Motion Calculation

Group	Segment	Instrumented Vertebrae	Total ROM (ROM_{TOTAL})	Local ROM
Group A	T1-T6 T7-T12	T2, T3, T4, T5 T8, T9, T10, T11	T2-T5 T8-T11	T2-T3; T3-T4; T4-T5 T8-T9; T9-T10; T10-T11
Group B	T1-T12	T2, T6, T10, T11	T2-T11	T6-T10; T10-T11
Group C	T1-T12	T2, T7, T10, T11	T2-T11	T10-T11

ROM, range of motion; T, thoracic

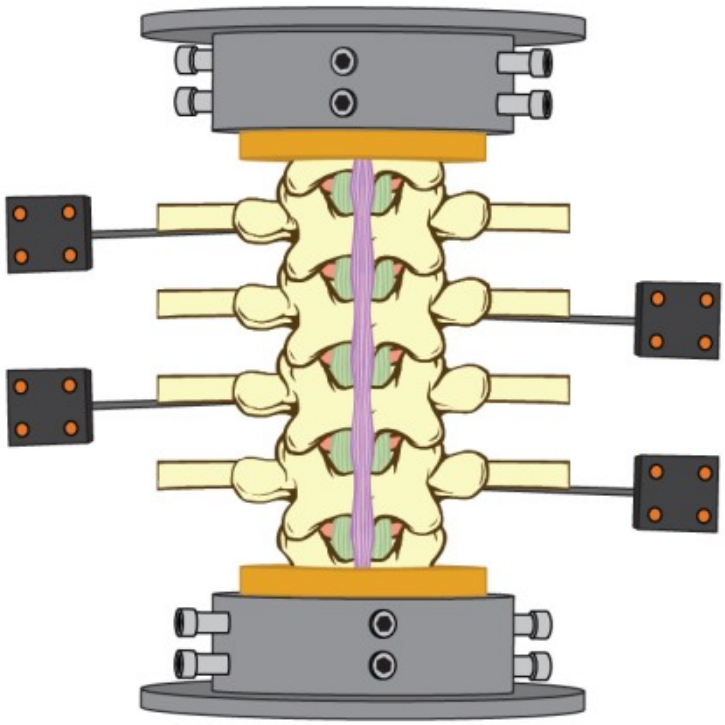

Figure 7. Representative photo depicting motion tracker flag locations for specimens in *Group A*, i.e. placing instrumentation at T2, T3, T4 and T5 in upper hemi-thoracic segments, or placing instrumentation at T8, T9, T10 and T11 in lower hemi-thoracic segments.

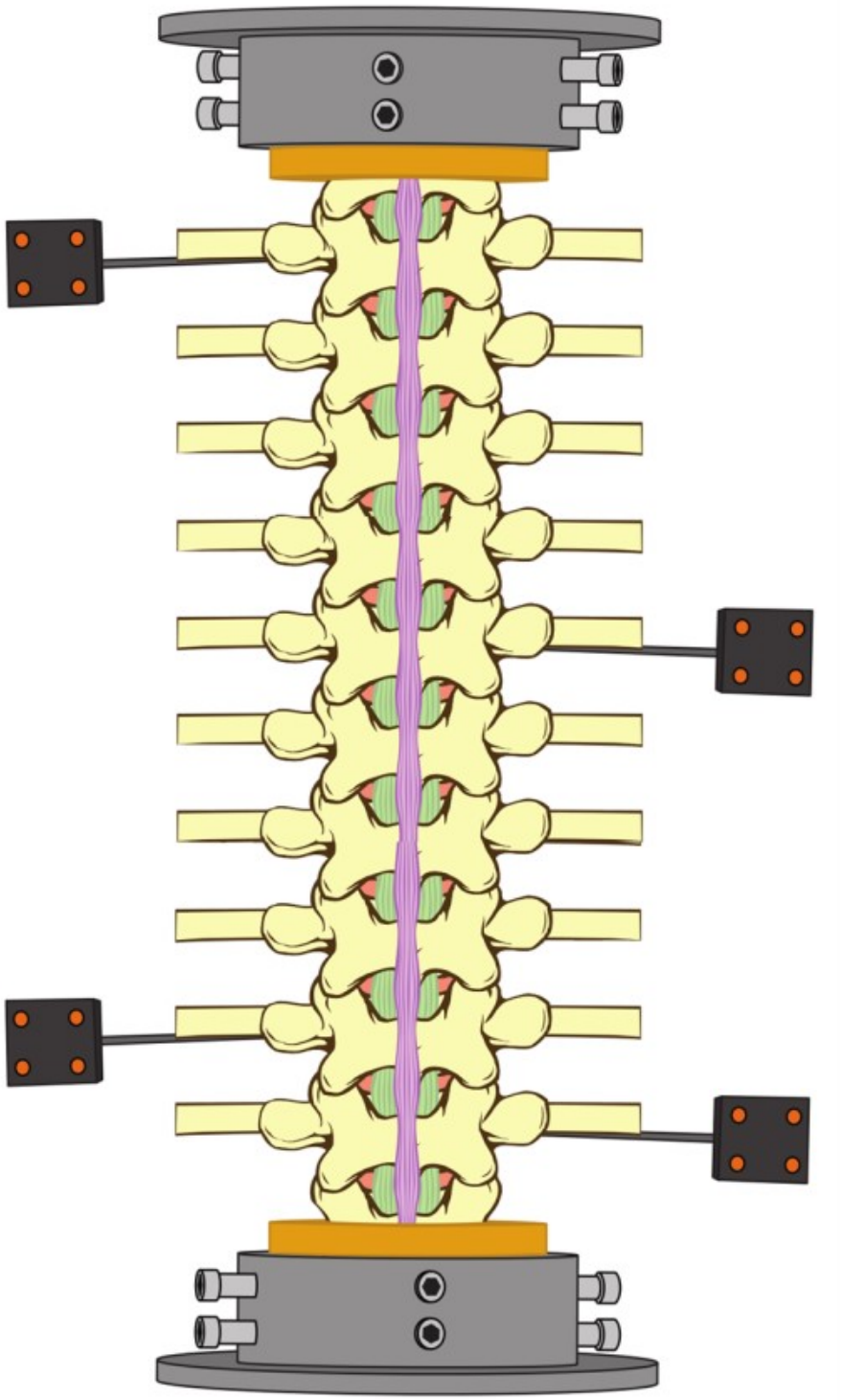

Figure 8. Representative photo depicting motion tracker flag locations for specimens in *Group B*, i.e. placing instrumentation at T2, T6, T10 and T11.

To create local reference frames for each of the four vertebral bodies, desired points on each instrumented body were digitized to create local coordinate axes. Three-dimensional range of motion in each plane was measured throughout testing. The motion tracking flags attached to each vertebra provided a set of three-dimensional coordinates on each vertebral body, which allowed real time tracking of the rigid body's three rotations and three translations. All range of motion measurements were calculated as the relative motion of the superior vertebra of interest with respect to the inferior vertebra of interest.[24] The relative motions were reported as Euler angles.[24]

Motion of each instrumented vertebrae was continuously recorded throughout all loading, and motion from the maximum loading steps, i.e. ± 6Nm for ***Group A*** and ± 4Nm for ***Group B*** and ***Group C***, was used for analysis. Total range of motion (ROM_{TOTAL}) was defined as the range of motion of the superior most instrumented vertebra with respect to the inferior most instrumented vertebra.

In addition to ROM_{TOTAL}, local ROM was recorded for specimens in each group. In ***Group A***, local ROM at each vertebral level was measured. Unlike ***Group A***, where three sequential posterior releases were performed on three levels, in ***Group B***, different releases were performed at different levels. Specifically, and as described earlier, 9 *en bloc* total bilateral facetectomies were performed from T2-T11. Then, sequential osteotomies were performed from T6-T10. Therefore, in addition to evaluating the increases in total ROM following each release, which compared the use of facetectomies at all levels with each supplemental osteotomy, a separate analysis was performed from T6-T10. The local T6-T10 ROM ($ROM_{T6\text{-}T10}$) was

evaluated to compare the use of four bilateral total facetectomies to 4 sequential osteotomies at the same levels.

Finally, in ***Group C***, local ROM at T10-T11 ($ROM_{T10\text{-}T11}$) was recorded intact, and following sequential releases, each of which was performed at the T10-T11 level.

For each of the above described ROM analyses, the primary and coupled motions were reduced. Primary ROM was defined as the motion of the spine in the direction of loading. For example, during flexion-extension loading, the primary ROM was rotation in the sagittal plane. Similarly, during axial rotation loading, the primary ROM was rotation in the transverse plane, and during lateral bending rotation, the primary ROM was rotation in the coronal plane. Coupled ROM was defined as the motions of the spine outside of the primary loading plane. For example, during flexion-extension loading where the primary ROM consisted of rotation in the sagittal plane, off-planar motions in the transverse and coronal planes were coupled motions. In other words, flexion-extension moments produced primary ROM in the sagittal plane, and simultaneously produced coupled ROM in the transverse and coronal plane.

2.3.1.7 Statistical Analyses

SPSS 15.0 statistical analysis software (IBM Corporation, Armonk, NY) was used to conduct all analyses. The statistical analysis was designed to evaluate the effects of surgical release on ROM in each of the loading directions. Paired-samples *t* tests were performed to compare measurements in the various specimen conditions. The *t* tests were repeated for measurements in each of the loading directions, that is, flexion-extension, lateral bending, and axial rotation. The specific tests are outlined below.

Group A: For ***Group A***, the total ROM (ROM_{T2-T5} or ROM_{T7-T11}) measurements following the intact condition were compared to the total ROM measurements following each of the sequential osteotomies using paired-samples *t* tests. Specifically, the following comparisons were performed: intact versus 1-level Ponte osteotomy, intact versus 2-level Ponte osteotomies, and intact versus 3-level Ponte osteotomies. Additionally, separate paired-samples *t* tests were performed to compare l-level Ponte osteotomy to 2-level Ponte osteotomies, and 2-level Ponte osteotomies to 3-level Ponte osteotomies.

For each of the comparisons described above, two separate paired-samples *t* tests were performed. First, a set of paired *t* tests were performed to compare the raw total ranges of motion (ROM_{total}), in degrees. Second, all ranges of motion were normalized against the intact condition, and subsequently reported as a percent increase in motion. A set of paired *t* tests were then performed to compare these normalized flexibility measurements (% increases).

Group B: Similarly, for ***Group B*** total ROM (ROM_{T2-T11}), the following comparisons to the intact condition were performed: intact versus 9 *en bloc* total facetectomies, intact versus 1-level Ponte osteotomy, intact versus 2-level Ponte osteotomy, intact versus 3-level Ponte osteotomy, and intact versus 4-level Ponte osteotomy. In addition, to determine the significance of each osteotomy as compared to the *en bloc* total facetectomies, the following comparisons were also performed: total facetectomies versus 1-level Ponte osteotomy, total facetectomies versus 2-level Ponte osteotomy, total facetectomies versus 3-level Ponte osteotomy, and total facetectomies versus 4-level Ponte osteotomy.

In addition to the above analyses, additional comparisons were made using the local ROM (ROM_{T6-T10}). In order to compare the effectiveness of 4 bilateral total facetectomies with 4

Ponte osteotomies at the same levels, $ROM_{T6\text{-}T10}$ was compared. Specifically, the following $ROM_{T6\text{-}T10}$ comparisons were made: intact versus 4 total bilateral facetectomies, intact versus 4 sequential Ponte osteotomies, and 4 total bilateral facetectomies versus 4 sequential Ponte osteotomies.

For each of the comparisons described above, two separate paired-samples *t* tests were performed. First, a set of paired *t* tests were performed to compare the raw ranges of motion, in degrees. Second, all ranges of motion were normalized against the intact condition, and subsequently reported as a percent increase in motion. A set of paired *t* tests was then performed to compare these normalized flexibility measurements (% increases). These tests were performed for the total ROM ($ROM_{T2\text{-}T11}$), as well as local ROM ($ROM_{T6\text{-}T10}$).

Group C: For ***Group C***, the following comparisons were performed: intact versus total facetectomies, intact versus 1-level Ponte osteotomy, and total facetectomies versus 1-level Ponte osteotomy.

For each of the comparisons described above, two separate paired-samples *t* tests were performed. First, a set of paired *t* tests were performed to compare the raw ranges of motion, in degrees. Second, all ranges of motion were normalized against the intact condition, and subsequently reported as a percent increase in motion. A set of paired *t* tests were then performed to compare these normalized flexibility measurements (% increases). These tests were performed for the local ROM ($ROM_{T10\text{-}T11}$) at the level in which the posterior releases were performed.

2.3.2 Multi-Planar Loading

2.3.2.1 Overview

Aim 3 was achieved by applying a novel multi-planar loading protocol to full-length human cadaveric thoracic spines before and after sequential release.

2.3.2.2 Specimens

Each of the 10 full-length cadaveric thoracic spines in specimen ***Group B*** underwent *Multi-Planar Loading*, according to the protocol outlined below.

2.3.2.3 Load Frame

For *Multi-Planar Loading*, all specimens were tested using the 8-degree-of-freedom MTS spine simulator, described earlier. The machine was configured with the same setup as *Single Plane Pure Moments*. Specifically, bending moments were applied through the upper and lower gimbals, while axial load (cranial-caudal) and torsional moments were applied through the upper actuator. Once again, the spine was free to translate in the transverse plane, as the xz-tables remained unconstrained. Similar to *Single Plane Pure Moments*, the axial load was maintained at 0N throughout loading, allowing cranial-caudal translation.

2.3.2.4 Loading Protocol

For *Multi-Planar Loading*, each specimen in ***Group B*** was tested in two simultaneous, multi-planar loading combinations:

(1) Axial rotation with combined flexion-extension

(2) Axial rotation with combined lateral bending

The *Single Plane Pure Moment* results were used to determine the single-plane flexibility of each spine in each plane (coronal, sagittal and transverse). Then, a multi-planar position of the caudal vertebra was predicted based on a combination of the single-plane rotations, using custom-derived formulations based on the gimbals of the machine (Figure 9).

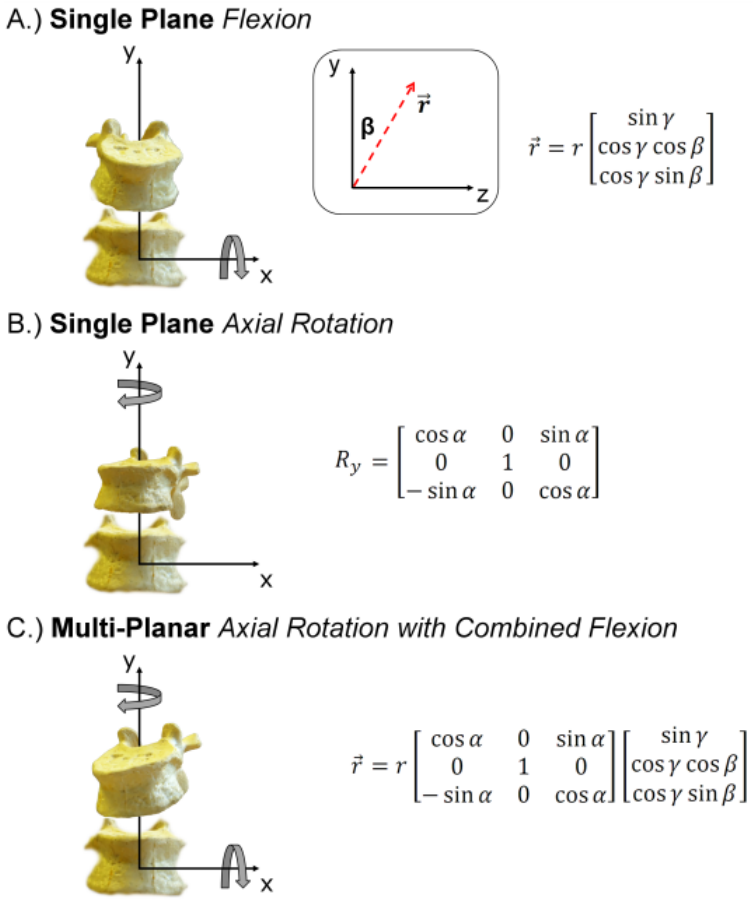

Figure 9. Schematic overview of the calculations performed to estimate and predict the gimbal positions for producing combined flexion with axial rotation. The calculation used the a.) flexion Euler angle and the b.) Euler angle in axial rotation measured during single plane pure moment testing of Group B specimens. From these Euler angles, the predicted c.) combined position was determined. The load frame was then programmed to rotate the spine towards this predicted position in space.[250]

An algorithm was then designed and implemented to simultaneously apply rotations about two anatomical axes, i.e. rotations in the transverse and sagittal planes, simulating axial rotation with combined flexion-extension, to produce motion towards the predicted end position. This entire procedure was then repeated for combined axial rotation and lateral bending, providing two multi-planar combinations in total.

Multi-Planar Loading Schematic Derivation

Controls

The 8-*degree-of-freedom* MTS spine simulator is equipped with a set of gimbals attached to the upper biaxial actuator of the machine. The gimbals allow for simultaneous and independent control of spine rotation about two orthogonal axes. Therefore, the full range of motion of the two gimbals parameterize a half-sphere, with the inner gimbals governing one rotation (γ), and outer gimbals governing a second rotation (β). In order to parameterize the half-sphere, an imaginary vector was created which represents the location of the center of the spine mounting plate, i.e. the plate to which a potted vertebral body is attached (Figure 10).

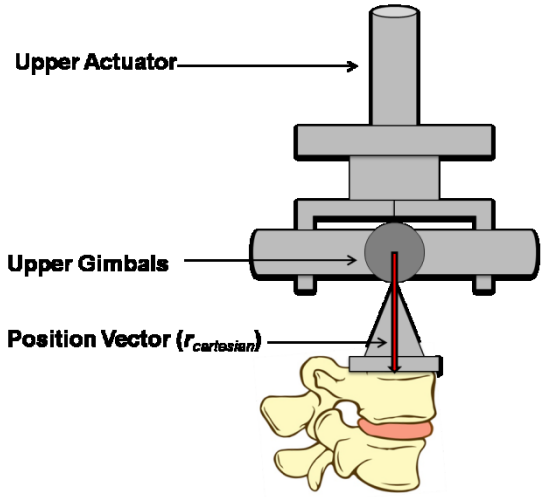

Figure 10. Position vector, representing the position of the mounting plate (vertebral body) with respect to the central axis of rotation of the two gimbals (inner and outer, i.e. flexion-extension and lateral bending rotations).

Throughout the following derivation, the assumption is made that the end of the position vector located at the center of the spine mounting plate approximates the position of the superior vertebral body, as the vertebral body is rigidly attached to the mounting plate. Moreover, the vertebral body is aligned with the axes of the plate, which in turn are aligned with the axes of the load frame.

The position vector, defined as the vector which describes the position of the mounting plate with respect to the central rotation axis of the gimbals, is defined by the following equation based on Cartesian coordinates: $r_{\mathbf{cartesian}} = r\,[sin(\gamma);\ cos(\gamma)cos\beta);\ cos(\gamma)sin(\beta)]$.

Note that in the above equation, when the gimbals are both in their neutral position, that is, when

$$\gamma = \beta = 0$$

, position vector points along the vertical axis of the machine, as intended:

$$\boldsymbol{r}_{cartesian} = r\begin{bmatrix}0\\1\\0\end{bmatrix}$$

If the gimbals were the only forms of rotation of the plate, this would be the final equation based on the gimbals rotations. However, a third rotation is possible as the orthogonal gimbals are rigidly connected to the upper rotational actuator. Specifically, rotation about the y-axis can be produced through torsional rotation of the upper actuator (α). This rotation about the y-axis, α, can be represented using the basic rotation matrix for rotation about the y-axis, $R_y(\alpha)$, as follows:

$$\boldsymbol{R_y}(\alpha) = \begin{bmatrix}\cos\alpha & 0 & \sin\alpha\\ 0 & 1 & 0\\ -\sin\alpha & 0 & \cos\alpha\end{bmatrix}$$

Now, incorporating the rotation about the y-axis (α), and the rotation about the x- and z-axes due to the gimbals (β,γ), the equation becomes:

$$\boldsymbol{r} = r\begin{bmatrix}\cos\alpha & 0 & -\sin\alpha\\ 0 & 1 & 0\\ \sin\alpha & 0 & \cos\alpha\end{bmatrix}\begin{bmatrix}\sin\gamma\\ \cos\gamma\cos\beta\\ \cos\gamma\sin\beta\end{bmatrix}$$

The final degree of freedom in the machine is translation along the y-axis, provided by the upper actuator of the machine. This is incorporate d by adding a simple linear translation term. The final equation then becomes:

$$\boldsymbol{r} = r\begin{bmatrix}\cos\alpha & 0 & -\sin\alpha \\ 0 & 1 & 0 \\ \sin\alpha & 0 & \cos\alpha\end{bmatrix}\begin{bmatrix}\sin\gamma \\ \cos\gamma\cos\beta \\ \cos\gamma\sin\beta\end{bmatrix} + \begin{bmatrix}0 \\ l \\ 0\end{bmatrix}$$

Here, *r* corresponds to the magnitude of the position vector (i.e. distance between center of rotation of the gimbals and the center position of the plate), the 3 x 3 matrix corresponds to the rotation about the y-axis, the 3 x 1 matrix corresponds to rotation of the inner and outer gimbals, , and *l* corresponds to the axial translation motion of the upper actuator.

As discussed, the above equation parameterizes a half sphere governed by the three controllable angles, α, β, and γ. By combining these parameters, the position vector of the plate, **r**, can describe any point of the half-sphere. Imagine now that we are viewing this problem from the stationary, global coordinate system, given by the gimbals. In this view, therefore, the global axes align with both the gimbals, and the anatomical axes of the spine. Because the combination of the machine parameters α, β and γ parameterize a half sphere, they also parameterize an infinite amount of half-circles, that when combined together, create the imaginary half sphere. When viewing the situation from the anatomical axes, in each two-dimensional plane, the sphere appears as a half-circle.

For the purpose of the present section, the derivation for combined axial rotation with flexion-extension is described.

In this case, the spine was controlled to rotate in flexion-extension, given an initial position in space. For this, the following convention was assumed:

Flexion-Extension: Rotation about the x-axis

Lateral Bending: Rotation about the z-axis

Axial Rotation: Rotation about the y-axis

Given an initial position, in order to create flexion, the spine was rotated along the path given by the circle in the yz-plane (anatomical sagittal plane). Given an initial position, x,y,z, in order to rotate the spine about the anatomical x-axis, $\vec{r}$ was rotated in the yz-plane in order to reach a new desired position, (x',y',z'). Given r', determined from the magnitude of *r* governed from the points (0, 0, 0) and (x, y, z), and inputting the desired angle of flexion, η, the new y- and z-coordinates, **y'** and **z',** were determined, as follows:

$$y' = r' \cos(\eta)$$

$$z' = r' \sin(\eta)$$

Where,

η ≡ Angle in anatomical coordinate system of rotation about the x-axis mapped on the yz-plane

r' ≡ magnitude of the imaginary vector drawing the radius of the circle created by rotating about the anatomical x-axis

y' ≡ new desired y-coordinate

z' ≡ new desired z-coordinate

Now, all three of the desired coordinates **x, y'**, and **z'**, have been determined. Notice, the x-coordinate has not changed from the initial x-coordinate, as a rotation would occur in only the yz-plane. Therefore, the new desired position is:

(x, y', z')

Therefore, to rotate the vector in the yz-plane by η, the position vector must rotate from (x,y,z) to (x,y',z'); however, η is not controllable by the gimbals. Instead, given these new coordinates, β and γ must be solved for to determine the controllable parameters to reach the desired location. More specifically, a combination of gimbal rotations, β and γ, must be determined which would produce rotation in the sagittal plane by η. Using the initial formulation for the position vector, $\vec{\boldsymbol{r}}$, a system of three equations was produced based on the expansion of the position vector equation, as follows:

$$\vec{\boldsymbol{r}} = r \begin{bmatrix} \cos(\alpha) & 0 & \sin(\alpha) \\ 0 & 1 & 0 \\ -\sin(\alpha) & 0 & \cos(\alpha) \end{bmatrix} \begin{bmatrix} \sin(\gamma) \\ \cos(\gamma)\cos(\beta) \\ \cos(\gamma)\sin(\beta) \end{bmatrix}$$

Following expansion, the system of equations for x, y, and z becomes,

$$x = r\cos(\alpha)\sin(\gamma) + r\sin(\alpha)\cos(\gamma)\sin(\beta)$$

$$y = r\cos(\gamma)\cos(\beta)$$

$$z = -r\sin(\alpha)\sin(\gamma) + r\cos(\alpha)\cos(\gamma)\sin(\beta)$$

Given this system of equations, and given α, x, y' and z', β and γ were determined.

Let

$$q = \cos(\alpha)$$

$$p = \sin(\alpha)$$

$$x = rq\sin(\gamma) + rp\cos(\gamma)\sin(\beta) \qquad (1)$$

$$y = r\cos(\gamma)\cos(\beta) \qquad (2)$$

$$z = -rp\sin(\gamma) + rq\cos(\gamma)\sin(\beta) \qquad (3)$$

From (3)

$$z + rp\sin(\gamma) = rq\cos(\gamma)\sin(\beta)$$

$$\cos(\gamma)\sin(\beta) = \frac{z + rp\sin(\gamma)}{rq}$$

Plug into (1) and solve for γ

$$x = rq\sin(\gamma) + rp\left[\frac{z + rp\sin(\gamma)}{rq}\right]$$

$$x = rq\sin(\gamma) + \frac{rpz}{rq} + \frac{r^2p^2\sin(\gamma)}{rq}$$

$$x = rq\sin(\gamma) + \frac{pz}{q} + \frac{rp^2\sin(\gamma)}{q}$$

$$x - \frac{pz}{q} = rq\sin(\gamma) + \frac{rp^2\sin(\gamma)}{q}$$

$$x - \frac{pz}{q} = \sin(\gamma)\left[rq + \frac{rp^2}{q}\right]$$

$$\sin(\gamma) = \frac{x - \frac{pz}{q}}{rq + \frac{rp^2}{q}}$$

$$\gamma = \sin^{-1}\left(\frac{x - \frac{pz}{q}}{rq + \frac{rp^2}{q}}\right)$$

With γ, plug into (2)

$$\cos(\beta) = \frac{y}{r\cos(\gamma)}$$

$$\beta = \cos^{-1}\left(\frac{y}{r\cos(\gamma)}\right)$$

Now, in order to move the spine in the anatomical plane of flexion-extension by η, the gimbals were moved by β and γ.

Combined Loading Path

From the above derivations, three major components can be controlled: (1) α, β, γ, (2) the position of **r**, and (3) anatomical-plane movements given any initial position of the actuator. With the combination of these controls, the combined protocol was established.

Because the superior gimbal axes rotate with rotation of the actuator, any combined position of the superior plate of the machine is sequence independent. For example, if the actuator is rotated by α and the superior gimbals by β, the position vector, **r**, would be equivalent to the vector created when the gimbals are first rotated by β and then rotated by α.

Given the initial single plane motions, established in *Single Plane Pure Moments*, the combined path was derived. For example, given α = 10° (single plane axial rotation ROM) and β = 10° (single plane flexion ROM), in order to create an idealized path of the combined motion, **r**

can be derived for all values of α and β, increasing each from 0° to 10°. Note that the smaller the increment of increase, the smoother the idealized path.

For this example, imagine that 1000 points were traced, as follows:

$$\alpha = 1{:}\,0.01{:}\,10$$

$$\beta = 1{:}\,0.01{:}\,10$$

$$\boldsymbol{r_{path}} = [\boldsymbol{x_i}, \boldsymbol{y_i}, \boldsymbol{z_i}]$$

$$i = 0{:}1000$$

With the above equations, the entire set of points, [x y z], along the path towards the combined position, are known. This path was created by increasing only two parameters, α and β. Now, in order to rotate the spine along this path by only creating anatomical movements, all three controlled parameters, α β and γ, must be controlled. Specifically, for example, once the actuators are rotated by α, the axes of the load frame and the gimbals no longer align with the anatomical axes of the specimen. Therefore, following rotation by α, a combination of β and γ must be applied in order to rotate in the anatomical sagittal plane by η.

To begin the process, the spine was first flexed by a given angle, β*. The position of the spine was then defined by the following:

$$\mathbf{r}\ (\alpha^*, \beta^*, \gamma^*) = [x_1, y_1, z_1]$$

Now, the spine had to be axially rotated. In order to axially rotate the spine, the x- and z-coordinates must change, while keeping the y coordinate constant, thus moving in the xz-plane (axial rotation). In order to follow the combined path, the spine had to be axially rotated back

towards the curve given by $\mathbf{r_{path}}$. To do so, the point at which y_1 is equivalent to the y-coordinate of a point along the combined path was determined. This point along the path is described by the following:

$$\boldsymbol{r_{path}} = [\hat{\boldsymbol{x}}, \hat{\boldsymbol{y}}, \hat{\boldsymbol{z}}]$$

As discussed, the y-coordinate remained constant. Therefore, the above equation becomes:

$$\boldsymbol{r_{path}} = [\hat{\boldsymbol{x}}, \hat{\boldsymbol{y}}, \hat{\boldsymbol{z}}] = [\hat{\boldsymbol{x}}, \boldsymbol{y_1}, \hat{\boldsymbol{z}}]$$

Then, given $\hat{\boldsymbol{x}}, \boldsymbol{y_1}, \hat{\boldsymbol{z}}$, **β*, and γ*** (remember, in this initial case, γ* = 0), α can be determined, given by the following derivation:

FOR γ ≠ 0,

Recall back to our original formulation of the position vector, **r**,

$$\vec{\boldsymbol{r}} = r \begin{bmatrix} \cos(\alpha) & 0 & \sin(\alpha) \\ 0 & 1 & 0 \\ -\sin(\alpha) & 0 & \cos(\alpha) \end{bmatrix} \begin{bmatrix} \sin(\gamma) \\ \cos(\gamma)\cos(\beta) \\ \cos(\gamma)\sin(\beta) \end{bmatrix}$$

The matrix form of **r** can be transformed into three equations for x, y and z.

$$x = r\cos(\alpha)\sin(\gamma) + r\sin(\alpha)\cos(\gamma)\sin(\beta) \qquad (1)$$

$$y = r\cos(\gamma)\cos(\beta) \qquad (2)$$

$$z = -r\sin(\alpha)\sin(\gamma) + r\cos(\alpha)\cos(\gamma)\sin(\beta) \qquad (3)$$

From (1),

$$\cos(\alpha) = \frac{x - r\sin(\alpha)\cos(\gamma)\sin(\beta)}{r\sin(\gamma)}$$

Plugging into (3)

$$z = -r\sin(\alpha)\sin(\gamma) + r\cos(\gamma)\sin(\beta)\left[\frac{x - r\sin(\alpha)\cos(\gamma)\sin(\beta)}{r\sin(\gamma)}\right]$$

$$z = -r\sin(\alpha)\sin(\gamma) + \left[\frac{r\cos(\gamma)\sin(\beta)\,x}{r\sin(\gamma)}\right] - \left[\frac{r^2\sin(\alpha)\cos(\gamma)^2\sin(\beta)^2}{r\sin(\gamma)}\right]$$

$$z - \left[\frac{r\cos(\gamma)\sin(\beta)\,x}{r\sin(\gamma)}\right] = -r\sin(\alpha)\sin(\gamma) - \left[\frac{r^2\sin(\alpha)\cos(\gamma)^2\sin(\beta)^2}{r\sin(\gamma)}\right]$$

$$z - \left[\frac{\cos(\gamma)\sin(\beta)\,x}{\sin(\gamma)}\right] = -\sin(\alpha)\left[r\sin\gamma + \frac{r\cos(\gamma)^2\sin(\beta)^2}{\sin(\gamma)}\right]$$

$$\boldsymbol{\sin(\alpha) = -\frac{z - \left[\frac{\cos(\gamma)\sin(\beta)\,x}{\sin(\gamma)}\right]}{\left[r\sin\gamma + \frac{r\cos(\gamma)^2\sin(\beta)^2}{\sin(\gamma)}\right]}, \quad \gamma \neq 0}$$

FOR $\gamma = 0$,

When $\gamma = 0$,

$$x = r\sin(\alpha)\sin(\beta)$$

$$z = r\cos(\alpha)\sin(\beta)$$

$$\boldsymbol{\sin(\alpha) = \frac{x}{r\sin\beta}, \quad \gamma = 0}$$

By rotating the actuator by α, the spine was rotated to a location along the combined path, $\mathbf{r}_{\mathbf{path}}$, by rotating about the anatomical y-axis.

The above procedures were repeated continuously to cycle between the two described processes:

1. Flexion about the anatomical x-axis
2. Axial rotation by rotating the actuator about the anatomical y-axis, and bringing the vector back to a position that lies along the combined path, $\mathbf{r}_{\mathbf{path}}$.

The combined loading path was then defined, as well as a set of [α, β, γ] that travels along this path. These controls were programmed in the 8-*dof* simulator to produce combined loading. Note that in the above example, the primary controlled motions were flexion and axial rotation. A similar derivation was used to produce the combined loading of axial rotation and extension, and axial rotation and lateral bending. All motions were applied until a maximum moment of ±4 Nm is applied, along any of the three anatomical axes (M_x, M_y, or M_z).

2.3.2.5 Range of Motion Measurements

Similar to *Single Plane Pure Moments*, all motions were continuously recorded throughout *Multi-Planar Loading* using an Optotrak 3020 motion capture system (Northern Digital Inc, Waterloo, Ontario, Canada). For ***Group B*** specimens, LED motion flags were attached to T2, T6, T10, and T11. Total range of motion was measured, and reported as the motion of T2 with respect to T11. Throughout loading, the motions in all planes were simultaneously measured, that is, flexion-extension, lateral bending, and axial rotation.

2.3.2.6 Experimental Analysis

For *Multi-planar Loading*, the primary outcome variables were the simultaneous flexion-extension, lateral bending, and axial rotation ranges of motion under each of the two loading modes, i.e. axial rotation with combined flexion-extension and axial rotation with combined lateral bending. The motions obtained during *Multi-planar Loading* were compared with the results obtained during *Single Plane Pure Moments*. The comparisons were made for the intact condition, and following each of the sequential posterior releases.

2.3.3 Intraoperative Simulation and Direct Vertebral Rotation (DVR) to Failure

2.3.3.1 Overview

Aim 4, Aim 5, Aim 6 and Aim 7 were achieved by applying simulated direct vertebral rotation to failure to full-length human cadaveric thoracic spines.

Note that in the following intraoperative simulation, thoracic spine specimens were loaded until failure occurred. Once all testing was complete, safe limits of DVR were established. Then, separate analyses were performed for the results at 25%, 50%, and 75% failure (intraoperative simulation), as well as at failure (DVR-to-Failure).

2.3.3.2 Vertebral Derotation Simulator (VDS)

Design

Design Concept

A custom-made vertebral derotation simulator (VDS) was fabricated to mount to the upper actuator of the MTS load frame, allowing control through the existing MTS software. The simulator was designed to simulate Direct Vertebral Rotation (DVR),[6,7] a popularized correction maneuver used in combination with all-pedicle screw constructs for scoliosis correction. Based off of the design for the clinically used apparatuses, such as the Vertebral Column Manipulator (VCM, Medtronic, Minneapolis, MN),[7] the VDS enabled moment-application through pedicle screw-vertebral body linkages in a variety of combinations, including 1-level (bilateral pedicle screws), 2-level, 3-level, and 4-level linkages (bilateral pedicle screws at four levels, i.e. quadrangular linkage).

Component Design

The most basic assembly of the VDS was the single vertebral linkage bar. The linkage bar was designed to attach bilaterally to two pedicle screws at a given level of the spine, e.g. T7. A targeting ball-joint was first attached to each pedicle screw at the left and right side of the spine. Then, the two targeted ball joints were linked together using an orthogonal linkage-bar, creating a triangular linkage with the pedicle screws. An individual stainless steel pusher-bar was then attached to this triangular linkage through which a moment could be applied (Figure 11).

a.) 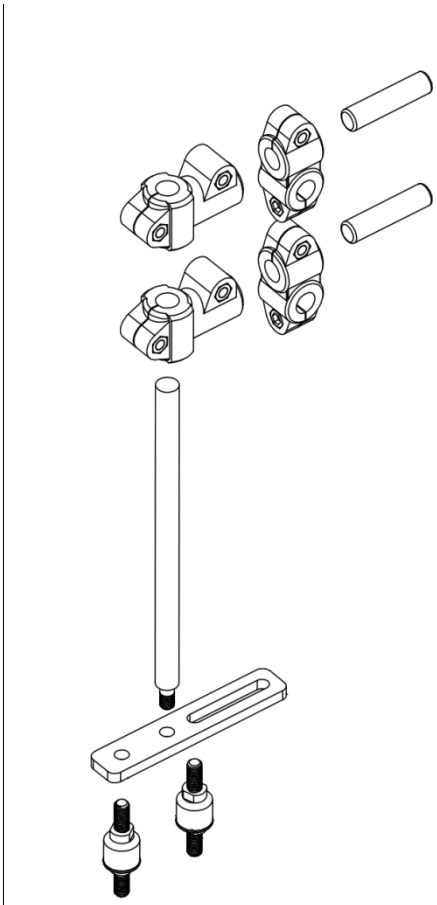 b.) 

Figure 11. Single vertebral body connection assembly. This assembly is attached to each of 4 vertebrae. The 4 assemblies are then linked together (See Figure 12). a.) Individual components. b.) Assembled.

In total, four individual linkage-bars were assembled and instrumented. Once linked to the spine at adjacent levels, the four individual linkage-bars were linked together, creating a rigid quadrangular structure (Figure 12).

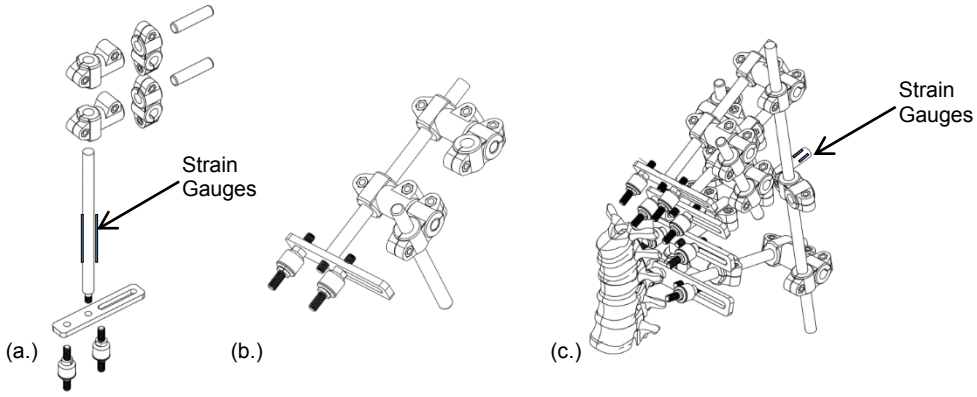

Figure 12. Custom designed vertebral derotation simulator (VDS). a.) Individual vertebral body linkage bar with strain gauges; b.) Assembled individual linkage bar. c.) Assembled quadrangular linkage, including 4-vertebral linkage bars joined as a rigid structure for application of applied torque.

The moment was then applied through the entire apparatus, effectively sharing the load across four vertebral bodies and eight bone-screw interfaces (Figure 13). This allowed the application of larger applied moments compared to single level linkages. In other words, larger moments could be applied prior to failure of the spine. The applied moment was designed to simulate the typical correction maneuver and forces applied clinically with the use of the DVR devices, e.g. the VCM.

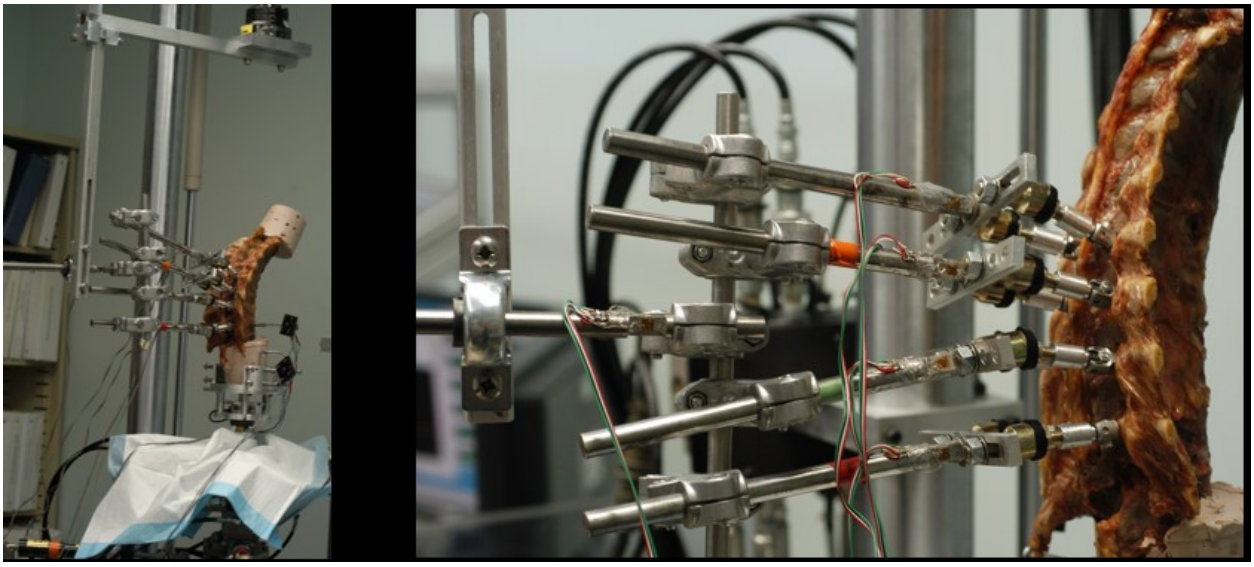

Figure 13. Custom DVR simulator attached to the spine through each of 8 pedicle screws, creating a quadrangular linkage. The DVR simulator is instrumented with strain gauges at each level to measure the simulated surgical loads.

Strain Gauging

The VDS was instrumented with strain gauges to measure the real-time moments applied through the device during loading. Specifically, strain was measured using SGD-2/350-XY11 biaxial precision strain gauges (OMEGA Engineering, Inc., Stamford, CT), with a resistance of 350 Ohms and a gauge factor of 2.14. The strain gauges were placed in the following locations: the left and right aspects of the each of the individual vertebral body linkage bars (8 total gauges), and on the left and right aspects of the single bar that was used to apply the rotational torque (2 total gauges).

As described, on each bar, two biaxial strain gauges were applied such that one measured the tension side of the bar, and the other measured the compression side of the bar in bending. The pair of biaxial strain gauges was wired in a single full-wheatstone bridge configuration. The bridge was then connected to a signal conditioning box, which in turn was connected to a

computer dedicated to the collection of the strain signals. The signal was conditioned, and amplified at 500X for data collection.

The individual linkage bars were machined from ½" 52100 stainless steel rods. In order to produce enough bending of the bar during moment application for changes in strain detectable by the gauges, the bars were modified. The bars satisfied two conditions: (1) strain was detected at small applied moments; and (2) the bar had to be able to withstand the maximum applied moment without plastic deformation. According to previous studies, and using a quadrangular linkage, the maximum applied moment was an average of 42.5 Nm (19.0 Nm – 61.5 Nm).[245] Therefore, in a worst case scenario where the entirety of the applied moment was applied through only one linkage bar, the bar would need to withstand an average of 42.5 Nm prior to plastic deformation.

For the individual linkage bars, 52100 steel ½" rods were used. These bars had an elastic modulus, E, of 210E9 N/m^2. The published yield strength of this material is 427 MPa. Consequently, the strain at yield, ε_{yield} is approximately 2030 microstrain (με). Accordingly, in order to withstand the worst-case moment magnitude (~42.5 Nm), each bar was machined to a 9-mm cross section, just distal to the triangular linkage. This ensured that the bar did not yield under maximum moment. Further, with this cross section, 100 με was detectable at approximately 2.5 Nm, and thus was sensitive enough to capture small changes in applied moment.

Each strain gauge was applied to the bar using a TT300 Adhesive Kit (OMEGA Engineering, Inc, Stamford, CT). The 9-mm cross section of the bar was first cleaned using acetone. Then, the surface was smoothed using several steps of sanding, beginning with coarse

grain and transitioning to a finer grain paper, completing the process with 400-grade paper. The surface was then cleaned with a conditioner, and neutralized. The strain gauges were then applied to the cross section of the bar using a resin compound, and cured for 3 hours at 100° C. The process was designed to ensure sensitivity of the gauge in detecting small strains, and to ensure strong adhesion for the duration of the experiments.

Once installed and set, the strain gauges and corresponding lead wires were protected using 3140 RTV coating, a room temperature curing silicone rubber (Dow Corning, Midland, MI).

The strain gauges were wired to a circuit such that they measured maximum compression and tension strains from bending loads on each bar. From these strains, the applied rotational torque on the spine was both calculated and calibrated.

2.3.3.3 Load Frame

All loading was performed in the 8-*dof* MTS spine simulator. Unlike the protocols for *Single Plane Pure Moments* and *Multi-planar Loading*, the upper gimbals were not attached to the MTS machine for the *Intraoperative Simulation*. As the torsional moment was applied through the custom-designed VDS, the upper gimbals were removed. The lower gimbals, however, remained attached and active for specimen positioning (Figure 14).

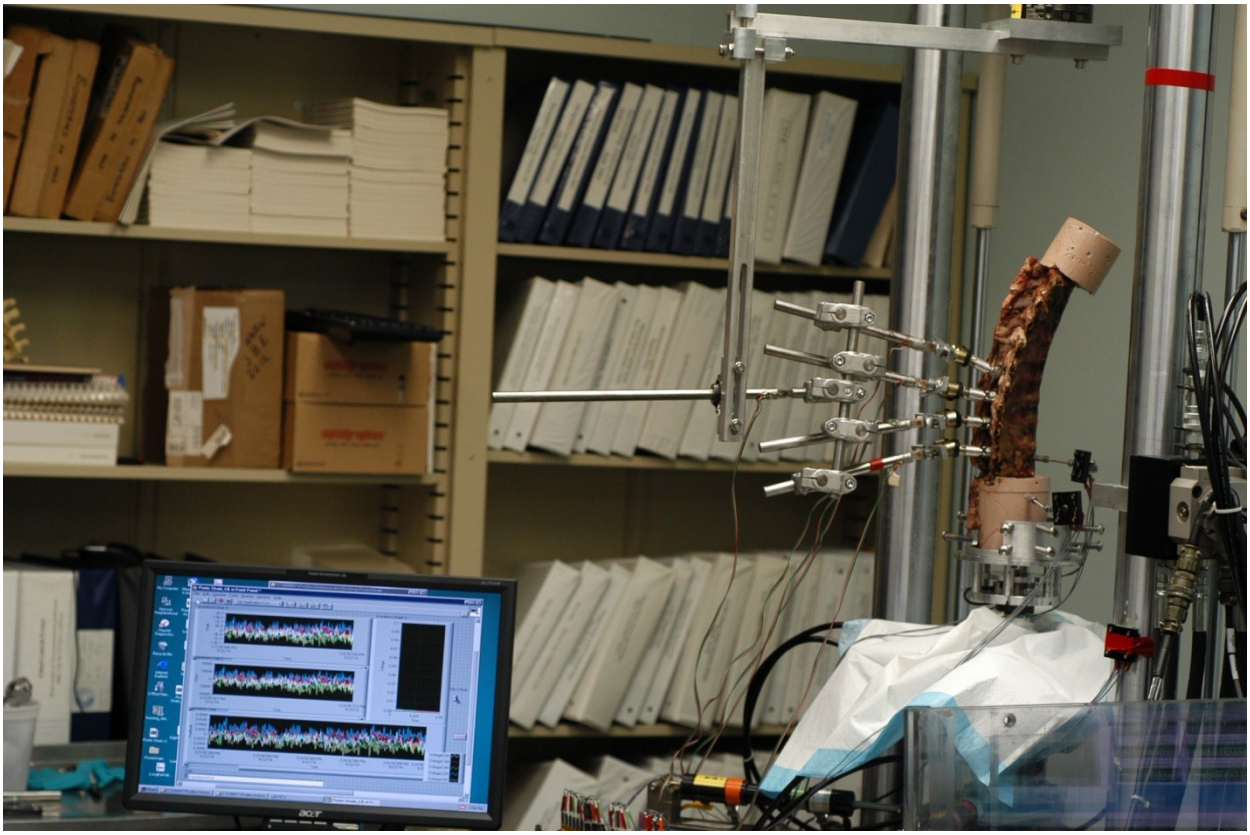

Figure 14. Representative photo of Simulated DVR experimental setup, with the upper gimbals removed, the lower gimbals engaged, and the DVR simulator attached to the upper actuator.

A 2-*dof* axial-torsional load cell (MTS Systems, Eden Prairie, MN) mounted on the base of the MTS load frame just below the bottom gimbals was used to control the main actuator and in turn, the VDS simulator. The load cell had an axial capacity of 25,000N and a torsional capacity of 250Nm.

2.3.3.4 Loading Protocol

Each specimen was mounted in the VDS simulator in an upright, vertical position, with the inferior-potted vertebrae attached to the bottom gimbals. The specimen was aligned such that the axes of the T10-T11 disc space coincided with the axes of the MTS load frame. Then, the

MTS was programmed to apply a torsional moment through the VDS, simulating a typical correction maneuver. The MTS was programmed to apply a ramping, step-wise moment. Specifically, motion was applied at a rate of 0.5°/s to 4 Nm increments, until failure. At each 4 Nm increment, a 5 second hold was applied, allowing for viscoelastic effects. This process was continued until failure occurred. Failure was defined as a quick, drastic drop in the moment-rotation curve, creating an inflection point at the maximum moment.

The simulator measured the simulated surgical loads via strain gauges mounted on every linkage throughout the DVR simulator. Specifically, and as discussed previously, biaxial precision strain gauges (OMEGA Engineering, Inc., Stamford, CT) were applied to four bars attached at each of the T7, T8, T9, and T10 vertebral pedicle screws, as well as to a bar through which the torsional moment is transferred to the quadrangular linkages. The strain gauges were calibrated to measure the compression and tension strains throughout simulated DVR, which were then used to determine the applied load simulating a surgeon's maneuvers.

2.3.3.5 Measurements

Range of Motion

All motions were recorded using the optical motion tracker, as described previously. Local $ROM_{T10\text{-}T11}$ was recorded and measured continuously throughout the DVR simulation.

Intervertebral Disc Moment (T10-T11)

Throughout the VDS simulation, the moments of the T10-T11 disc were approximated by the axial-torsional load cell mounted at the base of the MTS machine, just inferior to the potted T11-T12 vertebrae.

Strain in the VDS

The strain in the VDS was continuously measured throughout loading in each of the five strain gauge locations.

2.3.3.6 Statistical Analyses

The primary input variable was applied moment. The primary outcome variables were strain in the VDS, axial rotation local $ROM_{T10\text{-}T11}$ at failure, and moment at failure. Statistical measures, including mean, median, minimum, and maximum were used to establish the failure characteristics of the human thoracic spine at T10-T11 for each of the outcome variables. Additionally, a correlation analysis was performed to quantify the relationship between torsional failure strength and thoracic bone density.

For the intraoperative simulation, several statistical tests were performed. Paired-samples *t* tests were performed to compare the increase in motion at 25%, 50%, 75%, and 100% torsional strength to the increase in motion at the typical in-vitro loading magnitude of 4 Nm. Separate *t* tests were performed for the raw-motion increases and the normalized motion increases.

In addition to the statistical tests described above, one-sample t-tests were performed to compare the failure moments (applied moment and intervertebral disc moment) with the purported clinical torque of 100 Nm, as well as the reported failure strengths of the spine in torsion[244] and the bone-screw interfaces under DVR-type loading.[142,245]

2.4 Supplemental Analyses

2.4.1 Overview

Aim 8 was achieved by evaluating the results derived from the above described biomechanical tests as a function of intervertebral disc health. ***Aim 9*** was achieved by performing a systematic review of the previous literature reporting on the range of motion of intact cadaveric thoracic spine specimens.

2.4.2 Radiographic Analysis of Degeneration

Each of the radiographs of the specimens in ***Group B*** and ***Group C*** were classified according standard intervertebral disc degeneration grading criteria established by Mimura *et al*.[196] and Lane *et al*.[254] to evaluate the intervertebral disc health of each specimen. The classification by Mimura *et al*. included a 1-4 grading system based on changes in disc height, osteophytes formation, and endplate sclerosis (Table 4). The classification by Lane *et al*. included a 0-3 grading system based on joint space narrowing, osteophytes, and sclerosis (Table 5).

Table 4. X-Ray grading system proposed by Mimura *et al*.[196]

Score	Disc Height Changes (% of adjacent discs)	Osteophyte Formation*	Endplate Sclerosis
0	None (Normal)	0 points	None
1	> 75% (Mild)	1-4 points	Either endplate
2	> 50% (Moderate)	5-8 points	Both endplates
3	> 25% (Severe)	9-12 points	
4	< 25% (Very Severe)	13-16 points	

*Sum of points (< 3mm = 1 point; > 3mm = 2 points) on 8 Edges: lateral left, lateral right, anterior, posterior edge of superior and inferior vertebral bodies

Intervertebral disc grade determined by the sum of the scores for each of the three categories (Disc Height Changes, Osteophyte Formation, and Sclerosis)

Grade 1: Score = 0-1.5
Grade 2: Score = 2-3.5
Grade 3: Score = 4-6
Grade 4: Score > 6

Table 5. X-Ray grading system proposed by Lane *et al*.[254]

Score	Joint Space Narrowing	Osteophytes	Sclerosis
0	None	None	None
1	Definite (mild) narrowing	Small	Present
2	Moderate	Moderate	
3	Severe (complete loss of joint space)	Large	
Grade 0	Normal (0 for Joint Space Narrowing and Osteophytes)		
Grade 1	Mild (1) Joint Space Narrowing or Mild (1) Osteophytes		
Grade 2	Moderate-severe (2-3) Joint Space Narrowing and/or moderate-severe (2-3) Osteophytes		

In addition to the radiographic analyses, specimens in ***Group C*** were also graded according to the MRI-based degeneration scoring system developed by Pfirrmann *et al*.[255] The scoring system is based on an I-V scoring system.

Following radiographic analysis, outcome variables measured in ***Group B*** and ***Group C*** for each experiment were correlated with intervertebral disc health, according to grade. The Spearman correlation coefficient was determined, and coefficients greater than 0.5 associated with a p-value of less than 0.05 were considered significant. For the outcome variables which

were significantly correlated with x-ray graded degeneration, the above described t-tests and ANOVAs were repeated following grouping the specimens on the basis of disc health.

2.4.3 Histological Analysis of Degeneration

Following biomechanical testing, histological analysis of intervertebral discs in ***Group B*** and ***Group C*** was performed. The desired motion segment(s) from each specimen was extracted by transversely sectioning the segment using a water-cooled band saw (EXAKT, Gottingen, Germany), equipped with a 0.3 mm thick cutting band. For specimens in ***Group B*** and ***Group C***, the T10-T11 motion segments were extracted. Each motion segment was sectioned in the sagittal plane to obtain two-3mm sagittal slices. The sagittal disc specimens were prepared and stained with hematoxylin and eosin (H&E). All slides were evaluated under light microscopy and polarized light.

Each of the stained sections were graded using a modified 0-10 point scoring system developed by Rutges *et al*.[147] The scoring system was based on endplate changes, the morphology of the annulus fibrosus and nucleus pulposus, the boundary between the annulus and nucleus, cellularity of the nucleus, and the organization of the nucleus matrix (Table 6).

Table 6. Modified histological (microscopic) grading system proposed by Rutges *et al.*[147]

Score	Endplate	Annulus Fibrosus Morphology	Boundary Between Annulus Fibrosus and Nucleus Pulposus	Nucleus Pulposus Cellularity	Nucleus Pulposus Matrix
0	Homogeneous structure; regular thickness	Well-organized, half ring-shaped structure, collagen lamellae	Clear boundary between AF and NP tissue	Normal cellularity; no cell clusters	Well-organized structure of nucleus matrix
1	Slight irregularity with limited number of microfractures and locally decreased thickness	Partly ruptured annulus fibrosus; loss of half ring-shaped structure	Boundary less clear; loss of annular-nuclear demarcation	Mixed cellularity; normal pattern with some cell clusters	Partly disorganized structure of nucleus matrix
2	Severe irregularity with multiple microfractures and generalized decreased thickness	Completely ruptured annulus fibrosus; no intact half ring-shaped collagen lamellae	No distinguishable boundary between AF and NP tissue	Mainly clustered cellularity, chondroid nests present	Complete disorganization and loss of nucleus matrix

Total score determined by the sum of the scores for each of the 5 categories: Endplate, Annulus Fibrosus Morphology, Boundary Between Annulus Fibrosus and Nucleus Pulposus, Nucleus Pulposus Cellularity, and Nucleus Pulposus Matrix

Similarly to the analysis for radiographic grading, following histological analysis, outcome variables measured in ***Group B*** and ***Group C*** for each experiment were correlated with intervertebral disc health, according to histological degeneration grade. The Spearman correlation coefficient was determined, and coefficients greater than 0.5 associated with a p-value of less than 0.05 were considered significant. For the outcome variables which were significantly correlated with histologically graded degeneration, the above described t-tests and ANOVAs were repeated following grouping the specimens on the basis of disc health.

2.4.4 Establishing Typical Thoracic Spine Range of Motion

2.4.4.1 Systematic Search

A systematic MEDLINE search was performed to identify in-vitro thoracic spine biomechanics studies which evaluated thoracic spine ROM. Specifically, a MEDLINE search

was performed using the search terms “thoracic spine”, “motion”, and “cadaver”. All of the abstracts yielded from the above search terms were reviewed to identify articles of interest. Articles which performed biomechanical testing on thoracic spine specimens were identified, and the full manuscripts were reviewed. In order to ensure that no articles were missed using the above search terms, the references cited by all of the identified articles were also reviewed. Finally, once an article was identified and chosen for inclusion in this study, the ‘Related Citations’ option of PubMed was used to identify any additional articles missed by the initial search criteria and/or the references of the included articles.

Only studies which reported the ROM of intact human cadaveric thoracic spines were included. Studies reporting thoracic ROM only after simulated injury or treatment were excluded. Studies involving only cervical or lumbar motion segments were excluded. Additionally, studies performing biomechanical testing on non-human specimens, e.g. canine specimens, were also excluded. Clinical studies and computational studies were excluded as well.

Within the potential articles, there were instances where a group of authors published multiple articles, each of which reported the same intact motion data from the same groups of specimens. In these cases, only the article with the most comprehensive reporting of the intact ROM data was included.

2.4.4.2 Extracted Variables

Once the relevant articles were identified, each was reviewed, and the relevant independent and dependent variables were extracted. Specifically, the independent variables extracted included the tested motion segments (e.g. T1-T2 or T4-T7), number of specimens,

specimen age, presence of ribcage (yes or no), type of loading (e.g. pure moment, cantilever bending, or 4 point bending), preload, type of loading control (i.e. displacement or moment), loading rate, and maximum bending moment (or load) in each direction, that is, flexion-extension, lateral bending and axial rotation. These variables were extracted to assess the trends in employed biomechanical testing methods.

The dependent variables extracted from each study were the ranges of motion in each reported anatomical plane: flexion-extension, lateral bending, and/or axial rotation. All ROM data extracted measured in degrees was included. For studies which only reported mean motions in unilateral/unidirectional directions, e.g. mean flexion ROM and mean extension ROM, the means were summed to provide average values for bilateral/bidirectional motions, e.g. flexion-extension ROM. Means and standard deviations were extracted. In few cases, only medians were reported, and this data was recorded separately. For those studies which reported raw motion measurements for each individual specimen, means and standard deviations were calculated. Only data which was clearly reported was used. Finally, in studies which report did not report the motions in the text or in tables, the values were extracted from the corresponding graphs.

2.4.4.3 Segmental Motion Estimation

As the studies tested different levels of the spine, e.g. T1-T12, T2-T5, or T4-T12, and many of them reported multi-segment motion, e.g. T1-T12 motion as opposed to the motion at each segment, the reported motions were used to approximate single level motions. Specifically, the reported motions were divided by the number of motion segments included in the

measurement. Then, the single level values were used as approximations of motion for each of the individual levels.

For example, if the reported T1-T12 ROM was 44°, the total motion was divided by 11 motion segments. In turn, the single level estimated motion would be 4° per level. In this case, an entry was made for each of the 11 motion segments, e.g. T1-T2, T2-T3, …, and T11-T12, each with a motion of 4°. This approximation was necessary in order to maximize the number of studies that were included.

Segmental motions were estimated for all studies which (1) applied loading to thoracic spines without the ribcage intact, and (2) reported bilateral/bidirectional ROM (e.g. flexion-extension) or both unilateral/unidirectional motions in a given plane (e.g. flexion and extension).

2.4.4.4 Statistical Analyses

All statistical analyses were performed using SPSS 19.0 statistical software (IBM, Armonk, NY). The median, minimum, and maximum values of the estimated segmental motions among the studies were reported. High-low plots were used to visually represent the spread in the estimated segmental motions. Additionally, for studies which applied standard pure moment testing to cadaveric thoracic specimens without the ribcage and reported ROM means and standard deviations, pooled means and pooled standard deviations were calculated based on the range of motion for each of the estimated motion segments (T1-T2, T2-T3…, and T11-T12) in each of the three loading directions: flexion-extension, lateral bending, and axial rotation.

The above analysis served as a context of discussion for the results derived from the biomechanical testing described in the proposed work.

3 Results

3.1 Single Plane Pure Moments

3.1.1 Group A

3.1.1.1 Summary of Results

The results from the *Single Plane Pure Moment* testing of ***Group A*** specimens were published previously (Appendix A),[28] and reported as they pertain to the present work below. *Single Plane Pure Moments* were applied to each of the n=7 hemi-thoracic spine specimens to produce flexion-extension, lateral bending, and axial rotation, to a maximum of ±6 Nm. During testing, two specimens fractured during the intact testing. Consequently, these two fractured specimens were excluded, and the analysis was based on the n=5 specimens which survived the entirety of the testing protocol. Three of these specimens were lower hemi-thoracic segments, i.e. T7-T12, and two were upper hemi-thoracic segments, i.e. T1-T6. As described in the Materials and Methods section, for the specimens in ***Group A***, ROM_{TOTAL} was defined as the motion across the hemi-thoracic segment, that is, T2-T5 ROM or T8-T11 ROM. For each loading direction, i.e. flexion-extension, lateral bending, and axial rotation, a moment-rotation hysteresis curve was produced (Figure 15).

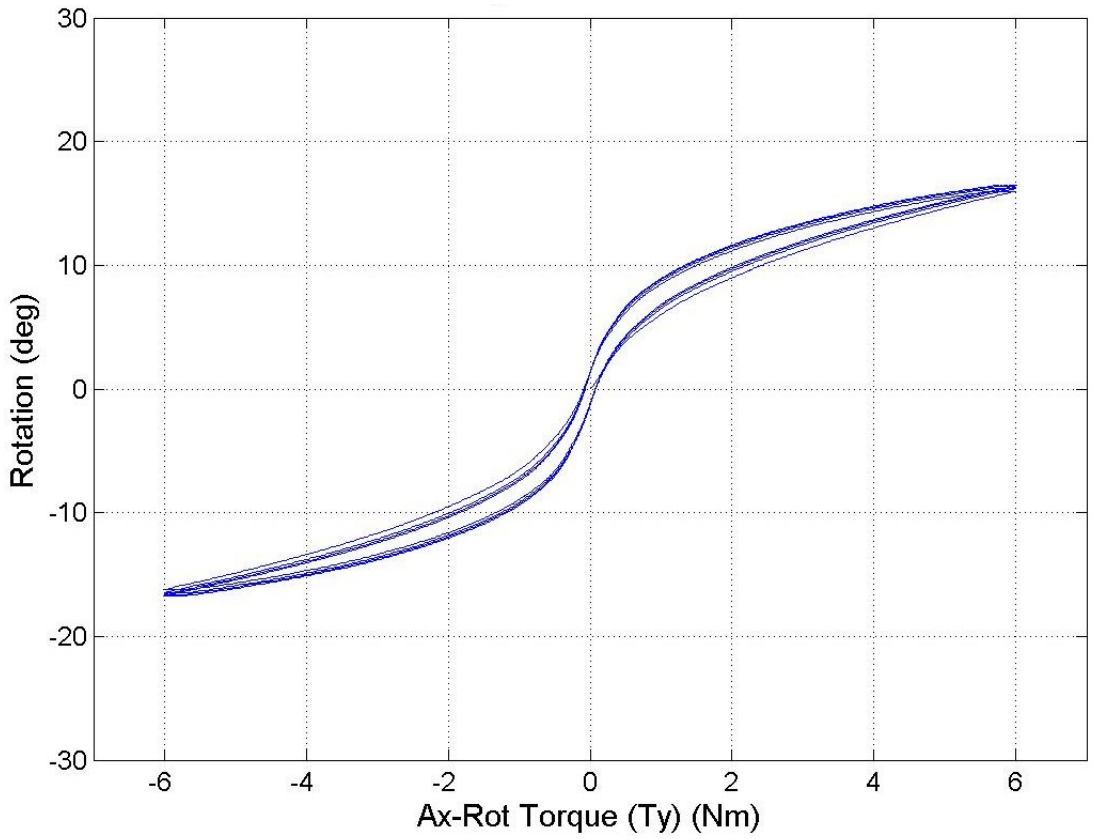

Figure 15. Representative moment-rotation hysteresis curve from the pure moment testing of the cadaveric thoracic spine specimens. Range of motion (ROM) is calculated as the differences between the endpoints of the hysteresis loop.

Overall, intact ROM_{TOTAL} was largest in axial rotation, with an average ROM_{TOTAL} of 10.6°±7.2°, compared to either flexion-extension or lateral bending. Specifically, the average intact ROM_{TOTAL} was 5.7°±4.9° in flexion-extension and 7.9°±5.7° in lateral bending. The three sequential posterior destabilizations, i.e. Ponte osteotomies, had a clear effect on thoracic ROM in flexion-extension and axial rotation, producing additive increases following each sequential release. In lateral bending, while each sequential release provided additive increases, the magnitudes of these increases were negligible.

3.1.1.2 Changes in Flexion-Extension

The changes in flexion-extension ROM_{TOTAL} were calculated as a function of sequential posterior releases, with the increases measured with respect to the intact condition. ROM_{TOTAL} increased following each sequential release, i.e. each Ponte osteotomy, with increases ranging from -0.2° to 2.6° for each individual release. As discussed, each osteotomy provided additive increases in ROM_{TOTAL}, with the ROM_{TOTAL} increasing from 5.7° ± 4.9° intact, to 6.5° ± 5.6° (p=0.08), 7.6° ± 6.5° (p=0.07), and 8.5° ± 7.3° (p=0.09) following one, two, and three osteotomies, respectively (Table 7). Note that the p-values correspond to the comparison of the ROM_{TOTAL} following each sequential release with the ROM_{TOTAL} in the intact condition.

Table 7. Flexion-Extension Range of Motion (Degrees) across Thoracic Spine Segment (T2-T5, or T8-T11)[28]

	Flexion-Extension (Degrees)			
Measure	Intact	1-Level Ponte	2-Level Ponte	3-Level Ponte
Mean (SD)	5.7 (4.9)	6.5 (5.6)	7.6 (6.5)	8.5 (7.3)
Range	1.0-11.0	1.5 - 13.1	1.7 - 15.6	1.6 - 18.2
	p = 0.08			
	p = 0.07			
	p = 0.09			

In addition to the raw increases in ROM_{TOTAL}, reported in degrees, increases in motion were also analyzed as a ratio. Specifically, ROM_{TOTAL} increases were analyzed as a % increase compared to the intact condition. Compared to the intact condition, flexion-extension ROM_{TOTAL} increased by 20% ± 16% (p=0.05), 41% ± 24% (p=0.02), and 54% ± 33% (p=0.02), following each osteotomy (Figure 16). The total increase following the three sequential osteotomies ranged widely, ranging from 14% to 101%.

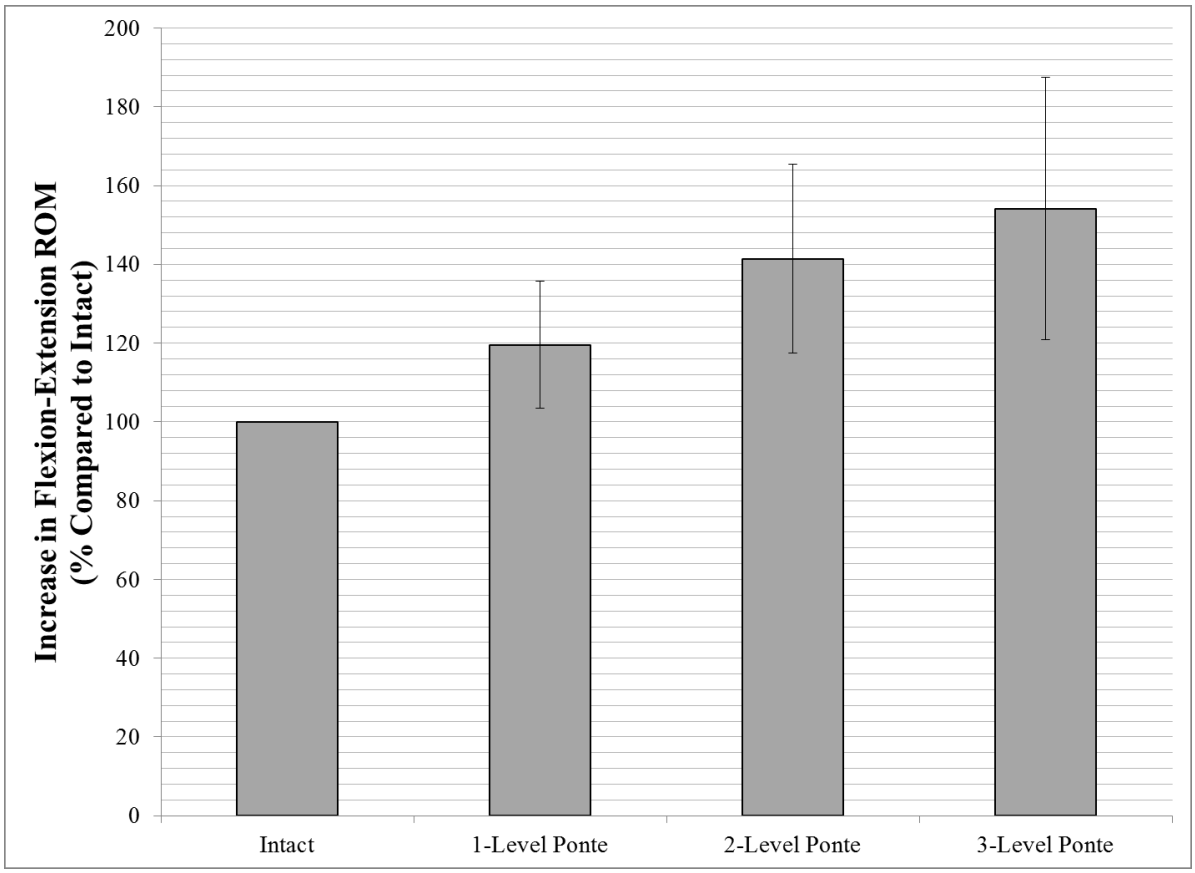

Figure 16. Increase (%) in total hemi-thoracic flexion-extension range of motion as a function of sequential Ponte osteotomies compared to the intact condition.

Coupled motions were small during flexion-extension loading, with intact coupled motions of 0.7° ± 0.5° in lateral bending and 0.9° ± 1.3° in axial rotation. Following osteotomy, average changes in coupled motions were less than 0.3°.

3.1.1.3 Changes in Flexion

In addition to analyzing the flexion-extension ROM_{TOTAL}, flexion and extension were evaluated separately due to the asymmetric anatomy in the anterior and posterior columns of the spine. Specifically, in extension, the motion of the spine is resisted primarily by the anterior disc space and the anterior longitudinal ligament. Alternatively, in flexion, the motion of the spine is

resisted primarily by the posterior disc space, the posterior longitudinal ligament, and the posterior column ligaments such as the ligamentum flavum, the facet capsular ligaments, and the supraspinous and interspinous ligaments.

The changes in flexion ROM_{TOTAL} were calculated as a function of sequential posterior releases, with the increases measured with respect to the intact condition. ROM_{TOTAL} increased following each sequential release, with increases ranging from -0.1° to 1.6° for each individual release. Each osteotomy provided additive increases in ROM_{TOTAL}, with the ROM_{TOTAL} increasing from 2.7 ± 1.9° intact, to 3.2° ± 2.3° (p=0.11), 3.9° ± 2.8° (p=0.05), and 4.4° ± 3.2° (p=0.07) following one, two, and three osteotomies, respectively (Table 8). Note that, once again, the p-values correspond to the comparison of the ROM_{TOTAL} following each sequential release with the ROM_{TOTAL} in the intact condition.

Table 8. Flexion Range of Motion (Degrees) across Thoracic Spine Segment (T2-T5, or T8-T11)[28]

	Flexion (Degrees)			
Measure	Intact	1-Level Ponte	2-Level Ponte	3-Level Ponte
Mean (SD)	2.7 (1.9)	3.2 (2.3)	3.9 (2.8)	4.4 (3.2)
Range	0.5 - 5.3	1.1 - 5.9	1.1 - 7.1	1.1 - 7.9
		p = 0.11		
		p = 0.05		
		p = 0.07		

Similar to the raw motion increases, there was additive percentage increases in ROM_{TOTAL} with each posterior release, compared to the intact condition. Specifically, compared to the intact condition, flexion ROM_{TOTAL} increased by 33% ± 44% (p=0.17), 56% ± 38% (p=0.03), and 69% ± 39% (p=0.02), following one, two, and three osteotomies, respectively (Figure 17). The total percentage increase in ROM_{TOTAL} following the completion of all three osteotomies ranged from 24% to 115%.

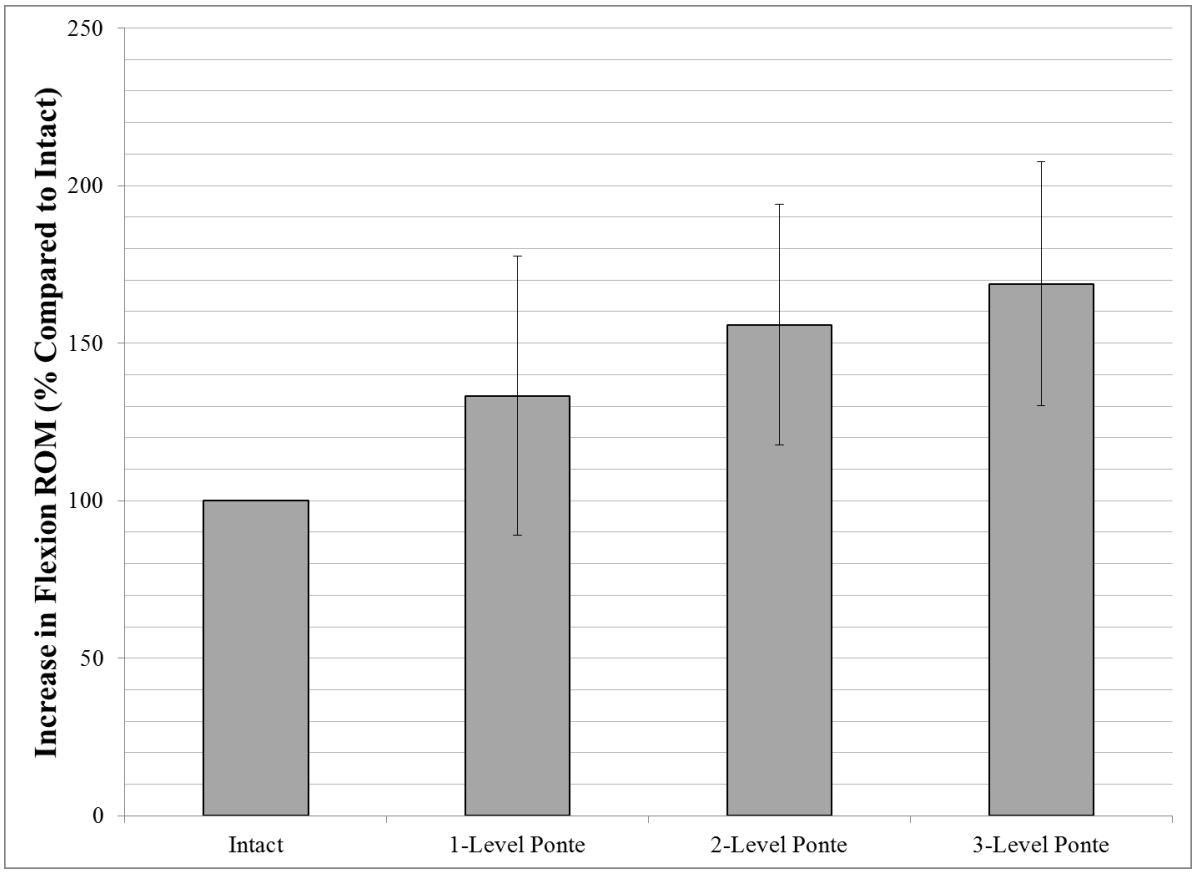

Figure 17. Increase (%) in total hemi-thoracic flexion range of motion as a function of sequential Ponte osteotomies compared to the intact condition.

3.1.1.4 Changes in Extension

The changes in extension ROM_{TOTAL} were calculated as a function of sequential posterior releases, with the increases measured with respect to the intact condition. Compared to the changes in flexion ROM_{TOTAL}, increases in extension ROM_{TOTAL} were smaller in magnitude. Specifically, in extension, ROM_{TOTAL} increased following each sequential release, with increases ranging from -0.2° to 1.5° for each individual release. Each osteotomy provided additive increases in extension ROM_{TOTAL}, with the extension ROM_{TOTAL} increasing from 3.0 ± 3.1° intact, to 3.3° ± 3.4° (p=0.16), 3.7° ± 3.7° (p=0.09), and 4.1° ± 4.2° (p=0.13) following one, two,

and three osteotomies, respectively (Table 9). Note that, once again, the p-values correspond to the comparison of the extension ROM_{TOTAL} following each sequential release with the extension ROM_{TOTAL} in the intact condition.

Table 9. Extension Range of Motion (Degrees) across Thoracic Spine Segment (T2-T5, or T8-T11)[28]

	Extension (Degrees)			
Measure	Intact	1-Level Ponte	2-Level Ponte	3-Level Ponte
Mean (SD)	3.0 (3.1)	3.3 (3.4)	3.7 (3.7)	4.1 (4.2)
Range	0.5 - 7.1	0.4 - 7.6	0.6 - 8.8	0.4 - 10.3
	p = 0.16			
	p = 0.09			
	p = 0.13			

Similar to the raw motion increases, the percentage increases in extension ROM_{TOTAL} were smaller than those in flexion. Specifically, compared to intact specimens, extension ROM_{TOTAL} increased by 12% ± 32% (p=0.44), 34% ± 38% (p=0.12), and 56% ± 95% (p=0.26) following each of the three sequential osteotomies, respectively (Figure 18). While the mean percentage increases in extension motion were smaller than those reported in flexion, the maximum percentage increase was larger. Specifically, the maximum total percentage increase in extension ROM_{TOTAL} following the completion of all three osteotomies was 223%, compared to only 115% in flexion.

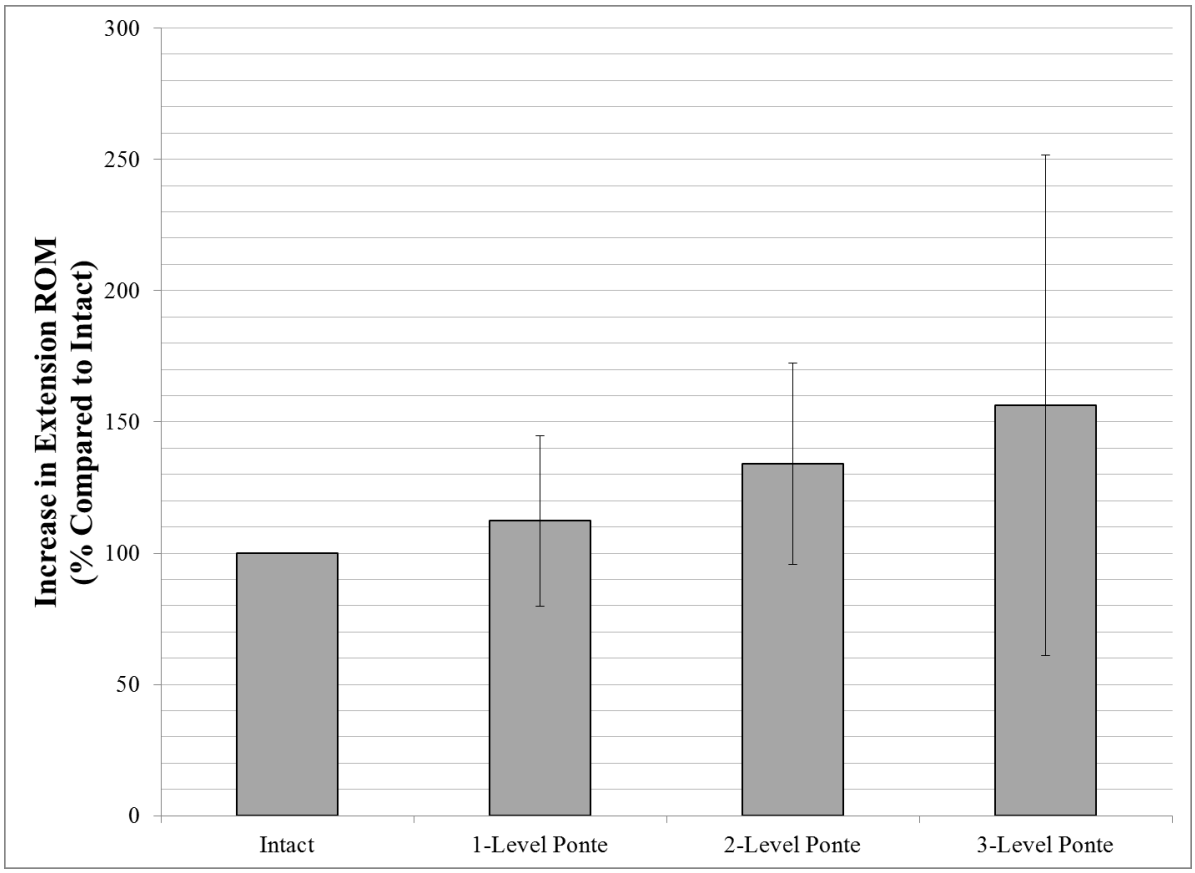

Figure 18. Increase (%) in total hemi-thoracic extension range of motion as a function of sequential Ponte osteotomies compared to the intact condition.

3.1.1.5 Changes in Lateral Bending

The changes in lateral bending ROM_{TOTAL} were calculated as a function of sequential posterior releases, with the increases measured with respect to the intact condition. Compared to either the increases in flexion-extension ROM_{TOTAL} or axial rotation ROM_{TOTAL}, the increases in lateral bending ROM_{TOTAL} were smaller. Therefore, the sequential posterior releases had little to no effect on lateral bending ROM_{TOTAL}.

Lateral bending ROM_{TOTAL} increases ranged from 0.1° to 0.5° following each individual release. Average changes in lateral bending ROM_{TOTAL} were small compared to the intact

condition. Specifically, lateral bending ROM_{TOTAL} increased from 7.9° ± 5.7° intact, to 8.1° ± 5.9° (p=0.16) and 8.3° ± 6.0° (p=0.07) following one and two osteotomies, respectively (Table 10). Average lateral bending ROM_{TOTAL} remained the same following the 3rd osteotomy, as compared to the average ROM_{TOTAL} following the 2nd osteotomy. The reported p-values correspond to the comparisons of the lateral bending ROM_{TOTAL} following each osteotomy as compared to the intact condition.

Table 10. Lateral Bending Range of Motion (Degrees) across Thoracic Spine Segment (T2-T5, or T8-T11)[28]

	Lateral Bending (Degrees)			
Measure	Intact	1-Level Ponte	2-Level Ponte	3-Level Ponte
Mean (SD)	7.9 (5.7)	8.1 (5.9)	8.3 (6.0)	8.3 (6.0)
Range	1.6 - 14.8	1.5 - 15.3	1.5 - 15.5	1.5 - 15.4
	p = 0.16			
	p = 0.07			
	p = 0.07			

Similar to the raw increases in lateral bending motion, the percentage increases in lateral bending ROM_{TOTAL} were small, as compared to the intact condition. Specifically, as compared to intact, the lateral bending ROM_{TOTAL} increased by 2% ± 6% (p=0.43) following the three osteotomies (Figure 19). The maximum percentage increase in lateral ROM_{TOTAL} following the completion of the three osteotomies was only 8%.

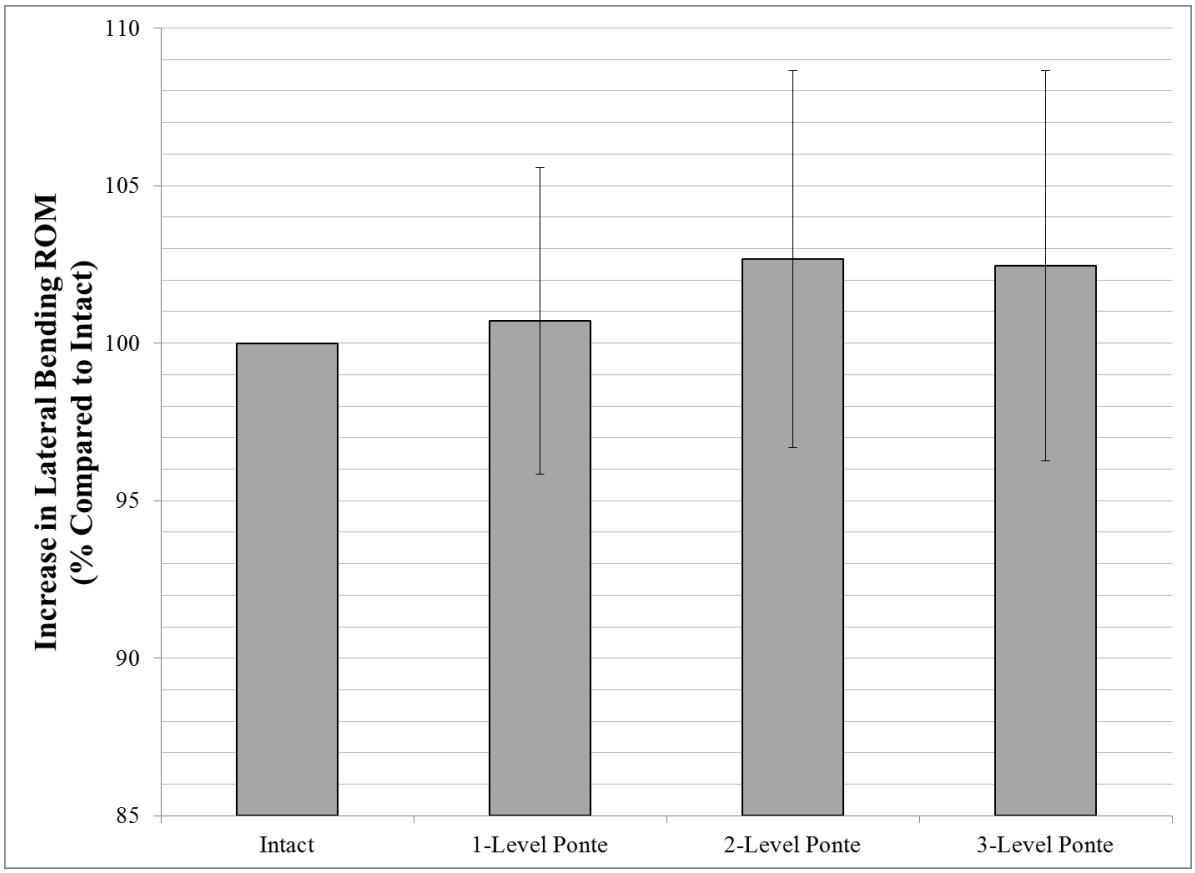

Figure 19. Increase (%) in total hemi-thoracic lateral bending range of motion as a function of sequential Ponte osteotomies compared to the intact condition.

Similarly to flexion-extension loading, coupled motions were small during lateral bending loading, with intact coupled motions of 1.0° ± 0.7° in flexion-extension and 1.0° ± 0.5° in axial rotation. Following osteotomy, average changes in coupled motions were less than 0.3°.

3.1.1.6 Changes in Axial Rotation

The changes in axial rotation ROM_{TOTAL} were calculated as a function of sequential posterior releases, with the increases measured with respect to the intact condition. Overall, increases in axial rotation ROM_{TOTAL} were smaller than those in flexion-extension, but

substantially larger than those in lateral bending. Similar to flexion-extension, as well as the individual analyses of flexion and extension, axial rotation ROM_{TOTAL} increased following each sequential posterior release.

Specifically, axial rotation ROM_{TOTAL} increases ranged from 0.1° to 2.8° following each individual release. The maximum increase in axial rotation ROM_{TOTAL} of 2.8° exceeded the maximum increases in flexion, extension, and lateral bending. Similar to flexion-extension, there was an additive effect of the sequential posterior releases on the axial rotation motion. Specifically, average axial rotation ROM_{TOTAL} increased from 10.6° ± 7.2° in the intact condition, to 11.7° ± 8.2° (p=0.08), 12.8° ± 9.0° (p=0.07), and 13.8° ± 9.1° (p=0.04) following one, two, and three osteotomies, respectively (Table 11). The reported p-values correspond to the comparisons of the axial rotation ROM_{TOTAL} following each osteotomy as compared to the intact condition.

Table 11. Axial Rotation Range of Motion (Degrees) across Thoracic Spine Segment (T2-T5, or T8-T11)[28]

	Axial Rotation (Degrees)			
Measure	Intact	1-Level Ponte	2-Level Ponte	3-Level Ponte
Mean (SD)	10.6 (7.2)	11.7 (8.2)	12.8 (9.0)	13.8 (9.1)
Range	3.4 - 19.7	3.9 - 22.2	4.1 - 23.6	4.3 - 23.9
	p = 0.08			
	p = 0.07			
	p = 0.04			

Like the raw increases in axial rotation ROM_{TOTAL}, the percentage increases in axial rotation ROM_{TOTAL} were a function of each sequential osteotomy. Specifically, compared to the intact condition, axial rotation ROM_{TOTAL} increased by 9% ± 6% (p=0.02), 20% ± 7% (p<0.01), and 34% ± 20% (p=0.02) following each of the three sequential osteotomies, respectively

(Figure 20). The total percentage increase in axial rotation ROM_{TOTAL} following the completion of all three posterior releases ranged from 16% to 64%.

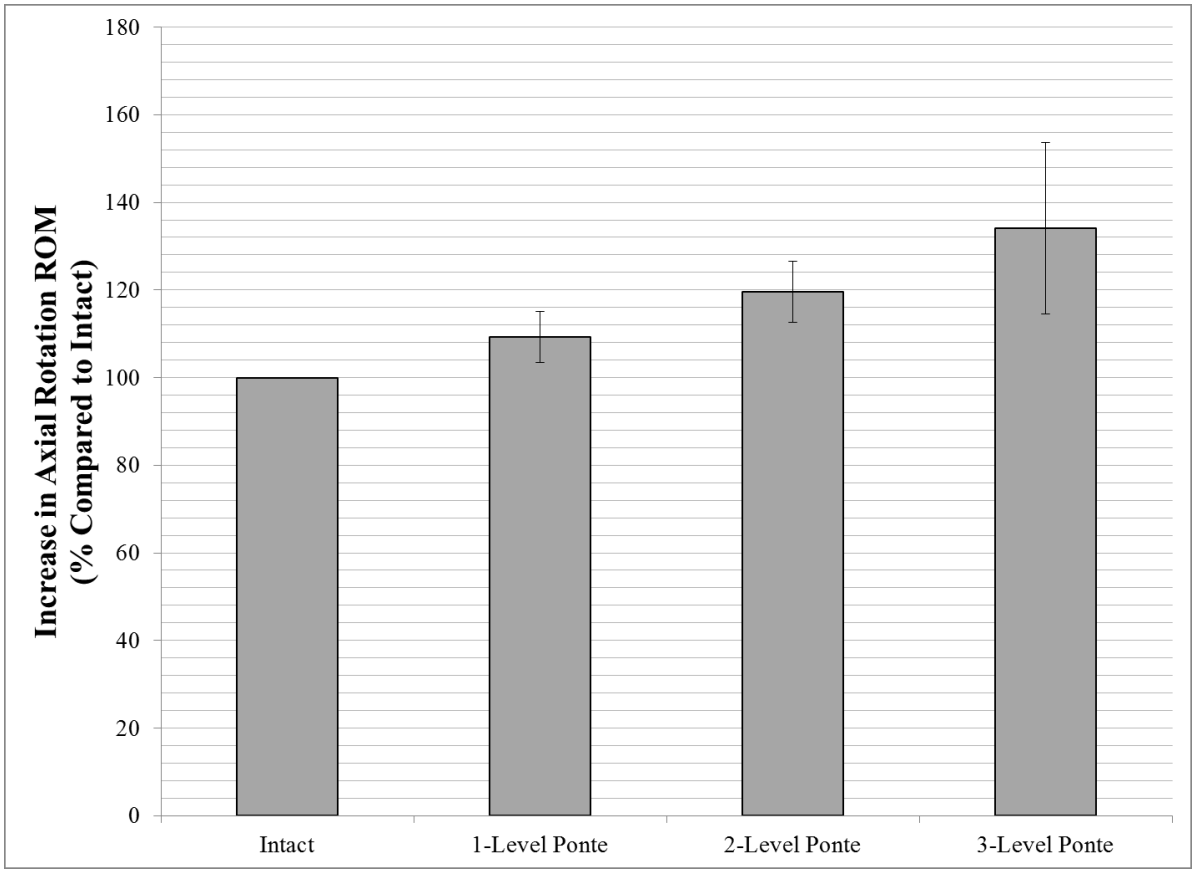

Figure 20. Increase (%) in total hemi-thoracic axial rotation range of motion as a function of sequential Ponte osteotomies compared to the intact condition.

Coupled motions during axial rotation loading were small in flexion-extension rotation, with intact coupled flexion-extension of 0.8° ± 0.6°. Coupled lateral bending rotation was larger, with average coupled lateral bending of 2.0° ± 2.4°. Following osteotomy, average changes in coupled motions were less than 0.2°.

3.1.2 Group B

3.1.2.1 Summary of Results

The *Single Plane Pure Moment* results of the specimens in ***Group B*** were published previously (Appendix A),[250] and are reported as they pertain to the present work below. *Single Plane Pure Moments* were applied to each of the n=10 full-length human cadaveric thoracic spine specimens to produce flexion-extension, lateral bending, and axial rotation, to a maximum of ±4 Nm. The first specimen of ***Group B*** was tested on multiple non-consecutive days over several hours, with several freeze-thaw cycles. Consequently, this specimen was excluded, and the analysis was based on the remaining n=9 specimens. These n= 9 specimens were all tested under the full protocol without incidence. As described in the Materials and Methods section, for the specimens in ***Group B***, ROM_{TOTAL} was defined as the motion of T2 with respect to T11. In addition to ROM_{TOTAL}, the T6-T10 motion was also analyzed, denoted by $ROM_{T6\text{-}T10}$.

Overall, the *Single Plane Pure Moment* testing of ***Group B*** produced similar increases in flexibility following the sequential osteotomies as specimens in ***Group A***. Despite ***Group B*** including full-length specimens, and despite applying a smaller maximum moment, i.e. 4Nm compared to 6Nm, the osteotomies had a similar effect. In addition, beyond the analysis provided in ***Group A***, for specimens in ***Group B***, the effects of the osteotomies were compared to the routinely used total facetectomies, a less invasive, more commonly used procedure. Overall, the four supplemental osteotomies provided significant increases in ROM_{TOTAL} beyond that provided by the routinely performed total facetectomies in flexion-extension, lateral bending, and axial rotation (Figure 21). Similar to the specimens in ***Group A***, even in the most destabilized

condition, i.e. after 9 total facetectomies and 4 supplemental osteotomies, the increases in ROM_{TOTAL} were smallest in lateral bending, with less than 10% overall increase in ROM_{TOTAL}.

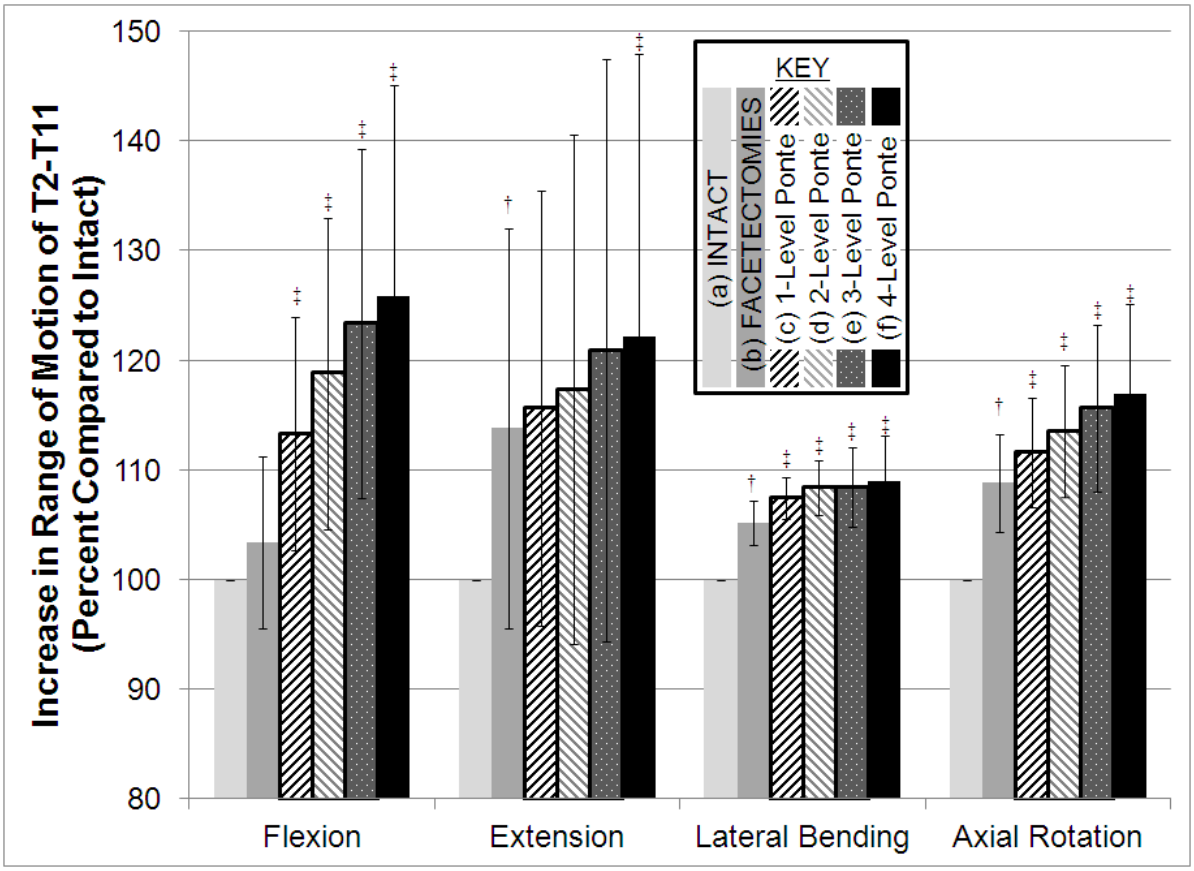

Figure 21. Summary of Group B Specimens. % Increase in total T2-T11 range of motion (ROM), compared to the intact total ROM, following bilateral total facetectomies, and each of four sequential Ponte osteotomies.[250]
† Bilateral total facetectomies compared to intact ($p<0.05$) (Paired-samples t-tests)
‡ Ponte osteotomies compared to bilateral total facetectomies ($p<0.05$) (Paired-samples t-tests)

3.1.2.2 Changes in Flexion-Extension

Similar to ***Group A***, changes in flexion-extension ROM_{TOTAL} were calculated as a function of the five sequential posterior release combinations, with the increases measured in two ways. First, the increases were measured after each release with respect to the intact condition.

Second, the increase following each supplemental osteotomy was calculated with respect to the total facetectomy condition.

Following each posterior release, on average, flexion-extension ROM_{TOTAL} increased. Of these, the largest increases were seen after the total facetectomies (Figure 22).

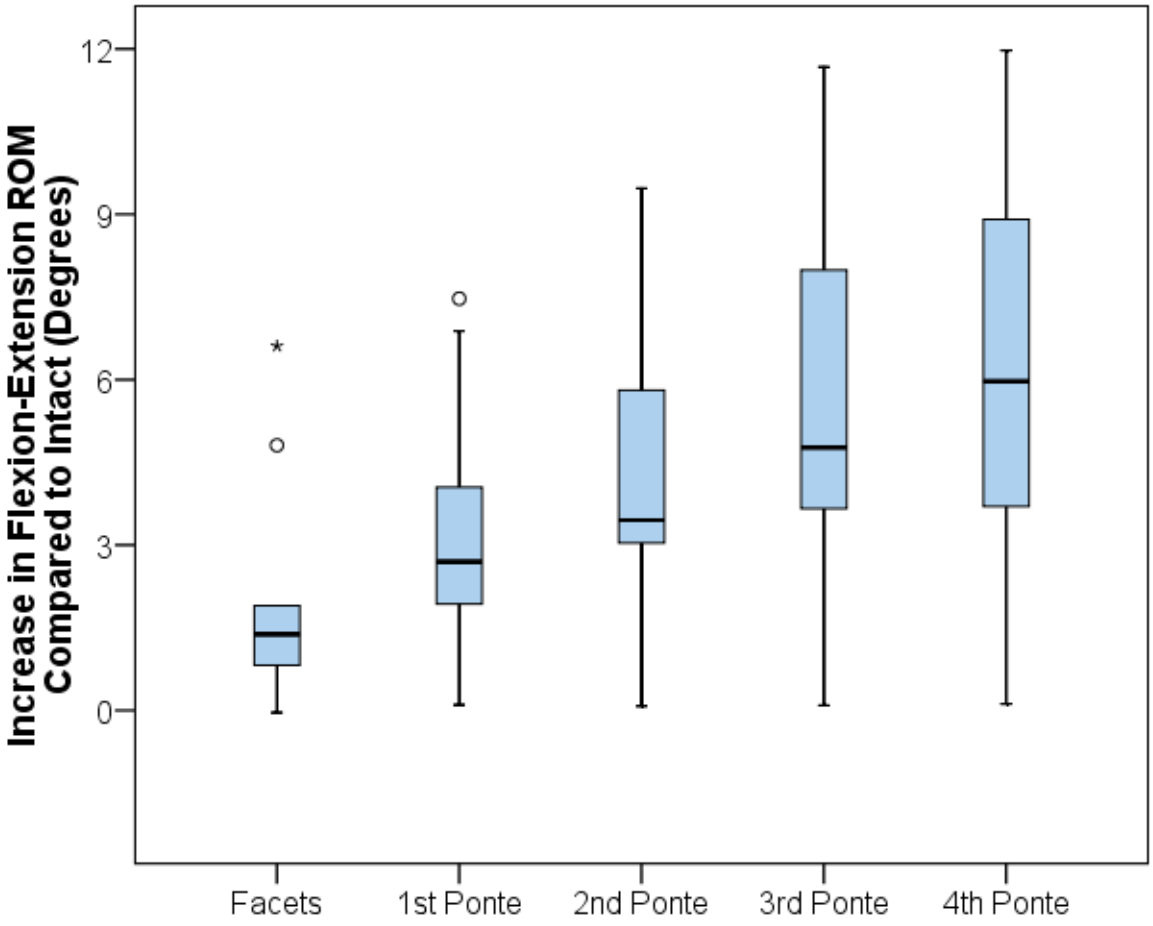

Figure 22. Increase in Flexion-Extension following each posterior release, compared to Intact.

On average, the 9 bilateral total facetectomies produced an increase in flexion-extension ROM_{TOTAL}, increasing from 21.5° ± 11.5° intact to 23.6° ± 12.8° following the total facetectomies ($p=0.02$). Each sequential, supplemental osteotomy then provided additive increases in flexion-extension ROM_{TOTAL}, increasing to 24.9° ± 13.5° ($p<0.01$), 25.8° ± 14.0°

($p<0.01$), 26.9° ± 14.8° ($p<0.01$), and 27.3° ± 15.0° ($p<0.01$) following the supplemental osteotomies at T7-T8, T8-T9, T6-T7, and T9-T10, respectively. It should be noted that the standard deviations in extension were larger than those in flexion. Note that the p-values correspond to the comparison of the ROM_{TOTAL} following each sequential posterior release with the ROM_{TOTAL} in the intact condition.

Compared to the total facetectomies, each supplemental osteotomy provided significant increases in flexion-extension ROM_{TOTAL} ($p<0.01$) (Figure 23).

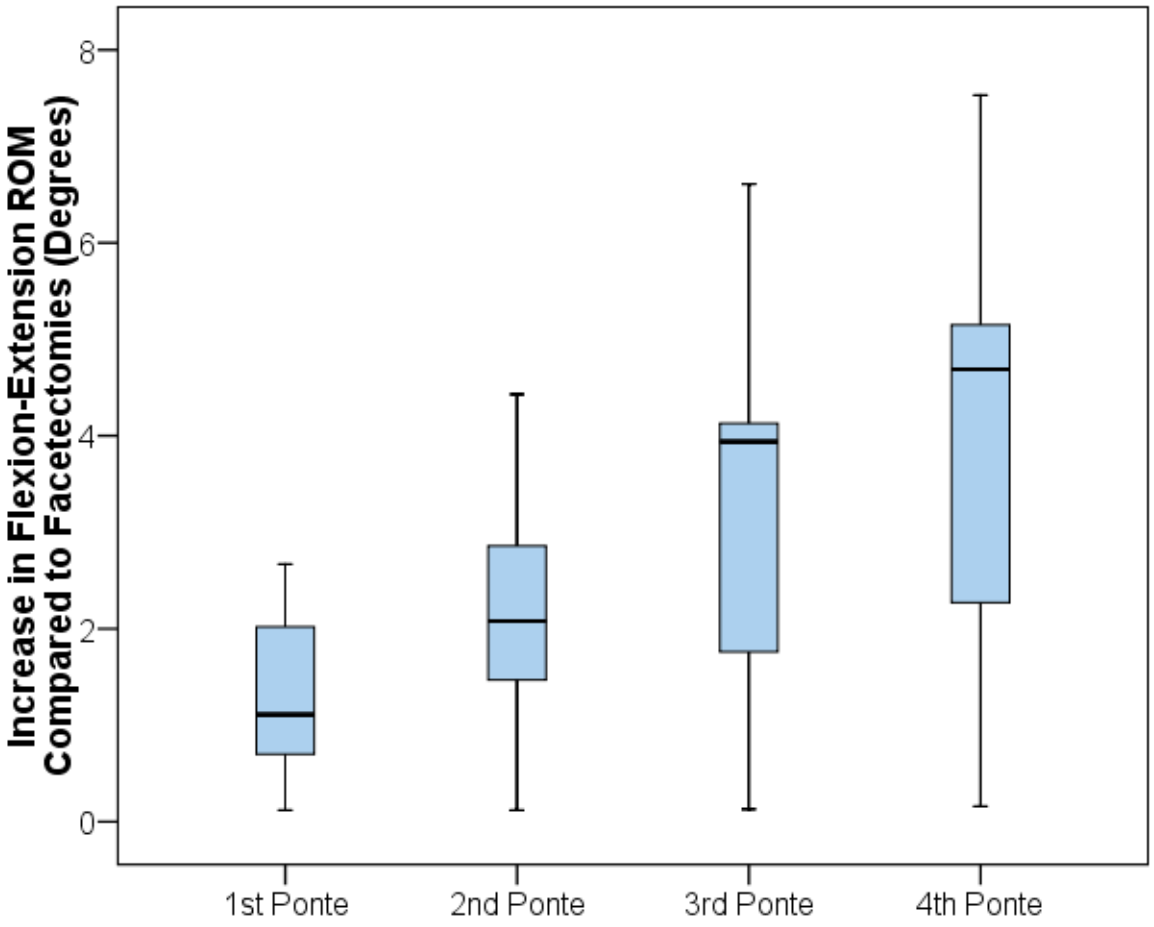

Figure 23. Increase in Flexion-Extension ROM following each of 4 sequential Ponte osteotomies, compared to Facetectomies.

Additionally, each osteotomy provided significant increases in motion beyond that provided by the preceding release. Specifically, the 2nd osteotomy provided significant increases in flexion-extension ROM_{TOTAL} as compared to the 1st osteotomy ($p<0.01$), the 3rd provided significant increases compared to the 2nd ($p<0.01$), and the 4th provided significant increases compared to the 3rd ($p=0.02$).

Similar to the raw motion results, there were additive percentage increases in flexion-extension ROM_{TOTAL} following the total facetectomies, as well as each of the supplemental osteotomies, as compared to the intact condition (Table 12). Specifically, compared to the intact condition, flexion-extension ROM_{TOTAL} increased by 8% ± 8% following facetectomies ($p=0.01$). Each osteotomy then provided additive increases. Specifically, following the 4 supplemental osteotomies, flexion-extension ROM_{TOTAL} increased by 14% ± 7% ($p<0.01$), 18% ± 8% ($p<0.01$), 22% ± 10% ($p<0.01$), and 24% ± 11% ($p<0.01$), respectively, and compared to the intact condition. The total percentage increase in ROM_{TOTAL} following the completion of the total facetectomies and the four supplemental osteotomies ranged from 8%-39%.

In addition to the increases compared to the intact condition, each osteotomy provided significant increases in normalized flexion-extension flexibility, as compared to the total facetectomies ($p<0.01$). In addition, each additional osteotomy had a significant effect compared to the previous. Specifically, the 2-level osteotomy provided significant percentage increase in flexion-extension ROM_{TOTAL} compared to the 1-level osteotomy ($p=0.01$), the 3-level provided significant increases beyond the 2-level osteotomy ($p<0.01$), and the 4-level osteotomy provided significant increases beyond the 3-level ($p=0.01$).

Table 12. Flexion-Extension - Ratio to Intact (T2-T11)

Flexion-Extension

Measure	Intact	TF	1-Level Ponte	2-Level Ponte	3-Level Ponte	4-Level Ponte
Mean (SD)	1.00 (0)	1.08 (0.08)	1.14 (0.07)	1.18 (0.08)	1.22 (0.10)	1.24 (0.11)
Range	1.00-1.00	0.97-1.22	1.06-1.26	1.06-1.31	1.06-1.38	1.08-1.39

	Intact	TF	1-Level Ponte	2-Level Ponte	3-Level Ponte	4-Level Ponte
Intact	x	**p=0.01**	**p<0.01**	**p<0.01**	**p<0.01**	**p<0.01**
Facetectomies		x	**p<0.01**	**p<0.01**	**p<0.01**	**p<0.01**
1-Level Ponte			x	**p=0.01**	**p<0.01**	**p<0.01**
2-Level Ponte				x	**p<0.01**	**p<0.01**
3-Level Ponte					x	**p<0.01**
4-Level Ponte						x

TF, Total Facetectomies; Ponte, Ponte Osteotomy; SD, Standard Deviation

In order to isolate the effects of the total facetectomies as compared to the osteotomies, an additional analysis was performed. Specifically, the increases in $ROM_{T6\text{-}T10}$ were analyzed before and after two four-level release: 4-level bilateral total facetectomies (first release), and following 4-level Ponte osteotomies (fifth and final release). Overall, $ROM_{T6\text{-}T10}$ increased following each release, with a larger effect due to the osteotomies as compared to the facetectomies. Specifically, $ROM_{T6\text{-}T10}$ increased, on average, by 0.6°±0.7° following 4 bilateral total facetectomies, compared to the intact condition ($p=0.05$). In comparison, following the 4 sequential Ponte osteotomies, larger increases were seen, with $ROM_{T6\text{-}T10}$ increasing by an additional 2.2°±1.7° ($p<0.01$).

3.1.2.3 Changes in Flexion

Once again, due to the asymmetrical anatomy of the anterior and posterior columns of the spine, flexion and extension were subsequently analyzed separately. Similarly to the specimens in ***Group A***, changes in flexion ROM_{TOTAL} were calculated as a function of the five sequential posterior release combinations, with the increases measured in two ways. First, the increases were measured after each release with respect to the intact condition. Second, the increase following each supplemental osteotomy was calculated with respect to the total facetectomy condition.

Flexion ROM_{TOTAL} increased following each posterior release, with the largest increase provided by the osteotomies. Specifically, the maximum increase following the total facetectomies was 1.6°, while each osteotomy provided a maximum increase of 1.8° (Figure 24).

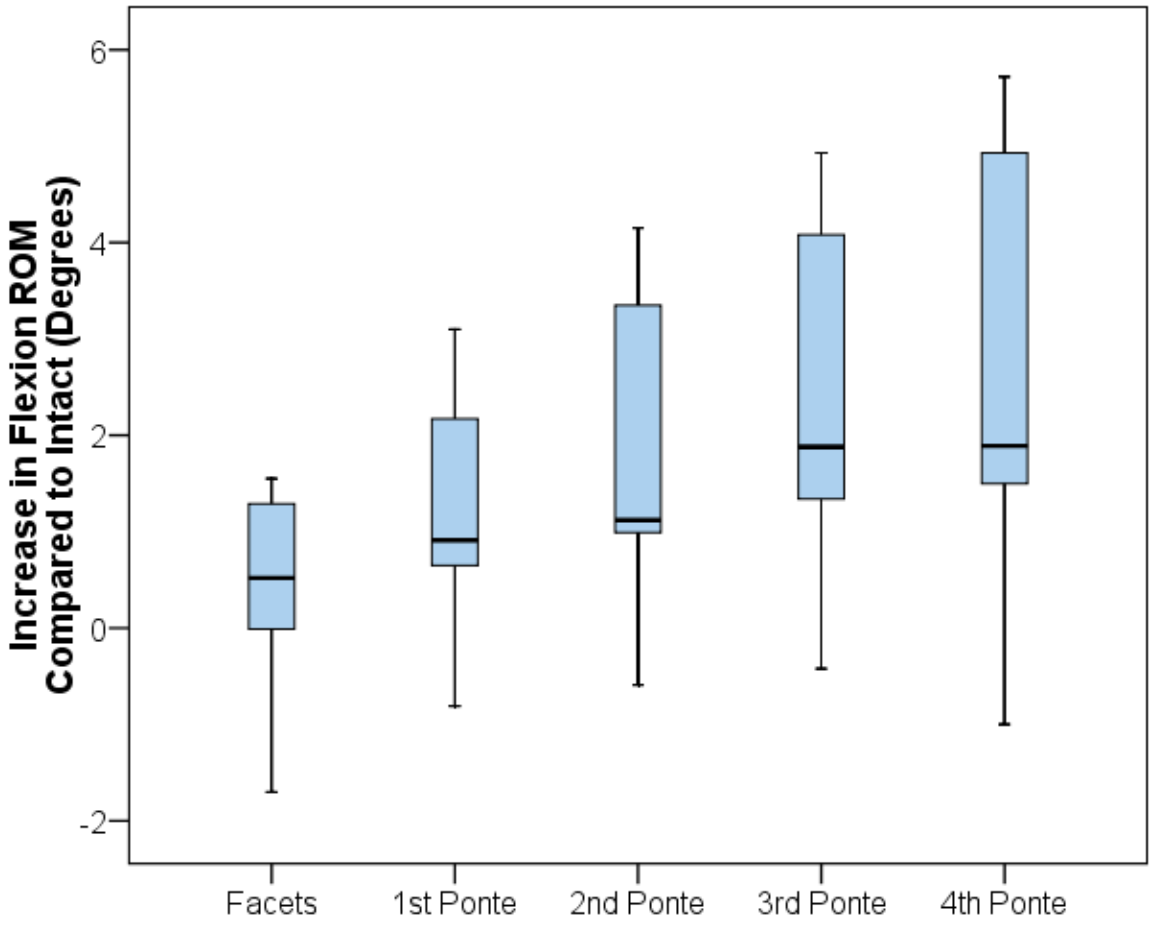

Figure 24. Increase in Flexion following each posterior release, compared to Intact.

The 9-bilateral total facetectomies produced an increase in flexion ROM_{TOTAL}, increasing from 11.3° ± 5.8° intact to 11.8° ± 6.2° following the facetectomies (p=0.23). Each sequential Ponte osteotomy provided additive increases in flexion ROM_{TOTAL}, increasing to 12.6° ± 6.6° (p=0.02), 13.2° ± 6.9° (p=0.01), 13.7° ± 7.2° (p<0.01), and 14.1° ± 7.5° (p<0.01) following the supplemental osteotomies at T7-T8, T8-T9, T6-T7, and T9-T10, respectively. Note that the p-values correspond to the comparison of the ROM_{TOTAL} following each sequential posterior release with the ROM_{TOTAL} in the intact condition.

As compared to the total facetectomies, each osteotomy provided significant increases in flexion ROM_{TOTAL} ($p<0.01$) (Figure 25).

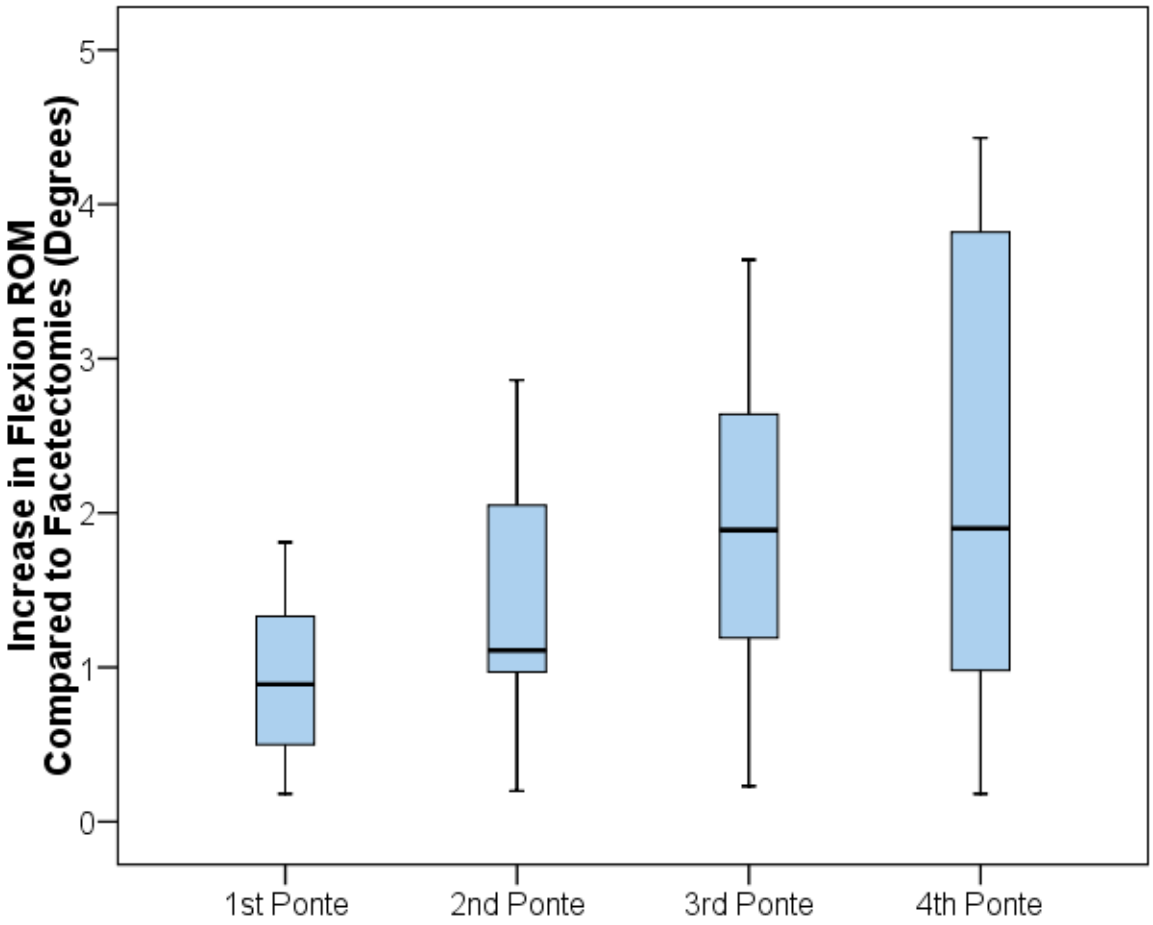

Figure 25. Increase in Flexion following each sequential osteotomy, compared to Facetectomies.

In addition, the first 3 sequential osteotomies each provided significant supplemental increase beyond the previous condition. Specifically, the 2nd osteotomy provided significant increase beyond that provided by the 1st osteotomy ($p=0.01$), and the 3rd provided significant increases beyond that provided by the 2nd ($p<0.01$). The 4th osteotomy, however, provided smaller raw motion increases compared to the 3rd osteotomy ($p=0.07$).

Similar to the raw increases in flexion ROM_{TOTAL}, there was additive percentage increases in ROM_{TOTAL} following the total facetectomies, as well as each of the supplemental osteotomies, as compared to the intact condition (Table 13). Specifically, compared to the intact condition, flexion ROM_{TOTAL} increased by 3% ± 8% following facetectomies ($p=0.23$). Following the 4 supplemental osteotomies, flexion ROM_{TOTAL} increased by 13% ±11% ($p=0.01$), 19% ± 14% ($p<0.01$), 23% ± 16% ($p<0.01$), and 26% ± 19% ($p<0.01$), respectively, and compared to the intact condition. The maximum total percentage increase in ROM_{TOTAL} following the completion of the total facetectomies and the four supplemental osteotomies was 65%.

Compared to the total facetectomies, each supplemental osteotomy provided significant increases in normalized flexion ROM_{TOTAL} ($p<0.01$). Additionally, the 2-level and 3-level osteotomies provided significant increases beyond the previous condition ($p<0.01$). However, in flexion, the 4-level osteotomy did not provide a significant increase in flexibility as compared to the 3-level osteotomy ($p=0.22$).

Table 13. Flexion - Ratio to Intact (T2-T11)

Flexion

Measure	Intact	TF	1-Level Ponte	2-Level Ponte	3-Level Ponte	4-Level Ponte
Mean (SD)	1.00 (0)	1.03 (0.08)	1.13 (0.11)	1.19 (0.14)	1.23 (0.16)	1.26 (0.19)
Range	1.00-1.00	0.87-1.11	0.94-1.28	0.95-1.47	0.97-1.55	0.92-1.65

	Intact	TF	1-Level Ponte	2-Level Ponte	3-Level Ponte	4-Level Ponte
Intact	x	p=0.23	**p=0.01**	**p<0.01**	**p<0.01**	**p<0.01**
Facetectomies		x	**p<0.01**	**p<0.01**	**p<0.01**	**p<0.01**
1-Level Ponte			x	**p=0.01**	**p<0.01**	**p<0.01**
2-Level Ponte				x	**p<0.01**	**p=0.02**
3-Level Ponte					x	p=0.22
4-Level Ponte						x

TF, Total Facetectomies; Ponte, Ponte Osteotomy; SD, Standard Deviation

3.1.2.4 Changes in Extension

Changes in extension ROM_{TOTAL} were calculated as a function of the five sequential posterior release combinations, with the increases measured in two ways. First, the increases were measured after each release with respect to the intact condition. Second, the increase following each supplemental osteotomy was calculated with respect to the total facetectomy condition.

Similar to flexion ROM_{TOTAL}, extension ROM_{TOTAL} increased following each posterior release; however, the largest increase was provided by the total facetectomies. Specifically, the maximum increase following the 9 bilateral total facetectomies was 8.3°, while each supplemental osteotomy provided a maximum increase of 2.0° (Figure 26).

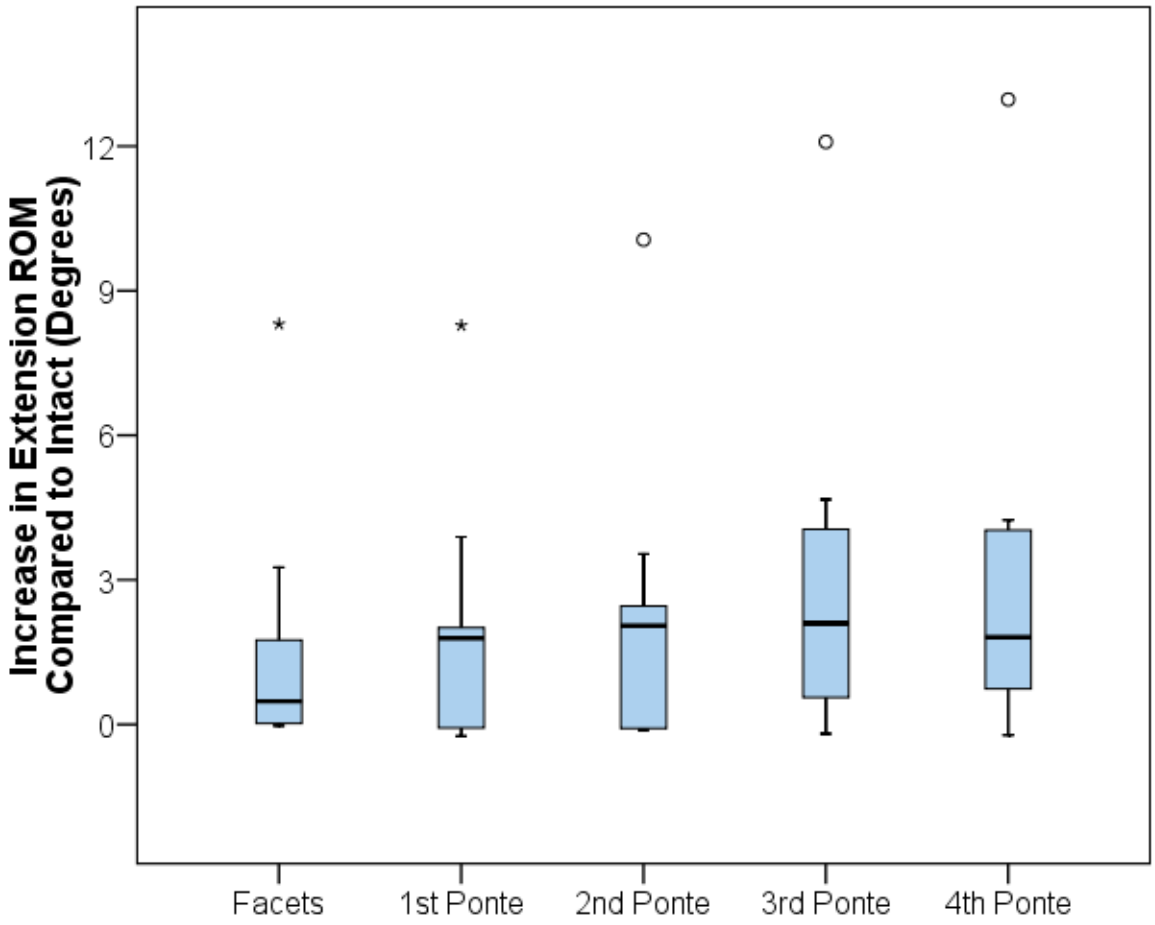

Figure 26. Increase in Extension following each posterior release, compared to Intact.

On average, the bilateral total facetectomies produced an increase in extension ROM_{TOTAL}, increasing from an intact ROM_{TOTAL} of 10.2° ± 6.6° to a ROM_{TOTAL} of 11.9° ± 8.1° following the facetectomies (p=0.10). Each sequential, supplemental osteotomy provided additive increases in extension ROM_{TOTAL}, increasing to 12.2° ± 8.5° (p=0.06), 12.5° ± 8.9° (p=0.06), 13.1° ± 9.6° (p=0.05), and 13.2° ± 9.8° (p=0.06) following the supplemental osteotomies at T7-T8, T8-T9, T6-T7, and T9-T10, respectively. It should be noted that the standard deviations in extension were larger than those in flexion. Note that the p-values

correspond to the comparison of the ROM_{TOTAL} following each sequential posterior release with the ROM_{TOTAL} in the intact condition.

Compared to the total facetectomies, significant increases were provided by 2, 3, and 4-levels of osteotomies ($p<0.06$); however, the first osteotomy provided only small increases ($p=0.15$) (Figure 27).

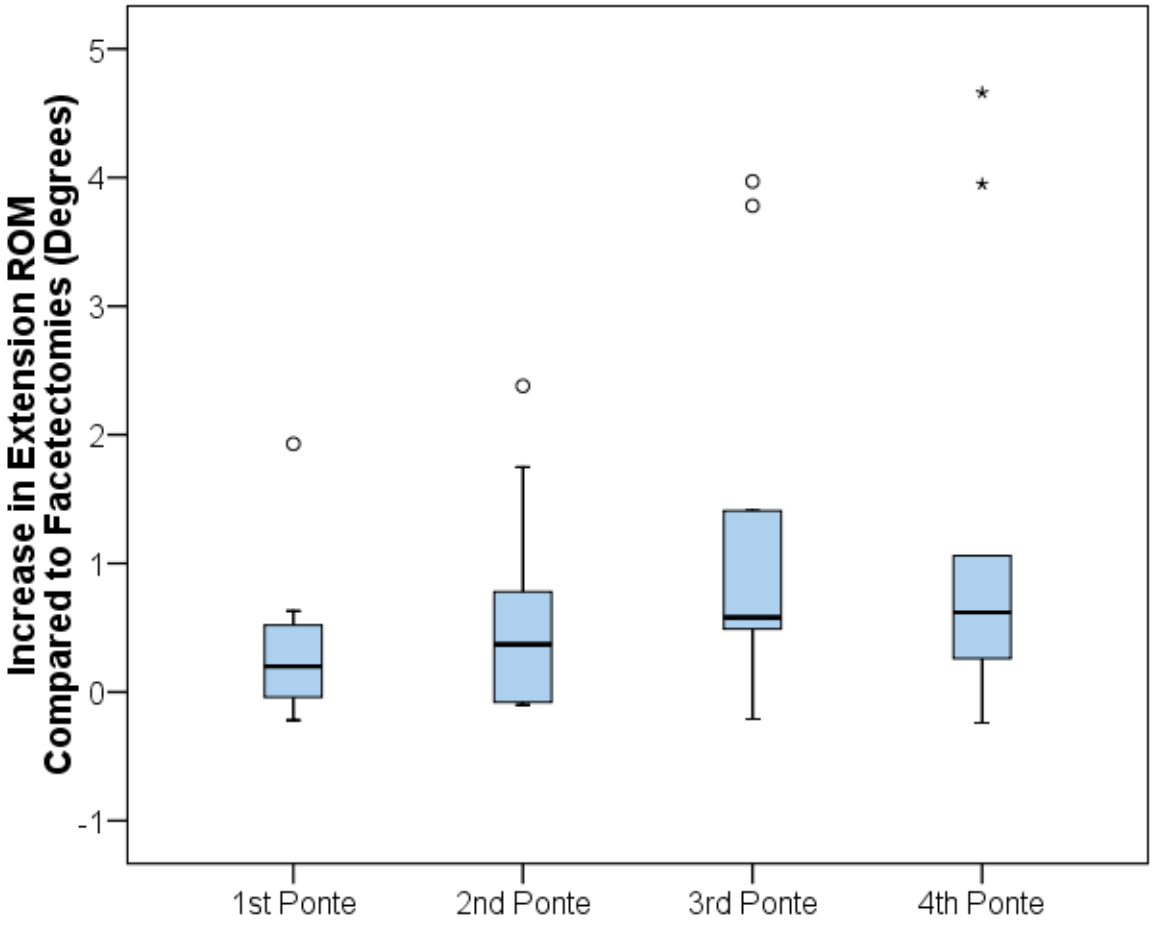

Figure 27. Increase in Extension following each of 4 sequential Ponte osteotomies, compared to Facetectomies.

Additionally, on average, each level osteotomy had a different effect with respect to the previous condition. For example, the 2nd osteotomy provided only incremental increases over the

1st osteotomy, and the 4th provided negligible increases beyond the 3rd osteotomy; however, the 3rd osteotomy provided significant increases above the 2nd (p=0.05).

There were additive percentage increases in extension ROM_{TOTAL} following the total facetectomies, as well as each of the supplemental osteotomies, as compared to the intact condition (Table 14). Specifically, compared to the intact condition, extension ROM_{TOTAL} increased by 14% ± 18% following facetectomies (p=0.05). Following the 4 supplemental osteotomies, flexion ROM_{TOTAL} increased by 16% ± 20% (p=0.05), 17% ± 23% (p=0.06), 21% ± 27% (p=0.05), and 22% ± 26% (p=0.03), respectively, and compared to the intact condition. The maximum total percentage increase in ROM_{TOTAL} following the completion of the total facetectomies and the four supplemental osteotomies was 72%.

Table 14. Extension - Ratio to Intact (T2-T11)

	Extension					
Measure	Intact	TF	1-Level Ponte	2-Level Ponte	3-Level Ponte	4-Level Ponte
Mean (SD)	1.00 (0)	1.14 (0.18)	1.16 (0.20)	1.17 (0.23)	1.21 (0.27)	1.22 (0.26)
Range	1.00-1.00	0.96-1.46	0.91-1.46	0.85-1.56	0.83-1.67	0.93-1.72

	Intact	TF	1-Level Ponte	2-Level Ponte	3-Level Ponte	4-Level Ponte
Intact	x	**p=0.05**	**p=0.05**	p=0.06	**p=0.05**	**p=0.03**
Facetectomies		x	p=0.26	p=0.18	p=0.08	**p=0.04**
1-Level Ponte			x	p=0.29	p=0.09	p=0.06
2-Level Ponte				x	p=0.07	p=0.06
3-Level Ponte					x	p=0.45
4-Level Ponte						x

TF, Total Facetectomies; Ponte, Ponte Osteotomy; SD, Standard Deviation

Unlike normalized flexion ROM_{TOTAL}, significant increases in normalized extension ROM_{TOTAL} beyond the facetectomies were not realized until all four Ponte osteotomies were completed ($p=0.04$). Additionally, the 3-level osteotomy provided increases in normalized extension ROM_{TOTAL} compared to the 2-level osteotomy ($p=0.07$); however, the 4-level osteotomy did not significantly add to the percentage increase in total flexibility ($p=0.45$), compared to the 3-level osteotomy.

3.1.2.5 Changes in Lateral Bending

Similar to flexion-extension, the increases in lateral bending ROM_{TOTAL} were calculated as a function of the sequential posterior releases, that is, the facetectomies and sequential osteotomies. The increases were measured with respect to the intact condition. Similar to ***Group A***, the increases in lateral bending ROM_{TOTAL} in ***Group B*** were the smallest in magnitude amongst the bending directions. Smaller increases were seen in lateral bending compared with flexion-extension, flexion, extension, or axial rotation. Additionally, the 2nd, 3rd, and 4th supplemental osteotomy had little effect on lateral bending ROM_{TOTAL}.

In lateral bending, the total facetectomies had the largest effect of the posterior releases on ROM_{TOTAL}. Specifically, lateral bending ROM_{TOTAL} increases ranged from 0-3.2° following the total facetectomies. Meanwhile, following each osteotomy ROM_{TOTAL} increased by a maximum of only 1.4° (Figure 28).

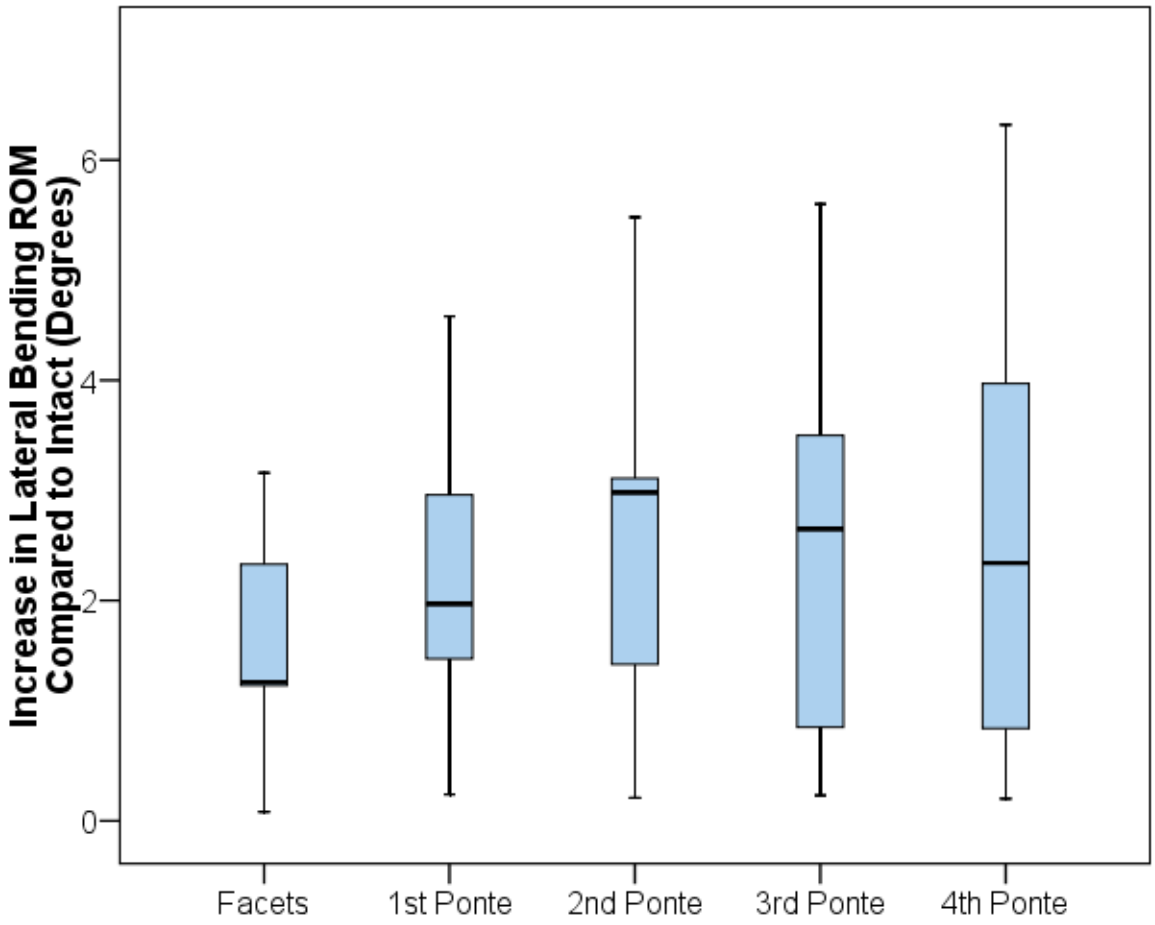

Figure 28. Increase in Lateral Bending ROM following each posterior release, compared to Intact.

On average, lateral bending ROM_{TOTAL} increased from 28.5° ± 13.4° intact to 30.2° ± 14.3° following the 9 bilateral total facetectomies ($p<0.01$). Lateral bending ROM_{TOTAL} further increased to 30.7° ± 14.6° ($p<0.01$) and 31.1° ± 14.9° ($p<0.01$) following the first two osteotomies, respectively; however, following the 3rd and 4th osteotomies, ROM_{TOTAL} remained the same or showed negligible changes. The reported p-values correspond to the comparisons of the lateral bending ROM_{TOTAL} following each osteotomy as compared to the intact condition.

Compared to the total facetectomies, each supplemental osteotomy provided increases in lateral bending ROM_{TOTAL} (Figure 29).

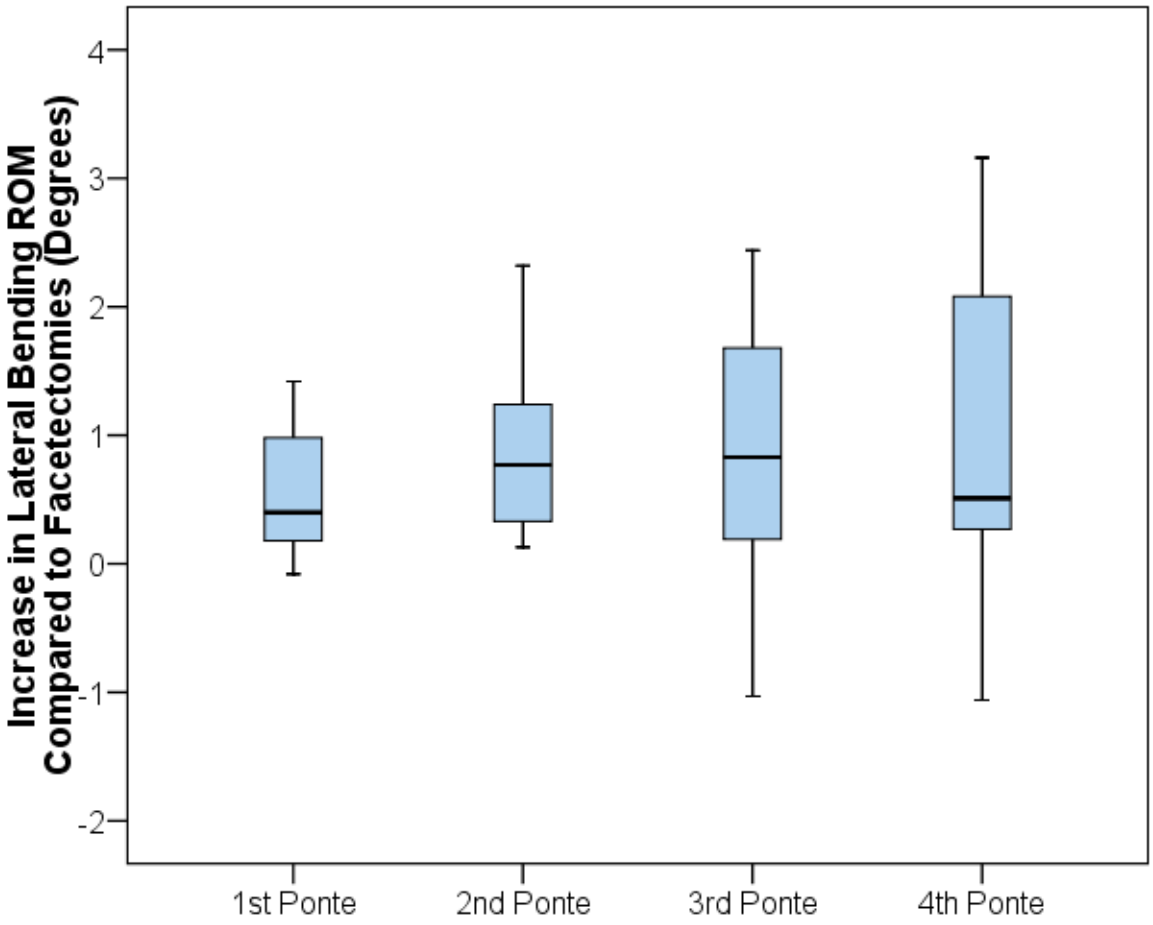

Figure 29. Increase in Lateral Bending ROM following each of 4 sequential Ponte osteotomies, compared to Facetectomies.

Specifically, increases were demonstrated following 1-level ($p=0.01$), 2-levels ($p<0.01$), 3-levels ($p=0.05$), and 4-levels of osteotomies ($p=0.06$). In addition, the second osteotomy provided significant increase in motion compared to the 1st osteotomy ($p=0.03$). The 3rd and 4th osteotomies, however, did not provided increases beyond the 2-level osteotomy ($p>0.29$).

Normalized increases showed similar trends (Table 15). Specifically, compare to the intact condition, lateral bending ROM_{TOTAL} increased by 5% ± 2% following total facetectomies ($p<0.01$). Following the four supplemental osteotomies, normalized motion increased by 7% ± 2% ($p<0.01$), 8% ± 2% ($p<0.01$), 8% ± 4% ($p<0.01$), and 9% ± 4% ($p<0.01$), respectively, and

compared to the intact condition. In the most destabilized condition, i.e. following the total facetectomies and the four osteotomies, ROM_{TOTAL} increases ranged from 1% to 15%.

Compared to the total facetectomies, in lateral bending, the normalized ROM_{TOTAL} significantly increased following each of the four supplemental osteotomies ($p<0.03$). Additionally, the 2-level osteotomy provided significant increases in normalized flexibility beyond the 1-level osteotomy ($p=0.05$). However, the 3-level and 4-level osteotomies did not have a significant effect on total flexibility ($p>0.27$).

Table 15. Lateral Bending - Ratio to Intact (T2-T11)

	Lateral Bending					
Measure	Intact	TF	1-Level Ponte	2-Level Ponte	3-Level Ponte	4-Level Ponte
Mean (SD)	1.00 (0)	1.05 (0.02)	1.07 (1.02)	1.08 (0.02)	1.08 (0.04)	1.09 (0.04)
Range	1.00-1.00	1.02-1.08	1.05-1.11	1.05-1.13	1.01-1.13	1.01-1.15

	Intact	TF	1-Level Ponte	2-Level Ponte	3-Level Ponte	4-Level Ponte
Intact	x	**p<0.01**	**p<0.01**	**p<0.01**	**p<0.01**	**p<0.01**
Facetectomies		x	**p<0.01**	**p<0.01**	**p=0.02**	**p=0.02**
1-Level Ponte			x	**p=0.05**	p=0.29	p=0.20
2-Level Ponte				x	p=0.93	p=0.56
3-Level Ponte					x	p=0.28
4-Level Ponte						x

TF, Total Facetectomies; Ponte, Ponte Osteotomy; SD, Standard Deviation

Similar to previous analyses, in addition to the analysis comparing the effects of the four supplemental osteotomies to the 9 bilateral total facetectomies, a surgically relevant condition,

the lateral bending $ROM_{T6\text{-}T10}$ was analyzed to compare equal-level releases. Similar to the analysis of ROM_{TOTAL}, the posterior releases had little effect on $ROM_{T6\text{-}T10}$.

Specifically, increases in lateral bending $ROM_{T6\text{-}T10}$ following posterior releases were smaller than those in flexion-extension or axial rotation. On average, lateral bending $ROM_{T6\text{-}T10}$ increased by 0.2°±0.5° following the 4-level total facetectomies (p=0.22), and by an additional 0.2°±0.6° following the four sequential Ponte osteotomies (p=0.32).

3.1.2.6 Changes in Axial Rotation

Changes in axial rotation ROM_{TOTAL} were calculated as a function of the five sequential posterior release combinations, with the increases measured in two ways. First, the increases were measured after each release with respect to the intact condition. Second, the increase following each supplemental osteotomy was calculated with respect to the total facetectomy condition. Overall, the sequential releases provided additive effects to the flexibility of the full length thoracic spines, with increases larger in magnitude than those in lateral bending.

As discussed, axial rotation ROM_{TOTAL} increased following each posterior release. The largest increases were provided by the total facetectomies, with increases ranging from 0-8.1°. Meanwhile, increases following each supplemental osteotomy ranged from 0-3.1° (Figure 30).

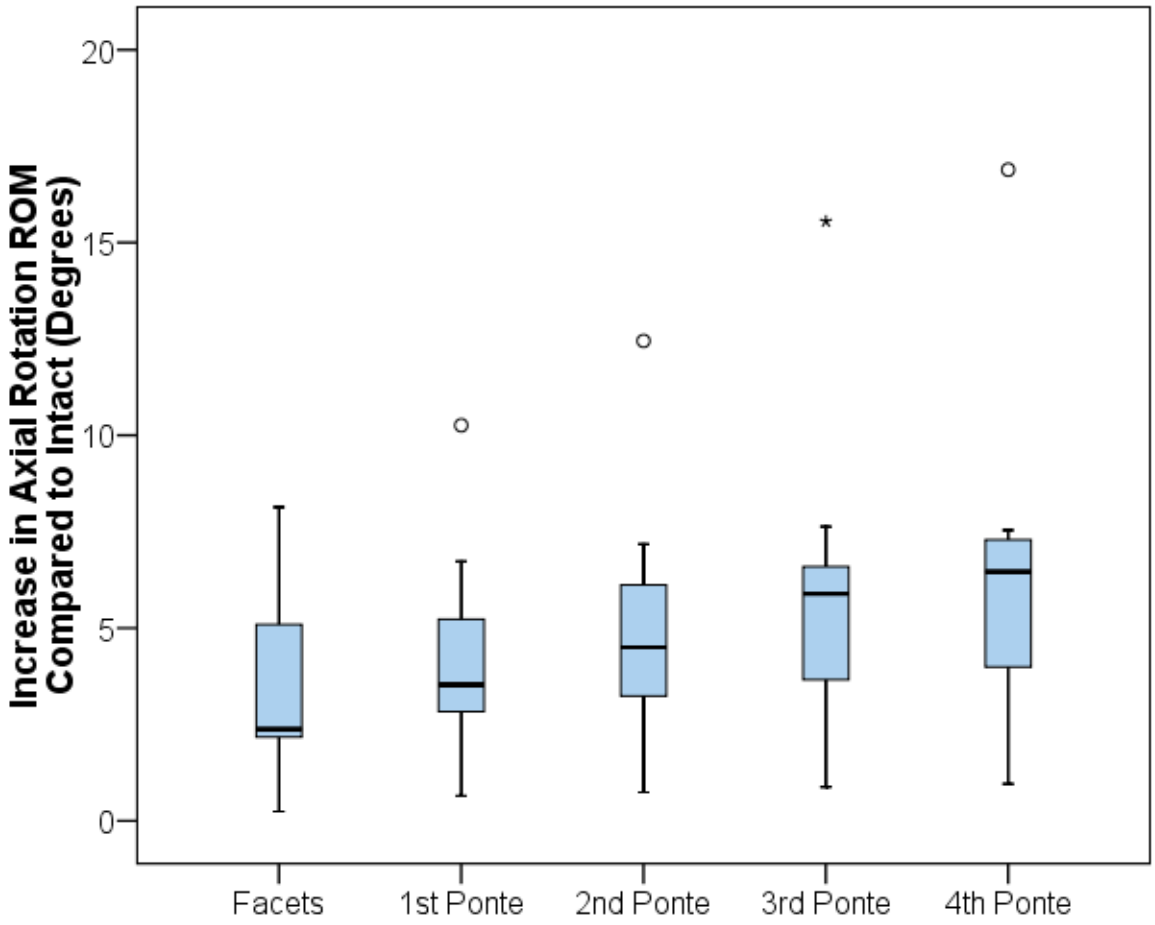

Figure 30. Increase in Axial Rotation ROM following each posterior release, compared to Intact

On average, the bilateral total facetectomies produced an increase in axial rotation ROM_{TOTAL}, with ROM_{TOTAL} increasing from 36.4° ± 15.3° intact to 39.9° ± 17.1° following the facetectomies ($p<0.01$). Similarly to the other bending directions, each sequential Ponte osteotomy provided additive increases in axial rotation ROM_{TOTAL}, increasing to 40.7° ± 17.4° ($p<0.01$), 41.5° ± 17.9° ($p<0.01$), 42.3° ± 18.4° ($p<0.01$), and 42.8° ± 18.6° ($p<0.01$) following the four supplemental osteotomies from T6-T10, respectively. Note that the p-values correspond to the comparison of the ROM_{TOTAL} following each sequential posterior release with the ROM_{TOTAL} in the intact condition.

As compared to the total facetectomies, each Ponte osteotomy provided significant increases in axial rotation ROM_{TOTAL} ($p<0.02$) (Figure 31).

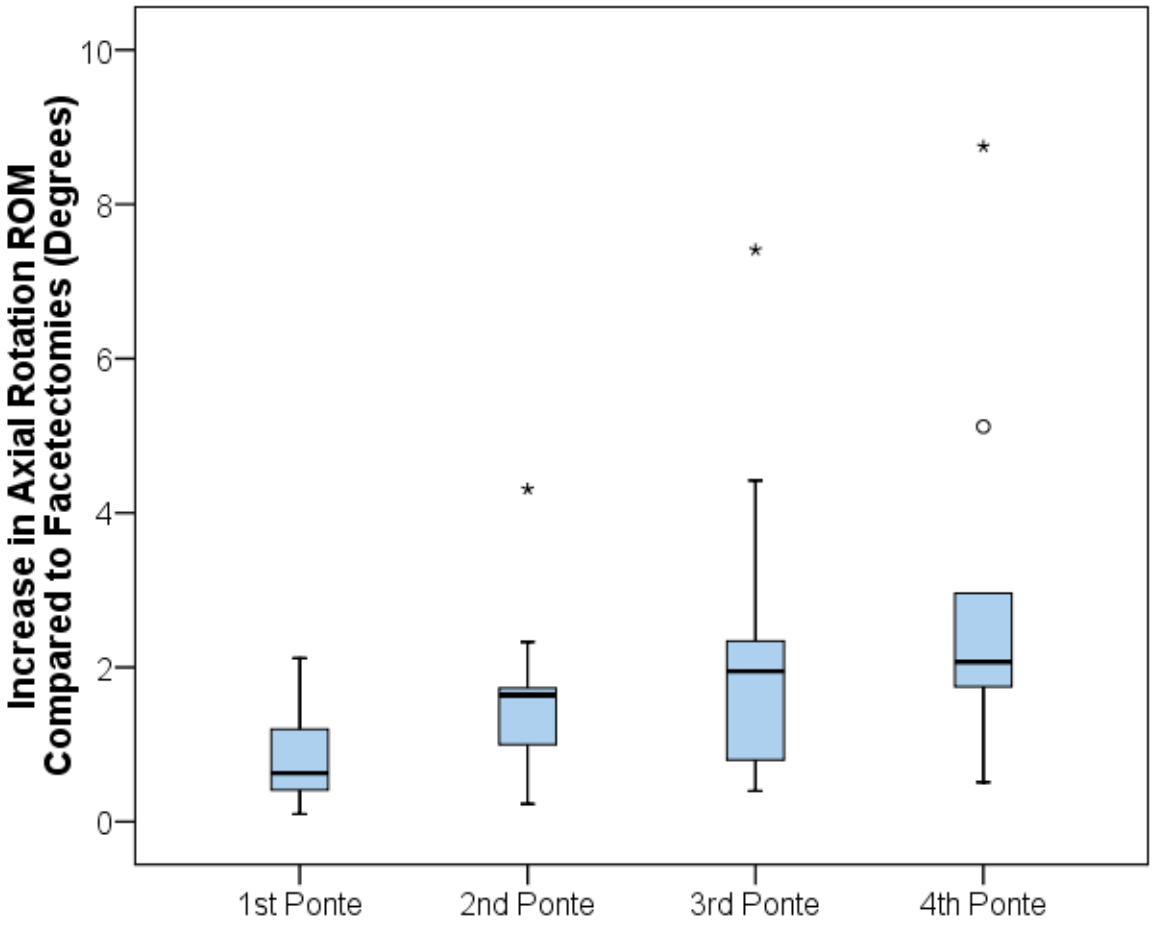

Figure 31. Increase in Axial Rotation ROM following each of 4 sequential Ponte osteotomies, compared to Facetectomies

Additionally, each osteotomy provided significant increases in motion beyond that provided by the preceding release. Specifically, the 2-level osteotomy provided significant increases in axial rotation ROM_{TOTAL} as compared to the 1-level osteotomy ($p<0.01$), the 3-level osteotomy provided significant increases beyond the 2-level osteotomy ($p=0.06$), and the 4-level osteotomy provided increases beyond the 3-level osteotomy ($p=0.02$).

There was also an additive percentage increase in axial rotation ROM_{TOTAL} following the series of posterior releases (Table 16). Specifically, axial rotation ROM_{TOTAL} increased by 9% ± 5% following total facetectomies ($p<0.01$), compared to the intact condition. Additive increases were then produced following each supplemental osteotomies, with percent increases in axial rotation ROM_{TOTAL} compared to the intact condition of 12% ± 5% ($p<0.01$), 13% ± 6% ($p<0.01$), 16% ± 8% ($p<0.01$), and 17% ± 8% ($p<0.01$) following the four osteotomies, respectively. Overall, following the entire sequence of posterior releases, that is, following the total facetectomies and the four osteotomies, axial rotation ROM_{TOTAL} increases ranged from 9%-37%.

In addition to the increases compared to the intact condition, each osteotomy provided significant increases in normalized axial rotation flexibility, as compared to the total facetectomies ($p<0.01$). In addition, each additional osteotomy had a significant effect compared to the previous ($p<0.04$). Specifically, the 2-level osteotomy provided significant percentage increase in axial rotation ROM_{TOTAL} compared to the 1-level osteotomy ($p<0.01$), the 3-level provided significant increases beyond the 2-level osteotomy ($p=0.03$), and the 4-level osteotomy provided significant increases beyond the 3-level ($p<0.01$).

Table 16. Axial Rotation - Ratio to Intact (T2-T11)

Axial Rotation

Measure	Intact	TF	1-Level Ponte	2-Level Ponte	3-Level Ponte	4-Level Ponte
Mean (SD)	1.00 (0)	1.09 (0.05)	1.12 (0.05)	1.13 (0.06)	1.16 (0.08)	1.17 (0.08)
Range	1.00-1.00	1.05-1.18	1.07-1.23	1.08-1.27	1.09-1.34	1.09-1.37

	Intact	TF	1-Level Ponte	2-Level Ponte	3-Level Ponte	4-Level Ponte
Intact	x	**p<0.01**	**p<0.01**	**p<0.01**	**p<0.01**	**p<0.01**
Facetectomies		x	**p=0.01**	**p<0.01**	**p<0.01**	**p<0.01**
1-Level Ponte			X	**p<0.01**	**p<0.01**	**p<0.01**
2-Level Ponte				x	**p=0.03**	**p<0.01**
3-Level Ponte					x	**p<0.01**
4-Level Ponte						x

TF, Total Facetectomies; Ponte, Ponte Osteotomy; SD, Standard Deviation

It should also be noted that, in some cases, the standard deviations suggest the possibility of a decrease in flexibility. However, this is due to the inherent assumptions in the calculations of the standard deviations around the mean. More specifically, it is assumed that there is a symmetric distribution on either side of the mean, that is, above and below the mean. However, in this case, like many other cases in the scientific literature, this is not the case. For example, negative energy cannot be produced; however, in electrical engineering, standard deviations around a mean may suggest that it could. Similarly, in this case, negative flexibility cannot be produced.

In addition to the above analysis which compares the additive effects of the four supplemental osteotomies to the 9 bilateral total facetectomies, a surgically relevant condition, the axial rotation $ROM_{T6\text{-}T10}$ was analyzed to compare equal-level releases. Specifically, the

$ROM_{T6\text{-}T10}$ was analyzed to compare the effect of 4 total facetectomies to 4 osteotomies, at the same levels. Overall, increases in axial rotation $ROM_{T6\text{-}10}$ were similar in trend to the increases in ROM_{TOTAL}.

Specifically, axial rotation $ROM_{T6\text{-}T10}$ increased, on average, by 1.0°±1.3° following 4 bilateral total facetectomies, increasing from 14.2°±9.6° in the intact condition to 15.2°±10.5° following the facetectomies (p=0.06). Following the 4 sequential Ponte osteotomies, axial rotation $ROM_{T6\text{-}T10}$ increased to 17.3°±11.3°. Therefore, axial rotation $ROM_{T6\text{-}T10}$ increased by an additional 1.5°±1.7° (p=0.03), beyond the total facetectomies.

3.1.3 Group C

3.1.3.1 Summary of Results

Single Plane Pure Moments were applied to each of the n=11 full-length human cadaveric thoracic spine specimens to produce flexion-extension, lateral bending, and axial rotation, to a maximum of ±4 Nm. As described in the Materials and Methods section, ROM_{TOTAL} was defined as the relative motion of T2 with respect to T11. In addition, local ROM was measured at the T10-T11 disc space, with $ROM_{T10\text{-}T11}$ defined as the relative motion of T10 with respect to T11. Unlike ***Group A*** and ***Group B***, specimens in ***Group C*** were tested in the intact condition, following facetectomy at T10-T11, and again following Ponte osteotomy at T10-T11.

Similar to the *Single Plane Pure Moment* testing results of ***Group A*** and ***Group B***, significant increases in total (T2-T11) ROM in flexion-extension and axial rotation were produced following both total facetectomy and Ponte osteotomy at T10-T11 (Table 17). Once again, changes in lateral bending were small.

Overall, ROM_{TOTAL} across T2-T11 was largest in axial rotation, and smallest in flexion-extension. Specifically, intact flexion-extension was ROM_{TOTAL} 11.7±9.4°, intact lateral bending ROM_{TOTAL} was 25.5±15.3°, and intact axial rotation ROM_{TOTAL} was 40.5±19.3°. Sequential increases in ROM_{TOTAL} were seen following both posterior releases in flexion-extension and axial rotation; changes in lateral bending were small.

Table 17. Total (T2-T11) ROM Paired Statistics

	Flexion-Extension (Degrees)			Lateral Bending (Degrees)			Axial Rotation (Degrees)		
	Intact	Facet	Ponte	Intact	Facet	Ponte	Intact	Facet	Ponte
Mean	11.7	13.4	14.5	25.5	24.8	24.5	40.5	41.0	42.0
Std Dev	9.4	10.4	12.2	15.3	15.5	15.8	19.3	19.4	19.6
	Intact	Facet	Ponte	Intact	Facet	Ponte	Intact	Facet	Ponte
Intact		p=0.013	p=0.042		p=0.410	p=0.356		p=0.003	p=0.009
Facet			p=0.178			p=0.445			p=0.016
Ponte									

3.1.3.2 Changes in Flexion-Extension

On average, flexion-extension ROM_{TOTAL} increased following both posterior releases (Table 17). Specifically, following facetectomy, flexion-extension ROM_{TOTAL} increased from 11.7° ± 9.4° intact to 13.4° ± 10.4° following the facetectomy (p=0.013). Compared to the total facetectomy, the ROM_{TOTAL} increased further following the osteotomy, with an average motion of 14.5° ± 12.2° (p=0.178). Compared to the intact condition, ROM_{TOTAL} increases ranged from 0.1-5.1° following the facetectomy and from -0.3-10.9° following the Ponte osteotomy.

Similar to the raw motion results, there were additive percentage increases in flexion-extension following both posterior releases (Table 18). Specifically, compared to intact, flexion-extension motion increased by 35%±66% following Ponte osteotomy (p=0.147).

Table 18. Flexion-Extension - Ratio to Intact (T2-T11 ROM_{TOTAL})

	Intact	Total Facetectomy (T10-T11)	Ponte Osteotomy (T10-T11)
Mean (SD)	1.00 (0)	1.31 (0.50)	1.35 (0.66)
Range	1.00-1.00	1.01-2.63	0.93-3.07
Intact	X	p=0.103	p=0.147
Total Facetectomy (T10-T11)		X	p=0.121
Ponte Osteotomy (T10-T11)			X

3.1.3.3 Changes in Lateral Bending

Compared to the changes in motion in flexion-extension and axial rotation, changes in lateral bending were small (Table 17). Specifically, intact lateral bending ROM_{TOTAL} was 25.5±15.3°. Following the facetectomy at T10-T11, motion changed by less than one degree (p=0.410). Similarly, following Ponte osteotomy, change in ROM_{TOTAL} was less than one degree, compared to the total facetectomy (p=0.445). In terms of normalized increases in ROM_{TOTAL}, changes were also small (p>0.200) (Table 19). Maximum increases in lateral bending ROM_{TOTAL} were 2.5° following the facetectomy and 3.8° following the osteotomy, compared to the intact condition.

Table 19. Lateral Bending - Ratio to Intact (T2-T11 ROM_{TOTAL})

	Intact	Total Facetectomy (T10-T11)	Ponte Osteotomy (T10-T11)
Mean (SD)	1.00 (0)	0.96 (0.07)	0.95 (0.10)
Range	1.00-1.00	0.83-1.05	0.76-1.07
Intact	X	p=0.203	p=0.205
Total Facetectomy (T10-T11)		X	p=0.439
Ponte Osteotomy (T10-T11)			X

3.1.3.4 Changes in Axial Rotation

Similar to flexion-extension, ROM_{TOTAL} increased following both posterior releases (Table 17). Specifically, following facetectomy, axial rotation ROM_{TOTAL} increased from 40.5° ± 19.3° intact to 41.0° ± 19.4° following the facetectomy (p=0.003). Compared to the total facetectomy, the ROM_{TOTAL} increased further following the osteotomy, with an average axial rotation motion of 42.0° ± 19.6° (p=0.016). Compared to the intact condition, increases ranged from 0-1.3° following the facetectomy and from -0.1-3.9° following the osteotomy.

Similar to the raw motion results, there were additive percentage increases in axial rotation ROM_{TOTAL} following both posterior releases (Table 20). Specifically, compared to intact, axial rotation ROM_{TOTAL} increased by 2%±1% following total facetectomy (p=0.002), and 4%±3% following Ponte osteotomy (p=0.006).

Table 20. Axial Rotation - Ratio to Intact (T2-T11 ROM_{TOTAL})

	Intact	Total Facetectomy (T10-T11)	Ponte Osteotomy (T10-T11)
Mean (SD)	1.00 (0)	1.02 (0.01)	1.04 (0.03)
Range	1.00-1.00	1.00-1.03	1.00-1.10
Intact	X	p=0.002	p=0.006
Total Facetectomy (T10-T11)		X	p=0.250
Ponte Osteotomy (T10-T11)			X

In axial rotation, the local ROM at T10-T11 ($ROM_{T10-T11}$) was also evaluated for a comparison to the simulated DVR and DVR-to-Failure results presented later in this work. Local bidirectional axial rotation $ROM_{T10-T11}$ increased from 4.5±2.3° intact to 5.2±3.0° following the osteotomy (p=0.058) (Table 21).

Unidirectional axial rotation right, which was the motion evaluated in simulated DVR and DVR-to-Failure, increased from 1.8°±0.7° intact to 2.1°±1.0° following the osteotomy (p=0.055). Increases following the Ponte osteotomy ranged from 0-0.9°, compared to the intact condition. In other words, unidirectional increases in right axial rotation $ROM_{T10-T11}$ were small under pure moment loads (4 Nm).

Table 21. Local (T10-T11) ROM under Pure Moment Loading

	Axial Rotation Right (Degrees)			Bidirectional Axial Rotation (Degrees)		
	Intact	Total Facetectomy (T10-T11)	Ponte Osteotomy (T10-T11)	Intact	Total Facetectomy (T10-T11)	Ponte Osteotomy (T10-T11)
Mean	1.8	2.0	2.1	4.5	5.5	5.2
Std Dev	0.7	0.8	1.0	2.3	2.9	3.0
	p=0.148			p=0.319		
	p=0.055			p=0.058		

3.2 Multi-Planar Loading

3.2.1 Group B

3.2.1.1 Summary of Results

The results of the *Multi-Planar Loading* of specimens in ***Group B*** were published previously (Appendix A),[250] and are reported as they pertain to the present work below. In addition to *Single Plane Pure Moment* loading, specimens in ***Group B*** also underwent testing according to the novel *Multi-Planar Loading* protocol. Under the two *Multi-Planar Loading* schemes, that is, axial rotation with combined lateral bending and axial rotation combined with flexion-extension, increases in 3-dimensional motion were seen following each of the sequential posterior releases. The maximum increases in ROM were largest following the 9-level bilateral total facetectomies. However, despite the smaller increases, the supplemental osteotomies provide additive increases in 3-dimensional motion, similar to the *Single Plane Pure Moment* results.

3.2.1.2 Flexion-Extension with Combined Axial Rotation

Under the first *Multi-Planar Loading* direction, that is, flexion-extension with combined axial rotation, the largest increases in three-dimensional motion were produced following the total facetectomies. Specifically, intact motion was 10.8°±6.9° in flexion-extension, 10.6°±6.1° in lateral bending, and 33.4°±14.2° in axial rotation, increasing to 12.7°±8.3° in flexion-extension, 11.6°±6.6° in lateral bending, and 36.2°±15.6° in axial rotation following the facetectomies (Table 22). Additional increases were provided in all three directions following each sequential osteotomy, with three-dimensional motion increasing to 13.8°±8.8° in flexion-

extension, 12.6°±7.2° in lateral bending, and 38.3°±16.8° in axial rotation following the 4-level Ponte osteotomy.

Table 22. Multi-Planar Motions - Axial Rotation with Flexion-Extension: Difference in ROM Following Each Sequential Release (T2-T11)[250]

	Flexion-Extension (Deg)		Lateral Bending (Deg)		Axial Rotation (Deg)	
	Mean (SD)	Range	Mean (SD)	Range	Mean (SD)	Range
Facetectomies - Intact	1.8 (1.6)	0.1-5.2	1.0 (0.7)	-0.1-2.4	2.7 (1.9)	0.1-5.4
Ponte 1 - Facetectomies	0.4 (0.4)	-0.2-0.9	0.3 (0.3)	-0.2-1.0	0.7 (0.4)	0.1-1.1
Ponte 2 - Ponte 1	0.4 (0.4)	-0.3-0.9	0.3 (0.4)	0.0-1.2	0.6 (0.5)	-0.1-1.4
Ponte 3 - Ponte 2	0.3 (0.5)	-0.3-1.4	0.3 (0.4)	0.0-1.3	0.6 (0.8)	-0.1-2.2
Ponte 4 - Ponte 3	0.1 (0.4)	-0.5-0.7	0.1 (0.3)	-0.1-0.6	0.2 (0.2)	-0.1-0.7

In addition to the mean increases in three-dimensional motion, the maximum increases in three-dimensional motion were largest under combined flexion-extension with axial rotation following the total facetectomies, as compared each supplemental osteotomy. Specifically, total facetectomies increased ROM_{TOTAL} in each bending plane simultaneously up to 5.2° in flexion-extension, 2.4° in lateral bending, and 5.4° in axial rotation. Each osteotomy, on the other hand, provided a maximum simultaneous increase in ROM_{TOTAL} of 1.4° in flexion-extension, 1.3° in lateral bending, and 2.2° in axial rotation.

Similar to the raw three-dimensional motions, changes in three-dimensional normalized ROM_{TOTAL} were produced following each posterior-release. Specifically, as compared to the intact condition, the total facetectomies produced simultaneous increases in all three directions, with increases of 16%±7% in flexion-extension, 10%±7% in lateral bending, and 8%±4% in axial rotation. Each supplemental osteotomy provided additive increases in flexibility in the coronal and transverse planes, i.e. lateral bending and axial rotation; however, the increases were

unpredictable in flexion-extension. Specifically, lateral bending and axial rotation ROM_{TOTAL} increased incrementally to 20%±14% in lateral bending and 14%±6% in axial rotation following the 4-level osteotomies. In contrast, in flexion-extension, ROM_{TOTAL} increased to 30%±31% following the first osteotomy, but decreased to 17%±35% following the 4th osteotomy.

3.2.1.3 Lateral Bending with Combined Axial Rotation

Under the second *Multi-Planar Loading* protocol, that is, lateral bending with combined axial rotation, similar results were found, with the largest increases produced by total facetectomies as compared to the supplemental osteotomies. However, the magnitudes of increase were smaller than the first *Multi-Planar Loading* protocol, i.e. flexion-extension with combined axial rotation.

Specifically, the three-dimensional ROM_{TOTAL} increased from 3.8°±2.5° in flexion-extension, 21.5°±10.6° in lateral bending, and 28.7°±14.2° in axial rotation, to 4.3°±3.2° in flexion-extension, 22.3°±10.9° in lateral bending, and 30.0°±15.2° in axial rotation between the intact and total facetectomies conditions (Table 23). On average, however, the changes following each supplemental osteotomy were small. Specifically, the motions following 4-levels of osteotomies resulted in three-dimensional ROM_{TOTAL} of only 4.0°±3.3° in flexion-extension, 23.2°±11.9° in lateral bending, and 30.9°±15.6° in axial rotation.

Table 23. Multi-Planar Motions - Axial Rotation with Lateral Bending: Difference in ROM Following Each Sequential Release (T2-T11)[250]

	Flexion-Extension (Deg)		Lateral Bending (Deg)		Axial Rotation (Deg)	
	Mean (SD)	Range	Mean (SD)	Range	Mean (SD)	Range
Facetectomies - Intact	0.5 (1.1)	-0.6-2.7	0.9 (0.9)	-0.2-2.7	1.3 (1.7)	-0.7-4.5
Ponte 1 - Facetectomies	-0.2 (0.4)	-1.0-0.4	0.3 (0.7)	-1.1-1.2	0.5 (0.7)	-0.2-2.1
Ponte 2 - Ponte 1	0.1 (0.1)	-0.1-0.4	0.3 (0.6)	-0.3-1.6	0.3 (0.5)	-0.4-1.2
Ponte 3 - Ponte 2	-0.1 (0.3)	-0.9-0.2	0.0 (0.5)	-0.8-0.6	0.0 (0.5)	-1.0 (0.5)
Ponte 4 - Ponte 3	-0.1 (0.3)	-0.8-0.4	0.2 (0.6)	-0.4-1.5	0.1 (0.5)	-0.3 (1.1)

Similarly, the maximum increases in three-dimensional motion under lateral bending with combined axial rotation were larger following the total facetectomies compared with the Ponte osteotomies. Specifically, total facetectomies provided simultaneous increases in ROM_{TOTAL} of up to 2.7° in flexion-extension, 2.7° in lateral bending, and 4.5° in axial rotation. In comparison, a single osteotomy provided simultaneous increases in total ROM of up to 0.4° in flexion-extension, 1.6° in lateral bending, and 2.1° in axial rotation.

In contrast to the first *Multi-Planar Loading* protocol, under combined lateral bending with axial rotation, the three-dimensional flexibility increases were near-universally smaller than 10%, even following the maximally destabilized condition, i.e. following the facetectomies and 4-level osteotomies. Specifically, as compared to the intact condition, the total facetectomies produced simultaneous increases in normalized ROM_{TOTAL} in all three directions, with increases of 12%±28% in flexion-extension, 4%±4% in lateral bending, and 3%±6% in axial rotation, all smaller than the first *Multi-Planar Loading* protocol.

Similar to the first *Multi-Planar Loading* protocol, each supplemental osteotomy provided additive increases simultaneously in lateral bending and axial rotation; however, the

changes were small in magnitude. Specifically, following the 4th osteotomy, normalized ROM_{TOTAL} increased simultaneously by 8%±5% in lateral bending and 7%±7% in axial rotation, compared to the intact condition. In flexion-extension on the other hand, changes were negligible, with changes of less than 2%.

3.3 Intraoperative Simulation and DVR-to-Failure

3.3.1 DVR-to-Failure

On average, under simulated DVR, the intervertebral disc moment at failure was 33.3±12.1 Nm (Table 24). The applied force to produce failure was 138.6±52.0 N. At failure, unidirectional right axial rotation at T10-T11 was 11.6°±5.6°. The load was applied at an average distance away from the spine of 350.9 mm.

Table 24. DVR-to-Failure Results and Observations

Exp	Disc Moment (Nm)	Applied Force (N)		Observations
1	43.2	190.6	Loosening (s)	
			Fracture(s)	
			Disc Instability	
2	21.7	109.6	Loosening (s)	R-T7; L-T9; R-T10; L-T10
			Fracture(s)	Fracture at left lamina of T10, just inferior to screw and superior to osteotomy site; Fracture at T10 just posterior to ALL
			Disc Instability	Yes
3	30.7	135.2	Loosening (s)	R-T10; L-T10
			Fracture(s)	Fracture at left T10 inferior to screw insertion site
			Disc Instability	None noted
4	13.7	20.3	Loosening (s)	
			Fracture(s)	
			Disc Instability	
5	36.9	160.1	Loosening (s)	
			Fracture(s)	
			Disc Instability	
6	35.8	154.6	Loosening (s)	L-T10
			Fracture(s)	Osteophyte fracture
			Disc Instability	Yes. Disc bulging when bending.
7	47.4	172.8	Loosening (s)	L-T7; R-T9; L-T9; Rt-T10
			Fracture(s)	
			Disc Instability	
8	54.7	202.7	Loosening (s)	
			Fracture(s)	
			Disc Instability	
9	23.3		Loosening (s)	R-T10; L-T10
			Fracture(s)	
			Disc Instability	
10	25.5	114.4	Loosening (s)	L-T7; R-T10; L-T10
			Fracture(s)	
			Disc Instability	
11	33.2	125.5	Loosening (s)	R-T8; L-T8; R-T10; L-T10
			Fracture(s)	
			Disc Instability	

On average, strain was largest at the T10 linkage, where strain at failure was 3.30E-04 (Table 25). Strain decreased across the linkages, moving away from the T10-T11 disc space. In other words, strain was largest at T10, decreasing to a minimum strain at failure of 1.18E-04 at the T7 linkage.

Table 25. DVR-to-Failure Strength, Force, and Strain Results

	Disc Moment Nm	Applied Force (Surgical) N	Strain (T7)	Strain (T8)	Strain (T9)	Strain (T10)
Mean	33.3	138.6	1.18E-04	1.47E-04	2.70E-04	3.30E-04
Std Dev	12.1	52.0	1.26E-04	9.04E-05	1.42E-04	1.65E-04
Min	13.7	20.3	4.59E-07	2.34E-05	3.45E-05	1.52E-04
Max	54.7	202.7	4.46E-04	3.11E-04	4.75E-04	6.45E-04

For the specimens in ***Group C***, BMD ranged from 0.616-0.992 g/cm^2 at T7, 0.625-0.992 g/cm^2 at T8, 0.643-1.035 g/cm2 at T9, and 0.652-1.151 g/cm^2 at T10 (Table 26). Average BMD across the linked vertebrae, i.e. T7-T10, ranged from 0.640-1.042 g/cm^2.

Table 26. Group C Specimen BMD Results across Linked Vertebrae

	T7 BMD g/cm2	T8 BMD g/cm2	T9 BMD g/cm2	T10 BMD g/cm2	Avg BMD g/cm2
Mean	0.788	0.815	0.85	0.878	0.833
Std Dev	0.124	0.13	0.138	0.161	0.134
Min	0.616	0.625	0.643	0.652	0.640
Max	0.992	0.991	1.035	1.151	1.042

The failure moment was significantly correlated with average BMD across the quadrangular linkage, with a Pearson correlation coefficient of r=0.609 (p=0.047) (Table 27, Figure 32).

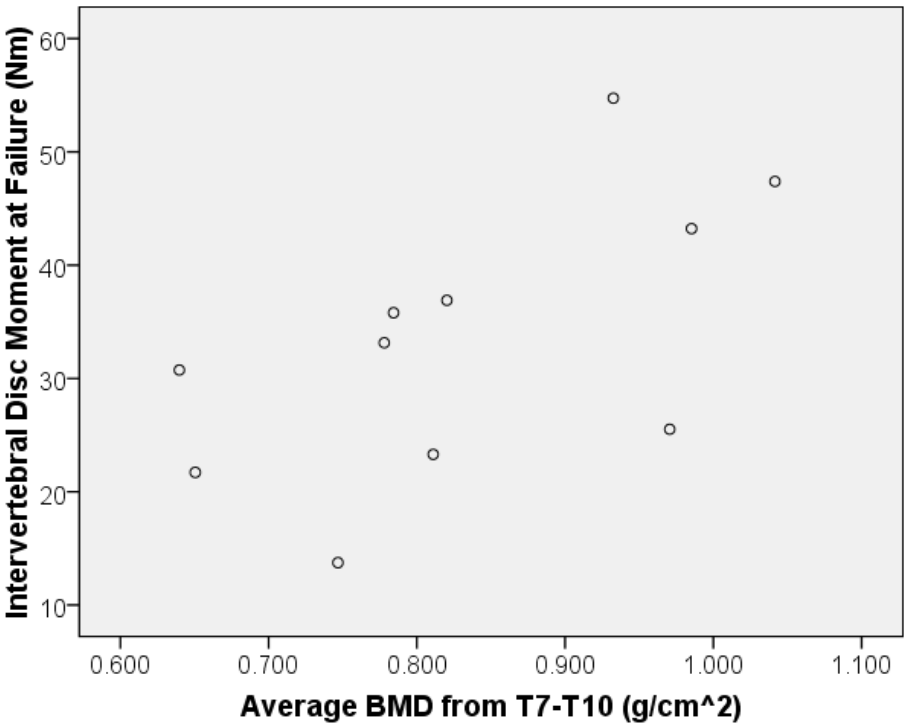

Figure 32. Correlation between the intervertebral disc moment at failure and the average BMD across the instrumented T7-T10 vertebral bodies.

Table 27. Correlation with Avg BMD

	Disc Moment	Applied Force
Pearson	0.609	0.514
p value	0.047	0.129
Spearman	0.664	0.636
p value	0.026	0.048

Similarly, the applied force to produce failure was correlated with average BMD, with a Pearson correlation coefficient of r=0.514 (p=0.129) (Figure 33).

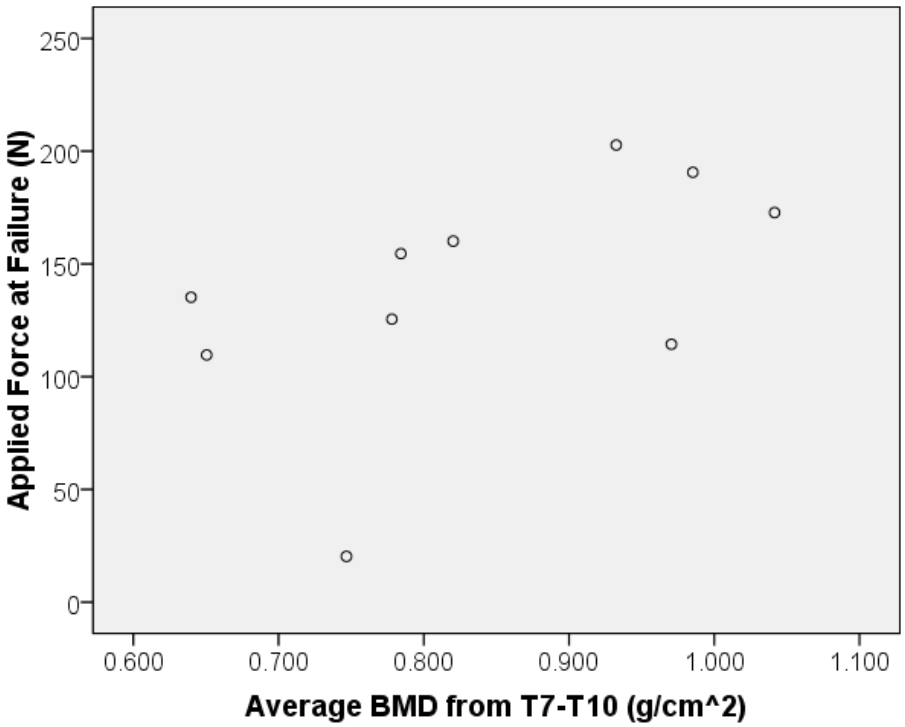

Figure 33. Correlation between the intervertebral disc moment at failure and the average BMD across the instrumented T7-T10 vertebral bodies.

There were also strong correlations between failure moment and intervertebral disc health. Specifically, failure moment was positively correlated with radiographic degeneration grade (Spearman's rho>0.662, p<0.04) and MRI degeneration grade (Spearman's rho=0.742, p=0.014). Note that full disc health results are presented later in this work.

3.3.2 Intraoperative Simulation

As discussed previously in this work, the average disc moment at failure was 33.3±12.1 Nm. Subsequently, average moments at 75%, 50%, and 25% of the failure moment were calculated (Table 28).

Table 28. Intervertebral Disc Failure Moment Calculations

	Failure	75% Failure	50% Failure	25% Failure
	Nm	Nm	Nm	Nm
Mean	33.3	25.0	16.6	8.3
Std Dev	12.1	9.1	6.0	3.0
Min	13.7	10.3	6.9	3.4
Max	54.7	41.1	27.4	13.7

In order to compare the simulated DVR results with those obtained from traditional pure moment testing, the unidirectional right axial rotation $ROM_{T10\text{-}T11}$ under simulated DVR were compared to the right axial rotation $ROM_{T10\text{-}T11}$ under pure moments. As presented earlier for ***Group C*** specimens, under pure moment loading (4 Nm), right axial rotation (ARR) at T10-T11 was 1.8±0.7° intact, increasing to 2.1±1.0° following the osteotomy. Increases in ARR at T10-T11 were 0.25±0.31°, with a maximum increase in ARR at T10-T11 was 0.9°.

In contrast to the increases produced under 4Nm pure moments, the increases produced under simulated DVR were significantly larger (Figure 34). Compared to the T10-T11 right axial rotation ROM under simulated DVR at 4 Nm (nominally equivalent load as that applied during pure moments), significant increases in motion were produced at 25%, 50%, 75%, and 100% of the failure moment ($p<0.001$) (Table 29). Specifically, T10-T11 ARR ROM increased from 2.7±1.5° under 4 Nm simulated DVR to 11.6±5.6° at failure ($p<0.001$).

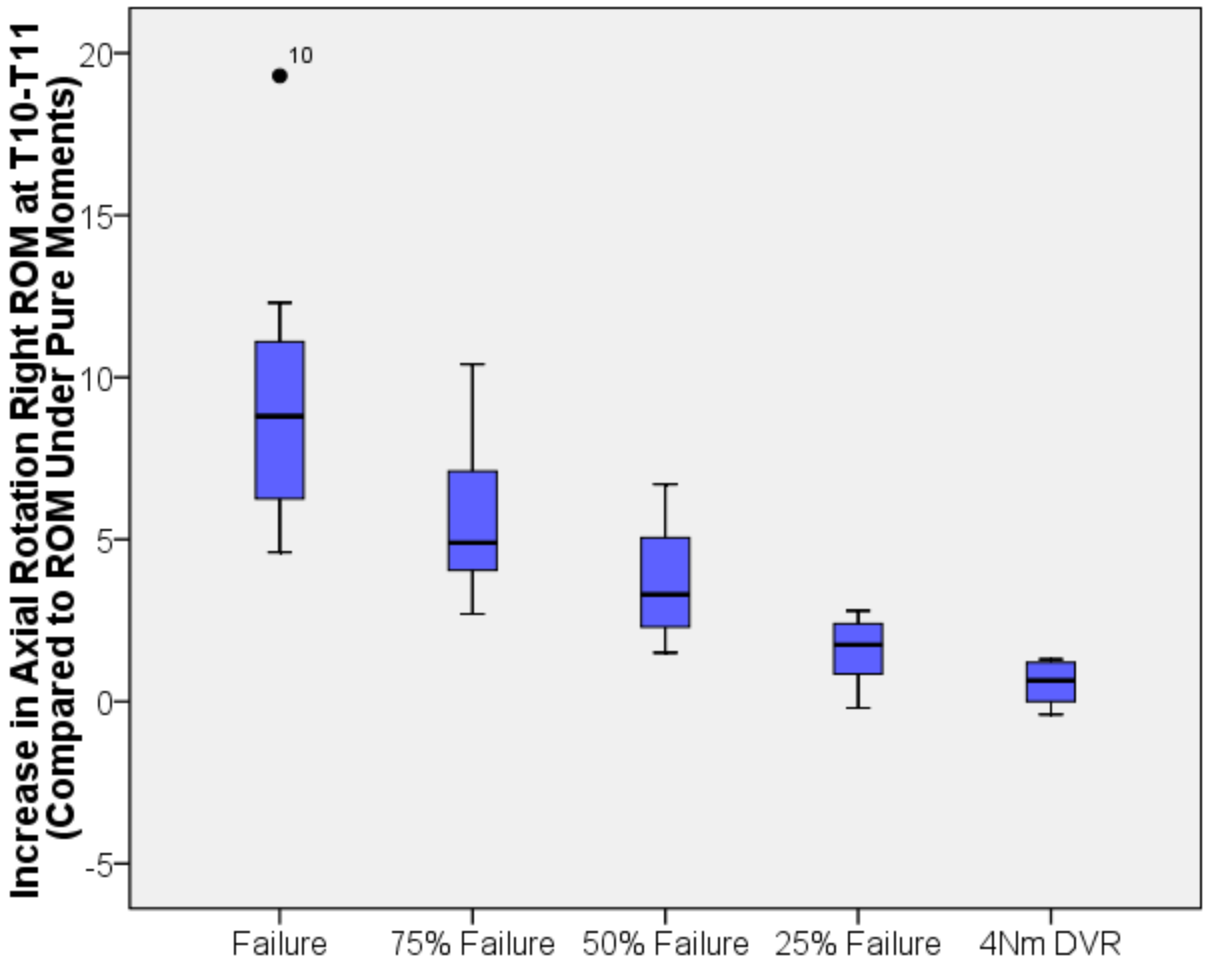

Figure 34. Increases in axial rotation right ROM under simulated DVR compared to ROM under pure moment testing. All increases significant compared to ROM under pure moments (p<0.001).

Table 29. Local (T10-T11) Right Axial Rotation ROM Under Simulated DVR

	4 Nm		Percentage of Failure Moment			
	Pure Moments (deg)	DVR (deg)	25% (deg)	50% (deg)	75% (deg)	100% (deg)
Mean	2.1	2.7	3.7	5.8	7.7	11.6
Std Dev	1.0	1.5	1.8	2.6	3.3	5.6
	p=0.001					
		p<0.001				
			p<0.001			
				p<0.001		
					p<0.001	

When considering the maximum increases in motion, similar trends were found (Table 30). Specifically, compared to maximum increase in ARR ROM at T10-T11 of 0.9° following posterior release under pure moments, maximum increases of 19.3° were produced under simulated DVR-to-Failure. Even at 50% of the failure moment (16.6±6.0 Nm), maximum increases in ARR ROM at T10-T11 were more than four times those achieved under pure moments.

Table 30. Increase in T10-T11 Right Axial Rotation ROM (Compared to Previous)

	4 Nm		Percentage of Failure Moment			
	Pure Moments (deg)	DVR (deg)	25% (deg)	50% (deg)	75% (deg)	100% (deg)
Range	0.0-0.9	-0.4-1.3	-0.2-2.0	0.8-4.3	0.9-3.7	1.4-8.9

3.4 Supplemental Analyses

3.4.1 Biomechanics as a Function of Disc Degeneration

3.4.1.1 Group B

3.4.1.1.1 Overview of Biomechanical Data

As discussed earlier, n=9 specimens from ***Group B*** were included in the biomechanical analysis presented above. For the secondary analysis presented here, that is, analyzing the biomechanics pre- and post- destabilization as a function of intervertebral disc health, n=7 specimens were available for grading. Consequently, this secondary analysis is based on those n=7 specimens. As such, the kinematic data, in terms of means and standard deviations, changed slightly for this subgroup of 7 specimens compared to the full group of 9 specimens. As such, a brief overview of these kinematic results is presented below.

In summary, during *Single Plane Pure Moment* loading, intact ROM_{TOTAL} was 21.7±7.2° in flexion-extension, 30.1±10.0° in lateral bending, and 39.9±11.3° in axial rotation. Local T10-T11 ROM, i.e. $ROM_{T10\text{-}T11}$, was 2.4±1.3°, 2.5±1.6°, and 3.2±1.8° in flexion-extension, lateral bending, and axial rotation, respectively.

Overall, total ROM_{TOTAL} significantly increased in all directions following both bilateral total facetectomies and 4-sequential Ponte osteotomies (Table 31).

Table 31. T2-T11 Range of Motion Results (All Specimens)

	Flexion-Extension (degrees)			Lateral Bending (degrees)			Axial Rotation (degrees)		
	Intact	BTF	4 PO	Intact	BTF	4 PO	Intact	BTF	4 PO
Mean	21.7	24.2	27.9	30.1	31.7	32.6	39.9	44.0	47.2
Std. Dev.	7.2	9.0	10.5	10.0	10.6	11.3	11.3	12.9	14.6
Min	10.7	11.2	11.9	14.3	14.8	15.1	19.0	20.2	20.7
Max	30.7	37.3	42.7	43.2	45.5	47.6	53.0	57.4	62.4
*P-Value**		0.026	0.004		0.001	0.007		0.004	0.007

*Compared to intact

Std. Dev., standard deviation; Min, minimum; Max, maximum; BTF, bilateral total facetectomies; 4 PO, 4-level Ponte osteotomies

On average, following the bilateral total facetectomies, ROM_{TOTAL} increased by 2.5±2.3° in flexion-extension, 1.6±0.8° in lateral bending, and 4.1±2.4° in axial rotation. Following 4-sequential Ponte osteotomies, ROM increased by 6.2±3.6° in flexion-extension, 2.5±1.7° in lateral bending, and 7.3±4.7° in axial rotation.

Following each osteotomy, flexion-extension ROM_{TOTAL} increased by 0.9±0.7°, lateral bending ROM_{TOTAL} increased by 1.1±0.5°, and axial rotation ROM_{TOTAL} increased by 3.1±0.8°. Maximum increases in ROM_{TOTAL} following a single osteotomy were 2.2°, 1.1°, and 3.1° in flexion-extension, lateral bending, and axial rotation, respectively.

3.4.1.1.2 Summary of Degeneration Results

Overall, thoracic ROM was negatively correlated with radiographic disc degeneration grade. Increases in ROM for healthier spines were at least two-fold larger than increases for degenerated spines, following destabilizations. Maximum increases in ROM for healthier spines

were also two-fold larger than degenerated spines. There were no correlations between age of the specimens and thoracic spine ROM.

3.4.1.1.3 Radiographic Analysis

According to Lane *et al.*'s[254] radiographic criteria (0-3), three specimens had mild degeneration (*Lane* Grade 1) and four specimens had moderate degeneration (*Lane* Grade 2). According to Mimura *et al.*'s[196] radiographic criteria (0-4), one specimen had mild degeneration (*Mimura* Grade 1), three specimens had moderate degeneration (*Mimura* Grade 2), and three specimens had severe degeneration (*Mimura* Grade 3). The two scoring systems were moderately correlated, with a Spearman's rho of 0.468; however, this correlation was not significant (p=0.290).

Overall, there was a negative correlation between the radiographic degeneration scores and intact thoracic spine ROM_{TOTAL} (Table 32).

Table 32. Correlation Between Intact Total (T2-T11) Range of Motion and Intervertebral Disc Health

		Intact Total (T2-T11) Range of Motion		
		Flexion-Extension	Lateral Bending	Axial Rotation
Lane *et al.*[254]	Spearman's rho	-0.577	-0.289	-0.433
	P-Value	0.175	0.530	0.332
Mimura *et al.*[196]	Spearman's rho	-0.501	**-0.849**	**-0.772**
	P-Value	0.252	**0.016**	**0.042**
Rutges *et al.*[147]	Spearman's rho	-0.438	-0.438	-0.319
	P-Value	0.325	0.325	0.486

The strongest negative correlations were produced between *Mimura* radiographic degeneration grades and lateral bending and axial rotation ROM_{TOTAL}, with Spearman's rho

magnitudes of -0.849 and -0.772, respectively. On the other hand, flexion-extension ROM_{TOTAL} was most strongly negatively correlated with *Lane* radiographic degeneration grades; however, this correlation was not significant (p=0.18).

Similarly, negative correlations were found between radiographic degeneration grades and local $ROM_{T10\text{-}T11}$, the disc space at which the spines were graded (Table 33).

Table 33. Correlation Between Intact Local (T10-T11) Range of Motion and Intervertebral Disc Health

		Intact Local (T10-T11) Range of Motion		
		Flexion-Extension	Lateral Bending	Axial Rotation
Lane *et al.*[254]	Spearman's rho	-0.577	**-0.866**	-0.577
	P-Value	0.175	**0.012**	0.175
Mimura *et al.*[196]	Spearman's rho	**-0.849**	-0.617	**-0.849**
	P-Value	**0.016**	0.140	**0.016**
Rutges *et al.*[147]	Spearman's rho	-0.438	-0.438	-0.438
	P-Value	0.325	0.325	0.325

For intact $ROM_{T10\text{-}T11}$, strong negative correlations were found between *Mimura* degeneration grades and flexion-extension and axial rotation $ROM_{T10\text{-}T11}$, with Spearman's rho of -0.849 (p=0.02). Lateral bending $ROM_{T10\text{-}T11}$ was most strongly negatively correlated with *Lane* degeneration grade, with a Spearman's rho of -0.866, the strongest of all the correlations (p=0.01).

Based on the strong correlations between intact ROM_{TOTAL} and Mimura degeneration grades in lateral bending and axial rotation ($p<0.05$), a second analysis was performed. Specifically, specimens of Mimura grade 2 (n=3) and Mimura grade 3 (n=3) were compared. As only one specimen was graded with a Mimura grade 1, this specimen was not included in the second analysis.

The mean intact thoracic ROM_{TOTAL} for the healthier grade 2 specimens was more than 12° larger than the more degenerated, grade 3 specimens in each bending direction (Figure 35).

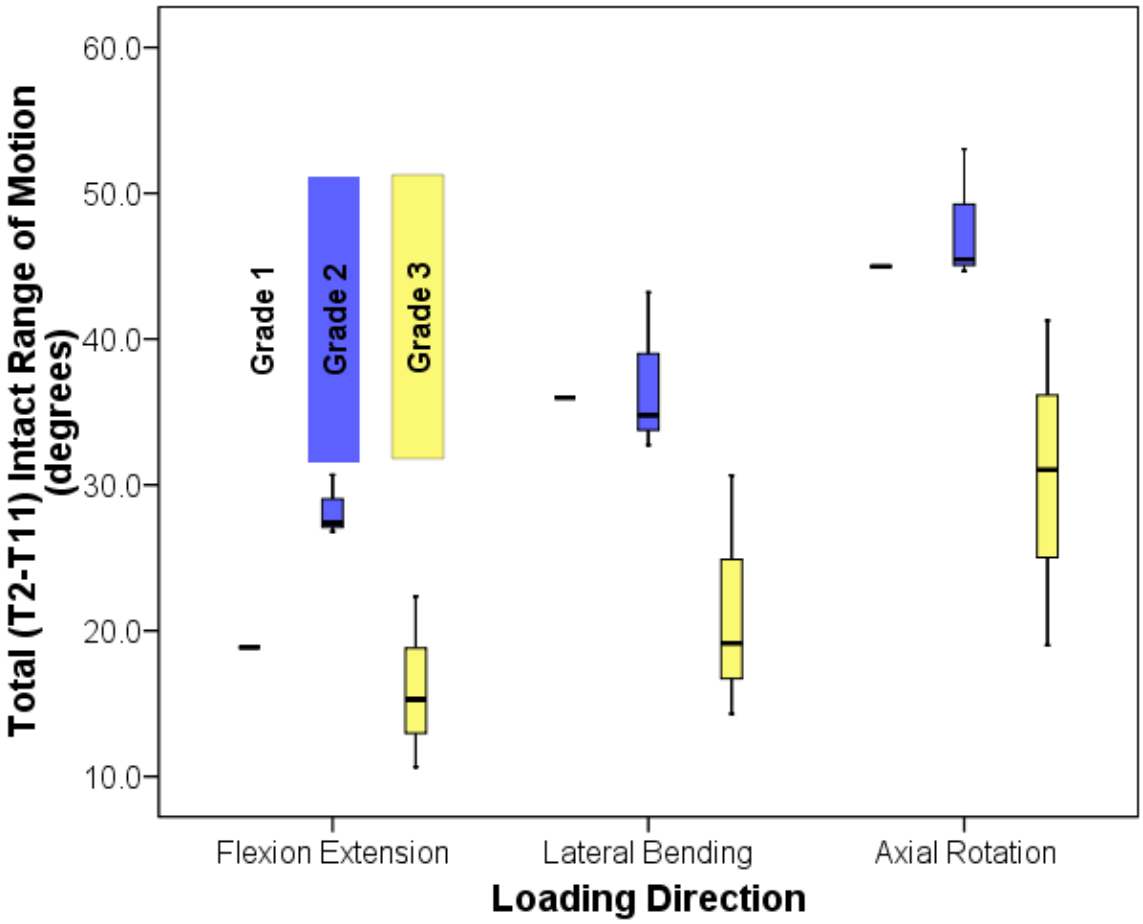

Figure 35. Total (T2-T11) intact range of motion in flexion extension, lateral bending, and axial rotation, according to the Mimura *et al*.[196] x-ray classification system.

Specifically, intact ROM_{TOTAL} was 28.3°±2.1° in flexion-extension for grade 2 specimens, compared to only 16.1°±5.9° for grade 3 specimens. In lateral bending, intact ROM_{TOTAL} was 36.9°±°5.6 for grade 2 specimens, compared to only 21.4°±8.4° for grade 3 specimens. Similarly, in axial rotation, intact ROM_{TOTAL} was 47.7°±4.6° for grade 2 specimens, compared to only 30.4°±11.1° for grade 3 specimens.

Following bilateral total facetectomies, mean increases in motion for the healthier, grade 2 spines were more than twice as large as mean increases in motion for the more degenerated, grade 3 spines (Figure 36).

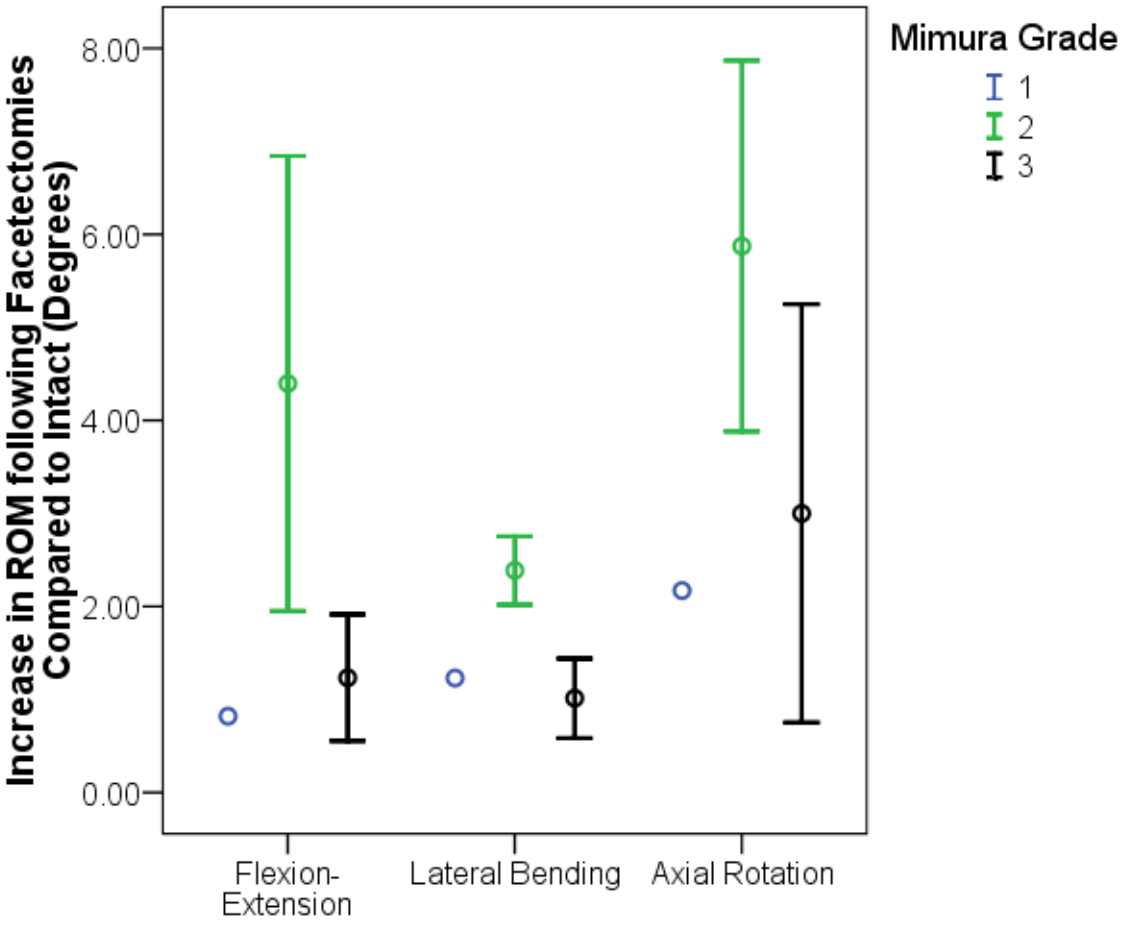

Figure 36. Increase in total (T2-T11) range of motion following *en bloc* bilateral total facetectomies, as compared to the intact condition, for Mimura *et al*.[196] grades.

Specifically, flexion-extension motion increased by 4.4°±2.4° for grade 2 compared to only 1.2°±0.7° for grade 3 ($p = 0.10$), lateral bending motion increased by 2.4°±0.4° for grade 2 compared to only 1.0°±0.4° for grade 3 ($p = 0.01$), and axial rotation motion increased by 5.9°±2.0° for grade 2 compared to only 3.0°±2.2° for grade 3 ($p = 0.17$).

Following four Ponte osteotomies, similar trends were seen (Figure 37). Specifically, flexion-extension motion increased by 9.3°±2.8° for grade 2 compared to only 3.1°±1.6° for grade 3 ($p = 0.03$), lateral bending motion increased by 3.6°±1.1° for grade 2 compared to only 0.9°±0.8° for grade 3 ($p = 0.03$), and axial rotation motion increased by 10.2°±5.8° for grade 2 compared to only 4.4°±2.9° for grade 3 ($p = 0.20$).

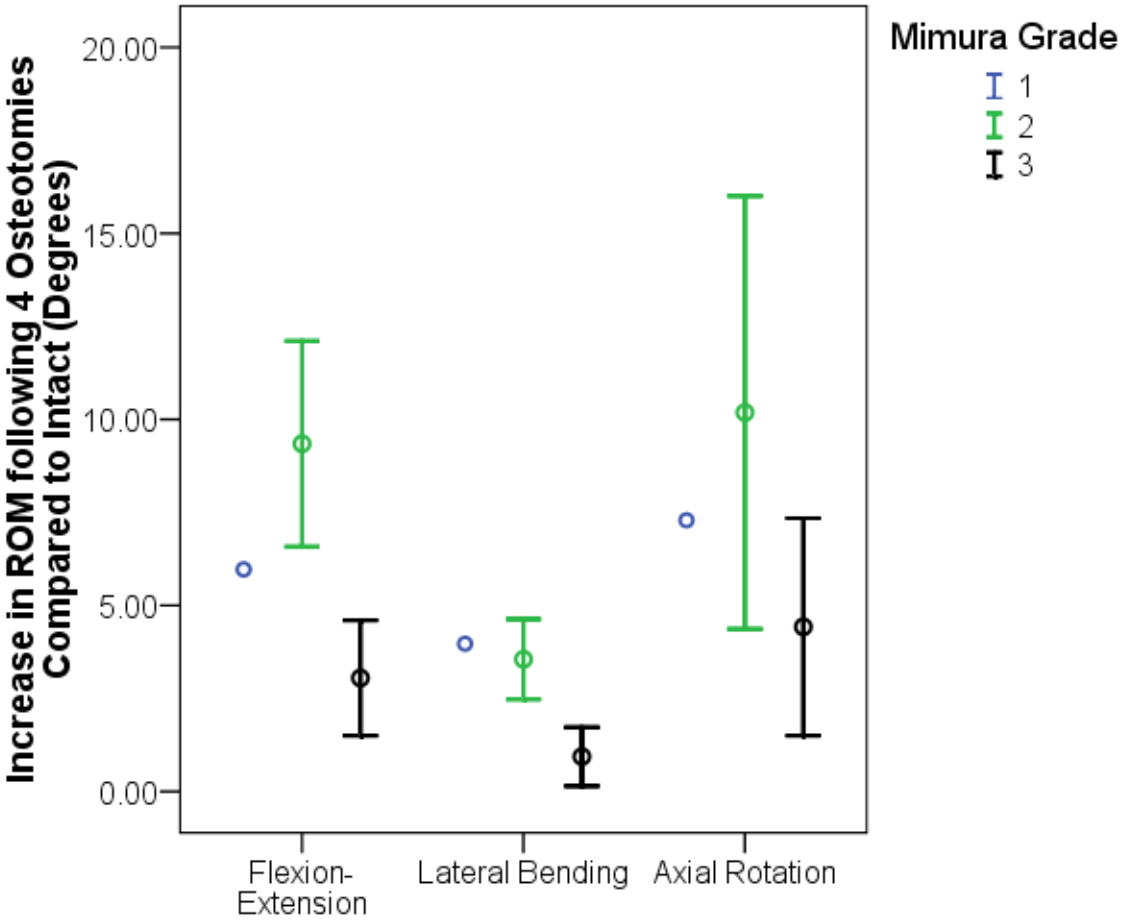

Figure 37. Increase in total (T2-T11) range of motion following four sequential Ponte osteotomies, as compared to the intact condition, for Mimura *et al*.[196] grades.

In addition to the increase in motion following the entirety of the posterior releases, the increases provided by each single osteotomy were significantly larger for healthier grade 2 specimens compared to the more degenerated grade 3 specimens. Specifically, in flexion-

extension, increases in ROM_{TOTAL} were 1.2°±0.8° for grade 2 specimens, compared to only 0.5°±0.5° for grade 3 specimens ($p<0.01$). In lateral bending, increases in ROM_{TOTAL} were 0.3°±0.5° in grade 2 specimens, and 0°±0.4° in grade 3 specimens. Finally, in axial rotation, increases in ROM_{TOTAL} were 1.1°±1.0° in grade 2 specimens, compared to only 0.4°±0.3° in grade 3 specimens.

Moreover, maximum increases in ROM following a single Ponte osteotomy were 2.2° in flexion-extension, 1.1° in lateral bending, and 3.1° in axial rotation for grade 2 specimens, compared to maximum increases of only 1.4° in flexion-extension, 0.5° in lateral bending, and 1.2° in axial rotation for grade 3 specimens.

A similar analysis was performed to compare the specimens according to *Lane* degeneration grade. Specifically, specimens with *Lane* grade 1 (n=3) and *Lane* grade 2 (n=4) were compared. However, the magnitude of the results was not as evident as those from the *Mimura* analysis, presented above. This is likely due to, overall, the weaker correlations between the biomechanics and the *Lane* degeneration grades. For example, despite larger magnitudes of intact ROM_{TOTAL} in each bending direction for grade 1 specimens compared to grade 2 specimens, the differences were not significant ($p>0.10$). This was likely due to the large standard deviations in ROM_{TOTAL} amongst the grade 2 specimens. Following each individual osteotomy, larger increases in flexion-extension ROM_{TOTAL} were produced in grade 1 specimens compared with grade 2 specimens ($p=0.09$). Specifically, in grade 1 specimens, increases in flexion-extension ROM_{TOTAL} were 1.1°±0.7°, compared to only 0.7°±0.7° in grade 2 specimens. In lateral bending and axial rotation, there were no significant differences between the increases in ROM_{TOTAL} following each osteotomy for specimens of grade 1 or grade 2.

3.4.1.1.4 Macroscopic Analysis

According to the Thompson *et al*.[256] macroscopic grading system (1-5), one specimen was grade 2, five specimens were grade 3, and one specimen was grade 4. There were no significant correlations between macroscopic grade and either total ROM ($0 > r > -0.310$, $p > 0.500$) or local ROM ($r = -0.134$, $p = 0.775$).

3.4.1.1.5 Histological Analysis

According to the modified Rutges scoring system (0-10), specimens were graded with mild to moderate degeneration (Figure 38). Specifically, two specimens had a total score of 3, four specimens had a total score of 4, and 1 specimen had a total score of 5. For all specimens, the endplates and nucleus pulposus matrix demonstrated mild degeneration (score=1); however, the scores for the annulus fibrosus morphology, the boundary between the annulus and nucleus, and the nucleus cellularity had variation (Figure 38). The total histological scores were positively correlated with both the scores according to Lane ($r=0.644$, $p=0.118$) and Mimura ($r=0.732$, $p=0.062$).

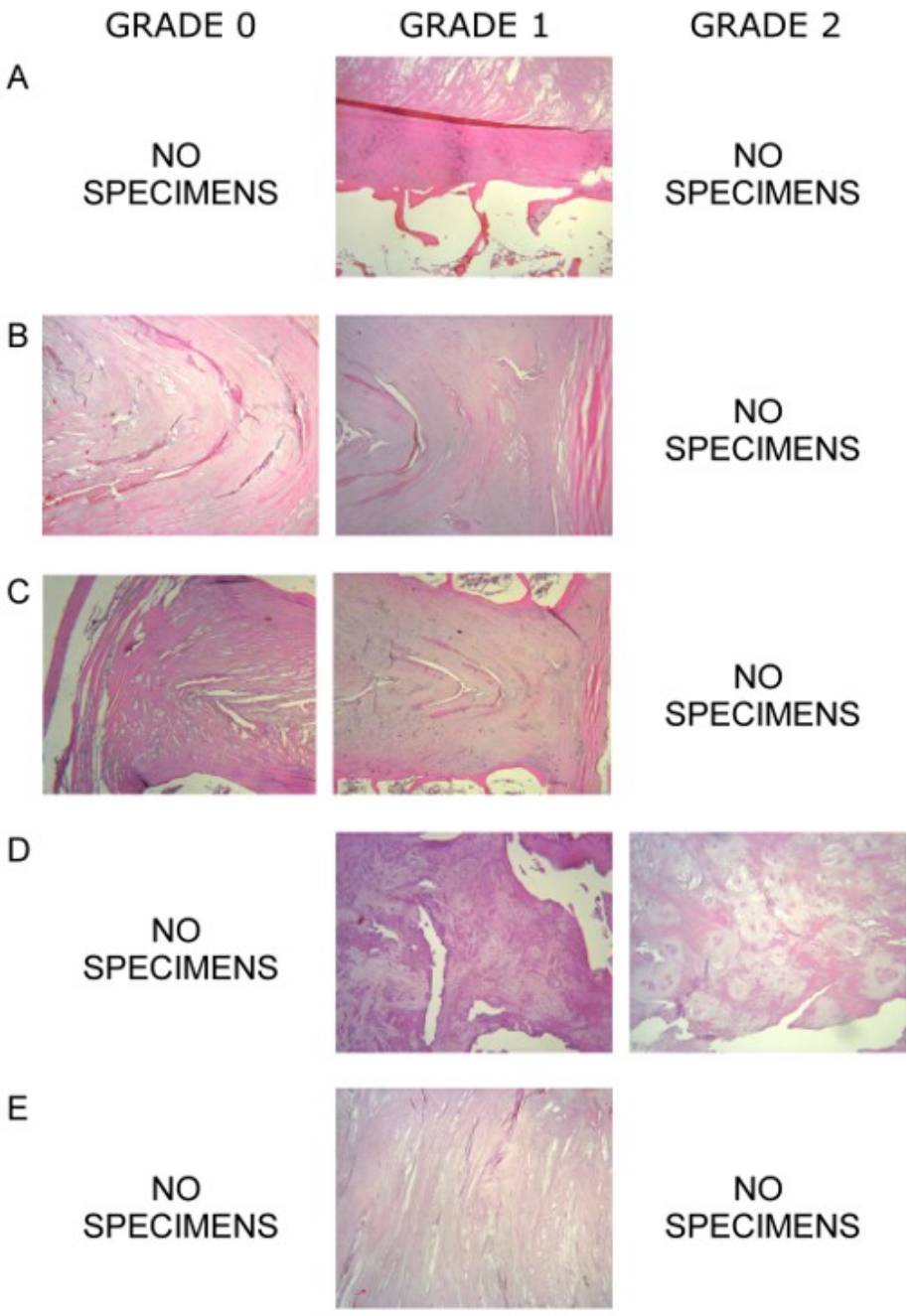

Figure 38. Representative histology images of the features graded in our subset of cadaveric thoracic spine specimens, including a.) Endplate (grade 1); b.) AF Morphology (Grade 0); c.) AF Morphology (Grade 1); d.) Boundary (Grade 0); e.) Boundary (Grade 1); f.) Cellularity (Grade 1); g.) Cellularity (Grade 2); h.) Matrix (Grade 1). Note that in our sample of specimens, some of the feature grades were not represented, e.g. Endplate Grade 0, and therefore, images of these features are not presented ("No Specimens").

Similar to the radiographic and macroscopic analyses, there was a negative correlation between histological degeneration scores and thoracic spine ROM; however, these correlations were not significant ($p>0.30$).

3.4.1.2 Group C

3.4.1.2.1 Overview of Biomechanical Data

As discussed, specimens in ***Group C*** were first tested under pure moments in the intact condition, following T10-T11 facetectomy, and following T10-T11 Ponte osteotomy. Following this testing, each specimen underwent simulated DVR and DVR-to-Failure loading. Of the n=11 specimens tested from ***Group C***, radiographic and MRI disc degeneration analyses were performed on n=10 specimens. As such, and similar to the analysis for ***Group B***, the kinematic and biomechanical data, in terms of means and standard deviations, changed slightly for the subgroup of 10 specimens. A brief overview of the results of those 10 specimens is presented below.

In summary, during *Single Plane Pure Moment* testing, intact ROM_{TOTAL} (T2-T11) was 12.4°±9.8° in flexion-extension, 25.2°±16.5° in lateral bending, and 38.7°±19.9° in axial rotation. Unidirectional right axial rotation at T10-T11 was 1.8°±0.8°. Overall, total ROM_{TOTAL} significantly increased in flexion-extension and axial rotation following Ponte osteotomy, compared to the intact condition (Table 34) ($p<0.05$). Maximum increases following osteotomy were 10.9° in flexion-extension, 3.8° in lateral bending, and 3.9° in axial rotation.

Table 34. T2-T11 Range of Motion (Group C Specimens)

	Flexion-Extension (deg)		Lateral Bending (deg)		Axial Rotation (deg)	
	Intact	Ponte	Intact	Ponte	Intact	Ponte
Mean	12.4	15.5	25.2	24.5	38.7	40.3
Std	9.8	12.7	16.5	17.0	19.9	20.3
Min	1.6	2.3	6.4	6.6	13.2	13.6
Max	27.1	38.0	50.7	54.5	65.3	69.2
p-value	*0.042*		*0.523*		*0.015*	

Local T10-T11 unidirectional right axial rotation ROM increased from 1.8±0.8° intact to 2.1±1.1° following osteotomy. Under simulated DVR, at 4 Nm, local T10-T11 ARR ROM was 2.9±2.0° (Table 35). The ARR ROM continuously increased throughout simulated DVR loading, increasing to 11.5±5.4° at failure. The moment at failure for this subgroup of specimens was 32.3±12.3Nm, with an average applied load of 132.8±51.6 N.

Table 35. Local (T10-T11) Right Axial Rotation ROM Under Simulated DVR (n=10 Group C Specimens for Degeneration Analysis)

	4 Nm		Percentage of Failure Moment			
	Pure Moments (deg)	DVR (deg)	25% (deg)	50% (deg)	75% (deg)	100% (deg)
Mean	2.1	2.9	3.9	6.0	8.0	11.5
Std Dev	1.1	2.0	2.2	3.2	3.9	5.4
	p=0.041					
		p=0.001				
			p<0.001			
				p<0.001		
					p=0.001	

3.4.1.2.2 Radiographic and MRI Analysis

According to Lane *et al.*'s[254] radiographic criteria (0-3), two specimens had no degeneration (*Lane* grade 0), four specimens had mild degeneration (*Lane* grade 1), and four

specimens had moderate degeneration (*Lane* grade 3). According to Mimura *et al*.'s[196] radiographic criteria (0-4), two specimens had mild degeneration (*Mimura* grade 1), three specimens had moderate degeneration (*Mimura* grade 2), three specimens had moderate-severe degeneration (*Mimura* grade 3), and two specimens had severe degeneration (*Mimura* grade 4). The two scoring systems were strongly correlated, with a Spearman's rho of 0.910 ($p<0.001$).

Overall, there was a negative correlation between x-ray degeneration scores and intact thoracic spine ROM_{TOTAL} in flexion-extension and lateral bending ($r<0.68$, $p<0.065$) (Table 36); however, there were no significant correlations between x-ray degeneration scores and global axial rotation ROM.

Table 36. Correlation Between Intact Total (T2-T11) Range of Motion and Intervertebral Disc Health

		Intact Total (T2-T11) Range of Motion		
		Flexion-Extension	Lateral Bending	Axial Rotation
Lane *et al.*[254]	Spearman's rho	-0.756	-0.850	0.283
	P-Value	0.030	0.015	0.538
Mimura *et al.*[196]	Spearman's rho	-0.683	-0.844	0.055
	P-Value	0.062	0.017	0.907
Pfirrmann *et al.*[255]	Spearman's rho	-0.866	-0.668	0.408
	P-Value	0.005	0.101	0.363

Compared to the x-ray degeneration grades, the MRI degeneration grades demonstrated less diversity among the specimens. Specifically, according to Pfirrmann *et al*.[255], one specimen was Grade 2, seven specimens were Grade 3, and two specimens were Grade 4. Similar trends were seen when evaluating the relationship between MRI degeneration grade, according to Pfirrmann, and ROM_{TOTAL}, with negative correlations between degeneration grade and flexion-extension and lateral bending.

Unlike the global ROM results, there were no significant correlations between the degeneration grades (x-ray or MRI) with local T10-T11 ROM under pure moments or under simulated DVR ($-0.33 < r < 0.408$, $p > 0.363$).

3.4.1.2.3 Histological Analyses

According to the modified Rutges scoring system (0-10), Group C specimens were graded with mild to moderate degeneration (Grades 2-7). Specifically, one specimen was Grade 2, one specimen was Grade 7, with the remaining specimens being graded 3, 4, or 5.

Similar to the analyses of Group B specimens, there was a negative correlation between histological degeneration scores and thoracic spine ROM; however, these correlations were once again not significant ($p > 0.42$). Additionally, unlike the radiographic degeneration scores, there was no correlation between histological degeneration grade and thoracic spine strength ($r = 0.150$, $p = 0.680$).

3.4.2 Typical Thoracic Spine Range of Motion

3.4.2.1 Search Results

The original MEDLINE search yielded 161 abstracts. Of the 161 abstracts, 27 articles were identified which included cadaver thoracic spine ROM measurements, in degrees.[11,25,26,31,35,41-43,47,48,58,129,131,135,136,158,252,257-266] After reviewing the references cited of each of the identified articles, as well as reviewing the abstracts of 9,223 'Related Citations', including repeats, 14 additional articles were identified.[9,13,27,28,133,134,174,251,267-272] This resulted in a total of 41 identified articles. Five articles reported redundant data, i.e. data from the same group of specimens and same author group, and thus were excluded.[257,258,262,268,269] Two studies which averaged lower thoracic motion with upper lumbar motion were excluded.[31,266] Finally, one of the identified articles was the original thesis written by Dr. Augustus A. White III.[9] As the original table of typical ROMs reported by White and Panjabi was largely based on this work, the motions were not included in the present analysis. Instead, the results of the present analysis were compared to the previously reported motions, discussed later. Following the exclusion of these eight articles, 33 unique articles remained for the present analysis.[11,13,25-28,35,41-43,47,48,58,129,131,133-136,158,174,251,252,259-261,263-265,267,270-272]

3.4.2.2 Overall Trends

Within the 33 included articles, a wide range of methods were applied, including differences in tested levels, intact specimen condition (i.e. with or without ribcage), type of loading, loading rate, and loading magnitude. Five studies tested full-length human thoracic spines,[25-27,129,158] three studies tested individual FSUs,[11,13,174] and the remaining studies tested multi-segment thoracic spine specimens. Mean specimen ages ranged from 43 to 83 years.

Of the included articles, 23 articles generally applied standard pure moments to thoracic spine specimens without the ribcage intact (Table 37, Table 38). There was a wide variation of reported means amongst these studies in each of the three loading directions. In these studies, moments ranging from 1.5 Nm to 8 Nm were applied to a variety of thoracic regions and specimen lengths. Displacement-controlled rotation rates ranged from 0.5°/s to 2°s, while load-controlled moment rates ranged from 0.3Nm/s to 1Nm/s; however, many of the articles did not report loading rate. Additionally, as many of the studies used weight-pulley loading systems, the loads were applied incrementally, e.g. steps of 2.25 Nm. Similar variations existed among the five studies which evaluated thoracic spine motion without the ribcage using 4 point bending loads, cantilever bending, or unknown loading types (Table 39).

Large variations were also observed in the seven articles reporting thoracic ROM in specimens with the ribcage intact (Table 40). Specifically, reported full length thoracic ROM (T1-T12) ranged from 7.93° to 33.9° in flexion-extension, 10.4° to 47.4° in lateral bending, and 23.0° to 44.9° in axial rotation.

Table 37. Reported Mean Thoracic Spine Range of Motion (Without Ribcage) from Pure Moment Testing

Author	n	Applied Moment	Reported Thoracic Motion Segment	Mean (SD) Range of Motion (degrees)		
				Flex-Ext	Lat Bend	Ax Rot
Brasiliense *et al*[131]†	8	7.5 Nm	T3-T4/T4-T5/T5-T6	5.7 (1.9)	4.2 (1.1)	4.3 (1.1)
			T7-T8	4.1 (1.1)	3.2 (0.3)	3.8 (0.7)
Deniz *et al*[264]	7	7.5 Nm	T8-T9	4.4 (1)	3.2 (0.6)	3.7 (1.2)
			T9-T10	4.2 (0.75)	3.48 (0.8)	3.5 (1.2)
Kuklo *et al*[35]	8	6 Nm	T4-T10	14.01 (4.9)	20.01 (7.04)	34.75 (9.38)
Chou *et al*[265]	21	3 Nm	T4-T6/T5-T7/T6-T8	4.6 (1.6)	8.9 (2.6)	11.7 (2.4)
Chang *et al*[42]	7	5 Nm	T10-T12	7.4 (1.77)	7.11 (1.59)	6.38 (1.08)
	7	5 Nm	T10-T12	5.85 (1.06)	6.89 (1.71)	7.39 (1.55)
Deviren *et al*[47]	8	4 Nm	T5-T11	17.5 (2)	30 (2)	39.5 (2)
	8	4 Nm	T5-T6	1.49 (1.39)		
Sran *et al*[252]	8	4 Nm	T6-T7	2.56 (1.68)		
	8	4 Nm	T7-T8	1.82 (1.4)		
Schultheiss *et al*[269]	6	3.75 Nm	T11-L1	10 (1.8)	11.2 (1.6)	5.3 (2.25)
Schultheiss *et al*[258]	6	3.75 Nm	T11-L1	6.3 (2.75)	7.3 (2.25)	4.2 (2.6)
Balabaud *et al*[43]	6	7.6 Nm	T6-T8	5.1 (2.4)	3.9 (3.1)	5.6 (4.1)
	6	7.6 Nm	T6-T8	3.8 (1.8)	2.5 (1.5)	5.7 (2.7)
Hitchon *et al*[263]	20	6 Nm	T10-T12	8.1 (2.3)	9.2 (6.3)	7.1 (3.3)
Panjabi *et al*[260]	10	7.5 Nm	T11-L1	12.7 (3.3)	12.6 (4.1)	4.7 (2.9)

Table 37 (cont.). Reported Mean Thoracic Spine Range of Motion (Without Ribcage) from Pure Moment Testing

Broc *et al*[41]	5	4 Nm	T4-T5	1.6 (1.1)	3.9 (2.3)	4.7 (2.7)
			T5-T6	1.7 (0.9)	3.4 (2.3)	4.4 (2.3)
			T6-T7	1.4 (0.6)	4.0 (2.3)	5.1 (1.3)
			T7-T8	1.4 (0.9)	3.6 (1.1)	4.6 (1.1)
			T8-T9	1.3 (0.3)	2.3 (0.9)	4.7 (0.4)
			T9-T10	1.4 (0.3)	2.9 (0.7)	4.3 (0.6)
			T10-T11	1.1 (0.6)	2.0 (1.0)	2.4 (1.0)
			T11-T12	1.7 (0.7)	2.3 (0.7)	1.6 (1.1)
Sangiorgio *et al*[28]	7	6 Nm	T2-T5/T8-T11	5.7 (4.9)	7.9 (5.7)	10.6 (7.2)
Kothe *et al*[134]	4	5 Nm	T5-T9/T6-T10	6.2 (1.4)	10.6 (3.2)	12.1 (2.4)
	4	5 Nm	T8-T12/T9-L1	5.7 (2.1)	6.7 (1.2)	4.8 (1.4)
Oxland *et al*[133]	11	7.5 Nm	T11-T12	5.1 (2.6)	7 (2.2)	3.6 (1.4)
Markolf *et al*[11]	6	5.7-6.5 Nm	FSUs (T7-T10)	2.95		
	13	5.7-6.5 Nm	FSUs (T10-L1)	3.15		
Lazaro *et al*[251]	7	6 Nm	T4-T6 or T5-T7	5.25 (1.8)	4.2 (1.2)	6.1 (1.56)
Ames *et al*[267]	7	1.5 Nm	T1-T2	3.38 (1.07)	2.07 (0.58)	2.42 (0.54)
Tan *et al*[272]	12	5 Nm	T10-T12	4.3 (1.2)	5.7 (1.7)	6.6 (2)
Watkins *et al*[27]‡	10	2-5 Nm	T1-T12	13.17	16.04	33.6

n, number of specimens tested; SD, standard deviation; Flex-Ext, flexion-extension; Lat Bend, lateral bending; Ax Rot, axial rotation

† Values from "Stage 4" condition, resection of 75% of the ribs

‡ Values from specimens following removal of sternum and ribcage

Table 38. Reported Median Thoracic Spine ROM (Without Ribcage) from Pure Moment Testing

Author	n	Applied Moment	Reported Thoracic Motion Segment	Median (SD) Range of Motion (Degrees)		
				Flex-Ext	Lat Bend	Ax Rot
Schultheiss *et al*[135]	6	3.75 Nm	T11-L1	10.3 (4.85)	10.8 (4.65)	5.6 (4.4)
	6	3.75 Nm	T11-L1	5.9 (8.25)	6.8 (5.39)	3 (6.9)
	6	3.75 Nm	T11-L1	6.6 (6.7)	5.7 (5.85)	3.5 (3.8)
Morgenstern *et al*[48]	12	8 Nm	T5-T8	11.5	18	20
	14	5 Nm	T2-T3			7
Wollowick *et al*[58]	14	5 Nm	T6-T7			5
	14	5 Nm	T10-T11			3.15

Table 39. Thoracic Spine (Without Ribcage) ROM in 4Pt Bend, Cantilever Bending, or Unknown Loading

Author	n	Load Type	Applied Moment (Load)	Reported Thoracic Motion Segment	Mean (SD) Range of Motion (Degrees)		
					Flex-Ext	Lat Bend	Ax Rot
Busscher *et al*[136,268]	6	4pt bend	4 Nm	T2-T3	6 (2.6)	6.1 (1.3)	7.2 (1.4)
	6	4pt bend	4 Nm	T6-T7	2.5 (1)	3.1 (1.3)	4.7 (1.5)
	6	4pt bend	4 Nm	T10-T11	2.5 (1.1)	2.8 (1)	3.2 (0.7)
	6	4pt bend	2 Nm	T2-T3	4.8 (2.3)	5 (1.5)	6.4 (1.5)
	6	4pt bend	2 Nm	T6-T7	1.9 (0.7)	2.4 (1.4)	3.3 (0.9)
	6	4pt bend	2 Nm	T10-T11	2.1 (1)	2 (0.8)	2.3 (0.6)
Stanley *et al*[271]	7		6-8 Nm	T2-T11	25.3 (10)	-	-
				T11-L1	8.2 (3.4)	-	-
Panjabi *et al*[13]	8	CB	43% BW	FSU§	*	-	
	9	CB	43% BW	FSUs§§	**	-	
Panjabi *et al*[174]	4		5.6 Nm	FSUs†	-	***	***
	2		5.6 Nm	FSUs††	-	****	****
	2		5.6 Nm	FSUs†††	-	*****	*****
Yu *et al*[259]	8		4 Nm	T1-T3	6.7 (1.5)	2.2 (0.6)	2.3 (0.75)

§Functional Spine Units (FSUs) tested: T1-T2 (n=1), T4-T5 (n=2), T5-T6 (n=1), T6-T7 (n=1), T8-T9 (n=1) T9-T10 (n=1), T11-T12 (n=1)

§§FSUs tested: T2-T3 (n=1), T3-T4 (n=1), T4-T5 (n=1), T6-T7 (n=1), T7-T8 (n=1), T8-T9 (n=2), T10-T11 (n=2)

†FSUs tested: T6-T7 (n=1), T7-T8 (n=1), T10-T11 (n=2); ††FSUs tested: T4-T5 (n=1), T10-T11 (n=1); †††FSUs tested: T6-T7 (n=1), T8-T9 (n=1)

*Flexion only reported: 1.35 (1); **Extension only: 1.07 (0.42)

***One side lateral bending: 1.46; One side axial rotation: 2.24

****One side lateral bending: 1.66; One side axial rotation: 1.7

*****One side lateral bending: 1.79; One side axial rotation: 1.68

Table 40. Reported Mean Thoracic Spine Range of Motion (with Ribcage Intact)

Author	n	Load Type	Applied Moment (Load)	Reported Thoracic Motion Segment	Mean (SD) Range of Motion (Degrees)		
					Flex-Ext	Lat Bend	Ax Rot
Healy *et al*[26]	9	PM	5 Nm	T1-T12	26.9 (10)	42.06 (19.04)	43.69 (16.87)
Brasiliense *et al*[131]	8	PM	7.5 Nm	T2-T5/T3-T6/T4-T7	1.3 (0.7)	2.2 (1.1)	0.5 (0.3)
Little *et al*[261]	10	PM	6 Nm	T3-T4	5.0 (1.8)	3.8 (1.1)	4.0 (0.9)
	6	CB	25N	T1-T12	28.4 (17.4)	-	-
Horton *et al*[25]	6	CB	25N	T1-T12	33.9 (28.7)	-	-
	6	CB	25N	T1-T12	28.5 (12.1)	-	-
Feiertag *et al*[129]	6		89N	T2-T10	11.34 (11.37)	13.6 (5.9)	-
Watkins *et al*[27]	10	PM	2-5 Nm	T1-T12	7.93	10.36	23.03
Lubelski *et al*[158]	10	PM	5 Nm	T1-T12	23.72 (11.36)	47.44 (14.77)	44.91 (18.79)

3.4.2.3 Estimated Segmental Thoracic Motions

From the 24 studies which reported mean thoracic ROM (either bilateral/bidirectional or both unilateral/bilateral directions) in cadaveric specimens without the ribcage intact, estimated segmental motions were calculated.[11,27,28,35,41-43,47,131,133-136,251,252,259,260,263-265,267,270-272] Estimated segmental motions ranged from 1.1° to 6.4° in flexion-extension, 1.1° to 7° in lateral bending, and 1.2° to 7.2° in axial rotation (Table 41).

Table 41. Estimated Segmental Thoracic Spine ROM (Without Ribcage)

Thoracic Motion Segment	Estimated Segmental Motion (Degrees)					
	Flexion-Extension		Lateral Bending		Axial Rotation	
	Median	Range	Median	Minimum	Median	Minimum
T1-T2	3.4	1.2-3.4	1.5	1.1-2.1	2.4	1.2-3.1
T2-T3	2.8	1.2-6.0	2.2	1.1-6.1	3.3	1.2-7.2
T3-T4	1.9	1.2-2.8	1.8	1.5-2.6	3.1	1.5-3.5
T4-T5	2.3	1.2-2.8	3	1.5-4.5	4.1	3.1-5.9
T5-T6	2.1	1.2-2.9	3	1.5-5.0	3.7	1.5-6.6
T6-T7	2.3	1.2-2.9	2.7	1.3-5.0	3.3	2.8-6.6
T7-T8	2.3	1.2-4.1	3.2	1.3-5.0	3.8	2.8-6.6
T8-T9	2.1	1.2-4.4	2.6	1.5-5.0	3.6	1.2-6.6
T9-T10	2.1	1.2-4.2	2.8	1.5-5.0	3.5	1.2-6.6
T10-T11	2.5	1.1-4.1	2.8	1.5-5.0	3.2	1.2-6.6
T11-T12	3.2	1.2-6.4	3.6	1.5-7.0	3.1	1.2-3.7

3.4.2.4 Pooled ROM Statistics from Pure Moment Testing

In order to comprehensively describe the ROM results from pure moment testing of thoracic spines without the ribcage, estimated segmental thoracic ROM pooled means and standard deviations were calculated. Only studies which reported mean and standard deviations were included. Pooled means ranged from 1.9° at T2-T3 and T3-T4 to 3.8° at T11-T12 in flexion-extension (Figure 39), 2.1° at T1-T2 to 4.4° at T11-T12 in lateral bending (Figure 40), and 2.4° at T1-T2 to 5.2° at T5-T6 in axial rotation (Figure 41). It should be noted that only one study was used for each the T1-T2 segment,[267] T2-T3 segment,[28] and the T3-T4 segment,[28] as only that particular study reported mean motions of specimens including those segments.

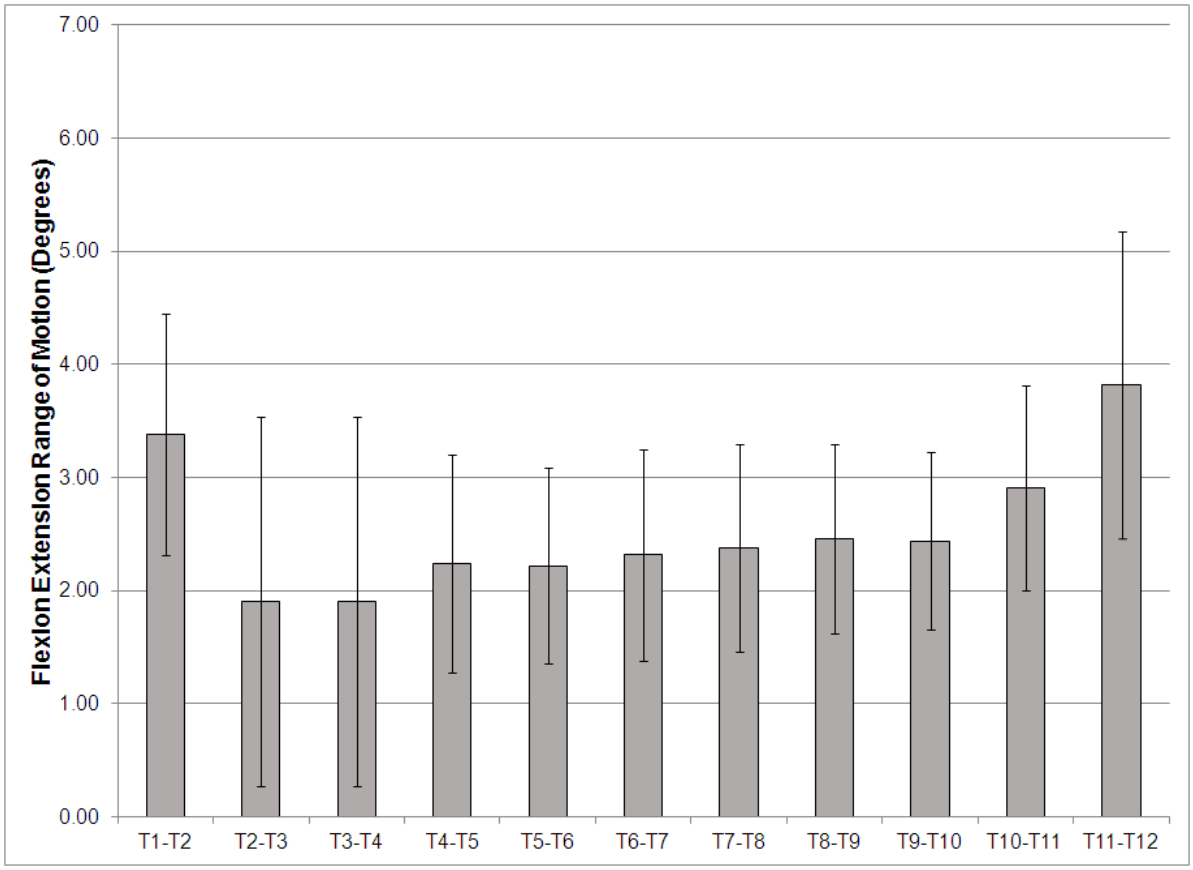

Figure 39. Pooled estimated segmental flexion-extension motion (pooled mean ± pooled standard deviation) for each level of the thoracic spine. Motions from articles measuring motions during standard Pure Moment testing of intact thoracic spines without ribcages were included in the pooled ROM calculations.

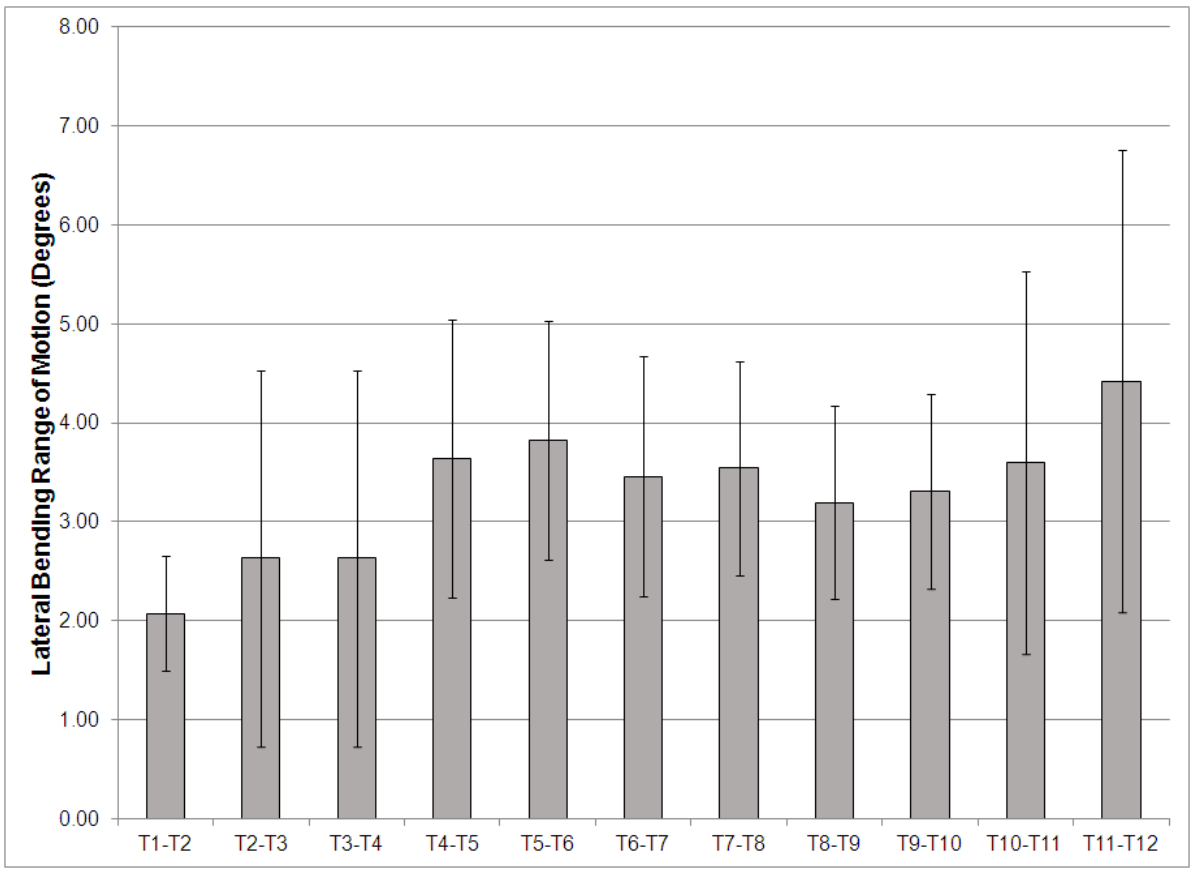

Figure 40. Pooled estimated segmental lateral bending motion (pooled mean ± pooled standard deviation) for each level of the thoracic spine. Motions from articles measuring motions during standard Pure Moment testing of intact thoracic spines without ribcages were included in the pooled ROM calculations.

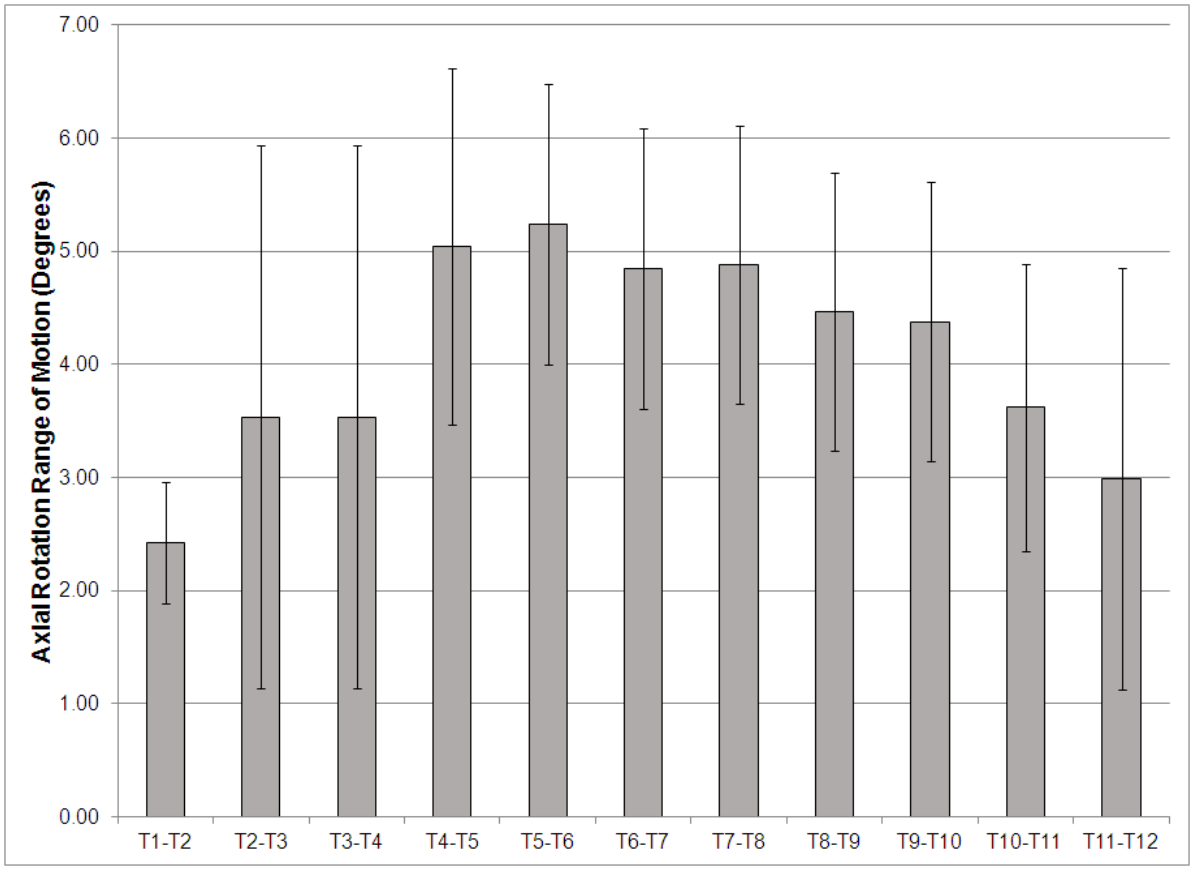

Figure 41. Pooled estimated segmental axial rotation motion (pooled mean ± pooled standard deviation) for each level of the thoracic spine. Motions from articles measuring motions during standard Pure Moment testing of intact thoracic spines without ribcages were included in the pooled ROM calculations.

Given the estimated segmental motions at each thoracic motion segment, an approximation for the total thoracic spine motion (T1-T12) was made based on the sum of the individual segments. Therefore, estimated total thoracic spine motion (T1-T12) was approximately 27.9° in flexion-extension, 36.3° in lateral bending, and 44.9° in axial rotation.

4 Discussion

4.1 Single Plane Pure Moments

4.1.1 Overview of Results

In the present work, under single plane pure moments, posterior release produced increases in motion in flexion-extension and axial rotation. The increases were produced following conservative posterior releases, i.e. total facetectomies, as well as more aggressive posterior releases, i.e. sequential Ponte osteotomies. Additionally, these releases provided significant increases in total ROM, both in flexion-extension and axial rotation, compared to using the conservative total facetectomies alone. The increases in flexion-extension motion are consistent with the indications for these procedures, which were originally used to correct sagittal plane deformities, such as Scheuermann's Kyphosis. Meanwhile, the increases in axial rotation suggest the potential use of these releases in correcting AIS deformities, where axial rotation-type maneuvers are used to achieve correction, such as DVR. Finally, and contrary to popular thought, even the osteotomies failed to significantly affect total ROM in lateral bending.

4.1.2 Comparison to Clinical Studies

Compared to clinical results of scoliosis and deformity correction, the increases following posterior release under single plane pure moments were substantially smaller. Throughout the clinical literature, studies have reported increases in sagittal correction ranging from approximately 5-15° with each Ponte osteotomy.[107,108,166] In the present work, maximum increases in flexion-extension moment for a single osteotomy were 2.6°, substantially smaller than those previous clinical reports. Following the *en bloc* total facetectomies, increases in flexion-extension were, on average, only 2.1°, with a maximum increase of 6.6°. This maximum,

however, was following 9-levels of conservative release, compared to the 5-15° increases reported following a single-level surgery.[108,166] Finally, following the most substantial release, that is 9 releases (5 level facetectomy, 4 level osteotomy), the average increase was 5.8°, with a maximum of 12.0°.

It must be noted that the cited clinical studies report correction following both the application of large correctional forces and torques, and the insertion of instrumentation during surgery. In contrast, the present study applied pure moment loading, which may be lower than forces applied during surgery.[7,24] In addition, no rod instrumentation was utilized in the present work. This may help explain the discrepancies in the findings.

The wide posterior release evaluated in the present work, the Ponte osteotomy, historically was described as a technique to reduce kyphotic deformity.[165] However, some surgeons have utilized the procedure as an effective means of improving apical lordosis in cases of idiopathic scoliosis. In the present study, increases in flexion of up to 1.6° per level of osteotomy were measured. These increases are consistent with the theory and justification of clinical observations of sagittal plane corrections; however, the magnitudes are still small.

Compared to coronal plane clinical corrections, and similar the sagittal plane corrections, the increases following posterior release under pure moments were smaller. While the coronal plane corrections are not as clear with respect to each individual release, conservative estimates in the literature range from 2.4-6° following wide release.[111,127,162,163] In contrast, in the present study, following a single osteotomy, increases in lateral bending ROM under pure moments were less than 1°. Following the most substantial releases (9-level release: 5-level total facetectomy and 4-level osteotomy), the average increase in lateral bending ROM was 2.7°, with a maximum

of 6.3°. The comparison is similar to that of the sagittal plane corrections, where the most destabilized in-vitro condition produced results similar to single-release clinical corrections.

Finally, in the axial plane, smaller motions were again observed in the present in-vitro studies compared to clinical reports. Specifically, and while estimated based on clinical reports, clinical axial corrections have ranged from approximately 5.1-17°.[6,169,170,172] In comparison, increases in excess of 3° were produced following each osteotomy, smaller than clinical reports. In contrast, as much as nearly 17° following the entirety of the posterior releases were produced in the present work, closer to those clinically reported corrections. However, as the clinical values are difficult to discern in terms of number of levels contributing towards the correction, comparisons are inconclusive.

In addition to evaluating the increases in ROM, the present work was the first to evaluate routinely performed *en bloc* facetectomies with supplemental Ponte osteotomies. Despite the various clinical reports, the effectiveness of Ponte osteotomies in comparison to the routinely performed total facetectomies remains controversially debated throughout the literature.[111,112,127,163] For example, Halanski *et al*.[127] evaluated the effectiveness of Ponte osteotomies and facetectomies in two groups of patients, concluding that both procedures performed equivalently. On the other hand, Pizones *et al*.[111] reported significantly improved correction outcomes following wide posterior release (e.g. Ponte osteotomy) compared to a standard release (e.g. facetectomy). Despite the controversy, the present work demonstrated that while *en bloc* total facetectomies can increase thoracic spine flexibility, significantly improved flexibility increases may be achieved with the use of supplemental osteotomies.

4.1.3 Comparison to Biomechanical Literature

Throughout the literature, several studies have evaluated the effects of posterior destabilization techniques and posterior surgical releases on thoracic spine range of motion.[25,29,58,129,130,164] However, and as discussed extensively in the Background section of this work, despite the presence of a 'standard', i.e. pure moment testing,[17,24] the results throughout the literature are difficult to compare due to differences in testing methodologies. In the context of posterior release literature, differences lie primarily in specimen type, loading protocol, and data presentation and analysis.[25,29,129,130,164] In addition, unlike the majority of the literature, the present study evaluated primarily multi-level releases, closely simulating an intraoperative environment.

Compared to single-level release studies, the most comparable investigations in the literature were performed by the Oda *et al*.[130], Oda *et al*.[29], and Anderson *et al*.[164]. Oda *et al*.[130] performed the most comparable study, in which pure moment loading was applied in a thoracic canine model to evaluate the increase in ROM following ablation of the posterior elements. Specifically, the destabilization involved the removal of all of the posterior elements, a procedure similar to a Ponte osteotomy, utilized in the present study. The authors reported higher increases in flexion-extension ROM; however, the normal ROM for canine specimens remains unknown. Moreover, how these ROMs compare to human thoracic spine ROM is unknown, making it difficult to draw comparisons to this study.

Later, the same group performed an evaluation of posterior destabilization procedures on a human thoracic spine model.[29] Specifically, Oda *et al*.[29] applied pure moments to functional spinal units following similar surgical procedures to the Ponte osteotomy. They reported higher

increases in ROM compared to the current study. Specifically, normalized increases in ROM (compared to intact) ranged from 38% to 45% in each of the three anatomical planes of bending, following release of the posterior structures. However, the authors did not report the raw magnitude of the motion increases. Instead, increases were only presented as a ratio of the intact motion. Oda *et al*.[29] evaluated the increase in ROM as a ratio of an individual FSU motion measurement, whereas in the present study, the increases in ROM were calculated as a ratio of the total thoracic ROM. Consequently, it is impossible to put into context the impact of their results as they pertain to the results presented herein. For example, in an FSU which had only 1° of motion in a given direction, a 50% increase would mean only 0.5°, which would have little clinical impact. Alternatively, if a given FSU had 10° of motion in a given direction, a 50% increase would be clinically significant, with a 5° increase at that level attributable to the posterior release. Similarly, Anderson *et al*.[164] evaluated the increase in motion of thoracic spine FSUs following posterior destabilization. They too reported higher increases in motion; however again, only ratios were presented. This highlights the need throughout the literature to present comprehensive motion results, both as ratios of intact motion and as raw magnitudes of change, as presented in the present work. This would enable stronger comparisons amongst the existing literature, as well as facilitate clinically relevant conclusions, and in turn, translation to clinical practice.

Additionally, studies of posterior techniques have been limited to single-level surgeries, with the exception of Horton *et al*.[25] In their study, four *en bloc* total facetectomies were performed before and after cantilever flexion-extension loading. Increases were observed in both flexion, where ROM increased by 1.7°, and extension, where ROM increased by 0.8°. Contrarily, in the present study, the *en bloc* facetectomies provided average increases in motion

of 0.4° and 1.7° in flexion and extension, respectively. The total percent increases in ROM were comparable. However, Horton *et al*.[25] applied cantilever bending type loading. Additionally, the ribcage and sternum were intact during loading. These differences may have, in part, contributed to the differences in the results of the two studies. Regardless of the differences, the increases were still substantially smaller across the studies than those reported clinically.[108,166]

Compared to the number of in-vitro studies which have evaluated the effects of posterior release on sagittal plane ROM, few have evaluated the effects on axial plane ROM. As discussed, posterior-only axial plane correction maneuvers have recently become popular for treating scoliosis deformities.[6,93,102,107,109,110] The axial plane techniques include derotation[113] and DVR.[6] The techniques rely on axially directed forces manually applied to the spine, which in the present work, corresponds to torsional loading and resulting axial rotation. In the present work, the sequential releases provided significant increases in ROM, with maximum increases of 3.1° following a single osteotomy, and up to 16.9° following the combination of releases (facetectomies combined with supplemental osteotomies). These increases were the largest in any anatomical direction, speaking towards the potential effectiveness of torsional loading-type maneuvers for correcting abnormally rotated spines.

Compared to a recent study by Wollowick *et al*.,[58] who evaluated the increase in thoracic torsional ROM under pure moment torsional loading, the single osteotomy results are similar. Specifically, Wollowick *et al*.[58] reported single level increases ranging from 0.8-1.9° following wide posterior release. However, despite the similar single level results, once again, the magnitudes of increase are less than clinical reports.

4.1.4 Lack of Increase in Lateral Bending

Unlike the increases in the sagittal and axial planes, the increases in lateral bending were negligible in comparison. Similarly, Feiertag *et al*.[129] and Oda *et al*.[29] reported negligible changes in lateral bending following posterior releases. Specifically, in the present study, following a single osteotomy, changes in lateral bending were on average less than 1°. This result is contrary to popular belief, which suggests effectiveness of the releases intraoperatively, measured by Cobb correction,[112,127] in correcting coronal plane deformities, and in turn, lateral bending ROM. However, as discussed, scoliosis is largely a deformity comprised of abnormal rotations in the transverse and sagittal planes,[6] creating a perceived coronal plane deformity. With this in mind, the ability to affect flexibility in the coronal plane becomes less important.

Furthermore, from a more fundamental biomechanical perspective, the results make intuitive sense. Specifically, the lack of increase in lateral bending ROM following posterior release are consistent with the anatomical positions of the posterior elements and ligaments relative to the neutral plane of bending (Figure 42).[28]

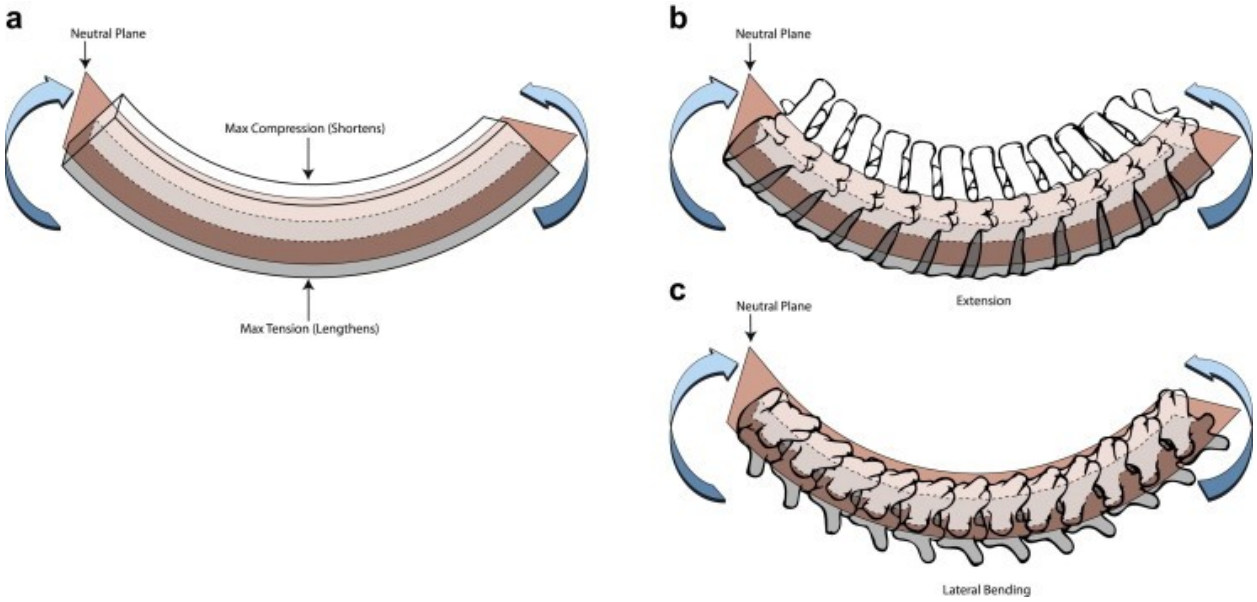

Figure 42. a.) Schematic diagram of a rectangular beam under bending loads depicting the neutral plane of bending and the maximum compression/tension forces experienced; b.) Schematic diagram of a spine under extension bending loads depicting the compression on the posterior aspects of the spine (posterior shortening) and tension on the anterior aspect of the spine (anterior lengthening); c.) Schematic diagram of a spine under lateral bending loads depicting neither lengthening nor shortening of the posterior elements, as the posterior structures lie along the neutral plane of bending.[28]

Specifically, under bending loads, one side of the spine lengthens, whereas the opposite side shortens. The neutral plane, which lies at the center of the structure, neither lengthens nor shortens. For example, under extension, the anterior longitudinal ligament and anterior disc fibers lengthen, whereas the posterior elements and posterior ligaments tend to compress and shorten. The neutral plane, which in this case would be the center of the discs, neither shortens nor lengthens. Based on this theory, if the posterior elements were removed, e.g. a wide posterior release, the resistance to shortening would be reduced. Hence, increases in extension ROM would occur, as demonstrated by the reported results. Contrarily, in lateral bending, the releases are being performed primarily in and around the neutral plane. Specifically, both the removed ligaments (interspinous and supraspinous) and the spinous processes lie largely along the neutral plane. Hence, the release should have a smaller effect compared to the other planes. This was in

fact the case, with negligible changes observed in lateral bending ROM following posterior release.

4.2 Multi-Planar Loading

While the single plane pure moment model enabled relative comparisons of the effects of posterior releases, e.g. the relative comparison of the effects of *en bloc* total facetectomies to the effects of supplemental osteotomies on total ROM, the magnitude of the increases in ROM did not agree with clinical reports. The noted discrepancies demonstrate the inability to comprehensively characterize the effects of posterior releases on thoracic ROM with pure moment testing alone. However, despite the evident need to expand testing, the majority of previous biomechanical studies have followed this typical protocol, that is, applying single plane pure moment type loading to thoracic spines before and after posterior release.[29,57,58,164]

One primary assumption in applying the pure moment model to deformity correction problems is that the increase in total ROM following a given posterior destabilization (e.g. wide posterior release) correlates to the increase in deformity correction achievable by surgeons intraoperatively.[138,273] Based on a relative comparison, the assumption was valid in predicting the relative performance of one release compared to another. For example, on the basis of the single plane analysis, the results of the present work suggest that sequential Ponte osteotomies provide significant increases in thoracic spine flexibility in axial rotation compared to *en bloc* total facetectomies. Similarly, throughout the literature, relative comparisons of different destabilization procedures could be performed. However, and as the discrepancies between the biomechanical and clinical results indicate, the assumption may fall short in assessing the magnitude of increase in thoracic ROM. This may be due to the fact that the process of assuming equivalence between biomechanical increases and deformity correction increases assumes that both the deformity and the correction of that deformity occur in one single plane; however, in

cases of scoliosis, the deformity presents with abnormal rotations and translations in all three anatomical planes.[6,63]

In the present study, a novel multi-planar loading protocol was applied to thoracic spines to expand upon the results provided using the single-plane pure moment model in an attempt to further elucidate the effects of posterior release in applications of three-dimensional deformities. Based on the results, both *en bloc* total facetectomies and supplemental sequential Ponte osteotomies provided simultaneous increases in ROM in all three planes. Specifically, simultaneous increases in ROM of up to 5.2°, 2.7°, and 5.4° in flexion-extension, lateral bending and axial rotation were produced under multi-planar loading following *en bloc* facetectomies. Additional simultaneous increases of 1.4°, 1.6°, and 2.2° were produced following each supplemental osteotomy. These simultaneous increases coincide with the single plane results. Specifically, the independent single plane increases under pure moments were 6.6°, 3.2°, and 8.1° following the total facetectomies in flexion-extension, lateral bending, and axial rotation, respectively. Following each osteotomy, additional increases of up to 2.6°, 1.4°, and 3.1° were produced in the three respective planes. The agreement between the results suggest the ability to maintain corrective power under three-dimensional moments, more representative of a typical clinical case where three-dimensional maneuvers are employed to correct three-dimensional deformities.[11,101,102]

These multi-planar testing results provide more evidence towards the current controversy surround the use of Ponte osteotomies in cases of AIS. Due to conflicting reports, there is a lack of consensus in the literature regarding the use of such wide posterior releases.[111,112,127] For example, while Pizones *et al*.[111] reported significant improvements in deformity correction using

wide-posterior releases compared to standard releases, Halanski *et al*.[127] reported no difference. According to the multi-planar results, and similar to the single plane testing results, the supplemental osteotomies provided added flexibility in three-dimensions beyond what was achieved using total facetectomies alone.

Additionally, beyond evaluating the effectiveness of supplemental osteotomies in comparison to standard releases, the multi-planar results demonstrate the effectiveness of the releases in three-dimensions. Without prospective clinical studies, it has been difficult to assess the validity and effectiveness of using Ponte osteotomy and similar wide posterior releases in cases of three-dimensional deformity, e.g. AIS. Consequently, some retrospective studies have suggested ineffectiveness. For example, Zhang *et al*.[222] concluded that while osteotomies may be effective in correcting sagittal deformity, they may be ineffective in correcting coronal plane deformities. In the present study where the variables are largely controlled, the multi-planar results suggested the effectiveness in three-dimensions. This result demonstrates the advantages of performing highly controlled biomechanical studies, as opposed to solely relying on retrospective clinical data for decision making and clinical conclusions.

These results demonstrated that to comprehensively predict the ability of various releases to produce three-dimensional corrections, multi-planar loading may be necessary. Together with the single plane pure moment results, assessments were made to evaluate (1) the relative performance of one release compared to another, and (2) the ability of the releases to maintain corrective power under three-dimensional loads. However, despite the fact that multi-planar loads were applied, the magnitudes of correction were still smaller than the clinical reports, which have suggested per-release increases of 5-15° in the sagittal plane,[107,108,166] 2.4-6° in the

coronal plane,[111,127,162,163] and 5.1-17° in the transverse plane.[6,169,170,172] These inconsistencies indicate the necessity to expand the testing model even further in order to fully characterize the potential of these releases in cases of AIS.

While the novel multi-planar loading protocol expanded the testing results to provide evaluation of the three-dimensional effectiveness of posterior releases, the loads were still applied at conservative, in-vitro magnitudes.[28,250] Once again, and similar to the majority of the biomechanical literature, the magnitudes were based on established limits designed to prevent soft-tissue damage during testing.[15-17,24] In addition to preventing damage, the loading magnitudes were intended to produce physiological motion.[45] However, based on clinical comparisons of preoperative bending films and postoperative films,[105,106] physiological motions are exceeded intraoperatively. Furthermore, in order to exceed physiological motions, high-magnitude intraoperative forces must be applied. Specifically, it has been suggested that torque in excess of 100-120 Nm has been applied intraoperatively.[7] Therefore, to further expand upon the characterization of the posterior-releases, an intraoperative simulation with high-magnitude forces was necessary.

4.3 Intraoperative Simulation and DVR-to-Failure

4.3.1 Strength of the Thoracic Spine under Simulated DVR

The pure moment model was designed to evaluate general thoracic spine properties, and to evaluate the effectiveness of various fusion devices. However, and as discussed thoroughly, the model was then applied to answer all questions surrounding preclinical testing of spine disorders, and namely, the effectiveness of correction releases and techniques. As demonstrated, the model was effective in helping to provide relative comparisons of one release versus another. For example, in the present study, when comparing the relative effect of utilizing Ponte osteotomies to supplement routinely performed *en bloc* facetectomies, the pure moment model offered a valid platform for analysis. However, due to the discrepancies between the in-vitro results and the clinical results, expansion upon this model was necessary.

One of the primary flaws in preclinical studies to date evaluating the effect of techniques and releases used intraoperatively for the correction of spine deformity is the loading magnitudes and maneuvers employed. Specifically, all of the studies to date which have evaluated the effectiveness of posterior release have done so at low torque magnitude, ranging from approximately 2-5 Nm.[29,58] Similarly, in the pure moment model applied herein, moments were applied at the 4Nm and 6Nm levels. Contrarily, with the advancement in surgical techniques, surgeons are capable of applying larger moments than previously achievable.[7] Specifically, the recent trend is to employ pedicle screw fixation at all levels along the length of the deformity, providing high fixation strength through three-column fixation.[76,101-104] This in turn allows the application of three-dimensional correction maneuvers to be applied, resulting in improved correction.[93,102,105,106] In the present study, DVR,[6] one such correction maneuver, was studied and

simulated. With this maneuver, surgeons have purportedly applied torques in excess of 100Nm directly to the spine.[7] These purported torques far exceed those applied in previous in-vitro studies, potentially accounting for the disparity in the results between clinical and in-vitro studies.

Unfortunately, despite the evident large torque magnitudes applied intraoperatively, both from the purported forces (e.g. 100 Nm)[7] and the intraoperative failures (e.g. screw plow, aortic abutment, pedicle fracture),[110,128,179,228] the strength limits of the thoracic spine under such torques are unknown. Moreover, the rotational response of the thoracic spine under these large torques after posterior release are also unknown. Therefore, with our simulated DVR model, we sought to expand the testing limitations of previous studies to provide more comprehensive analyses and understanding of the thoracic spine as they pertain to deformity correction. The first step in this process, then, was to evaluate the strength of the thoracic spine under simulated DVR to failure.

Unlike surgical reports, which have purported safe application of DVR moments in excess of 100Nm,[7] in the present study, thoracic spine torsional failure occurred at intervertebral disc moments ranging from 13.7 Nm to 54.7 Nm, with an average disc moment at failure of 33.3 Nm. The corresponding applied force was, on average, 138.6 N. These values are substantially lower than the purported 100 Nm intraoperative torque, as was expected based on previous in-vitro evaluations of the lumbar spine.[243,244]

Only two previous studies have evaluated the safety of applying derotational-type torques through pedicle screws in the thoracic spine;[142,245] however, neither study allowed motion of the spine. Consequently, the clinical relevance of the results is unknown, as intraoperatively, motion

would be allowed at the level of correction. Regardless, the studies provide an indication of the bone-screw interface strength in thoracic pedicles. According to the two studies, single screw-bone interface failure occurred at average values ranging from 4-12 Nm.[142,245] Meanwhile, using a quadrangular linkage, similar to the present study, failure occurred at an average of 42.5Nm,[245] comparable to the failures produced in the present study.

While these previous studies by Parent *et al*.[142] and Cheng *et al*.[245] provide insight into the thoracic pedicle screw-bone interface strength, the failures were isolated to this location as no motion was allowed. When motion is allowed, torque is transferred through the intervertebral disc as well, which could affect the results. However, prior to this work, no previous thoracic spine studies have evaluated the strength of the thoracic spine under torsional loading and axial rotation motion, with or without pedicle screw fixation. In the lumbar spine, more work has been performed. Miller *et al*.[243] applied torsional loads to lumbar FSUs, allowing motion at the disc. In their study, lumbar torsional failure occurred at moments less than 59Nm. Similarly, Bisschop *et al*.[244] performed a similar study, and reported an average torsional failure moment of 58.9 Nm in specimens with high BMD. In specimens with low BMD, lumbar spine failures were observed at as low as 23.7Nm. In the present study, similar torsional strengths were observed in the thoracic spine.

Moreover, and similar to Bisschop *et al*.,[244] thoracic spine BMD had a significant effect on the resulting failure moments. Thoracic spine BMD was significantly correlated with both the applied force at failure ($r=0.932$, $p<0.001$) and the intervertebral disc moment at failure ($r=0.609$, $p=0.047$). This may have substantial impact on future in-vitro studies for AIS and other pediatric and adolescent issues, as specimen selection may become of the utmost importance. The

majority of in-vitro studies are performed using elderly cadaveric spines, as adolescent specimens are virtually unattainable. Consequently, BMD must be considered in specimen selection. Additionally, the result may have an impact in cases of adult scoliosis, where effects of BMD may be paramount to intraoperative success.

Throughout these studies, spine failures have been observed at substantially smaller torque magnitudes than those purported clinically, both for the thoracic and the lumbar spines. This may explain the intraoperative failures which have been occurring clinically. Despite the intraoperative failures,[110,128,179] including pedicle screw plow, aortic abutment, and pedicle fracture, prior to this work, the safety limits had yet to be defined. This is the first study of its kind to evaluate the safety of a specific scoliosis correction maneuver in the thoracic spine.

4.3.2 Simulated DVR versus Conventional Biomechanical Methods (Pure Moments)

Despite the glaring controversies and gaps in the literature surrounding the effectiveness of posterior releases in correcting scoliosis deformities, the majority of the previous in-vitro studies applied the traditional *Pure Moment* model.[29,58,164] Accordingly, low-magnitude torques ranging from 2-6Nm have largely been applied. However, and as discussed extensively, these torques do not begin to simulate the typical torques applied intraoperatively. Consequently, in-vitro studies to date have produced results which have not coincided with either clinical reports or clinical belief.

In order to expand upon the typical low-magnitude model, the torsional limit of the thoracic spine had to first be established. As discussed, and reported above, the present study demonstrated an average thoracic spine failure moment of 33.3Nm, at an applied force of 138.6

N. With this failure limit established, the increase in ROM following posterior release at this limit could then be evaluated. Furthermore, the increase in ROM at fractional proportions of this failure load could also be evaluated to determine the effectiveness of the posterior releases at 'safe' torsional torque magnitudes.

Under failure-producing torque magnitudes, and compared to the typical pure moment load, e.g. 4Nm, unidirectional T10-T11 ROM increased from 2.1° to 11.6° following Ponte osteotomy. Moreover, the increases in unidirectional ROM at failure ranged from 4.6° to 19.3°, substantially larger than the increases in ROM reported previously in in-vitro studies of the thoracic spine.[25,28,58,250] Moreover, compared to the typical in-vitro loading magnitude of 4Nm, increases of up to 2° were observed at 25% failure, and an additional 4.3° when increasing the magnitude to 50% of the failure torque. Using the *Pure Moment* model, maximum increases in bilateral axial rotation ROM were approximately 3°.[28,250] Clearly, increased torque magnitudes produced larger increases in axial rotation ROM, providing a more accurate representation of the clinical environment.

As discussed, the improvement in axial plane deformity attributable to specific releases is difficult to ascertain from the literature, but approximate improvements range from 5.1-17°.[6,169,170,172] In comparison, the unidirectional T10-T11 ROM in the present study increased by as much as 19.3°. The simulated DVR model provided the most clinically comparable data to date in the biomechanical community. The increases alone demonstrate the importance of exploring high-magnitude loading scenarios in in-vitro prediction of clinical performance.

4.3.3 Risk-Benefit Analysis: Increase in Motion versus Increased Risk

With the DVR-to-failure and DVR simulation, the ultimate goal was to determine (1) safe limits of torque application during intraoperative correction of spine deformity and (2) evaluate the increased motion following posterior release under these safe limits. In the present study, the results indicated that the increase in ROM continues throughout loading, with a maximum increase in ROM occurring at the failure moment. However, clinically, the goal would be to achieve a desired correction prior to risking catastrophic failure. Specifically, surgeons would ideally apply magnitudes that achieved correction without producing pedicle screw plow, aortic abutment, vascular injury, or bony fracture, to name a few. Consequently, the results must be evaluated in the context of a risk-benefit analysis.

In the present study, the lowest failure moment observed was 13.7 Nm, corresponding to an applied load of 20.3 N. Meanwhile, the average moment at 25% failure was 8.3±3.0 Nm, the range of which falls below the minimum ultimate torsional failure moment. Irrespective of BMD, 25% failure moment may be an appropriate moment to achieve inherent confidence in the safety of the applied moment, as well as effectiveness in the produced results. Specifically, at 25% failure, increases in ROM were as much as 2°, increases which are above and beyond those provided at the 4Nm in-vitro loading magnitude. Consequently, at the increased loads, and compared to the Pure Moment results, the increases may be nearly doubled.

Moreover, when considering BMD, the true safety may be elucidated. In specimens where the BMD was greater than 0.9 (4 specimens, BMD ranging from 0.933-1.042), the intervertebral disc moments at failure were, on average, 42.7Nm. With sufficient thoracic spine BMD, stronger pedicle screw-bone interfaces may be achieved, and in turn, stronger thoracic spine strength

under DVR. With such considerations, the safe torque magnitudes may be increased, which would in turn improve the ROM increase following posterior release. In preclinical prediction of the deformity correction potential of various procedures, the relationship between BMD and strength should govern the safe limits, and in turn, the effectiveness in a given sample. This may serve to improve the preclinical deformity correction predictions for cases of AIS.

4.4 Supplemental Analyses

4.4.1 Biomechanics as a Function of Disc Degeneration

Despite the evident effects of disc degeneration and specimen health on the resulting spine biomechanics, as demonstrated by the wealth of studies performed on the lumbar and cervical spines,[183,196,201-205] the effects on thoracic spine biomechanics are unknown. Moreover, despite the majority of surgical release studies being aimed towards the adolescent and pediatric communities where disc degeneration is likely not present, all previous in-vitro studies of the thoracic spine have used adult cadaveric specimens without regard for specimen health.[10,27,29,58,129,164] Consequently, several supplemental analyses were performed in the present work to evaluate the effects of specimen health on the resulting thoracic spine biomechanics.

In the present work, thoracic spine ROM was negatively correlated with radiographic disc degeneration grade and MRI degeneration grade. Specifically, radiographic scoring was performed according to two grading systems proposed by Mimura *et al*.[196] and Lane *et al*.[254] Both x-ray scoring systems were significantly correlated with one another, demonstrating the similar ability of each to score the intervertebral discs. Similarly, both x-ray scoring systems were negatively correlated with total thoracic spine intact ROM in each of the three directions. The largest negative correlations were in axial rotation, where the Spearman's rho values were greater than 0.74. This coincides with many of the previous studies in the lumbar spine, which suggested consistent decreases in lumbar spine ROM with increasing degeneration.[183,196,203]

Despite the comprehensive negative correlations between x-ray degeneration grade and thoracic spine ROM, the MRI results were less clear. While negative correlations were observed between MRI degeneration grade and thoracic spine ROM in flexion-extension and lateral

bending, insignificant positive correlations were observed in axial rotation; however, the spread of MRI degeneration grades may have contributed to this finding. Specifically, 7 of the MRI graded specimens had a Pfirrmann grade III, whereas two had a Pfirrmann grade IV, and only one a Pfirrmann grade of II. Future work is needed to continue to evaluate the relationship between MRI degeneration grade and thoracic spine ROM, particularly as MRI-based grading may be the most clinically applicable in cases of spine disorders.

While thoracic spine degeneration has been reported,[274-279] the pathology is much less common than in the cervical or lumbar spines.[276,280] In our random sample of cadaveric thoracic spines, a mild to severe degree of degeneration was observed. The results of suggest a decrease in motion from moderate to severe degeneration, consistent with many previous studies of the lumbar spine.[183,196,203] In addition, and similar to some previous studies of the lumbar spine,[201,202,204] the results from ***Group B*** specimens suggest an increase in thoracic motion between mild and moderate degeneration; however, due to the limited sample size, and in particular only one spine with mild degeneration, this conclusion cannot be firmly established before a further study is conducted.

While there were negative correlations between histological degeneration grade and ROM in all directions, the correlations were not significant. Unlike the present study, Quint *et al*.[201] evaluated lumbar motion as a function of disc health, and found that histological grading was more associated with changes in ROM than radiographic criteria; however, thoracic motion was not evaluated. The lack of significant correlations in the present study may have been a result of the limited sample size. Moreover, nearly all of the specimens in the present study were given histological scores ranging from 3-5, i.e. mild to moderate degeneration. Despite the lack

of extreme scores, i.e. healthy or severely degenerated grades, the histological scoring system employed provided a simple and effective way to evaluate the discs. However, there was variation within each specimen. For example, the posterior half of the sagittal sections demonstrated clearer half circles in the AF, and in turn, the boundary between the AF and NP was clearer. The anterior half, on the other hand, showed much less clear organization. This observation was particularly noticeable under polarized light, which may be a useful tool in future investigations of the AF and AF/NP boundary. Typically, scores were equivalent for the AF, the AF/NP boundary, and the NP matrix; the cellularity, however, tended to differ, and may be a distinguishing factor between specimens. It should be noted that in such specimens with large variability between the anterior and posterior portions, the grade was based on the more degenerated regions. This was done because, in these specimens, there were few focal areas of healthy tissue, with the majority of the tissue having more severe degeneration.

Based on the strong negative correlations between thoracic spine ROM and radiographic-based disc health in the ***Group B*** specimens, cadaveric thoracic spine flexibility was further evaluated as a function of intervertebral disc health both before and after the sequential posterior destabilizations. Based on the results of ***Group B***, increases in ROM for healthier spines were at least two-fold larger than increases for degenerated spines, following destabilizations. Maximum increases in ROM for healthier spines were also two-fold larger than degenerated spines.

As discussed, while several studies have evaluated one-level destabilizations in the thoracic spine,[10,13,29,164] few studies to date have reported the effects of multi-level destabilizations, more closely representing a surgical environment. Horton *et al*.[25] evaluated total thoracic ROM increases following four total facetectomies, and found a mean increase of 2.5° in

flexion-extension, approximately half the magnitude of increase reported in the present study; however, in the present study, approximately twice the number of total facetectomies were performed. Similarly, under single plane pure moments, the present study demonstrated increases of approximately 3° in flexion-extension and axial rotation following three sequential Ponte osteotomies in hemi-thoracic spine segments. Following stratification by disc health, healthier spines showed increases of more than 4° in both flexion-extension and axial rotation following total facetectomies, and more than 9° following the osteotomies, far exceeding the increases reported in the previous studies. Clinically, surgical releases are typically performed during deformity correction surgery on pediatric patients, where disc degeneration likely does not exist. Therefore, by qualifying biomechanical results according to disc health, as done in the present study, more applicable data may be obtained for pediatric deformities, such as adolescent idiopathic scoliosis.

Unlike the total thoracic ROM results, specimen disc health had little effect on the increase in local ROM following posterior destabilization, particularly under the simulated DVR. Under simulated DVR, unidirectional axial rotation was applied locally at T10-T11, producing small motions compared to those produced under bidirectional axial rotation in ***Group B*** specimens. This may have contributed to the weak correlations between T10-T11 unidirectional axial rotation right ROM and disc health. Following osteotomy under low-magnitude in-vitro torques (i.e. 4Nm), the increases in motion compared to intact were, on average, less than 1°. Similar to the previous reasoning, the small magnitudes of increase may have been too small to decipher between degeneration grades.

Surprisingly, there were no correlations between the increase in motion under high-magnitude torque loading and intervertebral disc health. In this case, where the applied torque magnitudes exceed the typical elastic properties of the intervertebral disc, the degeneration seemed to have less of an effect. This makes sense as the degeneration likely affects the elastic response of the discs. However, again, as the sample size was limited, and the spread of degeneration grades was thin, it is difficult to make comprehensive conclusions to this point.

4.4.2 Typical Thoracic ROM

Intact thoracic spine range of motion was extracted from the literature to determine the spread of estimated segmental motions reported in previous studies and to calculate estimated segmental ROM pooled means and standard deviations in each anatomical plane. Overall, estimated segmental motions were smallest in magnitude in flexion-extension and largest in axial rotation. According to the pooled segmental ROM means and standard deviations, large variability in ROM existed at each thoracic motion segment in each of the three loading directions. Additionally, pooled estimated segmental motion in flexion-extension was largest at the superior- and inferior-most motion segments, whereas pooled estimated segmental motions in lateral bending and axial rotation were largest in the middle regions of the thoracic spine.

As discussed, previous literature frequently references the motions reported by White and Panjabi to evaluate the results of their respective research studies.[29,41,42,50,130,154,155,159,160] However, in contrast to the motions reported by White and Panjabi,[23] when considering all of the more recent studies conducted over the last three decades reviewed in the present study, estimated segmental motions were substantially smaller for nearly every thoracic motion segment in

flexion-extension (Figure 43), lateral bending (Figure 44), and axial rotation (Figure 45). The results are strikingly different, and both indicate a large variability amongst motions at each thoracic level.

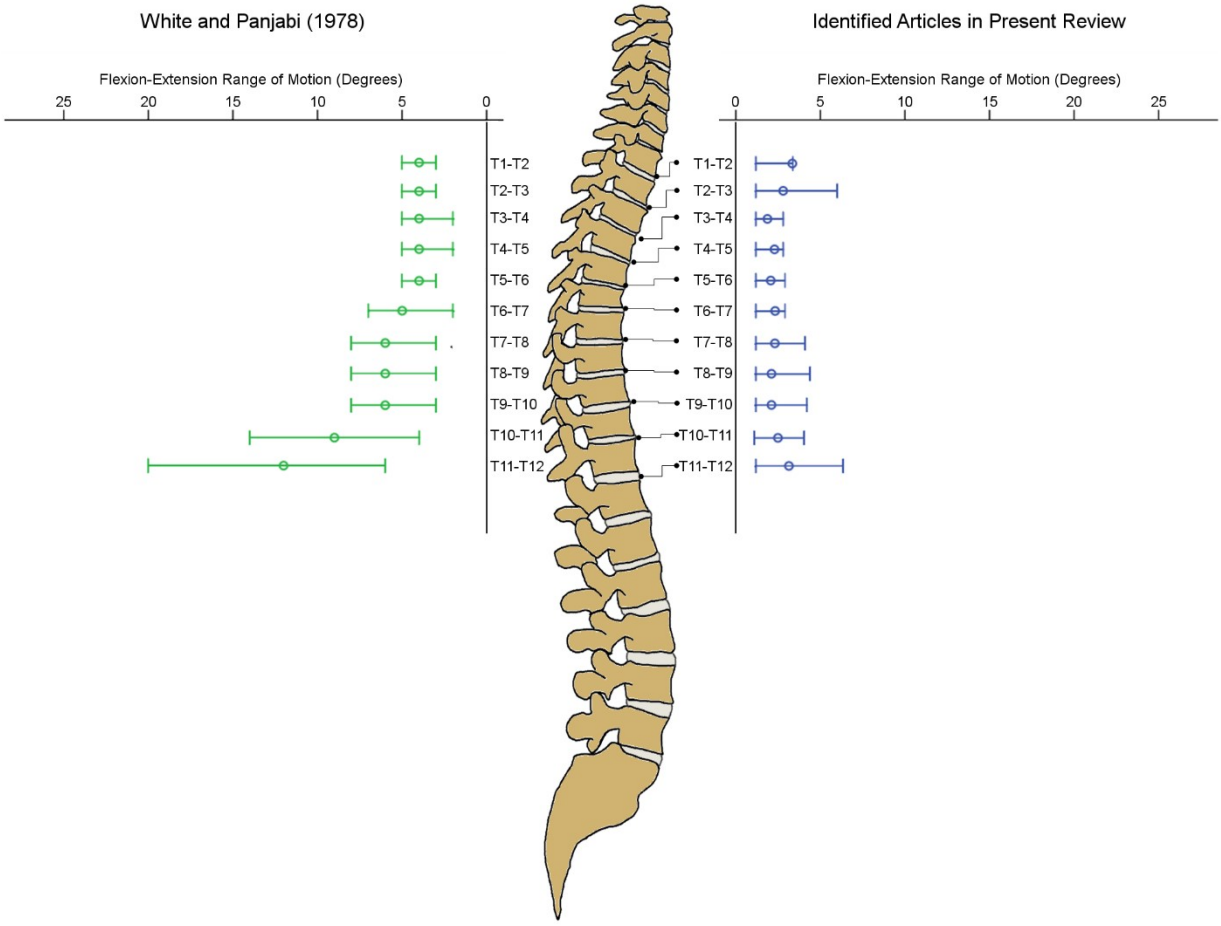

Figure 43. Left: flexion-extension ROM reported by White and Panjabi[23] shown in green (range of motion and ranges). Right: flexion-extension ROM reported by the 24 identified articles in the present study which tested specimens without ribcages. The median, minimum, and maximum values of the estimated segmental motions among the studies are shown.

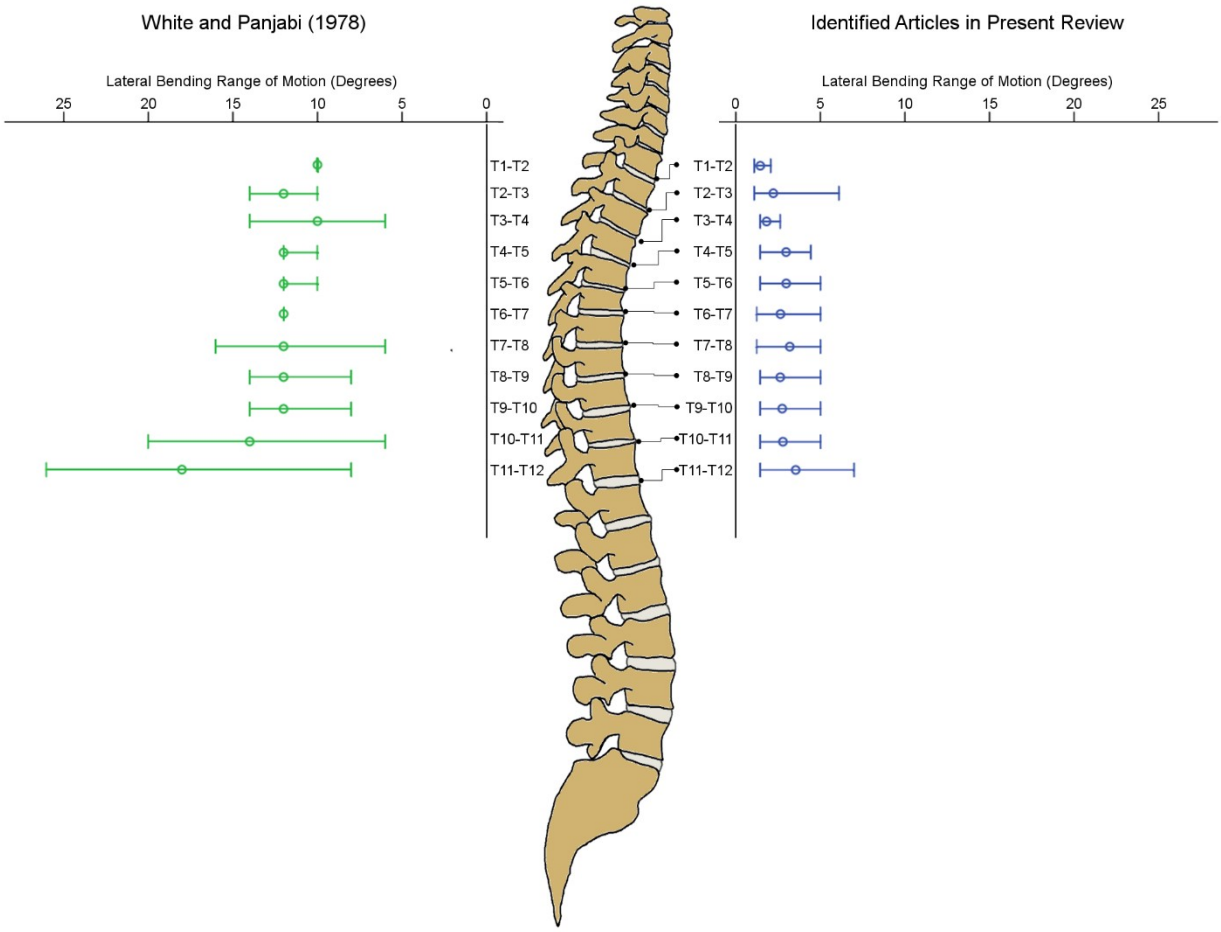

Figure 44. Left: lateral bending ROM reported by White and Panjabi[23] shown in green (range of motion and ranges). Right: lateral bending ROM reported by the 24 identified articles in the present study which tested specimens without ribcages. The median, minimum, and maximum values of the estimated segmental motions among the studies are shown.

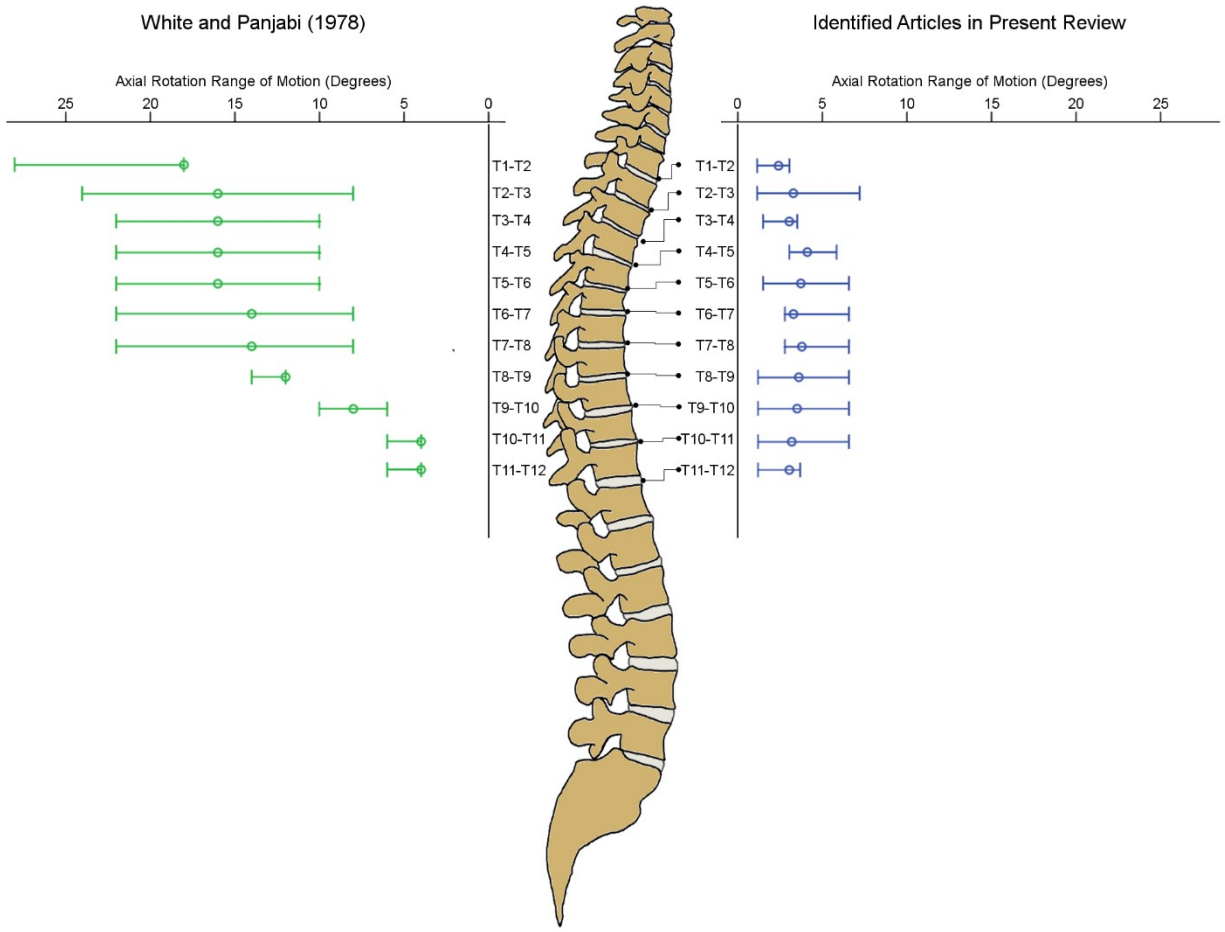

Figure 45. Left: axial rotation ROM reported by White and Panjabi[23] shown in green (range of motion and ranges). Right: axial rotation ROM reported by the 24 identified articles in the present study which tested specimens without ribcages. The median, minimum, and maximum values of the estimated segmental motions among the studies are shown.

Based on the reported ranges by White and Panjabi,[23] total thoracic ROM (T1-T12) would range from approximately 34°-90° in flexion-extension. In contrast, the sum of the pooled means in the present study (T1-T12) was approximately 28° in flexion-extension, substantially smaller than the previously reported range. Similarly, White and Panjabi reported an estimated total ROM of 94°-164° in lateral bending, compared to only 36° calculated in the present review,

also much smaller. Finally, White and Panjabi reported an estimated ROM of 108°-198° in axial rotation, whereas in the present review, estimated total ROM was only 45° in axial rotation.

The disparities may be attributed to differences in the loading mechanisms as well as the motion measurement methods. As discussed, the pooled means reported in the present study were based on the results of studies which generally employed pure moment testing standards.[17,24] In contrast, White's work was performed using off-axis compression loading modes for bending,[9] prior to the advent of pure moment testing standards. It should be noted however that despite this difference, motions in other studies using alternative types of loading, including cantilever bending[13,25] and 4-point bending,[136] have also reported motions substantially smaller than those reported by White and Panjabi,[23] suggesting an alternative reason for the differences. Another potential factor may be the method of motion measurement. Specifically, more recent techniques for motion measurements, such as optical motion tracking, may be more accurate than the methods employed by White's work, which included measurements using extensometers, displacement gauges, and radiographs.[9]

The biomechanical standards were specifically designed to allow comparisons of results across studies;[17] however, variability among the results clearly exists. As the standard should theoretically produce similar results, perhaps the variability in the results can be attributed to the inherent variability in cadaveric specimen flexibilities. As discussed, disc degeneration has been shown to affect the motions of the lumbar spine.[183,196,201-204] The present work demonstrates that the same is true in the thoracic spine. Additionally, experimental factors may play a role in the resultant motions, including, for example, loading magnitude, loading rate, and measurement apparatus. With improved reporting of the biomechanical methods, as well as improved

identification and reporting of specimen conditions, i.e. disc degeneration grade, presence of osteophytes, etc., the wide variance reported throughout the thoracic spine literature may be reduced.

Several studies have estimated and measured thoracic spine ROM in-vivo.[151-157] Reported full thoracic motion (T1-T12) in flexion-extension has ranged from approximately 25.6° to 71°,[153-156] lateral bending ROM has ranged from approximately 31.2° to 75°,[152,155,156] and axial rotation ROM has ranged from approximately 41.8° to 95.5°.[151,155-157] In comparison, the sum of the pooled motions in the present study (T1-T12) was 28°, 36°, and 45° in flexion-extension, lateral bending, and axial rotation, respectively. Each of these values fell within the lower ranges of reported in-vivo motion suggesting that, as intended, pure moment testing may produce physiological ranges of motion. In comparison to the values reported by White and Panjabi,[23] the clinical flexion-extension motions demonstrated similar ranges; however, the in-vivo measured lateral bending and axial rotation ROMs were substantially smaller, similar to those motions calculated in the present study.

The results of the present study may be limited by the method used to estimate the thoracic segmental ROM in each plane. With increased use of optical motion measurements and the increased capabilities of measuring motions at each spine segment, future studies should report both global and segmental motions. Once this data becomes routinely available, more accurate estimations may potentially be developed. Additionally, the analysis in the present study was limited to the details provided by the published literature. With more detailed explanations of experimental details, including loading rates, loading setups, etc., more thorough analyses may be performed.

Overall, estimated segmental thoracic ROM was established for each level of the thoracic spine in flexion-extension, lateral bending, and axial rotation. The estimated motions fell within the lower ranges of reported in-vivo motions, but were substantially smaller than the frequently referenced values of cadaveric motions previously established. The wide variation in the results suggests the need for improved characterization of experimental specimens, such as specimen health or intervertebral disc degeneration. Such improved specimen characterization, as well as improved reporting of experimental details and setups, may enable more accurate and comprehensive estimations to be developed in the future, ultimately establishing a set of normal motions at each level of the thoracic spine which could be beneficial for the diagnosis and treatment of thoracic spine disorders.

4.5 Limitations

As it is neither feasible nor possible to procure adolescent cadaveric specimens for preclinical testing, let alone those with untreated deformities, cadaveric specimens from adult donors were used in the present work. Therefore, the specimens employed in each of the models presented in this work may not be as flexible as those pediatric spines operated on during AIS surgeries, as adult spines suffer from poor bone quality, as well as disc and soft tissue degeneration. Additionally, the assumption was made that any increase in ROM observed during in-vitro testing would correlate to the increases observed intraoperatively. The assumptions associated with both the specimens, as well as the in-vitro to intraoperative correlation, may have affected the results.

In addition to these assumptions, in the present study, thoracic spines were tested with the ribcage and sternum removed, similar to previous work[13,29,164]. This too could have affected the magnitudes of increase observed following the releases, as the anterior structures could provide stability in the thoracic spine.[27,131,132] Specifically, Watkins *et al*.[27] reported increases in ROM as much as 66% following removal of these anterior structures. Similarly, Brasiliense *et al*.[131] demonstrated substantial stability provided by the ribcage and sternum.

Clearly, this model introduces errors into the study's approximations and estimates, and this limitation needs to be taken into account. On the other hand, there are good reasons to consider adult, non-scoliotic spines. These limitations and strengths are discussed below.

Adult spines are readily available, and there are simply no other available models that come as close as adult spines to the mechanical properties of adolescent spines. For example,

though the stiffness may be different, adult and adolescent ligament structures both have viscoelastic behavior which is extremely difficult to replicate with any other type of model.

A frequently discussed error involves the underlying assumption that the force required to bend (or torque) a straight spine into a deformed position is well approximated by the force required to bend a deformed spine into a straight position.[138] While there is no quantitative data to support its validity, this assumption does follow basic principles of mechanics, unless there is a significant asymmetry in mechanical properties of soft tissues in the scoliotic spine.

Even if scoliotic spines were readily available, these would not easily provide a good alternative model for this study, since each deformity is completely different in shape and stiffness. In contrast, a straight spine provides the most reproducible starting point for measurement of changes in flexibility.

Alternative methods of studying surgical biomechanical issues for scoliosis have included clinical reports and computational models (i.e. finite element models). Given the costs of spine deformity corrective surgeries and the amount of follow-up time and effort required to follow-up patients, clinical studies suffer from major limitations. On the other hand, computational models require input of material properties of the soft tissues.[281] These material properties for pediatric or scoliotic spines, however, are unknown. Therefore, computational models typically use mechanical properties of adult cadaveric soft tissues for scoliosis models, effectively introducing the same limitation as in cadaveric models.

In addition to the lack of deformity, adult cadaveric specimens possess varying disc degeneration, bone quality, and overall health, together resulting in a wide range of flexibility. It should be noted that a wide range of flexibility, in and of itself, is not unique to adult spines and

not a result of degeneration alone; rather, it is an inherent characteristic of the distribution of flexibilities of all human spines, young and old, healthy and deformed. For example, in one cohort of 76 AIS patients, standing Cobb angles ranged from 41.3°-95° and bending Cobb angles ranged from 9.1°-60.8°.[139] Similarly, in a cohort of 66 AIS patients, standing Cobb angles ranged from 48°-78° and bending Cobb angles ranged from 22°-47° .[105]

Recognizing the limitations of using adult spines, the present study explores and takes into account the error introduced by the differences among adult spines due to aging and degenerative changes. This study used the correlation between disc degeneration and spine flexibility to stratify the results. Taking this variable into account facilitates relating the data to adolescent scoliosis patients in a more quantitative and objective way.

Another limitation in the present study was the limited number of specimens for the supplemental analysis, particularly with MRI grading and histological grading. Consequently, a full range of degeneration grades was not represented, which may have affected the magnitude and statistical significance of the correlations. Additionally, only the T10-T11 disc space was graded. As this was a reanalysis of an already completed study, we were limited to evaluating this disc space; however, future studies should analyze the effects of disc degeneration on the kinematic response at each level of the spine.

Cadaveric models for the study of different methods to correct AIS deformities have clear advantages over clinical outcome studies, including shorter time, lower cost to the community and patients, and better control of numerous variables. Therefore, the results of the present study may serve to avoid the risk of suboptimal procedures that would otherwise be performed on

some of the youngest, and most clinically demanding orthopaedic patients, who require decades of clinical success from their surgeries.

4.6 Conclusions

The present work demonstrated results which will have immediate impacts in both the clinical and biomechanical communities. The overall goes of the present work was to expand upon the current in-vitro testing method to produce a more comprehensive model to evaluate spine deformity. Using the traditional *Pure Moment* model, it was demonstrated that supplemental wide posterior releases provided additional increases in thoracic spine flexibility, compared to the routinely performed total facetectomies. The result supports the use of wide releases as a supplement to provide added correction intraoperatively, helping to provide foundational data to alleviate the controversies in the clinical literature.

The traditional *Pure Moment* model was then expanded to include novel testing methods and supplemental analyses on the basis of intervertebral disc and bone health. Building upon the *Pure Moment* results, multi-planar loading and simulated DVR-to-failure models were employed. Under multi-planar loading, the surgical releases provided simultaneous three-dimensional increases in thoracic ROM, with the most pronounced effects in ROM occurring under combined transverse and sagittal plane loading. As these are the typical loading directions intraoperatively, the result suggests the potential of using similar releases intraoperatively in cases of three-dimensional deformity, such as AIS. Despite the recent popularization of these releases in cases of AIS, to date, no definitive data was available in this regard.

Further expanding the model, a novel apparatus was designed to develop a model which could evaluate the safety and efficacy of intraoperative techniques using in-vitro testing. Specifically, DVR, a popular posterior-only correction maneuver, was simulated in thoracic spines. Using the simulation, both the safety of the maneuver, as well as the added benefit of

increased ROM using the maneuver were evaluated. The thoracic spine strength under simulated DVR was measured to be 33.3 Nm, substantially smaller than purported clinical torques in excess of 100Nm. The result may explain the intraoperative failures which have occurred using such techniques, such as pedicle screw plow, pedicle fracture, and aortic abutment.

The safety of using such maneuvers must also be evaluated against the strength of the bone-screw interfaces along the length of the spine. Based on the strong correlations between thoracic spine BMD and thoracic spine strength, safety zones can be established. For example, in specimens where the BMD was greater than 0.9, the strength of the spine exceeded 40 Nm. Similar analyses may be made as future work continues to add to the database of knowledge surrounding this relationship.

While the strength limits of the thoracic spine have clearly been broached intraoperatively, the question of safety must be paralleled by the question of effectiveness at given applied loads. In the present work, following release, axial rotation ROM continually increased until failure was reached. At 25% failure load, the ROM increases were nearly twice as large as those achieved under typical in-vitro loading magnitudes, and were closer to those reported clinically. Using the information presented in the current work, more realistic and clinically relevant predictions may be performed, accounting for both the safety of the maneuver as well as the effectiveness of reducing the deformity.

Beyond the specific clinical questions at hand, the present work provides a platform for growth in the field of spine biomechanics. Based on the significant effects of intervertebral disc and vertebral bone health on the resulting biomechanics, inclusion criteria should be employed in specimen selection, just as surgeons would employ for their patients. This may maximize the

applicability of using elderly specimens for evaluating problems in the adolescent and pediatric communities, a limitation which, until now, was not addressed. Moreover, as demonstrated by the wide range of results throughout the thoracic spine literature in assessing the motion of the thoracic spine, the methods employed for testing should be purposeful.

In the present work, the traditional model was not sufficient to evaluate the problem at hand. Consequently, the model was expanded to include new testing methods, e.g. multi-planar loading and intraoperative simulation, as well as new analysis techniques, e.g. ROM as a function of disc degeneration. With purposeful experimental design and parameter selection, the questions of safety and efficacy could be addressed, producing the most clinically relevant biomechanical data to date in the evaluation of AIS correction techniques. With future work, and continued efforts towards problem-based biomechanical solutions, the field of spine biomechanics will begin to have a much greater impact on the clinical community, and in turn, on the treatment of orthopaedic patients.

In its entirety, this study established the safety and efficacy of commonly used intraoperative techniques for the treatment of scoliosis deformities. It provided quantitative information essential for the prediction of achievable correction under safe loading limits. The novel model provides a platform for the evaluation of other surgical releases and correction maneuvers, as well as future biomechanical models in evaluating spine disorders. With such well controlled and quantitative in-vitro models, we may ultimately improve the outcomes of our spine patients, including those from the pediatric and adolescent communities who require long-term permanency in their treatments.

5 Appendix A

5.1 Quantification of Increase in Three-Dimensional Spine Flexibility Following Sequential Ponte Osteotomies in a Cadaveric Model[28]

Spine Deformity

The Official Journal of the Scoliosis Research Society

May 2013 Volume 1, Issue 3, Pages 171–178

Quantification of Increase in Three-dimensional Spine Flexibility Following Sequential Ponte Osteotomies in a Cadaveric Model

Sophia N. Sangiorgio, PhD, Sean L. Borkowski, MS, Richard E. Bowen, MD, Anthony A. Scaduto, MD, Nathan L. Frost, MD, Edward Ebramzadeh, PhD

Received: August 24, 2012; Received in revised form: January 9, 2013; Accepted: January 13, 2013;

DOI: http://dx.doi.org/10.1016/j.jspd.2013.01.006

Abstract

Background

Posterior-only procedures are becoming more popular for treatment of rigid adolescent idiopathic scoliosis, but little is known about the quantitative correction potential for Ponte osteotomies. The objective of this study was to quantify and compare the range of motion of intact multilevel thoracic spine segments with the same segments after each of 3 sequential Ponte osteotomies.

Methods

We tested 5 human cadaveric thoracic spine segments, spanning T–T6, or T7–T12, in an 8-degree-of-freedom servo-hydraulic load frame, monitoring motion of each vertebra with an optical motion tracker. We measured range of motion while we applied cyclic, pure moment loading to produce flexion-extension, lateral bending, and axial rotation at a rate of 0.5°/second, to a maximum of ± 6 Nm. Each specimen was tested intact and after each of 3 sequential Ponte osteotomies.

Results

Total range of motion for the segments (either T2–T5 or T8–T11) increased by as much as 1.6° in flexion, 1.5° in extension, 0.5° in lateral bending, and 2.8° in axial rotation with each osteotomy. Because of the variation in initial specimen stiffness, we normalized motions to the intact values. In flexion, average range of motion increased after each osteotomy compared with intact, by 33%, 56%, and 69%. In extension, slightly smaller increases were seen, increasing by as much as 56% after the third osteotomy. In lateral bending, Ponte osteotomies had little effect on range of motion. In axial rotation, range of motion increased by 16%, 29%, and 65% after 3 osteotomies.

Conclusions

Sequential Ponte osteotomies increased range of motion in flexion, extension, and axial rotation, but not in lateral bending. These results suggest that the Ponte osteotomy may be appropriate when using derotational correction maneuvers, or to improve apical lordosis at the apex of curvature during posterior spinal fusion procedures. Although these techniques are effective in gaining correction for kyphotic deformities and rigid curvatures, they add time and blood loss to the procedure.

Keywords:

Scoliosis, Spine, Cadaver model, Biomechanics, Sequential destabilization, Deformity correction

INTRODUCTION

Adolescent idiopathic scoliosis affects approximately 2%–4% of adolescents [1], or 1.5–3 million children in the United States alone [2]. Surgical treatment traditionally consists of anterior releases, either alone or combined with a posterior release. More recently, because of the morbidity associated with anterior approaches and technological advances in pedicle-based instrumentation and implants, there have been advocates for posterior-only approaches [[3], [4], [5], [6], [7],[8]]. Although posterior-only approaches have been used to treat degenerative kyphosis, they have only recently been proposed for treatment of adolescent idiopathic scoliosis [4].

The Smith-Petersen osteotomy, sometimes referred to as a Ponte osteotomy [[3], [9], [10]], was introduced in 1945 [11]and was originally indicated for correction of kyphosis. Both the Smith-Petersen and Ponte osteotomies are posterior column shortening osteotomies originally described for the correction of rigid kyphosis. The Smith-Petersen osteotomy, first described by Smith-Petersen in 1945 in patients with ankylosing spondylitis and rigid kyphosis, involves resecting portions of the spinous processes, ossified interspinous ligament, and ankylosed facet joints. Closing the osteotomy allowed for correction of fixed kyphosis in these patients. Ponte originally described his osteotomy in the early 1980s as a posterior-only approach in patients with Scheuermann's kyphosis. His technique involves a wide posterior chevron osteotomy coupled with posterior instrumentation. The amount and location of bone resection are similar to those of the Smith-Petersen osteotomy, except that it occurs in the non-ankylosed spine. The clinical corrective potential for sagittal plane deformities using Ponte osteotomies has been reported to be approximately 5°–15° of correction per osteotomy [[3], [12]]; however, this is limited to the sagittal plane and has not been quantified in a well-controlled biomechanical model. Even less is known regarding the corrective potential of Ponte osteotomies in treating complex 3-dimensional deformities, such as scoliosis.

Previous biomechanical studies have investigated the role of different stabilizing structures in the thoracic spine [[13],[14], [15], [16], [17], [18], [19], [20], [21], [22]]; however, few have included posterior-only procedures, and none have isolated and quantified Ponte osteotomies. For example, Feiertag et al. [21] performed a unilateral facetectomy on a single level in a full thoracic cadaveric spine model and reported no significant increase in range of motion (ROM). Oda et al. [19] performed a total facetectomy and laminectomy; however the study only evaluated the effects of a single-level surgery on a single functional spinal unit. More recently, Anderson et al. [22] studied stiffness in flexion after a posterior procedure similar to the Ponte osteotomy; however, the authors did not evaluate extension, lateral bending, and axial rotation. In short, no studies to date have quantified the increase in 3-dimensional flexibility after sequential Ponte osteotomies in a multi-segment thoracic spine model. Consequently, it has been difficult to assess the potential of using Ponte osteotomies in treating 3-dimensional deformities.

The purpose of this study was to measure the 3-dimensional changes in thoracic spine mobility in a multi-segment human cadaveric thoracic spine model after sequential Ponte osteotomies.

METHODS

Specimen preparation

We used 7 fresh-frozen, 6-level thoracic spine segments in this study, dissected from 4 fresh-frozen human cadaveric thoracic spines (C7–L1) obtained from the International Institute for the Advancement of Medicine (Jessup, PA). There were 1 female and 3 male donors (mean, 72 ± 10 years). Before testing, we removed all attached soft tissues, leaving intact the vertebrae, discs, stabilizing ligaments, and posterior 5 cm of rib and associated costovertebral articulations [[23], [24]]. We took radiographs using an HP Faxitron Series X-ray system (43805N; Hewlett Packard Company, Palo Alto, CA) and assessed bone quality using dual-energy X-ray absorptiometry scans (Hologic, Inc., Bedford, MA) to determine general bone and disc health and exclude any gross abnormalities or previous surgeries.

We dissected the 4 cadaveric thoracic spines to obtain 8, 6-level (hemi-thoracic) spine segments, spanning T1–T6 or T7–T12. We excluded 1 T7–T12 lower hemi-thoracic specimen before testing because of severe calcification of the disc spaces, which left a total of 7 hemi-thoracic specimens for testing: 4 T1–T6 segments and 3 T7–T12 segments. The 7 experimental hemi-thoracic specimens (n = 7) underwent mechanical testing.

We potted the inferior (caudal) and superior (cranial) end vertebrae of each segment in low-temperature setting epoxy resin, then placed them in a custom-designed, 15-cm-diameter aluminum mounting ring. We used 2 triplanar laser levels to align the pot within the rings such that the vertebra was properly aligned with the axis of the load frame.

Loading and measurement protocol

In total, we applied the following loading and measurement protocol to each of the 7 hemi-thoracic specimens. We used an MTS 858 mini-bionix servo-hydraulic load frame equipped with the Flextest System (MTS Systems, Eden Prairie, MN) to conduct all experiments, as previously employed by the authors (Fig. 1) [25]. We mounted specimens in an inverted position. The caudal end was attached to the upper gimbals of the load frame, which in turn were attached to the axial-torsional actuator. The cranial end was attached to the lower gimbals and the lower gimbals were in turn mounted on a custom table with 2 perpendicular linear bearings, allowing free translation in the transverse plane to virtually minimize shear loading.

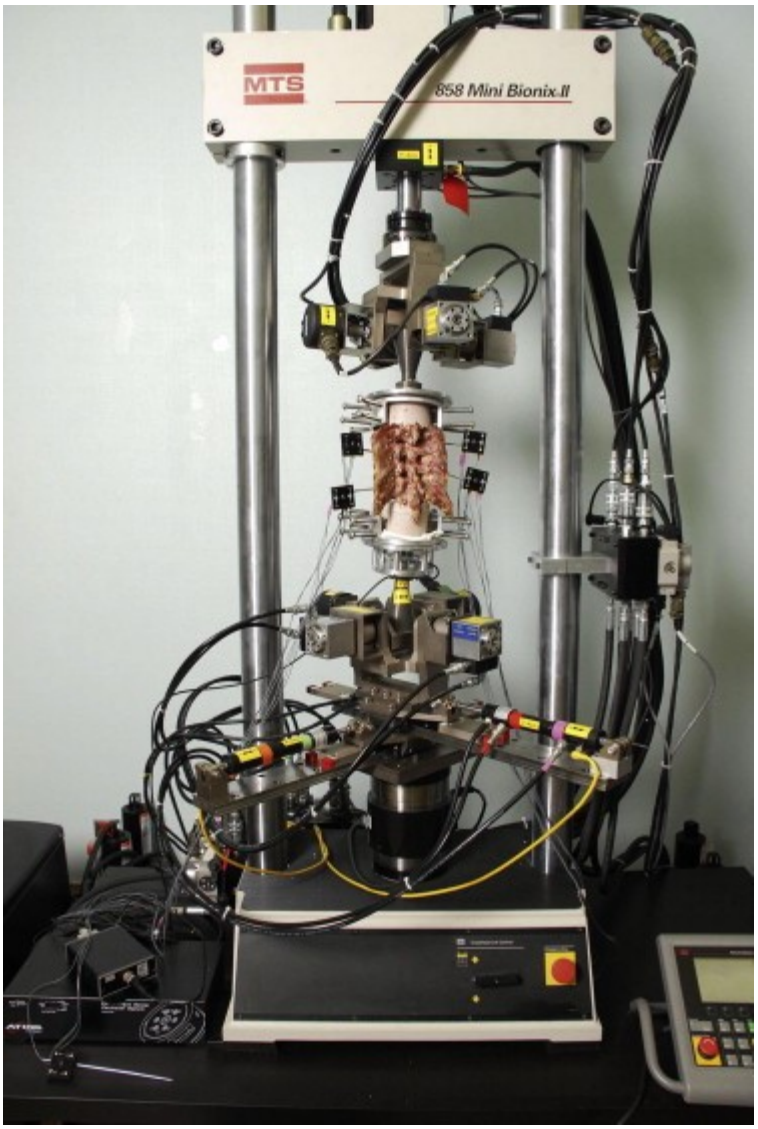

Fig. 1

Experimental setup. The hemi-thoracic spine specimen is in an inverted orientation, held by gimbals at each end, with square flags attached for optical motion tracking.

We applied loads as pure moments in position control with torque-controlled end points, at a rate of 0.5°/second [26] to a maximum of 6 Nm. Loads were applied in sequence as follows: flexion-extension (± 6 Nm), right and left lateral bending (± 6 Nm), and right and left axial rotation (± 6 Nm). For flexion-extension, we applied bending moments through both upper and lower gimbals, thus keeping the spinal segment aligned with the axis of the load frame. We carried out a similar process for the application of the lateral bending moments. For axial rotation, we applied rotational moments through the caudal aspect

with no axial preload. Each loading sequence was repeated for 5 cycles to minimize viscoelastic effects [[19], [26]]. The first 3 cycles served as preconditioning and the fourth cycle was used for analysis. We monitored and recorded loads throughout testing by a 6-degree-of-freedom load cell (ATI Industrial Automation, Apex, NC).

We recorded motion continuously throughout testing using an Optotrak 3020 3-dimensional motion tracking system (Northern Digital, Inc., Waterloo, Ontario, Canada). The motion tracking system has an accuracy of 0.1 mm and 0.1°. The resolution of the machine is 0.01 mm. Custom motion flags, equipped with 4 non-collinear, light-emitting diode markers, were attached to each vertebra in each spine segment (T2–T5 or T8–T11). In addition, we mounted 1 flag on the MTS load frame post to establish a fixed coordinate axis. The motion of each functional spinal unit and motion of the entire mobile segment (eg, T2–T5) were recorded continuously. We used a digitizing probe to establish planes of motion for each vertebra [27]. Total ROM across the segment (T2–T5 or T8–T11) was recorded as the motion of the superior vertebra with respect to the inferior vertebra.

We repeated the loading and measurement protocol described here for each specimen under the following conditions: 1) intact; 2) Ponte osteotomy at T2–T3 (or T7–T8); 3) Ponte osteotomy at T3–T4 (or T8–T9); and 4) Ponte osteotomy at T4–T5 (or T10–T11).

Destabilization procedures

After intact testing, we performed sequential Ponte osteotomies. Each Ponte osteotomy included a bilateral total facetectomy and resection of the following: the inferior half of the spinous process of the vertebra superior to the osteotomy site, interspinous ligament, and the ligamentum flavum (Fig. 2). We performed the osteotomies starting at the most superior level and then in sequence inferiorly until 3 sequential Ponte osteotomies were completed.

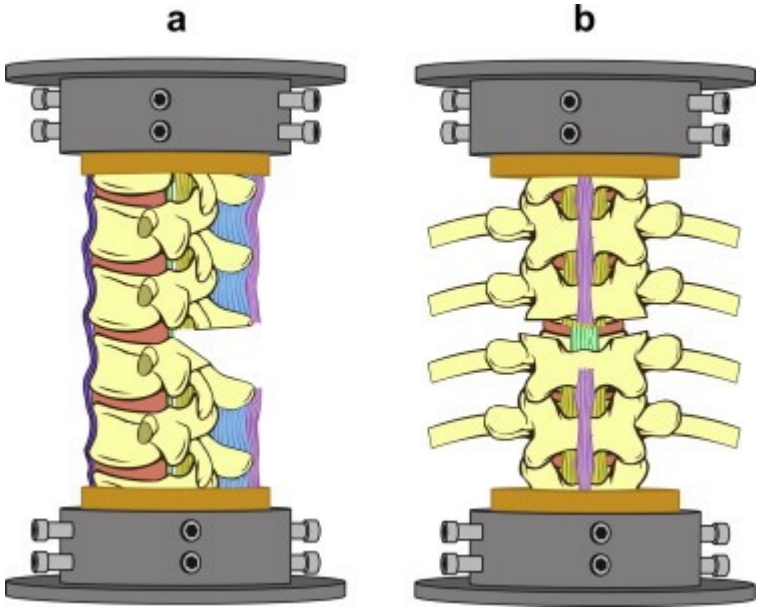

Fig. 2

Schematic diagram showing the resection for Ponte osteotomies in (a) the sagittal plane and (b) the coronal plane.

Statistical analysis

We used SPSS 15.0 statistical analysis software (Chicago, IL) to perform paired-samples *t* tests for the following pairs: intact versus 1-level Ponte, intact versus 2-level Ponte, and intact versus 3-level Ponte. We repeated each paired-samples *t* test for measurements in flexion, extension, lateral bending, and axial rotation.

We performed 2 separate *t* test analyses. A set of paired *t* tests was performed for the analysis of raw measurements in degrees of rotation (Table 1, Table 2, Table 3, Table 4, Table 5). The p values are presented in the Results section with the corresponding raw measurements (degrees).

Table 1 Flexion-extension range of motion (degrees) across thoracic spine segment (T2–T5, or T8–T11).

Measure	Flexion-extension (degrees)			
	Intact	**1-Level Ponte**	**2-Level Ponte**	**3-Level Ponte**
Mean (SD)	5.7 (4.9)	6.5 (5.6)	7.6 (6.5)	8.5 (7.3)
Range	1.0–11.0	1.5–13.1	1.7–15.6	1.6–18.2
		p=0.08		
			p=0.07	
				p=0.09

p-values are for comparison to intact.

Table 2 Flexion range of motion (degrees) across thoracic spine segment (T2–T5, or T8–T11).

Measure	Flexion (degrees)			
	Intact	**1-Level Ponte**	**2-Level Ponte**	**3-Level Ponte**
Mean (SD)	2.7 (1.9)	3.2 (2.3)	3.9 (2.8)	4.4 (3.2)
Range	0.5–5.3	1.1–5.9	1.1–7.1	1.1–7.9
		p=0.11		
			p=0.05	
				p=0.07

p-values are for comparison to intact.

Table 3 Extension range of motion (degrees) across thoracic spine segment (T2–T5, or T8–T11).

Measure	Extension (degrees)			
	Intact	**1-Level Ponte**	**2-Level Ponte**	**3-Level Ponte**
Mean (SD)	3.0 (3.1)	3.3 (3.4)	3.7 (3.7)	4.1 (4.2)
Range	0.5–7.1	0.4–7.6	0.6–8.8	0.4–10.3
		p=0.16		
			p=0.09	
				p=0.13

p-values are for comparison to intact.

Table 4 Lateral bending range of motion (degrees) across thoracic spine segment (T2–T5, or T8–T11).

Measure	Lateral bending (degrees)			
	Intact	**1-Level Ponte**	**2-Level Ponte**	**3-Level Ponte**
Mean (SD)	7.9 (5.7)	8.1 (5.9)	8.3 (6.0)	8.3 (6.0)
Range	1.6–14.8	1.5–15.3	1.5–15.5	1.5–15.4
		p=0.16		
			p=0.07	
				p=0.07

p-values are for comparison to intact.

Table 5 Axial rotation range of motion (degrees) across thoracic spine segment (T2–T5, or T8–T11).

Measure	Axial rotation (degrees)			
	Intact	**1-Level Ponte**	**2-Level Ponte**	**3-Level Ponte**
Mean (SD)	10.6 (7.2)	11.7 (8.2)	12.8 (9.0)	13.8 (9.1)
Range	3.4–19.7	3.9–22.2	4.1–23.6	4.3–23.9
		p=0.08		
			p=0.07	
				p=0.04

p-values are for comparison to intact.

Next, we divided the ROM after each osteotomy by the corresponding intact ROM to determine the normalized percent increase in flexibility. We performed a separate set of *t* tests for this normalized flexibility (Fig. 3). The p values are presented in the Results section with the corresponding normalized flexibility outcomes (percent increases).

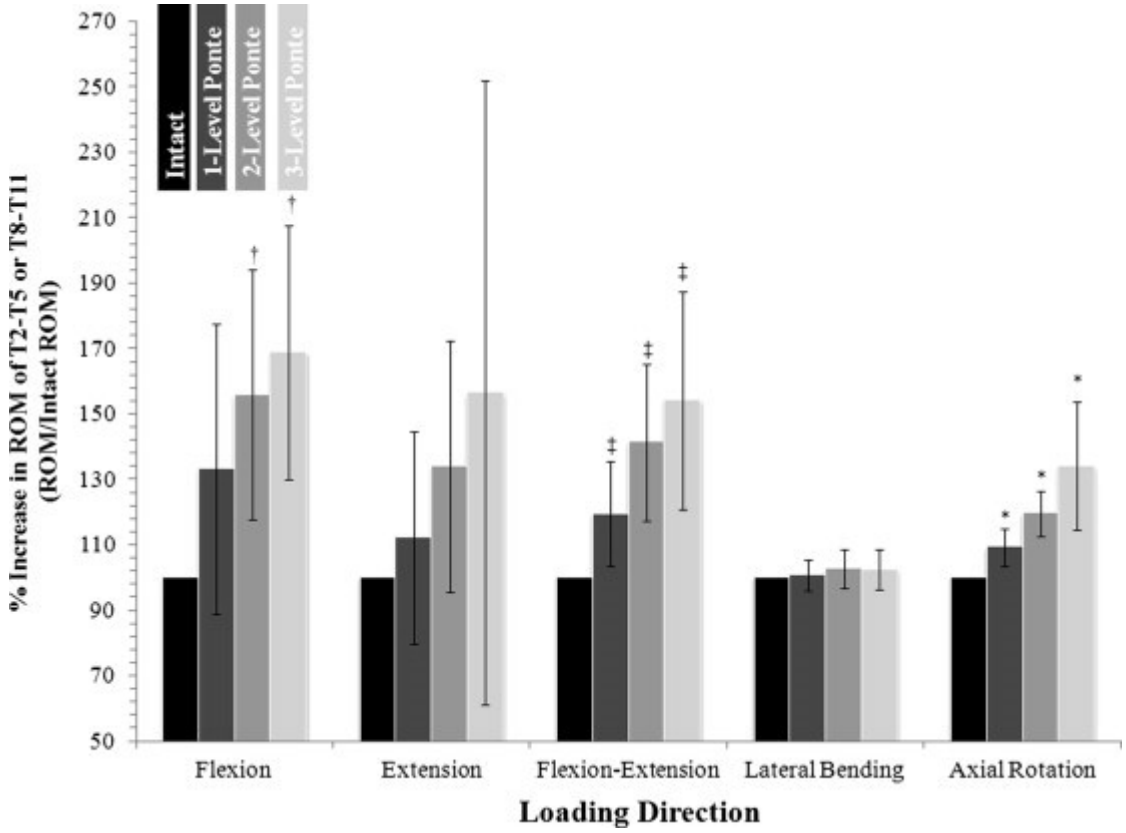

Fig. 3

Change in range of motion as a result of 1-level, 2-level, and 3-level Ponte osteotomies, shown as the percent increase compared with the range of motion of the intact spine. This increase is shown separately for flexion, extension, combined arc of flexion-extension, lateral bending, and axial rotation.

RESULTS

Changes in flexion-extension

We first measured total ROM across the entire segment, specifically either T2–T5 or T8–T11, in flexion-extension. Flexion-extension ROM increased after each osteotomy. Intact ROM was 5.7° ± 4.9° and increased to 6.5° ± 5.6°, 7.6° ± 6.5°, and 8.5° ± 7.3°, respectively after each of the 3 sequential Ponte osteotomies (Table 1). Each osteotomy increased flexion-extension by −0.2° to 2.6°. Compared with intact specimens, flexion-extension increased by 20% ± 16%, 41% ± 24%, and 54% ± 33% after each osteotomy (Fig. 3).

Coupled motions were small during flexion-extension loading, with intact coupled motions of 0.7° ± 0.5° in lateral bending and 0.9° ± 1.3° in axial rotation. After osteotomy, average changes in coupled motions were less than 0.3°.

Changes in flexion

Because flexion and extension are not symmetric, owing to different anterior and posterior anatomy, we also analyzed the 2 motions independently. Range of motion across the entire segment steadily increased in flexion after each osteotomy. Motion increased from 2.7° ± 1.9° in intact specimens to 4.4° ± 3.2° after the third osteotomy ($p = .07$) (Table 2). Each osteotomy increased flexion by −0.1° to 1.6°. Compared with intact specimens, flexion increased by 33% ± 44% ($p = .17$), 56% ± 38% ($p = .03$), and 69% ± 39% ($p = .02$) after each osteotomy (Fig. 3).

Changes in extension

The ROM of the complete hemi-spine increased in extension after each osteotomy, but to a lesser extent than in flexion. Specifically, extension increased from 3.0° ± 3.1° in intact specimens to 4.1° ± 4.2° after 3 osteotomies ($p = .13$) (Table 3). The mean increase resulting from individual osteotomies was −0.2° to 1.5°, similar to that observed in flexion. Compared with intact specimens, extension increased by 12% ± 32%, 34% ± 38%, and 56% ± 95%, respectively, after sequential osteotomies (Fig. 3).

Changes in lateral bending

Sequential Ponte osteotomies had little effect on lateral bending motion. Mean ROM in lateral bending changed from 7.9° ± 5.7° in intact specimens to 8.1° ± 5.9° after 1 osteotomy, and 8.3° ± 6.0° after the third osteotomy (Table 4). The increase in ROM after a single osteotomy ranged from −0.1° to 0.5°. Compared with intact specimens, lateral bending ROM increased by 2% ± 6% after 3 osteotomies (Fig. 3).

Similar to flexion-extension loading, coupled motions were small during lateral bending loading, with intact coupled motions of 1.0° ± 0.7° in flexion-extension and 1.0° ± 0.5° in axial rotation. After osteotomy, average changes in coupled motions were less than 0.3°.

Changes in axial rotation

Axial rotation ROM increased after each osteotomy: from 10.6° ± 7.2° in intact specimens to 13.8° ± 9.1° after the third sequential osteotomy (p = .04) (Table 5). Each osteotomy increased axial rotation by 0.1° to 2.8°. Compared with intact specimens, axial rotation increased by 34% ± 20% after the third osteotomy (p = .02) (Fig. 3).

Coupled motions during axial rotation loading were small in flexion-extension rotation, with intact coupled flexion-extension of 0.8° ± 0.6°. Coupled lateral bending rotation was larger, with average coupled lateral bending of 2.0° ± 2.4°. After osteotomy, average changes in coupled motions were less than 0.2°.

DISCUSSION

In this study, we quantified increases in thoracic ROM in each plane after sequential Ponte osteotomies. Motion increased in flexion and extension, consistent with original indications for the use of the Ponte osteotomy in patients with kyphotic deformities. Similarly, axial rotation motion increased with each osteotomy; however, sequential osteotomies did not increase lateral bending. Normal cadaveric ROMs in the thoracic spine have been reported for the motion segments evaluated in the present study (T2–T11), with per-level motions ranging from 2° to 14° in flexion-extension, 6° to 20° in lateral bending, and 4° to 24° in axial rotation [28]. Compared with these typical motions, maximum increases in flexion-extension and axial rotation resulting from a single osteotomy in this study provide large increases in motion.

These observations are consistent with positions of the posterior elements and ligaments relative to the neutral plane of the bending moment (Fig. 4). Under bending loads, 1 aspect of the structure lengthens, whereas the opposite shortens (Fig. 4a). The neutral plane, generally at the center, neither lengthens nor shortens; therefore, structures in this plane have no major role in resisting bending. Under extension, the anterior aspect of the spine lengthens, whereas the posterior aspect shortens (Fig. 4b). Under this type of bending, the spinous processes tend to compress toward each other, thereby resisting compression—that is, extension. A Ponte osteotomy profoundly reduces this type of resistance, increasing ROM in extension. On the other hand, in lateral bending, the spinous processes and interspinous and supraspinous ligaments are in the neutral plane, and therefore do not resist lateral bending (Fig. 4c). Consequently, a Ponte osteotomy should have a smaller effect on ROM in lateral bending, consistent with the results of the present study.

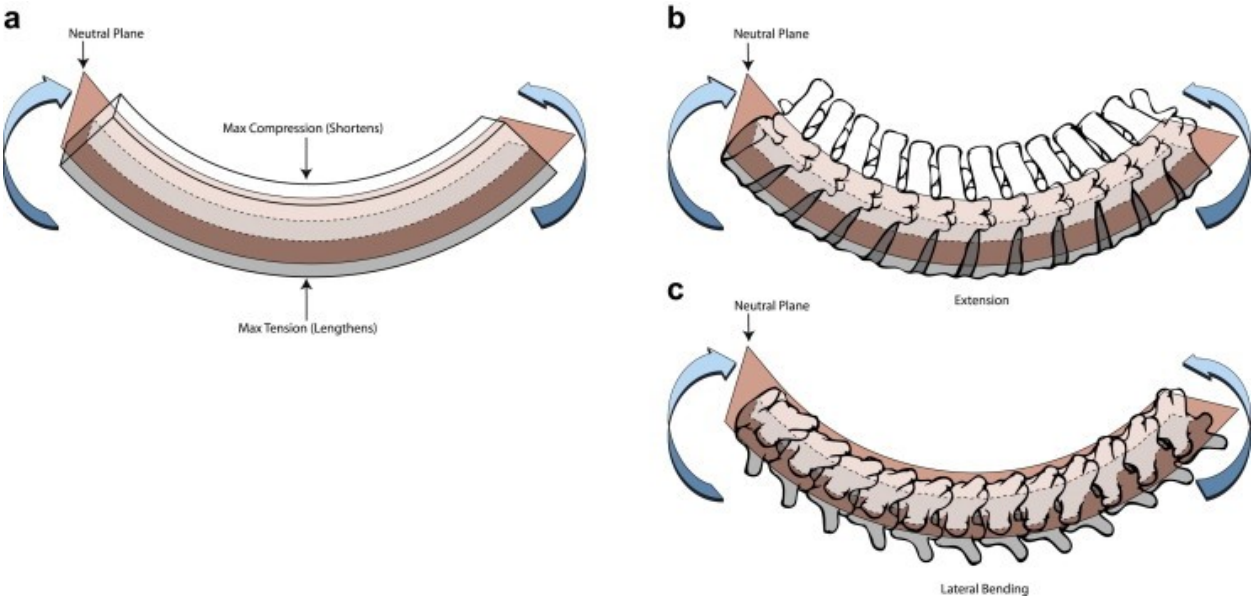

Fig. 4

Schematic diagram of (a) beam under bending depicting the surface of maximum tension, which lengthens under bending, surface of maximum compression, which shortens under bending, and the neutral plane in the center, which neither lengthens or shortens under bending in this plane; (b) a spine segment under bending to produce extension, showing that the spinous processes are undergoing maximum compression as the anterior column experiences maximum tension; and (c) a spine segment under bending to produce lateral bending, showing that the spinous processes and interspinous ligament are positioned within the neutral plane, and therefore do not have a major role in resisting bending.

Clinical studies have reported 5° to 15° of sagittal correction (ie, flexion-extension) per level of Ponte osteotomy [[3], [12]]. The maximum increase in flexion-extension motion for a given osteotomy in this study was 2.6°, lower than the clinical reports. Separating flexion and extension, a single osteotomy resulted in maximum increases of 1.6° in flexion and 1.5° in extension. The cited clinical studies report correction after both the application of large correctional forces and torques and the insertion of instrumentation during surgery. In contrast, the present study applied pure moment loading, which may be lower than forces applied during surgery. In addition, we used no instrumentation, which may explain the discrepancies in the findings.

Previous studies have investigated posterior destabilization techniques; however, results are difficult to compare because of differences in specimen type, loading protocol, and data presentation (Table 6) [[18], [19], [20], [21], [22]]. In addition, studies of posterior techniques have been limited to single-level surgeries, with the exception of the article by Horton et al. [20]. Those authors performed 4 non-sequential, total facetectomies, and reported findings similar to the present study in flexion-extension; however, they did not measure lateral bending and axial rotation. The most comparable investigation to the current study was that performed by Oda et al. [18], which entailed removal of all posterior elements in a canine thoracic model. Those authors reported higher increases in flexion-extension ROM; nevertheless, the normal ROM for canine specimens, as well as compared with human thoracic spines, remains unknown.

Table 6 Comparison of Results to the Literature.

Author, Year	Segment	Surgical Release (# of Levels)	Applied Load or Motion			Increase in ROM (degrees)			Increase in ROM (%)		
			FE	LB	AR (Preload)	FE	LB	AR	FE	LB	AR
Present Study	T2–T5; T8–T11	Ponte Osteotomy (3)	±6 Nm	±6 Nm	±6 Nm	2.8	0.3	3.3	54%	2%	34%
Present Study	Single Level	Ponte Osteotomy	±6 Nm	±6 Nm	±6 Nm	0.9	0.1	1.1			
Feiertag, 1995	T2–T10	Unilateral Total Facetectomy (l)	89 N	89 N		0.22°	0.45°		−1%	0%	
Oda, 1996	T6–T7	Removal of Posterior Elements	±0.45 Nm	±0.45 Nm	±0.45 Nm	3.8°	0.6°	0.8°			
Oda, 2002	Thoracic FSUs	Laminectomy + Total Facetectomy	±2 Nm	±2 Nm	±2 Nm (100 N)				38%	37%	45%
Horron, 2005	C7-L1	Total Facetectomy (4)	25 N			2.5°			13%		
Anderson, 2009	Thoracic FSUs	Removal of Posterior Structures	±2.8°						68%		

Abbreviations: FE (Flexion-Extension); LB (Lateral Bending); AR (Axial Rotation).

*Supraspinous and interspinous ligament, bilateral facet joints, ligamentum flavum resected.

**Bilateral supratransverse process hook and bilateral supralaminar hook site preparations, bilateral pedicle screw placement and removal, supraspinous and interspinous ligament resection, and removal of all remaining posterior structures.

Oda et al. [19] and Anderson et al. [22] performed similar surgical procedures on functional human spinal units, and reported higher increases in ROM compared with the current study. However, neither study reported motion in degrees, which makes it difficult to put the percent-increase values into a context for comparison. Throughout the literature, there is a need to report not only percent increase in ROM compared with the intact condition, but also the raw data in degrees. This would provide a more consistent measure across different studies.

The Ponte osteotomy was originally described as a means to improve kyphotic deformity, but some surgeons have found it to be even better at improving the apical lordosis present in adolescent idiopathic scoliosis. The present study measured increases in flexion of up to 1.6° per level of osteotomy. Overall flexibility increased by 69% ± 39% compared with the intact state after 3 sequential osteotomies ($p = .02$). This large increase is consistent with previous clinical observations.

With the success and technological advancement of pedicle-based instrumentation systems, derotation has become an increasingly popular technique to treat scoliosis deformity [[4], [5], [6], [7], [8], [29]]. The techniques of derotation apply axially directed forces to the spine, which in the current model corresponds with axial rotation. Each sequential osteotomy provided significant increases in axial rotation compared with the intact condition ($p < .05$; Fig. 3), with a maximum increase of 2.8° for a given osteotomy. Because the Ponte osteotomy is a posterior-only approach and bypasses the difficulties associated with anterior procedures, this may be an attractive option whenever derotational techniques are used during scoliosis surgery.

One assumption in the present study is that the increase in ROM after each Ponte osteotomy in a cadaveric spine is correlated with the amount of deformity correction attainable during surgery [[30], [31]]. This assumption has been used throughout the biomechanical literature studying destabilization procedures in cadaveric spines followed by simulated loading. In contrast, during surgery, surgeons manually apply these forces and torques to the spine using instrumentation and hardware after

destabilization procedures. Few studies have investigated the forces and torques applied using instrumentation during surgery [[32], [33]]. Therefore, it is difficult to compare loads applied during surgery to those applied in vitro. The load applied in the present study, 6 Nm in each plane, exceeded previously applied cadaveric thoracic spine moments (approximately 2–4 Nm) [[16], [19], [34]]. Still, higher loads may be applied during surgery.

This study quantifies the percent amount of increased spinal flexibility that is achieved with multiple Ponte osteotomies in a cadaver model. Care must be taken in extrapolating these data to the clinical situation. Patients with idiopathic scoliosis undergoing posterior instrumented spinal fusion present with varied curve severity and rigidity in all 3 planes. Thus, the surgical indication to perform concomitant Ponte osteotomies, and the optimal number of Ponte osteotomies, will be patient specific. Further clinical studies are necessary to address this question. There is little knowledge about the indications for and extent of Ponte osteotomies in pediatric scoliosis surgery. Halanski and Cassidy [35] recently published their experience of routine Ponte osteotomies in 18 patients compared with 19 patients with facetectomies alone undergoing posterior instrumented spinal fusion. In the osteotomy group, osteotomies were performed in 76% of instrumented levels. They found no difference in postoperative sagittal and coronal correction between groups. The curve magnitude in the osteotomy group was 59° ± 10°, which may be too small to show an effect with Ponte osteotomies. It is possible that Ponte osteotomies may have their greatest impact on intraoperative correction in stiff, severe curves.

It is difficult, if not impossible, to obtain pediatric cadaver specimens, let alone donors with untreated scoliosis; consequently, specimens in the present study were from adults with relatively normal alignment, or slight curvatures resulting from degenerative scoliosis. Because of poor bone quality and degenerative changes typical of elderly willed body donors, specimens in the current study were not as flexible as pediatric spines may be after surgical releases. Regardless, no alternatives are available for biomechanical testing. Therefore, data from this model may provide low estimates of correction potential,

which may be exceeded in surgery where larger forces and torques are applied to younger patients. In addition, because of the reliance on elderly donors experiencing various stages of degeneration, the intact stiffness of the specimens in the present study varied widely, which resulted in large standard deviations, an inherent limitation of cadaveric testing. The standard deviations are similar to those found in previous thoracic spine posterior release biomechanics studies [[18], [22]]. Future studies should investigate methods for normalizing biomechanical data based on the level of specimen quality and degeneration, to help make stronger conclusions. Despite these limitations, the trends suggest the correction potential of Ponte osteotomies in adolescent idiopathic scoliosis correction.

CONCLUSION

Sequential Ponte osteotomies increased thoracic ROM in flexion-extension and axial rotation, but had little effect on lateral bending. These findings are consistent with the indicated use of Ponte osteotomies for kyphosis. The increases in axial rotation may provide useful data for surgical planning of scoliosis when derotational techniques are considered. In addition, Ponte osteotomies may be useful in correcting apical lordosis.

REFERENCES

1. Asher, M.A. and Burton, D.C. Adolescent idiopathic scoliosis: natural history and long term treatment effects.*Scoliosis*. 2006; 1: 2

2. Howden LM, Meyer JA. Age and sex composition: 2010. 2010 Census Briefs 2011. Available at:http://www.census.gov/prod/cen2010/briefs/c2010br-03.pdf. Accessed January 30, 2013.

3. Geck, M.J., Macagno, A., Ponte, A., and Shufflebarger, H.L. The Ponte procedure: posterior only treatment of Scheuermann's kyphosis using segmental posterior shortening and pedicle screw instrumentation. *J Spinal Disord Tech*. 2007; 20: 586–593

4. Diab, M.G., Franzone, J.M., and Vitale, M.G. The role of posterior spinal osteotomies in pediatric spinal deformity surgery: indications and operative technique. *J Pediatr Orthop*. 2011; 31: S88–S98

5. Kim, Y.J., Lenke, L.G., Kim, J. et al. Comparative analysis of pedicle screw versus hybrid instrumentation in posterior spinal fusion of adolescent idiopathic scoliosis. *Spine (Phila Pa 1976)*. 2006; 31: 291–298

6. Suk, S.I., Kim, W.J., Lee, S.M. et al. Thoracic pedicle screw fixation in spinal deformities: are they really safe?.*Spine (Phila Pa 1976)*. 2001; 26: 2049–2057

7. Suk, S.I., Lee, C.K., Kim, W.J. et al. Segmental pedicle screw fixation in the treatment of thoracic idiopathic scoliosis. *Spine (Phila Pa 1976)*. 1995; 20: 1399–1405

8. Lehman, R.A. Jr., Lenke, L.G., Keler, K.A. et al. Operative treatment of adolescent idiopathic scoliosis with posterior pedicle screw-only constructs: minimum three-year follow-up of one hundred fourteen cases. *Spine (Phila Pa 1976)*. 2008; 33: 1598–1604

9. Ponte, A., Vero, B., and Siccardi, G. Surgical treatment of Scheuermann's hyperkyphosis. in: R. Winter (Ed.)Progress in Spinal Pathology: Kyphosis. Aulo Gaggi, Bologna, Italy; 1984: 75–80

10. Ponte, A. Posterior column shortening for Scheuermann's kyphosis. in: T. Haher, A. Merola (Eds.) Surgical Techniques for the Spine. Thieme Verlag, New York; 2003: 107–113

11. Smith-Petersen, M.N., Larson, C.B., and Aufranc, O.E. Osteotomy of the spine for correction of flexion deformity in rheumatoid arthritis. *J Bone Joint Surg Am*. 1945; 27: 1–11

12. Cho, K.J., Bridwell, K.H., Lenke, L.G. et al. Comparison of Smith-Petersen versus pedicle subtraction osteotomy for the correction of fixed sagittal imbalance. *Spine*. 2005; 30: 2030–2037 (discussion 2038)

13. White, A.A. III and Hirsch, C. The significance of the vertebral posterior elements in the mechanics of the thoracic spine. *Clin Orthop Relat Res*. 1971; 81: 2–14

14. Panjabi, M.M., Hausfeld, J.N., and White, A.A. III. A biomechanical study of the ligamentous stability of the thoracic spine in man. *Acta Orthop Scand*. 1981; 52: 315–326

15. Takeuchi, T., Abumi, K., Shono, Y. et al. Biomechanical role of the intervertebral disc and costovertebral joint in stability of the thoracic spine: a canine model study. *Spine*. 1999; 24: 1414–1420

16. Watkins, R. IV, Watkins, R. III, Williams, L. et al. Stability provided by the sternum and rib cage in the thoracic spine.*Spine*. 2005; 30: 1283–1286

17. Yoganandan, N., Maiman, D.J., Pintar, F.A. et al. Biomechanical effects of laminectomy on thoracic spine stability.*Neurosurgery*. 1993; 32: 604–610

18. Oda, I., Abumi, K., Lü et al. Biomechanical role of the posterior elements, costovertebral joints, and rib cage in the stability of the thoracic spine. *Spine*. 1996; 21: 1423–1429

19. Oda, I., Abumi, K., Cunningham, B.W. et al. An in vitro human cadaveric study investigating the biomechanical properties of the thoracic spine. *Spine*. 2002; 27: E64–E70

20. Horton, W.C., Kraiwattanapong, C., Akamaru, T. et al. The role of the sternum, costosternal articulations, intervertebral disc, and facets in thoracic sagittal plane biomechanics: a comparison of three different sequences of surgical release. *Spine*. 2005; 30: 2014–2023

21. Feiertag, M.A., Horton, W.C., Norman, J.T. et al. The effect of different surgical releases on thoracic spinal motion: a cadaveric study. *Spine*. 1995; 20: 1604–1611

22. Anderson, A.L., McIff, T.E., Asher, M.A. et al. The effect of posterior thoracic spine anatomical structures on motion segment flexion stiffness. *Spine*. 2009; 34: 441–446

23. Wilke, H.J., Jungkunz, B., Wenger, K. et al. Spinal segment range of motion as a function of in vitro test conditions: effects of exposure period, accumulated cycles, angular-deformation rate, and moisture condition. *Anat Rec*.1998; 251: 15–19

24. Sangiorgio, S.N., Sheikh, H., Borkowski, S.L. et al. Comparison of three posterior dynamic stabilization devices.*Spine (Phila Pa 1976)*. 2011; 36: E1251–E1258

25. Wilke, H.J., Wenger, K., and Claes, L. Testing criteria for spinal implants: recommendations for the standardization of in vitro stability testing of spinal implants. *Eur Spine J*. 1998; 7: 148–154

26. Crawford, N.R. and Dickman, C.A. Construction of local vertebral coordinate systems using a digitizing probe: technical note. *Spine (Phila Pa 1976)*. 1997; 22: 559–563

27. White, A.A. and Panjabi, M.M. Clinical Biomechanics of the Spine. 1st ed. JB Lippincott, Philadelphia; 1978

28. Lee, S.M., Suk, S.I., and Chung, E.R. Direct vertebral rotation: A new technique of three-dimensional deformity correction with segmental pedicle screw fixation in adolescent idiopathic scoliosis. *Spine (Phila Pa 1976)*. 2004;29: 343–349

29. Ashman, R.B., Birch, J.G., Bone, L.B. et al. Mechanical testing of spinal instrumentation. *Clin Orthop Relat Res*.1988; 227: 113–125

30. Ashman, R.B., bechtold, J., Edwads, WT. et al. In vitro spinal arthrodesis implant mechanical testing protocols.*J Spinal Disord*. 1989; 2: 274–281

31. Wiemann, J., Durrani, S., and Bosch, P. The effect of posterior spinal releases on axial correction torque: a cadaver study. *J Child Orthop*. 2011; 5: 109–113

32. Busscher, I., va der Veen, A.J., van Dieën, J.H. et al. In vitro biomechanical characteristics of the spine: a comparison between human and porcine spinal segments. *Spine (Phila Pa 1976)*. 2010; 35: E35–E42

33. Halanski MA, Cassidy JA. Do multilevel Ponte osteotomies in thoracic idiopathic scoliosis surgery improve curve correction and restore thoracic kyphosis? *J Spinal Disord Tech* In press (2011 Epub ahead of print).

Author disclosures: SNS (grants from President's Circle, and Doctor's Education and Research Fund; grants from NIH, and Amgen); SLB (none); RB (grants from President's Circle, Doctor's Education and Research Fund, employment with Orthopaedic Hospital, expert testimony for the Hardison Law Firm); AS (grants from President's Circle, Doctor's Education and Research Fund); NF (grants from President's Circle, Doctor's Education and Research Fund); EE (employment with UCLA, USC; grants from NIH, NIBIB).

5.2 Flexibility of Thoracic Spines Under Simultaneous Multi-Planar Loading[250]

European Spine Journal

10.1007/s00586-014-3499-0

Original Article

Flexibility of thoracic spines under simultaneous multi-planar loading

Sean L. Borkowski[1, 3], Sophia N. Sangiorgio[1, 2], Richard E. Bowen[1, 2], Anthony A. Scaduto[1, 2], Juliann Kwak[1, 2] and Edward Ebramzadeh[1, 2]

(1) J. Vernon Luck, Sr., M.D. Orthopaedic Research Center, Orthopaedic Institute for Children, 403 W. Adams Blvd., Los Angeles, CA 90007, USA

(2) Department of Orthopaedic Surgery, University of California, Los Angeles, USA

(3) Department of Biomedical Engineering, University of California, Los Angeles, USA

Received: 10 December 2013Revised: 28 July 2014Accepted: 29 July 2014Published online: 5 August 2014

ABSTRACT

Purpose

The corrective potential of two posterior-only destabilization procedures for scoliosis deformity was quantified under single and multi-planar loading using cadaveric spines.

Methods

Ten full-length human cadaveric thoracic spines were mounted in an 8-df servohydraulic load frame. Cyclic, pure moments were applied in: (1) flexion–extension, (2) lateral bending, (3) axial rotation, (4) flexion–extension with axial rotation, and (5) lateral bending with axial rotation at 0.5°/s, to ±4 Nm. Each specimen was tested intact, and again after nine en bloc bilateral total facetectomies, and one, two, three,

and four levels of Ponte osteotomies. Motion was measured throughout loading using optical motion tracking.

Results

Under single-plane loading, facetectomies and Ponte osteotomies increased thoracic spine flexibility in all three planes. Compared to total facetectomies, higher per-level increases were seen following Ponte osteotomies, with increases in total range of motion (total ROM) of up to 2.7° in flexion–extension, 1.4° in lateral bending, and 3.1° in axial rotation following each osteotomy. Compared to the facetectomies, four supplemental osteotomies increased total ROM by 23 % in flexion ($p < 0.01$) and 8 % in axial rotation ($p < 0.01$). Increases in lateral bending were smaller. Under multi-planar loading, each Ponte osteotomy provided simultaneous increases of up to 1.4°, 1.6°, and 2.2° in flexion–extension, lateral bending, and axial rotation.

Conclusions

Ponte osteotomies provided higher per-level increases in ROM under single-plane loading than total facetectomies alone. Further, Ponte osteotomies provided simultaneous increase in all three planes under multi-planar loading. These results indicated that, to predict the correction potential of a surgical release, multi-planar testing may be necessary.

Electronic supplementary material

The online version of this article (doi:10.1007/s00586-014-3499-0) contains supplementary material, which is available to authorized users.

Keywords

Biomechanics – Range of motion – Scoliosis – Simultaneous loading

INTRODUCTION

Recently, several studies have reported the clinical outcome of posterior-only approaches for the correction of adolescent idiopathic scoliosis (AIS) [*1*–*5*]. The Ponte osteotomy, originally described for correction of Scheuermann's kyphosis [*2*], is one such posterior-only procedure used for cases of AIS [*6*]. Despite some favorable clinical outcomes using these osteotomies and similar wide posterior releases [*6*–*10*], there is no consensus on using these for coronal plane correction or to supplement the routinely used total facetectomies [*10*]. Additionally, it is difficult to assess the potential of these procedures, as no prospective clinical studies have been performed. Moreover, the amount of correction following each supplemental osteotomy has not been quantified. Unfortunately, these issues have not been studied systematically in previous investigations of posterior-only surgical techniques using cadaveric models [*11*–*16*].

The majority of biomechanical studies which have tested surgical releases have followed the same general protocol for in vitro spine testing: pure moments applied independently in single planes to intact specimens, and again after sequential release [*14*, *16*]. The underlying assumption is that the increase in motion observed following release correlates to the amount of deformity correction achievable in surgery. However, this process assumes that both the deformity and the correction of the deformity occur in one plane, when in actuality these often occur three dimensionally.

In addition, many studies have used functional spine units (FSUs) [*11*, *14*–*16*], analyzing one operative level only, which ignores the contribution of the rest of the thoracic spine. Clinically, in posterior-only surgery for AIS cases, total facetectomies are performed, en bloc, on all instrumented levels of the spine. Supplemental osteotomies are then performed at specific levels to provide additional needed flexibility for correction. Clearly, the contribution of such supplemental releases cannot be compared to en bloc total facetectomies using an FSU model.

The purpose of this study was to apply a novel multi-planar testing protocol to cadaveric thoracic spines to quantify the increase in flexibility following two posterior-only surgical releases: (1) bilateral total

facetectomies and (2) sequential Ponte osteotomies. These increases may provide an indication of the deformity correction potential using each release.

METHODS

Specimen preparation and loading protocol

Ten fresh-frozen human cadaveric thoracic spines (T1–T12) were obtained (IIAM, Jessup, PA, USA). Specimens were dissected, leaving vertebrae, discs, stabilizing ligaments, and the posterior 5 cm of the ribs, with the costovertebral joints intact, as done previously [*14*, *15*, *17*]. High-resolution radiographs and DEXA scans (Hologic, Inc., Bedford, MA, USA) were taken to assess initial specimen conditions and to exclude those with gross abnormalities or poor bone health.

Specimens were loaded in an 8-df MTS 858 mini-bionix servohydraulic load frame equipped with the Flextest System (MTS Systems Corporation, Eden Prairie, MN, USA) in an inverted position (Fig. 1). The lower gimbals were mounted on an x–z table, equipped with two perpendicular linear bearings allowing translation in the transverse plane, while the upper gimbals were fixed to the actuator. All components of the loads and moments (F_x, F_y, F_z, M_x, M_y, M_z) were monitored to ensure that no load or moment was placed on the spine specimens (ATI Industrial Automation, Apex, NC, USA).

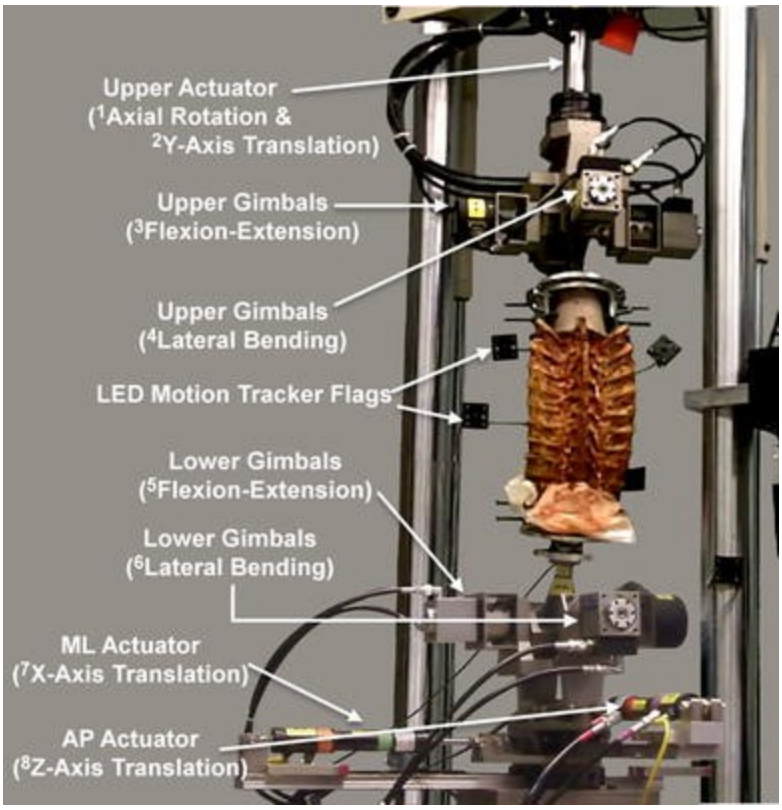

Fig. 1

Representative photo of the experimental setup and the 8-dof spine simulator. The degrees of freedom are denoted by the superscripts 1–8

Pure cyclic moments were applied using a combination of position and torque control to produce bending at a rate of 0.5 °/s to ± 4 Nm. The applied moments are within the range of magnitudes applied throughout the literature in the thoracic spine [*18*–*21*]. For each test, five cycles of bending were applied, with data from the third cycle used for analysis [*21*]. The specimens were first tested in the following single-plane loading directions: flexion–extension, bilateral lateral bending, and bidirectional axial rotation. As the present study aimed to analyze the flexibility of the spine following surgical releases that would be performed intraoperatively with a patient lying prone, no axial preload was applied. Single-plane loading results were used to determine the flexibility in each plane (coronal, sagittal, and transverse).

Following single-plane loading, specimens were tested in two multi-planar loading conditions: (1) combined axial rotation and flexion–extension, and (2) combined axial rotation and lateral bending (Electronic Supplementary Material).

Range of motion (ROM) was recorded throughout testing using an Optotrak 3020 motion tracking system (Northern Digital, Inc., Waterloo, ON, Canada). The motion capture system has an accuracy of 0.1 mm and 0.1°, and a resolution of 0.01 mm. The accuracy and precision of this machine has been independently validated [*22*]. Motion flags, equipped with four non-collinear light-emitting diode (LED) markers, were attached via bone screws to the T2, T6, T10, and T11 vertebral bodies, alternately on the left and right, to characterize motion of the spine (T2–T11). Additionally, one flag was mounted on the load frame to establish a fixed coordinate axis and to minimize the effects of any vibrations of the machine. Planes of motion for each of the instrumented vertebra were aligned using tri-planar lasers and a digitizing probe. Total ROM across the segment (T2–T11) was recorded as the motion of T2 with respect to T11. Segmental ROM from T6 to T10 (T6–T10 ROM) was recorded as the motion of T6 with respect to T10. All ROM measurements were calculated as the relative motions of the superior vertebra with respect to the inferior vertebra, and were based solely on the motion tracker markers/flags [*21*]. These relative motions were reported as Euler angles [*21*]. Due to differences in initial specimen flexibility, the data were normalized by calculating the percent increase in total ROM following each destabilization, as compared to the intact condition. Both raw total ROM and normalized total ROM are reported. In addition, as the majority of previous thoracic spine studies did not measure T2–T11 motion or T6–T10 motion, in the present study intact T10–T11 ROM was calculated to provide a direct comparison with previous studies (Electronic Supplementary Material). These measurements pertain to the intact spine prior to any surgical releases.

The loading protocol and measurements were repeated for each specimen under the following six conditions: (1) intact; (2) following bilateral total facetectomies between T2 and T11; and following Ponte osteotomy at (3) T7–T8; (4) T8–T9; (5) T6–T7; and (6) T9–T10.

Destabilization procedures

Following intact testing, sequential posterior-only surgical releases were performed to destabilize the spines. Nine en bloc bilateral total facetectomies were first performed from T2 to T11 (Fig. 2a). Each facetectomy included the bilateral removal of the inferior facet of the superior vertebra (Fig. 2c) [*4*]. After bilateral total facetectomies and testing, sequential Ponte osteotomies were performed to further destabilize the spine (Fig. 2b). For each Ponte osteotomy, in addition to the bilateral total facetectomy, resection of the following was performed: the inferior half of the spinous process of the vertebra superior to the osteotomy site, the interspinous ligament, and the ligamentum flavum (Fig. 2d) [*2*].

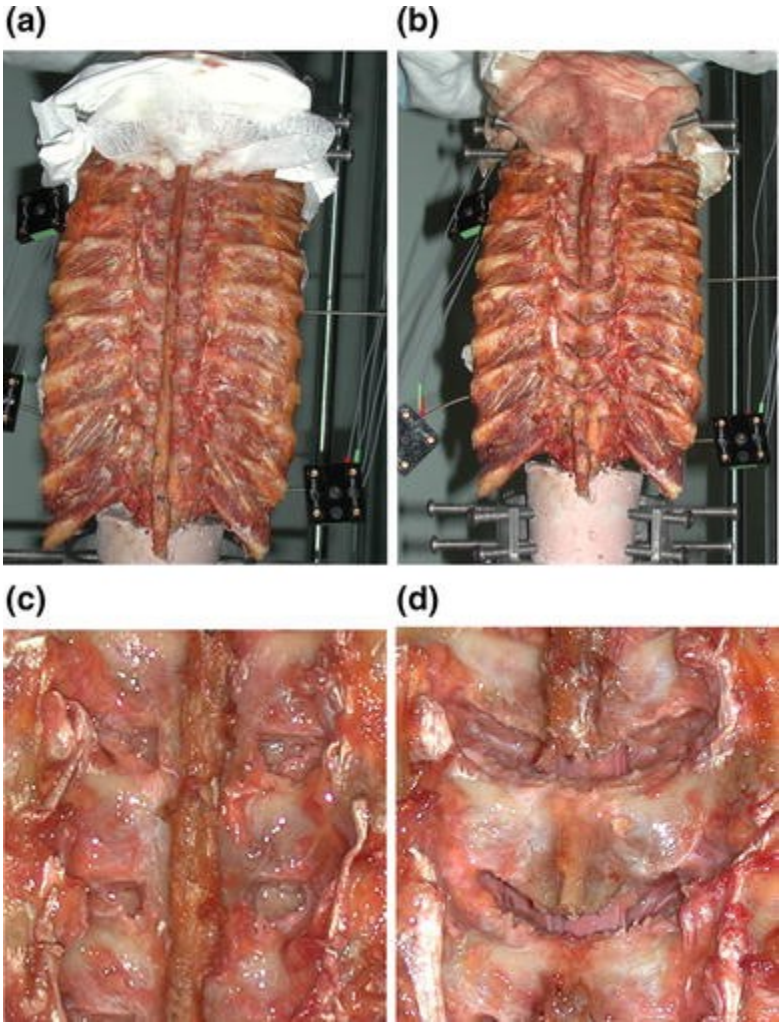

Fig. 2

a Full thoracic spine following nine en bloc bilateral total facetectomies from T2 to T11; **b** full thoracic spine following four sequential Ponte osteotomies from T6 to T10; **c** close-up of two example bilateral total facetectomies; **d** close-up of two example Ponte osteotomies

Statistical analysis

Normal distribution of the data was assured using the Shapiro–Wilk tests, followed by normal Q–Q plots. A multivariate general linear model was constructed to determine the relative effect of each input variable on the outcome variables, using SPSS 15.0 statistical analysis software (SPSS, Inc., Chicago, IL, USA). The input variables were specimen condition, destabilization, and loading direction. The primary outcome

variables were (1) total ROM between T2 and T11 in all three planes during single-plane loading, (2) T6–T10 ROM in all three planes during single-plane loading, and (3) total ROM between T2 and T11 in all three planes during multi-planar loading.

RESULTS

Altogether, ten specimens were tested under single-plane and multi-planar loading, intact and after each destabilization. The first specimen was tested on multiple days, with several freeze–thaw cycles, and consequently excluded from the analysis. The remaining nine specimens were all tested without incidence and were included for analysis.

Single-plane total range of motion (total ROM)

Flexion and extension were analyzed separately, due to asymmetrical anatomy in the anterior and posterior columns of the spine. In flexion, total ROM increased following each destabilization (Table 1). Bilateral total facetectomies increased total ROM by as much as 1.6°, while each osteotomy increased total ROM by up to 1.8°. Overall, total flexion ROM increased by 3 ± 8 % following facetectomies ($p = 0.58$) and 26 ± 19 % following 4 sequential osteotomies ($p < 0.01$, Fig. 3).

Table 1
Single-plane range of motion (T2–T11)

Loading direction	Measure	Intact	Facetectomies	1-level Ponte	2-level Ponte	3-level Ponte	4-level Ponte
Flexion	Mean (SD)	11.3 (5.8)	11.8 (6.2)	12.6 (6.6)	13.2 (6.9)	13.7 (7.2)	14.1 (7.5)
	Range	0.7–18.7	0.7–20.0	0.9–21.5	0.9–22.5	0.9–23.3	0.9–24.1
Extension	Mean (SD)	10.2 (6.6)	11.9 (8.1)	12.2 (8.5)	12.5 (8.9)	13.1 (9.6)	13.2 (9.8)
	Range	0.8–21.6	0.7–26.3	0.7–26.3	0.6–28.1	0.6–30.1	0.7–31.0
Lateral bending	Mean (SD)	28.5 (13.4)	30.2 (14.3)	30.7 (14.6)	31.1 (14.9)	31.0 (15.0)	31.2 (15.2)
	Range	3.5–43.2	3.6–45.7	3.7–47.1	3.7–48.0	3.8–48.2	3.8–48.9
Axial rotation	Mean (SD)	36.4 (15.3)	39.9 (17.1)	40.7 (17.4)	41.5 (17.9)	42.3 (18.4)	42.8 (18.6)
	Range	5.3–53.0	5.6–57.4	6.0–58.1	6.1–59.2	6.2–61.0	6.3–62.4

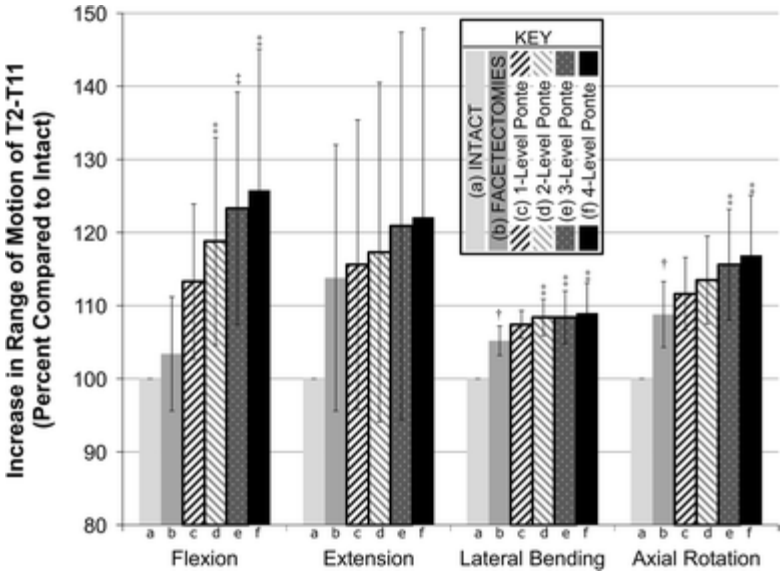

Fig. 3
% Increase in total T2–T11 range of motion (ROM), compared to the intact total ROM, following each sequential posterior release. †Bilateral total facetectomies compared to intact ($p < 0.05$). ‡Ponte osteotomies compared to bilateral total facetectomies ($p < 0.05$)

In extension, total ROM increased from 10.2° ± 6.6° intact to 11.9° ± 8.1° following total facetectomies (Table 1). Each sequential osteotomy provided additional increases, with total ROM increasing to 13.2° ± 9.8° following the fourth osteotomy. The maximum increase in total ROM was 8.3° following facetectomies and up to 2.0° following a single osteotomy. Overall, compared to intact, total extension ROM increased by 14 ± 18 % following facetectomies ($p = 0.17$) and by 22 ± 26 % following the fourth osteotomy ($p = 0.03$, Fig. 3).

Smaller increases in total ROM were seen in lateral bending compared to flexion, extension, or axial rotation (Table 1). The total ROM increase ranged from 0° to 3.2° following total facetectomies and from 0° to 1.4° following a single osteotomy. Compared to intact, total lateral bending ROM increased by 5 ± 2 % following total facetectomies ($p < 0.01$) and by only 9 ± 4 % following four sequential Ponte osteotomies ($p < 0.01$, Fig. 3).

Axial rotation total ROM increased following each destabilization procedure, increasing from 36.4° ± 15.3° intact, to 39.9° ± 17.1° following facetectomies, and further increased to 42.8° ± 18.6° following four sequential Ponte osteotomies (Table 1). Total ROM increases ranged from 0° to 8.1° following total facetectomies and from 0° to 3.1° following each single osteotomy. Compared to intact, total axial rotation ROM increased by 9 ± 5 % following total facetectomies ($p < 0.01$) and by 17 ± 8 % following sequential Ponte osteotomies ($p < 0.01$, Fig. 3). (It should be noted that while, on average, surgical releases always increased flexibility, the standard deviations suggest the possibility of decrease in flexibility due to inherent assumptions in the calculation of standard deviation around the mean.)

Single-plane T6–T10 range of motion (T6–T10 ROM)

In flexion–extension, T6–T10 ROM increased by an average of 0.6° ± 0.7° following four bilateral total facetectomies, compared to the intact condition ($p = 0.05$). Following four sequential Ponte osteotomies, T6–T10 flexion–extension ROM increased by an additional 2.2° ± 1.7° ($p < 0.01$).

In lateral bending, increases in T6–T10 ROM following posterior releases were smaller than those in flexion–extension or axial rotation. Specifically, T6–T10 lateral bending ROM increased an average of 0.2° ± 0.5° following the facetectomies ($p = 0.22$) and by an additional 0.2° ± 0.6° following the four sequential Ponte osteotomies ($p = 0.32$).

Finally, in axial rotation, T6–T10 ROM increased by an average of 1.0° ± 1.3° following four bilateral total facetectomies, compared to the intact condition ($p = 0.06$). Following four sequential Ponte osteotomies, T6–T10 axial rotation ROM increased by an additional 1.5° ± 1.7° ($p = 0.03$).

Multi-planar motions

Under multi-planar loading, the maximum increases in total ROM were larger following the nine-level en bloc total facetectomies; however, similar to the single-plane results, each Ponte osteotomy provided additional three-dimensional increases in motion.

Specifically, under combined flexion–extension with axial rotation, total facetectomies increased total ROM simultaneously up to 5.2° in flexion–extension, 2.4° in lateral bending, and 5.4° in axial rotation. Each osteotomy provided a maximum simultaneous increase in total ROM of 1.4° in flexion–extension, 1.3° in lateral bending, and 2.2° in axial rotation (Table 2).

Table 2
Multi-planar motions—axial rotation with flexion–extension: difference in ROM following each sequential release (T2–T11)

	Flexion–extension (°)		**Lateral bending (°)**		**Axial rotation (°)**	
	Mean (SD)	**Range**	**Mean (SD)**	**Range**	**Mean (SD)**	**Range**
Facetectomies–intact	1.8 (1.6)	0.1 to 5.2	1.0 (0.7)	−0.1 to 2.4	2.7 (1.9)	0.1 to 5.4
Ponte 1–facetectomies	0.4 (0.4)	−0.2 to 0.9	0.3 (0.3)	−0.2 to 1.0	0.7 (0.4)	0.1 to 1.1
Ponte 2–Ponte 1	0.4 (0.4)	−0.3 to 0.9	0.3 (0.4)	0.0 to 1.2	0.6 (0.5)	−0.1 to 1.4
Ponte 3–Ponte 2	0.3 (0.5)	–0.3 to 1.4	0.3 (0.4)	0.0 to 1.3	0.6 (0.8)	−0.1 to 2.2
Ponte 4–Ponte 3	0.1 (0.4)	−0.5 to 0.7	0.1 (0.3)	−0.1 to 0.6	0.2 (0.2)	−0.1 to 0.7

Under multi-planar loading combining lateral bending with axial rotation, the total facetectomies provided simultaneous increases in total ROM of up to 2.7° in flexion–extension, 2.7° in lateral bending, and 4.5° in axial rotation. In comparison, a single osteotomy provided simultaneous increases in total ROM of up to 0.4° in flexion–extension, 1.6° in lateral bending, and 2.1° in axial rotation (Table 3).

Table 3
Multi-planar motions—axial rotation with lateral bending: difference in ROM following each sequential release (T2–T11)

	Flexion–extension (°)		Lateral bending (°)		Axial rotation (°)	
	Mean (SD)	**Range**	**Mean (SD)**	**Range**	**Mean (SD)**	**Range**
Facetectomies–intact	0.5 (1.1)	−0.6 to 2.7	0.9 (0.9)	−0.2 to 2.7	1.3 (1.7)	−0.7 to 4.5
Ponte 1–facetectomies	−0.2 (0.4)	−1.0 to 0.4	0.3 (0.7)	−1.1 to 1.2	0.5 (0.7)	−0.2 to 2.1
Ponte 2–Ponte 1	0.1 (0.1)	−0.1 to 0.4	0.3 (0.6)	−0.3 to 1.6	0.3 (0.5)	−0.4 to 1.2
Ponte 3–Ponte 2	−0.1 (0.3)	−0.9 to 0.2	0.0 (0.5)	−0.8 to 0.6	0.0 (0.5)	−1.0 to 0.5
Ponte 4–Ponte 3	−0.1 (0.3)	−0.8 to 0.4	0.2 (0.6)	−0.4 to 1.5	0.1 (0.5)	−0.3 to 1.1

DISCUSSION

Single-plane and simultaneous multi-planar increases in thoracic spine total ROM following sequential posterior-only surgical releases were analyzed. Both en bloc bilateral total facetectomies and sequential Ponte osteotomies provided increases in all three planes. Moreover, both facetectomies and Ponte osteotomies provided simultaneous increases in total ROM under multi-planar loading.

Clinical studies have reported 5–15° of correction per level using Ponte osteotomies [*2*, *23*]. However, previous biomechanical studies have had trouble supporting this. One previous study [*17*] tested hemi-thoracic cadaveric segments under pure moments, intact and after three sequential Ponte osteotomies and, similar to the present study, reported maximum increases of up to 1.6° in flexion, 1.5° in extension, and 2.8° in axial rotation after each osteotomy, with little effect on lateral bending. These similarities demonstrate the repeatability in pure moment testing, regardless of specimen length. However, AIS is a complex three-dimensional deformity that combines sagittal, coronal, and transverse plane deformities [*24*]. Therefore, the multi-planar testing performed in the present study was intended to address this

complexity. Simultaneous maximum increases of 5.2°, 2.7°, and 5.4° in flexion–extension, lateral bending, and axial rotation following facetectomies, and additional simultaneous increases of 1.4°, 1.6°, and 2.2° following each osteotomy, suggested the potential to simultaneously increase flexibility in three dimensions. These results indicated that, to predict the correction potential of a surgical release, multi-planar testing may be necessary in preclinical studies.

Despite the fact that multi-planar loading of full thoracic spines was employed in the present study, the increases in range of motion were still below the clinically reported correction potential of 5–15° per osteotomy [*2*, *23*]. These discrepancies may be, in part, due to the fact that in the present study, and similar to numerous previous preclinical studies, the magnitudes of pure moments applied were based on established standards to prevent soft tissue rupture or damage [*14*, *25*]. However, it has been suggested that torque in excess of 100–120 Nm has been applied during surgery [*26*].

Previous biomechanical studies have analyzed the effects of various posterior-only sequential destabilizations in the thoracic spine [*11*–*16*]; however, most have analyzed single-level releases. In one such single-level study, Oda et al. [*14*] reported normalized increases in range of motion (compared to intact) of 38–45 % in each of the three planes of bending following resection of the posterior elements. In contrast, the normalized increases in range of motion in the present study were smaller, with increases ranging from 9 % in lateral bending to 26 % in flexion following the en bloc total facetectomies and sequential osteotomies. The differences in normalized motion increases may be due to the methods of analysis. In this study, increases following each surgical release were quantified as a percentage of total spine motion; in contrast, Oda et al. [*14*] analyzed increases following single-level surgery as a percentage of single-level motion.

Horton et al. [*13*] analyzed flexion–extension of full-length human thoracic spines following four en bloc total facetectomies. Facetectomies increased flexion by 1.7° and extension by 0.8°, representing a 12.7 % increase in flexion–extension. In contrast, in the present study, nine en bloc facetectomies provided

average increases of 0.4° in flexion and 1.7° in extension, or an 8 % increase in flexion–extension. However, Horton et al. [*13*] applied a perpendicular force to produce bending and kept the rib cage and sternum intact, both of which may, in part, account for the disparity in findings.

It remains controversial whether total facetectomies alone are sufficient to increase flexibility to achieve adequate deformity correction. For example, while Halanski et al. [*10*] reported no difference in coronal or sagittal curve correction following Ponte osteotomy as compared to facetectomies alone, Pizones et al. [*7*] reported significant improvement in coronal curve correction following wide posterior release (similar to Ponte osteotomy) compared to a standard posterior release, which in their study included more release than a typical facetectomy, inferring that the Ponte osteotomy would also provide improvement over facetectomy alone. Consequently, there is no consensus regarding the use of Ponte osteotomies, and similar wide posterior releases, for correction in the coronal plane [*6*, *7*, *9*, *10*]. The results of the present study suggest that while facetectomies alone can increase flexibility, supplemental osteotomies may be useful in providing additional flexibility. Further, the present study was able to quantify the sequential increase in spine flexibility following facetectomies and Ponte osteotomies, whereas clinical studies have had to rely on comparisons of average deformity correction in each patient group.

As it is not possible to obtain adolescent cadaveric specimens, let alone those with untreated deformities, for in vitro testing, cadaveric specimens from adult donors were used. Due to the limitations of elderly cadaveric specimens, such as poor bone quality and degeneration, specimens may not be as flexible as pediatric spines in surgery. Moreover, similar to other studies, the assumption was made that the increase in ROM following destabilization of non-deformed specimens corresponds to increases observed in deformed patients following the same posterior releases. Also, similar to previous studies [*14*, *15*, *17*], the ribcage was removed, leaving the posterior 5 cm of the ribs and costovertebral joints intact. This may have affected the magnitude of the resultant motions, as some studies have reported added stability provided by the ribcage [*18*, *27*, *28*]. Watkins et al. [*18*] reported that under pure moments, removal of the sternum and ribcage from cadaveric thoracic spines resulted in an increase in range of motion of 66 % in

flexion–extension, 54.8 % in lateral bending, and 45.9 % in axial rotation. Following the resections, only the posterior 3 cm of the ribs remained, similar to the condition of the intact spines in the present study. Brasiliense et al. [*27*] reported even larger increases in motion following resection of the ribcage and sternum, with only the posterior 25 % of the ribs intact, similar to the present study; however, the increases were calculated across three motion segments, in turn producing larger perceived percent increases in motion. In addition, unlike previous studies which apply pure moments to the spinal column, Brasiliense et al. [*27*] applied pure moments equally through the spine, ribcage and sternum, likely affecting the results.

Cadaveric models for the study of different methods to correct AIS deformities have clear advantages over clinical outcome studies, including shorter time, lower cost to the community and patients, and better control of numerous variables. Therefore, the results of the present study may serve to avoid the risk of suboptimal procedures that would otherwise be performed on some of the youngest and most clinically demanding orthopedic patients, who require decades of clinical success from their surgeries.

CONCLUSIONS

Ponte osteotomies provided higher per-level increases in ROM under single-plane loading than total facetectomies alone. Although Ponte osteotomies have been considered primarily for sagittal plane deformities, in this study they also provided simultaneous increase in all three planes under multi-planar loading, supporting clinical reports of coronal curve correction using Ponte osteotomies. Therefore, the results of the present study indicated that combined multi-planar loading of the spine can provide additional information beyond that obtained from previous single-plane loading models of surgical correction potential.

Acknowledgments

The study was supported by Doctor's Education and Research Fund, Orthopaedic Hospital.

Conflict of interest

None.

ELECTRONIC SUPPLEMENTARY MATERIAL

Below is the link to the electronic supplementary material.

Supplementary material 1 (DOC 40 kb) (http://link.springer.com/content/esm/art:10.1007/s00586-014-3499-0/file/MediaObjects/586_2014_3499_MOESM1_ESM.doc)

Supplementary material 2 (TIFF 2365 kb) (http://link.springer.com/content/esm/art:10.1007/s00586-014-3499-0/file/MediaObjects/586_2014_3499_MOESM2_ESM.tiff)

Supplementary material 3 (DOCX 12 kb) (http://link.springer.com/content/esm/art:10.1007/s00586-014-3499-0/file/MediaObjects/586_2014_3499_MOESM3_ESM.docx)

REFERENCES

1. Diab MG, Franzone JM, Vitale MG (2011) The role of posterior spinal osteotomies in pediatric spinal deformity surgery: indications and operative technique. J Pediatr Orthop 31(1 Suppl):S88–S98

2. Geck MJ, Macagno A, Ponte A, Shufflebarger HL (2007) The Ponte procedure: posterior only treatment of Scheuermann's kyphosis using segmental posterior shortening and pedicle screw instrumentation. J Spinal Disord Tech 20(8):586–593

3. Lehman RA Jr, Lenke LG, Keeler KA, Kim YJ, Buchowski JM, Cheh G, Kuhns CA, Bridwell KH (2008) Operative treatment of adolescent idiopathic scoliosis with posterior pedicle screw-only

constructs: Minimum three-year follow-up of one hundred fourteen cases. Spine (Phila Pa 1976) 33(14):1598–1604

4. Suk SI, Kim WJ, Lee SM, Kim JH, Chung ER (2001) Thoracic pedicle screw fixation in spinal deformities: are they really safe? Spine (Phila Pa 1976) 26(18):2049–2057

5. Suk SI, Lee CK, Kim WJ, Chung YJ, Park YB (1995) Segmental pedicle screw fixation in the treatment of thoracic idiopathic scoliosis. Spine (Phila Pa 1976) 20(12):1399–1405

6. Shah SA, Dhawale AA, Oda JE, Yorgova P, Neiss GI, Holmes L, Gabos PG (2013) Ponte osteotomies with pedicle screw instrumentation in the treatment of adolescent idiopathic scoliosis. Spine Deformity 1(3):196–204

7. Pizones J, Izquierdo E, Sanchez-Mariscal F, Alvarez P, Zuniga L, Gomez A (2010) Does wide posterior multiple level release improve the correction of adolescent idiopathic scoliosis curves? J Spinal Disord Tech 23(7):e24–e30

8. Shufflebarger HL, Clark CE (1998) Effect of wide posterior release on correction in adolescent idiopathic scoliosis. J Pediatr Orthop B 7(2):117–123

9. Shufflebarger HL, Geck MJ, Clark CE (2004) The posterior approach for lumbar and thoracolumbar adolescent idiopathic scoliosis: posterior shortening and pedicle screws. Spine 29(3):269–276 (discussion 276)

10. Halanski MA, Cassidy JA (2011) Do multilevel Ponte osteotomies in thoracic idiopathic scoliosis surgery improve curve correction and restore thoracic kyphosis? J Spinal Disord Tech 26(5):252–255

11. Anderson AL, McIff TE, Asher MA, Burton DC, Glattes RC (2009) The effect of posterior thoracic spine anatomical structures on motion segment flexion stiffness. Spine 34(5):441–446

12. Feiertag MA, Horton WC, Norman JT, Proctor FC, Hutton WC (1995) The effect of different surgical releases on thoracic spinal motion. A cadaveric study. Spine 20(14):1604–1611

13. Horton WC, Kraiwattanapong C, Akamaru T, Minamide A, Park JS, Park MS, Hutton WC (2005) The role of the sternum, costosternal articulations, intervertebral disc, and facets in thoracic sagittal plane biomechanics: a comparison of three different sequences of surgical release. Spine 30(18):2014–2023

14. Oda I, Abumi K, Cunningham BW, Kaneda K, McAfee PC (2002) An in vitro human cadaveric study investigating the biomechanical properties of the thoracic spine. Spine 27(3):E64–E70

15. Panjabi MM, Hausfeld JN, White AA 3rd (1981) A biomechanical study of the ligamentous stability of the thoracic spine in man. Acta Orthop Scand 52(3):315–326

16. White AA 3rd, Hirsch C (1971) The significance of the vertebral posterior elements in the mechanics of the thoracic spine. Clin Orthop Relat Res 81:2–14

17. Sangiorgio SN, Borkowski SL, Bowen RE, Scaduto AA, Frost NL, Ebramzadeh E (2013) Quantification of increase in three-dimensional spine flexibility following sequential Ponte osteotomies in a cadaveric model. Spine Deformity 1(3):171–178

18. Rt Watkins, Watkins R 3rd, Williams L, Ahlbrand S, Garcia R, Karamanian A, Sharp L, Vo C, Hedman T (2005) Stability provided by the sternum and rib cage in the thoracic spine. Spine 30(11):1283–1286

19. Deviren V, Acaroglu E, Lee J, Fujita M, Hu S, Lenke LG, Polly D Jr, Kuklo TR, O'Brien M, Brumfield D, Puttlitz CM (2005) Pedicle screw fixation of the thoracic spine: an in vitro biomechanical study on different configurations. Spine (Phila Pa 1976) 30(22):2530–2537

20. Balabaud L, Gallard E, Skalli W, Lassau JP, Lavaste F, Steib JP (2002) Biomechanical evaluation of a bipedicular spinal fixation system: a comparative stiffness test. Spine (Phila Pa 1976) 27(17):1875–1880

21. Wilke HJ, Wenger K, Claes L (1998) Testing criteria for spinal implants: recommendations for the standardization of in vitro stability testing of spinal implants. Eur Spine J 7(2):148–154

22. Schmidt J, Berg DR, Ploeg H-L, Ploeg L (2009) Precision, repeatability, and accuracy of optotrak optical motion tracking systems. Int J Exp Comput Biomech 1(1):114–127

23. Cho KJ, Bridwell KH, Lenke LG, Berra A, Baldus C (2005) Comparison of Smith-Petersen versus pedicle subtraction osteotomy for the correction of fixed sagittal imbalance. Spine 30(18):2030–2037 (discussion 2038)

24. Lee SM, Suk SI, Chung ER (2004) Direct vertebral rotation: a new technique of three-dimensional deformity correction with segmental pedicle screw fixation in adolescent idiopathic scoliosis. Spine (Phila Pa 1976) 29(3):343–349

25. Panjabi MM (1988) Biomechanical evaluation of spinal fixation devices: I. a conceptual framework. Spine (Phila Pa 1976) 13(10):1129–1134

26. Chang MS, Lenke LG (2009) Vertebral derotation in adolescent idiopathic scoliosis. Op Tech Orthop 19(1):19–23

27. Brasiliense LB, Lazaro BC, Reyes PM, Dogan S, Theodore N, Crawford NR (2011) Biomechanical contribution of the rib cage to thoracic stability. Spine (Phila Pa 1976) 36(26):E1686–E1693

28. Andriacchi T, Schultz A, Belytschko T, Galante J (1974) A model for studies of mechanical interactions between the human spine and rib cage. J Biomech 7(6):497–507

6 References

1. Lovett RW. The history of scoliosis. *Am J Orthop Surg* 1913;211:54-62.

2. Moen KY, Nachemson AL. Treatment of scoliosis. An historical perspective. *Spine (Phila Pa 1976)* 1999;24:2570-5.

3. Provencher MT, Abdu WA. Giovanni Alfonso Borelli: "Father of spinal biomechanics". *Spine (Phila Pa 1976)* 2000;25:131-6.

4. Boni T, Ruttimann B, Dvorak J, et al. Jean-Andre Venel. *Spine (Phila Pa 1976)* 1994;19:2007-11.

5. Harrington PR. Treatment of scoliosis. Correction and internal fixation by spine instrumentation. *J Bone Joint Surg Am* 1962;44-A:591-610.

6. Lee SM, Suk SI, Chung ER. Direct vertebral rotation: a new technique of three-dimensional deformity correction with segmental pedicle screw fixation in adolescent idiopathic scoliosis. *Spine (Phila Pa 1976)* 2004;29:343-9.

7. Chang MS, Lenke LG. Vertebral derotation in adolescent idiopathic scoliosis. *Operative Techniques in Orthopaedics* 2009;19:19-23.

8. Hirsch C, Nachemson A. New observations on the mechanical behavior of lumbar discs. *Acta Orthop Scand* 1954;23:254-83.

9. White AA, 3rd. Analysis of the mechanics of the thoracic spine in man. An experimental study of autopsy specimens. *Acta Orthop Scand Suppl* 1969;127:1-105.

10. White AA, 3rd, Hirsch C. The significance of the vertebral posterior elements in the mechanics of the thoracic spine. *Clin Orthop Relat Res* 1971;81:2-14.

11. Markolf KL. Deformation of the thoracolumbar intervertebral joints in response to external loads: a biomechanical study using autopsy material. *J Bone Joint Surg Am* 1972;54:511-33.

12. Nachemson AL, Schultz AB, Berkson MH. Mechanical properties of human lumbar spine motion segments. Influence of age, sex, disc level, and degeneration. *Spine (Phila Pa 1976)* 1979;4:1-8.

13. Panjabi MM, Hausfeld JN, White AA, 3rd. A biomechanical study of the ligamentous stability of the thoracic spine in man. *Acta Orthop Scand* 1981;52:315-26.

14. Maiman DJ, Sances A, Jr., Larson SJ, et al. Comparison of the failure biomechanics of spinal fixation devices. *Neurosurgery* 1985;17:574-80.

15. Panjabi MM, Brand RA, Jr., White AA, 3rd. Mechanical properties of the human thoracic spine as shown by three-dimensional load-displacement curves. *J Bone Joint Surg Am* 1976;58:642-52.

16. Panjabi MM, Brand RA, Jr., White AA, 3rd. Three-dimensional flexibility and stiffness properties of the human thoracic spine. *J Biomech* 1976;9:185-92.

17. Panjabi MM. Biomechanical evaluation of spinal fixation devices: I. A conceptual framework. *Spine (Phila Pa 1976)* 1988;13:1129-34.

18. Cotrel Y, Dubousset J, Guillaumat M. New universal instrumentation in spinal surgery. *Clin Orthop Relat Res* 1988;227:10-23.

19. Luque ER. Segmental spinal instrumentation for correction of scoliosis. *Clin Orthop Relat Res* 1982:192-8.

20. Dunn HK. Anterior stabilization of thoracolumbar injuries. *Clin Orthop Relat Res* 1984:116-24.

21. Dwyer AF, Newton NC, Sherwood AA. An anterior approach to scoliosis. A preliminary report. *Clin Orthop Relat Res* 1969;62:192-202.

22. Steffee AD, Biscup RS, Sitkowski DJ. Segmental spine plates with pedicle screw fixation. A new internal fixation device for disorders of the lumbar and thoracolumbar spine. *Clin Orthop Relat Res* 1986:45-53.

23. White AA, 3rd, Panjabi MM. *Clinical Biomechanics of the Spine*. 2nd ed. Philadelphia: J.B. Lippincott Company, 1978.

24. Wilke HJ, Wenger K, Claes L. Testing criteria for spinal implants: recommendations for the standardization of in vitro stability testing of spinal implants. *Eur Spine J* 1998;7:148-54.

25. Horton WC, Kraiwattanapong C, Akamaru T, et al. The role of the sternum, costosternal articulations, intervertebral disc, and facets in thoracic sagittal plane biomechanics: a comparison of three different sequences of surgical release. *Spine* 2005;30:2014-23.

26. Healy AT, Lubelski D, Mageswaran P, et al. Biomechanical analysis of the upper thoracic spine after decompressive procedures. *Spine J* 2014.

27. Watkins Rt, Watkins R, 3rd, Williams L, et al. Stability provided by the sternum and rib cage in the thoracic spine. *Spine* 2005;30:1283-6.

28. Sangiorgio SN, Borkowski SL, Bowen RE, et al. Quantification of increase in three-dimensional spine flexibility following sequential Ponte osteotomies in a cadaveric model. *Spine Deformity* 2013;1:171-8.

29. Oda I, Abumi K, Cunningham BW, et al. An in vitro human cadaveric study investigating the biomechanical properties of the thoracic spine. *Spine* 2002;27:E64-70.

30. Goel VK, Clark CR, Gallaes K, et al. Moment-rotation relationships of the ligamentous occipito-atlanto-axial complex. *J Biomech* 1988;21:673-80.

31. Panjabi MM, Oxland TR, Lin RM, et al. Thoracolumbar burst fracture. A biomechanical investigation of its multidirectional flexibility. *Spine (Phila Pa 1976)* 1994;19:578-85.

32. Crawford NR, Brantley AG, Dickman CA, et al. An apparatus for applying pure nonconstraining moments to spine segments in vitro. *Spine (Phila Pa 1976)* 1995;20:2097-100.

33. Wilke HJ, Claes L, Schmitt H, et al. A universal spine tester for in vitro experiments with muscle force simulation. *Eur Spine J* 1994;3:91-7.

34. Sangiorgio SN, Sheikh H, Borkowski SL, et al. Comparison of three posterior dynamic stabilization devices. *Spine* 2011;36:E1251-8.

35. Kuklo TR, Dmitriev AE, Cardoso MJ, et al. Biomechanical contribution of transverse connectors to segmental stability following long segment instrumentation with thoracic pedicle screws. *Spine (Phila Pa 1976)* 2008;33:E482-7.

36. Kikkawa J, Cunningham BW, Shirado O, et al. Biomechanical evaluation of a posterolateral lumbar disc arthroplasty device: an in vitro human cadaveric model. *Spine* 2010;35:1760-8.

37. Wilke HJ, Schmidt H, Werner K, et al. Biomechanical evaluation of a new total posterior-element replacement system. *Spine (Phila Pa 1976)* 2006;31:2790-6; discussion 7.

38. Lindsey DP, Swanson KE, Fuchs P, et al. The effects of an interspinous implant on the kinematics of the instrumented and adjacent levels in the lumbar spine. *Spine* 2003;28:2192-7.

39. Strube P, Tohtz S, Hoff E, et al. Dynamic stabilization adjacent to single-level fusion: part I. Biomechanical effects on lumbar spinal motion. *Eur Spine J* 2010;19:2171-80.

40. Panjabi M, Henderson G, Abjornson C, et al. Multidirectional testing of one- and two-level ProDisc-L versus simulated fusions. *Spine (Phila Pa 1976)* 2007;32:1311-9.

41. Broc GG, Crawford NR, Sonntag VK, et al. Biomechanical effects of transthoracic microdiscectomy. *Spine (Phila Pa 1976)* 1997;22:605-12.

42. Chang UK, Lim J, Kim DH. Biomechanical study of thoracolumbar junction fixation devices with different diameter dual-rod systems. *J Neurosurg Spine* 2006;4:206-12.

43. Balabaud L, Gallard E, Skalli W, et al. Biomechanical evaluation of a bipedicular spinal fixation system: a comparative stiffness test. *Spine (Phila Pa 1976)* 2002;27:1875-80.

44. Coe JD, Warden KE, Sutterlin CE, 3rd, et al. Biomechanical evaluation of cervical spinal stabilization methods in a human cadaveric model. *Spine (Phila Pa 1976)* 1989;14:1122-31.

45. Yamamoto I, Panjabi MM, Crisco T, et al. Three-dimensional movements of the whole lumbar spine and lumbosacral joint. *Spine (Phila Pa 1976)* 1989;14:1256-60.

46. Parsons JR, Chokshi BV, Lee CK, et al. The biomechanical analysis of sublaminar wires and cables using luque segmental spinal instrumentation. *Spine (Phila Pa 1976)* 1997;22:267-73.

47. Deviren V, Acaroglu E, Lee J, et al. Pedicle screw fixation of the thoracic spine: an in vitro biomechanical study on different configurations. *Spine (Phila Pa 1976)* 2005;30:2530-7.

48. Morgenstern W, Ferguson SJ, Berey S, et al. Posterior thoracic extrapedicular fixation: a biomechanical study. *Spine (Phila Pa 1976)* 2003;28:1829-35.

49. Shimamoto N, Kotani Y, Shono Y, et al. Static and dynamic analysis of five anterior instrumentation systems for thoracolumbar scoliosis. *Spine (Phila Pa 1976)* 2003;28:1678-85.

50. Puttlitz CM, Masaru F, Barkley A, et al. A biomechanical assessment of thoracic spine stapling. *Spine (Phila Pa 1976)* 2007;32:766-71.

51. Jones GA, Kayanja M, Milks R, et al. Biomechanical characteristics of hybrid hook-screw constructs in short-segment thoracic fixation. *Spine (Phila Pa 1976)* 2008;33:173-7.

52. Dick JC, Zdeblick TA, Bartel BD, et al. Mechanical evaluation of cross-link designs in rigid pedicle screw systems. *Spine (Phila Pa 1976)* 1997;22:370-5.

53. Henriques T, Cunningham BW, Olerud C, et al. Biomechanical comparison of five different atlantoaxial posterior fixation techniques. *Spine (Phila Pa 1976)* 2000;25:2877-83.

54. Hitchon PW, Goel VK, Rogge TN, et al. In vitro biomechanical analysis of three anterior thoracolumbar implants. *J Neurosurg* 2000;93:252-8.

55. Abumi K, Panjabi MM, Duranceau J. Biomechanical evaluation of spinal fixation devices. Part III. Stability provided by six spinal fixation devices and interbody bone graft. *Spine (Phila Pa 1976)* 1989;14:1249-55.

56. Shimamoto N, Cunningham BW, Dmitriev AE, et al. Biomechanical evaluation of stand-alone interbody fusion cages in the cervical spine. *Spine (Phila Pa 1976)* 2001;26:E432-6.

57. Oda I, Abumi K, Sell LC, et al. Biomechanical evaluation of five different occipito-atlanto-axial fixation techniques. *Spine (Phila Pa 1976)* 1999;24:2377-82.

58. Wollowick AL, Farrelly EE, Meyers K, et al. Anterior release generates more thoracic rotation than posterior osteotomy: a biomechanical study of human cadaver spines. *Spine (Phila Pa 1976)* 2013;38:1540-5.

59. Goel VK, Grauer JN, Patel T, et al. Effects of charite artificial disc on the implanted and adjacent spinal segments mechanics using a hybrid testing protocol. *Spine (Phila Pa 1976)* 2005;30:2755-64.

60. Schulte TL, Hurschler C, Haversath M, et al. The effect of dynamic, semi-rigid implants on the range of motion of lumbar motion segments after decompression. *Eur Spine J* 2008;17:1057-65.

61. Scoliosis [MedlinePlus Health Information], 2012. Available at: http://www.nlm.nih.gov/.

62. Whiting WC, Zernicke RF. *Biomechanics of Musculoskeletal Injury*. 2nd ed: Human Kinetics, 2008.

63. Stokes IA. Three-dimensional terminology of spinal deformity. A report presented to the Scoliosis Research Society by the Scoliosis Research Society Working Group on 3-D terminology of spinal deformity. *Spine (Phila Pa 1976)* 1994;19:236-48.

64. Keim HA, Hensinger RN. Spinal deformities. Scoliosis and kyphosis. *Clin Symp* 1989;41:3-32.

65. Kane WJ. Scoliosis prevalence: a call for a statement of terms. *Clin Orthop Relat Res* 1977:43-6.

66. Weinstein SL, Dolan LA, Cheng JC, et al. Adolescent idiopathic scoliosis. *Lancet* 2008;371:1527-37.

67. Bradford DS, Tay BK, Hu SS. Adult scoliosis: surgical indications, operative management, complications, and outcomes. *Spine (Phila Pa 1976)* 1999;24:2617-29.

68. AHRQ. Healthcare Cost and Utilization Project (HCUP) [HCUP Databases], 2011. Available at: http://hcupnet.ahrq.gov/.

69. Parent S, Newton PO, Wenger DR. Adolescent idiopathic scoliosis: etiology, anatomy, natural history, and bracing. *Instr Course Lect* 2005;54:529-36.

70. Konieczny MR, Senyurt H, Krauspe R. Epidemiology of adolescent idiopathic scoliosis. *J Child Orthop* 2013;7:3-9.

71. Kamerlink JR, Quirno M, Auerbach JD, et al. Hospital cost analysis of adolescent idiopathic scoliosis correction surgery in 125 consecutive cases. *J Bone Joint Surg Am* 2010;92:1097-104.

72. Larson AN, Aubin C, Polly D, Jr., et al. Are more screws better? A systematic review of anchor density and curve correction in adolescent idiopathic scoliosis. *Spine Deformity* 2013;1:237-47.

73. Kumar K. Spinal deformity and axial traction. *Spine (Phila Pa 1976)* 1996;21:653-5.

74. Humke T, Grob D, Scheier H, et al. Cotrel-Dubousset and Harrington Instrumentation in idiopathic scoliosis: a comparison of long-term results. *Eur Spine J* 1995;4:280-3.

75. Mariconda M, Galasso O, Barca P, et al. Minimum 20-year follow-up results of Harrington rod fusion for idiopathic scoliosis. *Eur Spine J* 2005;14:854-61.

76. McMaster MJ. Luque rod instrumentation in the treatment of adolescent idiopathic scoliosis. A comparative study with Harrington instrumentation. *J Bone Joint Surg Br* 1991;73:982-9.

77. Danielsson AJ, Nachemson AL. Radiologic findings and curve progression 22 years after treatment for adolescent idiopathic scoliosis: comparison of brace and surgical treatment with matching control group of straight individuals. *Spine (Phila Pa 1976)* 2001;26:516-25.

78. Cochran T, Irstam L, Nachemson A. Long-term anatomic and functional changes in patients with adolescent idiopathic scoliosis treated by Harrington rod fusion. *Spine (Phila Pa 1976)* 1983;8:576-84.

79. Gaines RW, Leatherman KD. Benefits of the Harrington compression system in lumbar and thoracolumbar idiopathic scoliosis in adolescents and adults. *Spine (Phila Pa 1976)* 1981;6:483-8.

80. Lee CS, Nachemson AL. The crankshaft phenomenon after posterior Harrington fusion in skeletally immature patients with thoracic or thoracolumbar idiopathic scoliosis followed to maturity. *Spine (Phila Pa 1976)* 1997;22:58-67.

81. Dubousset J, Herring JA, Shufflebarger H. The crankshaft phenomenon. *J Pediatr Orthop* 1989;9:541-50.

82. Padua R, Padua S, Aulisa L, et al. Patient outcomes after Harrington instrumentation for idiopathic scoliosis: a 15- to 28-year evaluation. *Spine (Phila Pa 1976)* 2001;26:1268-73.

83. Wenger DR, Carollo JJ, Wilkerson JA, Jr., et al. Laboratory testing of segmental spinal instrumentation versus traditional Harrington instrumentation for scoliosis treatment. *Spine (Phila Pa 1976)* 1982;7:265-9.

84. Davies AG, McMaster MJ. The effect of Luque-rod instrumentation on the sagittal contour of the lumbosacral spine in adolescent idiopathic scoliosis and the preservation of a physiologic lumbar lordosis. *Spine (Phila Pa 1976)* 1992;17:112-5.

85. Herring JA, Wenger DR. Segmental spinal instrumentation: a preliminary report of 40 consecutive cases. *Spine (Phila Pa 1976)* 1982;7:285-98.

86. Johnston CE, 2nd, Happel LT, Jr., Norris R, et al. Delayed paraplegia complicating sublaminar segmental spinal instrumentation. *J Bone Joint Surg Am* 1986;68:556-63.

87. Helenius I, Remes V, Yrjonen T, et al. Harrington and Cotrel-Dubousset instrumentation in adolescent idiopathic scoliosis. Long-term functional and radiographic outcomes. *J Bone Joint Surg Am* 2003;85-A:2303-9.

88. Lenke LG, Bridwell KH, Baldus C, et al. Cotrel-Dubousset instrumentation for adolescent idiopathic scoliosis. *J Bone Joint Surg Am* 1992;74:1056-67.

89. Bridwell KH, Betz R, Capelli AM, et al. Sagittal plane analysis in idiopathic scoliosis patients treated with Cotrel-Dubousset instrumentation. *Spine (Phila Pa 1976)* 1990;15:644-9.

90. Rhee JM, Bridwell KH, Won DS, et al. Sagittal plane analysis of adolescent idiopathic scoliosis: the effect of anterior versus posterior instrumentation. *Spine (Phila Pa 1976)* 2002;27:2350-6.

91. Kim YJ, Bridwell KH, Lenke LG, et al. Proximal junctional kyphosis in adolescent idiopathic scoliosis following segmental posterior spinal instrumentation and fusion: minimum 5-year follow-up. *Spine (Phila Pa 1976)* 2005;30:2045-50.

92. Lee GA, Betz RR, Clements DH, 3rd, et al. Proximal kyphosis after posterior spinal fusion in patients with idiopathic scoliosis. *Spine (Phila Pa 1976)* 1999;24:795-9.

93. Kim YJ, Lenke LG, Kim J, et al. Comparative analysis of pedicle screw versus hybrid instrumentation in posterior spinal fusion of adolescent idiopathic scoliosis. *Spine (Phila Pa 1976)* 2006;31:291-8.

94. Lowe TG, Betz R, Lenke L, et al. Anterior single-rod instrumentation of the thoracic and lumbar spine: saving levels. *Spine (Phila Pa 1976)* 2003;28:S208-16.

95. Hsu LC, Zucherman J, Tang SC, et al. Dwyer instrumentation in the treatment of adolescent idiopathic scoliosis. *J Bone Joint Surg Br* 1982;64:536-41.

96. Kohler R, Galland O, Mechin H, et al. The Dwyer procedure in the treatment of idiopathic scoliosis. A 10-year follow-up review of 21 patients. *Spine (Phila Pa 1976)* 1990;15:75-80.

97. Hammerberg KW, Rodts MF, DeWald RL. Zielke instrumentation. *Orthopedics* 1988;11:1365-71.

98. Horton WC, Holt RT, Johnson JR, et al. Zielke instrumentation in idiopathic scoliosis: late effects and minimizing complications. *Spine (Phila Pa 1976)* 1988;13:1145-9.

99. Trammell TR, Benedict F, Reed D. Anterior spine fusion using Zielke instrumentation for adult thoracolumbar and lumbar scoliosis. *Spine (Phila Pa 1976)* 1991;16:307-16.

100. Kaneda K, Shono Y, Satoh S, et al. New anterior instrumentation for the management of thoracolumbar and lumbar scoliosis. Application of the Kaneda two-rod system. *Spine (Phila Pa 1976)* 1996;21:1250-61; discussion 61-2.

101. Deacon P, Flood BM, Dickson RA. Idiopathic scoliosis in three dimensions. A radiographic and morphometric analysis. *J Bone Joint Surg Br* 1984;66:509-12.

102. Suk SI, Lee CK, Kim WJ, et al. Segmental pedicle screw fixation in the treatment of thoracic idiopathic scoliosis. *Spine (Phila Pa 1976)* 1995;20:1399-405.

103. Hackenberg L, Link T, Liljenqvist U. Axial and tangential fixation strength of pedicle screws versus hooks in the thoracic spine in relation to bone mineral density. *Spine (Phila Pa 1976)* 2002;27:937-42.

104. Liljenqvist U, Hackenberg L, Link T, et al. Pullout strength of pedicle screws versus pedicle and laminar hooks in the thoracic spine. *Acta Orthop Belg* 2001;67:157-63.

105. Dobbs MB, Lenke LG, Kim YJ, et al. Selective posterior thoracic fusions for adolescent idiopathic scoliosis: comparison of hooks versus pedicle screws. *Spine (Phila Pa 1976)* 2006;31:2400-4.

106. Kim YJ, Lenke LG, Cho SK, et al. Comparative analysis of pedicle screw versus hook instrumentation in posterior spinal fusion of adolescent idiopathic scoliosis. *Spine (Phila Pa 1976)* 2004;29:2040-8.

107. Diab MG, Franzone JM, Vitale MG. The role of posterior spinal osteotomies in pediatric spinal deformity surgery: indications and operative technique. *J Pediatr Orthop* 2011;31:S88-98.

108. Geck MJ, Macagno A, Ponte A, et al. The Ponte procedure: posterior only treatment of Scheuermann's kyphosis using segmental posterior shortening and pedicle screw instrumentation. *J Spinal Disord Tech* 2007;20:586-93.

109. Lehman RA, Jr., Lenke LG, Keeler KA, et al. Operative treatment of adolescent idiopathic scoliosis with posterior pedicle screw-only constructs: minimum three-year follow-up of one hundred fourteen cases. *Spine (Phila Pa 1976)* 2008;33:1598-604.

110. Suk SI, Kim WJ, Lee SM, et al. Thoracic pedicle screw fixation in spinal deformities: are they really safe? *Spine (Phila Pa 1976)* 2001;26:2049-57.

111. Pizones J, Izquierdo E, Sanchez-Mariscal F, et al. Does wide posterior multiple level release improve the correction of adolescent idiopathic scoliosis curves? *J Spinal Disord Tech* 2010;23:e24-30.

112. Shah SA, Dhawale AA, Oda JE, et al. Ponte osteotomies with pedicle screw instrumentation in the treatment of adolescent idiopathic scoliosis. *Spine Deformity* 2013;1:196-204.

113. Krismer M, Bauer R, Sterzinger W. Scoliosis correction by Cotrel-Dubousset instrumentation. The effect of derotation and three dimensional correction. *Spine (Phila Pa 1976)* 1992;17:S263-9.

114. Gardner-Morse M, Stokes IA. Three-dimensional simulations of the scoliosis derotation maneuver with Cotrel-Dubousset instrumentation. *J Biomech* 1994;27:177-81.

115. Chang KW. Cantilever bending technique for treatment of large and rigid scoliosis. *Spine (Phila Pa 1976)* 2003;28:2452-8.

116. Cheng I, Kim Y, Gupta MC, et al. Apical sublaminar wires versus pedicle screws--which provides better results for surgical correction of adolescent idiopathic scoliosis? *Spine (Phila Pa 1976)* 2005;30:2104-12.

117. Di Silvestre M, Bakaloudis G, Lolli F, et al. Posterior fusion only for thoracic adolescent idiopathic scoliosis of more than 80 degrees: pedicle screws versus hybrid instrumentation. *Eur Spine J* 2008;17:1336-49.

118. Helgeson MD, Shah SA, Newton PO, et al. Evaluation of proximal junctional kyphosis in adolescent idiopathic scoliosis following pedicle screw, hook, or hybrid instrumentation. *Spine (Phila Pa 1976)* 2010;35:177-81.

119. Lowenstein JE, Matsumoto H, Vitale MG, et al. Coronal and sagittal plane correction in adolescent idiopathic scoliosis: a comparison between all pedicle screw versus hybrid thoracic hook lumbar screw constructs. *Spine (Phila Pa 1976)* 2007;32:448-52.

120. Mulpuri K, Perdios A, Reilly CW. Evidence-based medicine analysis of all pedicle screw constructs in adolescent idiopathic scoliosis. *Spine (Phila Pa 1976)* 2007;32:S109-14.

121. Roach JW, Mehlman CT, Sanders JO. "Does the outcome of adolescent idiopathic scoliosis surgery justify the rising cost of the procedures?". *J Pediatr Orthop* 2011;31:S77-80.

122. Sanders JO, Diab M, Richards SB, et al. Fixation points within the main thoracic curve: does more instrumentation produce greater curve correction and improved results? *Spine (Phila Pa 1976)* 2011;36:E1402-6.

123. Senaran H, Shah SA, Gabos PG, et al. Difficult thoracic pedicle screw placement in adolescent idiopathic scoliosis. *J Spinal Disord Tech* 2008;21:187-91.

124. Storer SK, Vitale MG, Hyman JE, et al. Correction of adolescent idiopathic scoliosis using thoracic pedicle screw fixation versus hook constructs. *J Pediatr Orthop* 2005;25:415-9.

125. Yilmaz G, Borkhuu B, Dhawale AA, et al. Comparative analysis of hook, hybrid, and pedicle screw instrumentation in the posterior treatment of adolescent idiopathic scoliosis. *J Pediatr Orthop* 2012;32:490-9.

126. Vora V, Crawford A, Babekhir N, et al. A pedicle screw construct gives an enhanced posterior correction of adolescent idiopathic scoliosis when compared with other constructs: myth or reality. *Spine (Phila Pa 1976)* 2007;32:1869-74.

127. Halanski MA, Cassidy JA. Do Multilevel Ponte Osteotomies in Thoracic Idiopathic Scoliosis Surgery Improve Curve Correction and Restore Thoracic Kyphosis? *J Spinal Disord Tech* 2011.

128. Wagner MR, Flores JB, Sanpera I, et al. Aortic abutment after direct vertebral rotation: plowing of pedicle screws. *Spine (Phila Pa 1976)* 2011;36:243-7.

129. Feiertag MA, Horton WC, Norman JT, et al. The effect of different surgical releases on thoracic spinal motion. A cadaveric study. *Spine* 1995;20:1604-11.

130. Oda I, Abumi K, Lu D, et al. Biomechanical role of the posterior elements, costovertebral joints, and rib cage in the stability of the thoracic spine. *Spine* 1996;21:1423-9.

131. Brasiliense LB, Lazaro BC, Reyes PM, et al. Biomechanical contribution of the rib cage to thoracic stability. *Spine (Phila Pa 1976)* 2011;36:E1686-93.

132. Andriacchi T, Schultz A, Belytschko T, et al. A model for studies of mechanical interactions between the human spine and rib cage. *J Biomech* 1974;7:497-507.

133. Oxland TR, Lin RM, Panjabi MM. Three-dimensional mechanical properties of the thoracolumbar junction. *J Orthop Res* 1992;10:573-80.

134. Kothe R, Panjabi MM, Liu W. Multidirectional instability of the thoracic spine due to iatrogenic pedicle injuries during transpedicular fixation. A biomechanical investigation. *Spine (Phila Pa 1976)* 1997;22:1836-42.

135. Schultheiss M, Hartwig E, Sarkar M, et al. Biomechanical in vitro comparison of different mono- and bisegmental anterior procedures with regard to the strategy for fracture stabilisation using minimally invasive techniques. *Eur Spine J* 2006;15:82-9.

136. Busscher I, van der Veen AJ, van Dieen JH, et al. In vitro biomechanical characteristics of the spine: a comparison between human and porcine spinal segments. *Spine (Phila Pa 1976)* 2010;35:E35-42.

137. Hodges PW, Cresswell AG, Daggfeldt K, et al. In vivo measurement of the effect of intra-abdominal pressure on the human spine. *J Biomech* 2001;34:347-53.

138. Ashman RB, Bechtold JE, Edwards WT, et al. In vitro spinal arthrodesis implant mechanical testing protocols. *J Spinal Disord* 1989;2:274-81.

139. Hasler CC, Hefti F, Buchler P. Coronal plane segmental flexibility in thoracic adolescent idiopathic scoliosis assessed by fulcrum-bending radiographs. *Eur Spine J* 2010;19:732-8.

140. Halsall AP, James DF, Kostuik JP, et al. An experimental evaluation of spinal flexibility with respect to scoliosis surgery. *Spine (Phila Pa 1976)* 1983;8:482-8.

141. Yoganandan NPC, Joseph F. MD; Pintar, Frank A. PhD; Rao, Raj D. MD. Whiplash Injury Determination With Conventional Spine Imaging and Cryomicrotomy. *SPINE* 2001;26:2443-8.

142. Parent S, Odell T, Oka R, et al. Does the direction of pedicle screw rotation affect the biomechanics of direct transverse plane vertebral derotation? *Spine (Phila Pa 1976)* 2008;33:1966-9.

143. Benneker LM, Heini PF, Anderson SE, et al. Correlation of radiographic and MRI parameters to morphological and biochemical assessment of intervertebral disc degeneration. *Eur Spine J* 2005;14:27-35.

144. Christe A, Laubli R, Guzman R, et al. Degeneration of the cervical disc: histology compared with radiography and magnetic resonance imaging. *Neuroradiology* 2005;47:721-9.

145. Gunzburg R, Parkinson R, Moore R, et al. A cadaveric study comparing discography, magnetic resonance imaging, histology, and mechanical behavior of the human lumbar disc. *Spine (Phila Pa 1976)* 1992;17:417-26.

146. Boos N, Weissbach S, Rohrbach H, et al. Classification of age-related changes in lumbar intervertebral discs: 2002 Volvo Award in basic science. *Spine (Phila Pa 1976)* 2002;27:2631-44.

147. Rutges JP, Duit RA, Kummer JA, et al. A validated new histological classification for intervertebral disc degeneration. *Osteoarthritis Cartilage* 2013;21:2039-47.

148. Weiler C, Lopez-Ramos M, Mayer HM, et al. Histological analysis of surgical lumbar intervertebral disc tissue provides evidence for an association between disc degeneration and increased body mass index. *BMC Res Notes* 2011;4:497.

149. Amiot LP, Poulin F. Computed tomography-based navigation for hip, knee, and spine surgery. *Clin Orthop Relat Res* 2004:77-86.

150. Nolte LP, Slomczykowski MA, Berlemann U, et al. A new approach to computer-aided spine surgery: fluoroscopy-based surgical navigation. *Eur Spine J* 2000;9 Suppl 1:S78-88.

151. Fujimori T, Iwasaki M, Nagamoto Y, et al. Kinematics of the thoracic spine in trunk rotation: in vivo 3-dimensional analysis. *Spine (Phila Pa 1976)* 2012;37:E1318-28.

152. Fujimori T, Iwasaki M, Nagamoto Y, et al. Kinematics of the thoracic spine in trunk lateral bending: in vivo three-dimensional analysis. *Spine J* 2013.

153. Mannion AF, Knecht K, Balaban G, et al. A new skin-surface device for measuring the curvature and global and segmental ranges of motion of the spine: reliability of measurements and comparison with data reviewed from the literature. *Eur Spine J* 2004;13:122-36.

154. Morita D, Yukawa Y, Nakashima H, et al. Range of motion of thoracic spine in sagittal plane. *Eur Spine J* 2014;23:673-8.

155. Willems JM, Jull GA, J KF. An in vivo study of the primary and coupled rotations of the thoracic spine. *Clin Biomech (Bristol, Avon)* 1996;11:311-6.

156. Troke M, Moore AP, Cheek E. Reliability of the OSI CA 6000 Spine Motion Analyzer with a new skin fixation system when used on the thoracic spine. *Man Ther* 1998;3:27-33.

157. Heneghan NR, Hall A, Hollands M, et al. Stability and intra-tester reliability of an in vivo measurement of thoracic axial rotation using an innovative methodology. *Man Ther* 2009;14:452-5.

158. Lubelski D, Healy AT, Mageswaran P, et al. Biomechanics of the lower thoracic spine after decompression and fusion: a cadaveric analysis. *Spine J* 2014.

159. Takeuchi T, Abumi K, Shono Y, et al. Biomechanical role of the intervertebral disc and costovertebral joint in stability of the thoracic spine. A canine model study. *Spine* 1999;24:1414-20.

160. Wilke HJ, Geppert J, Kienle A. Biomechanical in vitro evaluation of the complete porcine spine in comparison with data of the human spine. *Eur Spine J* 2011;20:1859-68.

161. Suk SI, Kim JH, Kim SS, et al. Pedicle screw instrumentation in adolescent idiopathic scoliosis (AIS). *Eur Spine J* 2012;21:13-22.

162. Shufflebarger HL, Clark CE. Effect of wide posterior release on correction in adolescent idiopathic scoliosis. *J Pediatr Orthop B* 1998;7:117-23.

163. Shufflebarger HL, Geck MJ, Clark CE. The posterior approach for lumbar and thoracolumbar adolescent idiopathic scoliosis: posterior shortening and pedicle screws. *Spine* 2004;29:269-76; discussion 76.

164. Anderson AL, McIff TE, Asher MA, et al. The effect of posterior thoracic spine anatomical structures on motion segment flexion stiffness. *Spine* 2009;34:441-6.

165. Smith-Petersen MN, Larson CB, Aufranc OE. Osteotomy of the spine for correction of flexion deformity in rheumatoid arthritis. *J Bone Joint Surg Am* 1945;27:1-11.

166. Cho KJ, Bridwell KH, Lenke LG, et al. Comparison of Smith-Petersen versus pedicle subtraction osteotomy for the correction of fixed sagittal imbalance. *Spine (Phila Pa 1976)* 2005;30:2030-7; discussion 8.

167. Gill JB, Levin A, Burd T, et al. Corrective osteotomies in spine surgery. *J Bone Joint Surg Am* 2008;90:2509-20.

168. Lenke LG, Betz RR, Harms J, et al. Adolescent idiopathic scoliosis: a new classification to determine extent of spinal arthrodesis. *J Bone Joint Surg Am* 2001;83-A:1169-81.

169. Kadoury S, Cheriet F, Beausejour M, et al. A three-dimensional retrospective analysis of the evolution of spinal instrumentation for the correction of adolescent idiopathic scoliosis. *Eur Spine J* 2009;18:23-37.

170. Di Silvestre M, Lolli F, Bakaloudis G, et al. Apical vertebral derotation in the posterior treatment of adolescent idiopathic scoliosis: myth or reality? *Eur Spine J* 2013;22:313-23.

171. Fu G, Kawakami N, Goto M, et al. Comparison of vertebral rotation corrected by different techniques and anchors in surgical treatment of adolescent thoracic idiopathic scoliosis. *J Spinal Disord Tech* 2009;22:182-9.

172. Asghar J, Samdani AF, Pahys JM, et al. Computed tomography evaluation of rotation correction in adolescent idiopathic scoliosis: a comparison of an all pedicle screw construct versus a hook-rod system. *Spine (Phila Pa 1976)* 2009;34:804-7.

173. Kuklo TR, Potter BK, Polly DW, Jr., et al. Monaxial versus multiaxial thoracic pedicle screws in the correction of adolescent idiopathic scoliosis. *Spine (Phila Pa 1976)* 2005;30:2113-20.

174. Panjabi MM, Krag M, Summers D, et al. Biomechanical time-tolerance of fresh cadaveric human spine specimens. *J Orthop Res* 1985;3:292-300.

175. White AA, 3rd. Kinematics of the normal spine as related to scoliosis. *J Biomech* 1971;4:405-11.

176. Remes V, Helenius I, Schlenzka D, et al. Cotrel-Dubousset (CD) or Universal Spine System (USS) instrumentation in adolescent idiopathic scoliosis (AIS): comparison of midterm clinical, functional, and radiologic outcomes. *Spine (Phila Pa 1976)* 2004;29:2024-30.

177. Chang KW, Leng X, Zhao W, et al. Broader curve criteria for selective thoracic fusion. *Spine (Phila Pa 1976)* 2011;36:1658-64.

178. Dobbs MB, Lenke LG, Kim YJ, et al. Anterior/posterior spinal instrumentation versus posterior instrumentation alone for the treatment of adolescent idiopathic scoliotic curves more than 90 degrees. *Spine (Phila Pa 1976)* 2006;31:2386-91.

179. Di Silvestre M, Parisini P, Lolli F, et al. Complications of thoracic pedicle screws in scoliosis treatment. *Spine (Phila Pa 1976)* 2007;32:1655-61.

180. Li G, Lv G, Passias P, et al. Complications associated with thoracic pedicle screws in spinal deformity. *Eur Spine J* 2010;19:1576-84.

181. Soultanis KC, Sakellariou VI, Starantzis KA, et al. Late diagnosis of perforation of the aorta by a pedicle screw. *Acta Orthop Belg* 2013;79:361-7.

182. Zhu F, Sun X, Qiao J, et al. Misplacement Pattern of Pedicle Screws in Pediatric Patients with Spinal Deformity: A Computed Tomography Study. *J Spinal Disord Tech* 2013.

183. Ellingson AM, Mehta H, Polly DW, et al. Disc degeneration assessed by quantitative T2* (T2 star) correlated with functional lumbar mechanics. *Spine (Phila Pa 1976)* 2013;38:E1533-40.

184. Chiba M, McLain RF, Yerby SA, et al. Short-segment pedicle instrumentation. Biomechanical analysis of supplemental hook fixation. *Spine (Phila Pa 1976)* 1996;21:288-94.

185. Hitchon PW, Brenton MD, Serhan H, et al. In vitro biomechanical studies of an anterior thoracolumbar implant. *J Spinal Disord Tech* 2002;15:350-4.

186. Oda T, Panjabi MM. Pedicle screw adjustments affect stability of thoracolumbar burst fracture. *Spine (Phila Pa 1976)* 2001;26:2328-33.

187. Wheeler DJ, Freeman AL, Ellingson AM, et al. Inter-laboratory variability in in vitro spinal segment flexibility testing. *J Biomech* 2011;44:2383-7.

188. Hayes WC, Mockros LF. Viscoelastic properties of human articular cartilage. *J Appl Physiol* 1971;31:562-8.

189. Panjabi MM, Oxland TR, Kifune M, et al. Validity of the three-column theory of thoracolumbar fractures. A biomechanic investigation. *Spine (Phila Pa 1976)* 1995;20:1122-7.

190. Pelker RR, Duranceau JS, Panjabi MM. Cervical spine stabilization. A three-dimensional, biomechanical evaluation of rotational stability, strength, and failure mechanisms. *Spine (Phila Pa 1976)* 1991;16:117-22.

191. Clark JA, Hsu LC, Yau AC. Viscoelastic behaviour of deformed spines under correction with halo pelvic distraction. *Clin Orthop Relat Res* 1975:90-111.

192. Mac-Thiong JM, Labelle H, Poitras B, et al. The effect of intraoperative traction during posterior spinal instrumentation and fusion for adolescent idiopathic scoliosis. *Spine (Phila Pa 1976)* 2004;29:1549-54.

193. Nachemson A, Nordwall A. Effectiveness of preoperative Cotrel traction for correction of idiopathic scoliosis. *J Bone Joint Surg Am* 1977;59:504-8.

194. Letts RM, Palakar G, Bobecko WP. Preoperative skeletal traction in scoliosis. *J Bone Joint Surg Am* 1975;57:616-9.

195. Sanchez Marquez JM, Sanchez Perez-Grueso FJ, Fernandez-Baillo N, et al. Gradual scoliosis correction over time with shape-memory metal: a preliminary report of an experimental study. *Scoliosis* 2012;7:20.

196. Mimura M, Panjabi MM, Oxland TR, et al. Disc degeneration affects the multidirectional flexibility of the lumbar spine. *Spine (Phila Pa 1976)* 1994;19:1371-80.

197. Natarajan RN, Andersson GB. The influence of lumbar disc height and cross-sectional area on the mechanical response of the disc to physiologic loading. *Spine (Phila Pa 1976)* 1999;24:1873-81.

198. Sairyo K, Biyani A, Goel V, et al. Pathomechanism of ligamentum flavum hypertrophy: a multidisciplinary investigation based on clinical, biomechanical, histologic, and biologic assessments. *Spine (Phila Pa 1976)* 2005;30:2649-56.

199. Fukuyama S, Nakamura T, Ikeda T, et al. The effect of mechanical stress on hypertrophy of the lumbar ligamentum flavum. *J Spinal Disord* 1995;8:126-30.

200. Kirkaldy-Willis WH, Farfan HF. Instability of the lumbar spine. *Clin Orthop Relat Res* 1982:110-23.

201. Quint U, Wilke HJ. Grading of degenerative disk disease and functional impairment: imaging versus patho-anatomical findings. *Eur Spine J* 2008;17:1705-13.

202. Tanaka N, An HS, Lim TH, et al. The relationship between disc degeneration and flexibility of the lumbar spine. *Spine J* 2001;1:47-56.

203. Kettler A, Rohlmann F, Ring C, et al. Do early stages of lumbar intervertebral disc degeneration really cause instability? Evaluation of an in vitro database. *Eur Spine J* 2011;20:578-84.

204. Fujiwara A, Lim TH, An HS, et al. The effect of disc degeneration and facet joint osteoarthritis on the segmental flexibility of the lumbar spine. *Spine (Phila Pa 1976)* 2000;25:3036-44.

205. Galbusera F, van Rijsbergen M, Ito K, et al. Ageing and degenerative changes of the intervertebral disc and their impact on spinal flexibility. *Eur Spine J* 2014;23 Suppl 3:324-32.

206. Yahia H, Drouin G, Maurais G, et al. Degeneration of the human lumbar spine ligaments. An ultrastructural study. *Pathol Res Pract* 1989;184:369-75.

207. Wiemann J, Durrani S, Bosch P. The effect of posterior spinal releases on axial correction torque: a cadaver study. *J Child Orthop* 2011;5:109-13.

208. Lam FC, Groff MW, Alkalay RN. The effect of screw head design on rod derotation in the correction of thoracolumbar spinal deformity: laboratory investigation. *J Neurosurg Spine* 2013;19:351-9.

209. ASTM F2193-02. *Standard Specifications and Test Methods for Components Used in the Surgical Fixation of the Spinal Skeletal System*, 2007.

210. ASTM F1798-97. *Standard Guide for Evaluating the Static and Fatigue Properties of Interconnection Mechanisms and Subassemblies Using in Spinal Arthrodesis Implants*, 2008.

211. ASTM F2694. *Standard Practice for Functional and Wear Evaluation of Motion-Preserving Lumbar Total Facet Prostheses*, 2011.

212. ASTM F2790. *Standard Practice for Static and Dynamic Characterization of Motion Preserving Lumbar Total Facet Prostheses*, 2011.

213. ASTM F2423-11. *Standard Guide for Functional, Kinematic, and Wear Assessment of Total Disc Prostheses*, 2011.

214. ASTM F2624. *Standard Test Method for Static, Dynamic, and Wear Assessment of Extra-Discal Single Level Spinal Constructs*, 2011.

215. ASTM F2346-05. *Standard Test Methods for Static and Dynamic Characterization of Spinal Artificial Discs*, 2011.

216. ASTM F2267-04. *Standard Test Method for Measuring Load Induced Subsidence of Intervertebral Body Fusion Device Under Static Axial Compression*, 2011.

217. ASTM F1582-98. *Standard Terminology Relating to Spinal Implants*, 2011.

218. ASTM F2706. *Standard Test Methods for Occipital-Cervical and Occipital-Cervical-Thoracic Spinal Implant Constructs in a Vertebrectomy Model*, 2011.

219. ASTM F2759. *Standard Guide for Assessment of the Ultra High Molecular Weight Polyethylene (UHMWPE) Used in Orthopedic and Spinal Devices*, 2011.

220. ASTM F2077-11. *Test Methods for Intervertebral Body Fusion Devices*, 2011.

221. ASTM F1717-12. *Standard Test Methods for Spinal Implant Constructs in a Vertebrectomy Model*, 2012.

222. Zhang G, Zhang Y, Zhang X, et al. [Restoration of thoracic kyphosis with multilevel Ponte osteotomies in thoracic idiopathic scoliosis surgery]. *Zhongguo Xiu Fu Chong Jian Wai Ke Za Zhi* 2012;26:1197-201.

223. Mladenov KV, Vaeterlein C, Stuecker R. Selective posterior thoracic fusion by means of direct vertebral derotation in adolescent idiopathic scoliosis: effects on the sagittal alignment. *Eur Spine J* 2011;20:1114-7.

224. Hwang SW, Samdani AF, Lonner B, et al. Impact of direct vertebral body derotation on rib prominence: are preoperative factors predictive of changes in rib prominence? *Spine (Phila Pa 1976)* 2012;37:E86-9.

225. Hwang SW, Samdani AF, Gressot LV, et al. Effect of direct vertebral body derotation on the sagittal profile in adolescent idiopathic scoliosis. *Eur Spine J* 2012;21:31-9.

226. Hwang SW, Samdani AF, Cahill PJ. The impact of segmental and en bloc derotation maneuvers on scoliosis correction and rib prominence in adolescent idiopathic scoliosis. *J Neurosurg Spine* 2012;16:345-50.

227. Samdani AF, Hwang SW, Miyanji F, et al. Direct vertebral body derotation, thoracoplasty, or both: which is better with respect to inclinometer and scoliosis research society-22 scores? *Spine (Phila Pa 1976)* 2012;37:E849-53.

228. Faraj AA, Webb JK. Early complications of spinal pedicle screw. *Eur Spine J* 1997;6:324-6.

229. Sucato DJ, Duchene C. The position of the aorta relative to the spine: a comparison of patients with and without idiopathic scoliosis. *J Bone Joint Surg Am* 2003;85-A:1461-9.

230. Sandhu HK, Charlton-Ouw KM, Azizzadeh A, et al. Spinal screw penetration of the aorta. *J Vasc Surg* 2013;57:1668-70.

231. Mac-Thiong JM, Parent S, Poitras B, et al. Neurological outcome and management of pedicle screws misplaced totally within the spinal canal. *Spine (Phila Pa 1976)* 2013;38:229-37.

232. Suk SI, Kim JH, Kim SS, et al. Thoracoplasty in thoracic adolescent idiopathic scoliosis. *Spine (Phila Pa 1976)* 2008;33:1061-7.

233. Demura S, Yaszay B, Carreau J, et al. Maintenance of Thoracic Kyphosis in the 3D Correction of Thoracic Adolescent Idiopathic Scoliosis Using Direct Vertebral Derotation. *Spine Deformity* 2013;1:46-50.

234. Cidambi KR, Glaser DA, Bastrom TP, et al. Postoperative changes in spinal rod contour in adolescent idiopathic scoliosis: an in vivo deformation study. *Spine (Phila Pa 1976)* 2012;37:1566-72.

235. Lonner BS, Auerbach JD, Boachie-Adjei O, et al. Treatment of thoracic scoliosis: are monoaxial thoracic pedicle screws the best form of fixation for correction? *Spine (Phila Pa 1976)* 2009;34:845-51.

236. Lonner BS, Auerbach JD, Estreicher MB, et al. Thoracic pedicle screw instrumentation: the learning curve and evolution in technique in the treatment of adolescent idiopathic scoliosis. *Spine (Phila Pa 1976)* 2009;34:2158-64.

237. Sarlak AY, Tosun B, Atmaca H, et al. Evaluation of thoracic pedicle screw placement in adolescent idiopathic scoliosis. *Eur Spine J* 2009;18:1892-7.

238. Hicks JM, Singla A, Shen FH, et al. Complications of pedicle screw fixation in scoliosis surgery: a systematic review. *Spine (Phila Pa 1976)* 2010;35:E465-70.

239. Quan GM, Gibson MJ. Correction of main thoracic adolescent idiopathic scoliosis using pedicle screw instrumentation: does higher implant density improve correction? *Spine (Phila Pa 1976)* 2010;35:562-7.

240. Paik H, Kang DG, Lehman RA, Jr., et al. The biomechanical consequences of rod reduction on pedicle screws: should it be avoided? *Spine J* 2013;13:1617-26.

241. Osvalder AL, Neumann P, Lovsund P, et al. Ultimate strength of the lumbar spine in flexion--an in vitro study. *J Biomech* 1990;23:453-60.

242. Neumann P, Osvalder AL, Nordwall A, et al. The ultimate flexural strength of the lumbar spine and vertebral bone mineral content. *J Spinal Disord* 1993;6:314-23.

243. Miller JA, Schultz AB, Warwick DN, et al. Mechanical properties of lumbar spine motion segments under large loads. *J Biomech* 1986;19:79-84.

244. Bisschop A, van Dieen JH, Kingma I, et al. Torsion biomechanics of the spine following lumbar laminectomy: a human cadaver study. *Eur Spine J* 2013;22:1785-93.

245. Cheng I, Hay D, Iezza A, et al. Biomechanical analysis of derotation of the thoracic spine using pedicle screws. *Spine (Phila Pa 1976)* 2010;35:1039-43.

246. Coe JD, Warden KE, Herzig MA, et al. Influence of bone mineral density on the fixation of thoracolumbar implants. A comparative study of transpedicular screws, laminar hooks, and spinous process wires. *Spine (Phila Pa 1976)* 1990;15:902-7.

247. Berlemann U, Cripton P, Nolte LP, et al. New means in spinal pedicle hook fixation. A biomechanical evaluation. *Eur Spine J* 1995;4:114-22.

248. Panjabi MM, Abumi K, Duranceau J, et al. Biomechanical evaluation of spinal fixation devices: II. Stability provided by eight internal fixation devices. *Spine (Phila Pa 1976)* 1988;13:1135-40.

249. McAfee PC, Werner FW, Glisson RR. A biomechanical analysis of spinal instrumentation systems in thoracolumbar fractures. Comparison of traditional Harrington distraction instrumentation with segmental spinal instrumentation. *Spine (Phila Pa 1976)* 1985;10:204-17.

250. Borkowski SL, Sangiorgio SN, Bowen RE, et al. Flexibility of thoracic spines under simultaneous multi-planar loading. *Eur Spine J* 2014.

251. Lazaro BC, Deniz FE, Brasiliense LB, et al. Biomechanics of thoracic short versus long fixation after 3-column injury. *J Neurosurg Spine* 2011;14:226-34.

252. Sran MM, Khan KM, Zhu Q, et al. Posteroanterior stiffness predicts sagittal plane midthoracic range of motion and three-dimensional flexibility in cadaveric spine segments. *Clin Biomech (Bristol, Avon)* 2005;20:806-12.

253. Schmidt J, Berg DR, Ploeg H-L, et al. Precision, repeatability, and accuracy of Optotrak optical motion tracking systems. *Int. J. Experimental and Computational Biomechanics* 2009;1:114-27.

254. Lane NE, Nevitt MC, Genant HK, et al. Reliability of new indices of radiographic osteoarthritis of the hand and hip and lumbar disc degeneration. *J Rheumatol* 1993;20:1911-8.

255. Pfirrmann CW, Metzdorf A, Zanetti M, et al. Magnetic resonance classification of lumbar intervertebral disc degeneration. *Spine (Phila Pa 1976)* 2001;26:1873-8.

256. Thompson JP, Pearce RH, Schechter MT, et al. Preliminary evaluation of a scheme for grading the gross morphology of the human intervertebral disc. *Spine (Phila Pa 1976)* 1990;15:411-5.

257. Schultheiss M, Hartwig E, Claes L, et al. Influence of screw-cement enhancement on the stability of anterior thoracolumbar fracture stabilization with circumferential instability. *Eur Spine J* 2004;13:598-604.

258. Schultheiss M, Claes L, Wilke HJ, et al. Enhanced primary stability through additional cementable cannulated rescue screw for anterior thoracolumbar plate application. *J Neurosurg* 2003;98:50-5.

259. Yu Y, Xie N, Song S, et al. A biomechanical comparison of a novel thoracic screw fixation method: transarticular screw fixation vs traditional pedicle screw fixation. *Neurosurgery* 2011;69:ons141-5; discussion ons6.

260. Panjabi MM, Kifune M, Liu W, et al. Graded thoracolumbar spinal injuries: development of multidirectional instability. *Eur Spine J* 1998;7:332-9.

261. Little AS, Brasiliense LB, Lazaro BC, et al. Biomechanical comparison of costotransverse process screw fixation and pedicle screw fixation of the upper thoracic spine. *Neurosurgery* 2010;66:178-82; discussion 82.

262. Kifune M, Panjabi MM, Arand M, et al. Fracture pattern and instability of thoracolumbar injuries. *Eur Spine J* 1995;4:98-103.

263. Hitchon PW, Goel V, Drake J, et al. Comparison of the biomechanics of hydroxyapatite and polymethylmethacrylate vertebroplasty in a cadaveric spinal compression fracture model. *J Neurosurg* 2001;95:215-20.

264. Deniz FE, Brasiliense LB, Lazaro BC, et al. Biomechanical evaluation of posterior thoracic transpedicular discectomy. *J Neurosurg Spine* 2010;13:253-9.

265. Chou D, Larios AE, Chamberlain RH, et al. A biomechanical comparison of three anterior thoracolumbar implants after corpectomy: are two screws better than one? *J Neurosurg Spine* 2006;4:213-8.

266. Ruger M, Schmoelz W. Vertebroplasty with high-viscosity polymethylmethacrylate cement facilitates vertebral body restoration in vitro. *Spine (Phila Pa 1976)* 2009;34:2619-25.

267. Ames CP, Bozkus MH, Chamberlain RH, et al. Biomechanics of stabilization after cervicothoracic compression-flexion injury. *Spine (Phila Pa 1976)* 2005;30:1505-12.

268. Busscher I, van Dieen JH, Kingma I, et al. Biomechanical characteristics of different regions of the human spine: an in vitro study on multilevel spinal segments. *Spine (Phila Pa 1976)* 2009;34:2858-64.

269. Schultheiss M, Hartwig E, Kinzl L, et al. Axial compression force measurement acting across the strut graft in thoracolumbar instrumentation testing. *Clin Biomech (Bristol, Avon)* 2003;18:631-6.

270. Schultheiss M, Hartwig E, Kinzl L, et al. Thoracolumbar fracture stabilization: comparative biomechanical evaluation of a new video-assisted implantable system. *Eur Spine J* 2004;13:93-100.

271. Stanley SK, Ghanayem AJ, Voronov LI, et al. Flexion-extension response of the thoracolumbar spine under compressive follower preload. *Spine (Phila Pa 1976)* 2004;29:E510-4.

272. Tan JS, Singh S, Zhu QA, et al. The effect of cement augmentation and extension of posterior instrumentation on stabilization and adjacent level effects in the elderly spine. *Spine (Phila Pa 1976)* 2008;33:2728-40.

273. Ashman RB, Birch JG, Bone LB, et al. Mechanical testing of spinal instrumentation. *Clin Orthop Relat Res* 1988;227:113-25.

274. Arana E, Marti-Bonmati L, Molla E, et al. Upper thoracic-spine disc degeneration in patients with cervical pain. *Skeletal Radiol* 2004;33:29-33.

275. Goh S, Tan C, Price RI, et al. Influence of age and gender on thoracic vertebral body shape and disc degeneration: an MR investigation of 169 cases. *J Anat* 2000;197 Pt 4:647-57.

276. Niemelainen R, Battie MC, Gill K, et al. The prevalence and characteristics of thoracic magnetic resonance imaging findings in men. *Spine (Phila Pa 1976)* 2008;33:2552-9.

277. Otani K, Yoshida M, Fujii E, et al. Thoracic disc herniation. Surgical treatment in 23 patients. *Spine (Phila Pa 1976)* 1988;13:1262-7.

278. Teraguchi M, Yoshimura N, Hashizume H, et al. Prevalence and distribution of intervertebral disc degeneration over the entire spine in a population-based cohort: the Wakayama Spine Study. *Osteoarthritis Cartilage* 2014;22:104-10.

279. Wood KB, Garvey TA, Gundry C, et al. Magnetic resonance imaging of the thoracic spine. Evaluation of asymptomatic individuals. *J Bone Joint Surg Am* 1995;77:1631-8.

280. McInerney J, Ball PA. The pathophysiology of thoracic disc disease. *Neurosurg Focus* 2000;9:e1.

281. Little JP, Izatt MT, Labrom RD, et al. An FE investigation simulating intra-operative corrective forces applied to correct scoliosis deformity. *Scoliosis* 2013;8:9.